Synthesis and Ring-Opening Metathesis Polymerization of Norbornenes Containing Pendent Aromatic and Aliphatic Side Chains

by

Andrea L. Edel

A Thesis

Submitted to the Faculty of Graduate Studies

In Partial Fulfillment of the Requirements

For the Degree of

Masters of Science

in Chemistry

Department of Chemistry

The University of Manitoba

Winnipeg, Manitoba

THE UNIVERSITY OF MANITOBA

FACULTY OF GRADUATE STUDIES

*****

COPYRIGHT PERMISSION PAGE

Synthesis and Ring-Opening Metathesis Polymerization of Norbornenes Containing Pendent Aromatic and Aliphatic Side Chains

BY

Andrea L. Edel

A Thesis/Practicum submitted to the Faculty of Graduate Studies of The University of Manitoba in partial fulfillment of the requirements of the degree of

Master of Science

Abstract

A series of well-defined polynorbornenes containing pendent aromatic ether or aliphatic side chains have been prepared. Synthesis of the monomeric materials proceeded via initial cyclopentadienyliron-mediated nucleophilic aromatic substitution reactions and DCC-mediated condensation reactions, followed by removal of the metal moiety via photolytic demetallation. Structural analysis of both the metallated and nonmetallated compounds was accomplished using homo- and heteronuclear correlation spectroscopic techniques as well as IR, MS and C,H elemental analysis. Subsequent ring-opening metathesis polymerization of these building blocks was achieved in the presence of a ruthenium-based catalyst, namely bis(tricyclohexylphosphine)benzylidene ruthenium (IV) dichloride, which liberated the resulting polymeric materials in high conversion of the monomer to the polymer. Gel permeation chromatography of each of the polymers revealed high molecular weights as well as low to narrow polydispersity indices. Thermal analysis of the aromatic ether functionalized polynorbornenes was accomplished using differential scanning calorimetry (DSC) and thermogravimetric analysis (TGA). These results showed that when the number of aromatic groups pendent to the polymer chain increased (within each polymer repeat unit), a subsequent increase in the thermal stability was noted. TGA of the aliphatic-bridged systems revealed decreased thermal stability as the length of the aliphatic flexible spacer increased. Changing the spacer from a purely methylene-bridged system to one containing a tri(ethylene glycol) chain was found to increase the overall thermal properties of the resulting polymeric material.

Acknowledgements

To begin, I would like to acknowledge and thank my supervisor Dr. Alaa S. Abd-El-Aziz who has given me the opportunity to work with him. Being a part of his research group has been such a valuable and memorable experience for me that has enabled my growth as both a scientist and an individual.

I would also like to extend my thanks to both the University of Manitoba and Faculty of Graduate Studies for accepting me as a graduate student and The University of Winnipeg for providing the facilities for me to perform my research. Manitoba Hydro is also gratefully acknowledged for providing the funds for this research.

Several individuals who deserve special mention are ones who contributed towards the outcome of this thesis. These include Ed Segstro, for his insightful training on the mass spectrometer, Dr. Harold Hutton for his helpful NMR discussions and Terry Wolowiec at the University of Manitoba for running some of my NMR samples.

Of the members of my research group I would like to begin by thanking Leslie May for all of her hard work in reading and correcting this manuscript as well as her contribution towards the success of this project. I would also like to thank Erin Todd and Shelly Bernardin for their valued discussions throughout the course of my studies. Other individuals who have been an asset in my chemical studies are Dr. Karen Epp, Dr. Christine de Denus, Debbie Armstrong, Simone Smith, Khanh Tran, Nicole Gavel, Jonathan Fine, Wesley Budakowski and Shaune McFarlane.

I would next like to thank my husband Wayne, my parents, Freda and Earl White and my brother Greg for their continued support and love throughout the duration of my university studies. Your constant encouragement and prayers have meant so much to me that I cannot find words to express how blessed I am to have you as family. In addition, I would like to thank my new family, the Edel's, as well as my friends. I thank you all for your prayers and patience. I could not have done this without you all.

In closing, I would just like to thank my heavenly Father, Jesus Christ, for giving me this remarkable opportunity as well as providing me with the strength to fulfill all that was required.

Table of Contents

List of Figures

List of Tables

List of Abbreviations

APT	attached proton test
t-Bu	tertiary-butyl
COSY	correlation spectroscopy
Cp	cyclopentadienyl
Cy_3P	tricyclohexylphosphine
Cyp	cyclopentyl
d	doublet
dd	doublet of doublets
1-D	one-dimensional
2-D	two-dimensional
DCC	dicyclohexylcarbodiimide
DCMNBD	2,3-dicarbomethoxynorbornadiene
DCU	dicyclohexylurea
DMAc	dimethylacetamide
DMAP	dimethylaminopyridine
DMF	dimethylformamide
DMSO	dimethylsulphoxide
DSC	differential scanning calorimetry
DTAB	dodecyltrimethylammonium bromide
FIDs	free induction decays
FT	fourier transformation
GPC	gel permeation chromatography
HETCOR	heteronuclear correlation
Hz	hertz
$(i\text{-Pr})_3P$	triisopropylphosphine
IR	infrared
k_{rel}	relative rates
LC	liquid crystal
LCP	liquid crystal polymer
M	monomer
$M^{\cdot}$	molecular ion peak
MCLCPs	main chain liquid crystal polymers
Me	methyl
Mn	number average molecular weight
MS	mass spectroscopy
Mw	weight average molecular weight
m/z	mass to charge ratio
NBDF6	2,3-bis(trifluoromethyl)norbornadiene
NBDPA	(norbornene)diphenylanthracene
NMR	nuclear magnetic resonance
PAEKs	poly(aryletherketones)
PEK	poly(etherketone)
PEEK	poly(etheretherketone)

PDI	polydispersity index
Ph	phenyl
q	quartet
ROMP	ring-opening metathesis polymerization
s	singlet
SCLCPs	side chain liquid crystalline polymers
S_NAr	nucleophilic aromatic substitution
t	triplet
Tg	glass transition temperature
TGA	thermogravimetric analysis
THF	tetrahydrofuran
UC	uncomplexed

1.0 Ring-Opening Metathesis Polymerization of Highly Strained Bicyclo[2.2.1] Heptenes

1.1 Introduction

Polynorbornene, (Norsorex), has been manufactured industrially since 1976 by CdF Chimie and has found applications in the production of engine mountings, shock-proof bumpers and flexible couplings.[1-4] Over the past decade, there have been efforts to modify the thermal properties of polynorbornene as the demand for more thermally stable materials has escalated.[5-7] Previous studies have demonstrated that functionalization of the polynorbornene backbone leads to enhanced thermal properties of the resulting polymeric material.[6, 7] As aromatic groups are well known for their structural stability, efforts have been made to incorporate these groups onto the polymer backbone in an attempt to improve the overall thermal stability of the polymer. Of the many studies reporting the synthesis of functionalized polynorbornenes, only a few focus on the synthesis of fully aryl substituted polynorbornenes, however, none of them mention any of the thermal properties of the resulting polymeric materials.[8, 9]

Over the past few decades, significant strides have been made in the ring-opening metathesis polymerization (ROMP) of cycloalkenes and bicycloalkenes. This has primarily been accomplished with advances in the preparation of well-defined organotransition metal catalysts, beginning with the discovery of the Ziegler-Natta catalyst in the late 1950's.[4] Since then, catalysts consisting of Ti, Zr, Hf, V, Nb, Ta, Cr,

Mo, W, Tc, Re, Ru, Os, Co, Rh and Ir have been prepared and investigated in terms of their ability to facilitate ROMP.[1]

In 1960, Truett and coworkers detailed the polymerization of norbornene, a highly strained bicyclo[2.2.1]hept-2-ene, using catalysts derived from lithium aluminum tetraalkyls and titanium tetrachloride, as shown in Equation 1.1.[10] An interesting feature of this new type of polymerization was the formation of a site of unsaturation between each repeating unit within the polynorbornene backbone. Truett proposed that for this unsaturation to be present in the polymer chain, the initial step of the mechanism must involve breaking of the double bond within the monomer. He proposed that the monomer was able to coordinate to the metal catalyst at a specified site, and through a series of successive rearrangements and propagations, the resulting unsaturated polymeric material could be formed. This mechanism was later defined as "coordination polymerization." As this chemistry of breaking and building new double bonds had never been observed before in other cyclic olefin polymerizations, this mechanism was widely disputed, and was not accepted until further evidence was established.

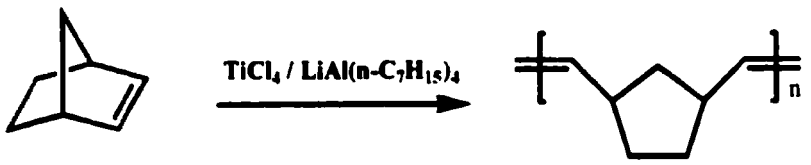

(1.1)

The first accepted report detailing the mechanism of the ROMP reaction was published in 1967 by Calderon and coworkers who defined this process as "olefin metathesis".[11, 12] It was proposed that the mechanism involved the interchange of carbon atoms between a pair of double bonds.[11, 12] Evidence for this exchange of atoms was

identified by these researchers with their finding that both acyclic olefins and cycloalkenes could be polymerized using the same initiator, $WCl_6/EtAlCl_2/EtOH$.[11, 12] This established that a common pathway existed for the polymerization of both types of monomers. It was determined that the mechanism proceeded via an initial breaking of the double bond within the monomer forming a highly strained metallacyclobutane complex, followed by a carbon atom exchange with an alkylidene ligand, as shown in Scheme 1.1. Additional evidence supporting this mechanism was obtained several years later based upon findings from isotope labeling studies.[11, 13-17] However, conclusive evidence for the olefin metathesis mechanism was not obtained until the early 1980's when ^1H and ^{13}C NMR spectroscopic data was used to confirm the intermediate metallacyclobutane complex.[1-3, 18-22]

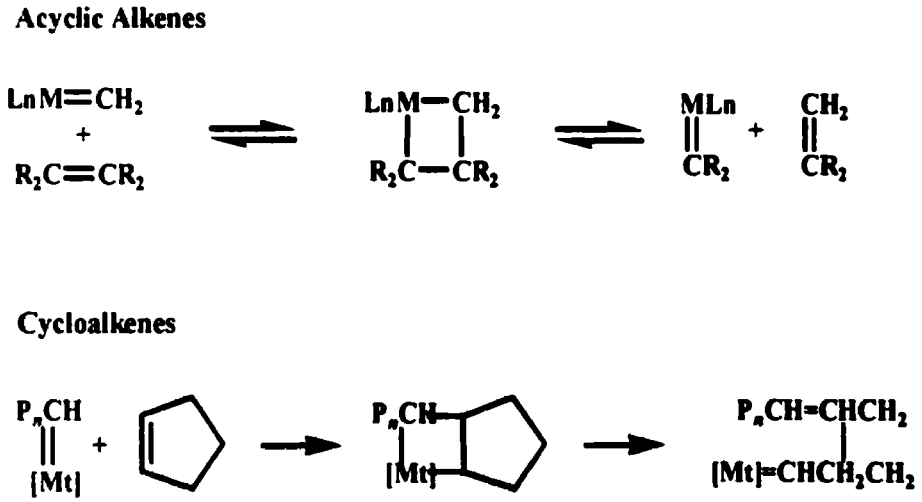

Scheme 1.1

Optimal control of the structural design of polymeric materials synthesized from ring-opening metathesis polymerization (ROMP) is best achieved in living systems. A

polymerization is defined as living if the propagating species does not undergo any chain transfer or termination steps.[4, 23] In order to ascertain whether or not a polymerization is living, several criteria must be observed. One factor involves the ability to prepare a homopolymer of a particular monomer, which is accomplished by the removal and quenching of an aliquot of the polymer followed by the addition of a second aliquot of the same monomer. Molecular weight analysis of the two polymers should show a significant increase in the overall molecular weight for the final polymer relative to the initial polymer. This methodology can also be used to synthesize various block copolymers. Another feature indicative of a living system is the linear relationship observed between molecular weight and the degree of conversion of monomer to polymer. This reveals that the number average molecular weight (Mn) in a living system is related to the stoichiometry of the overall reaction, and hence its degree of conversion.[23]

Since the initial discovery of polynorbornene forty years ago, significant strides have been made in the area of ring-opening metathesis polymerization. With the development of more well-defined metal-carbene ROMP catalysts displaying increased tolerance towards a wider variety of polar functional groups, the polymerization of a diverse range of functionalized norbornenes has been made possible. As a result, numerous types of polymeric materials have been prepared possessing a wide range of properties.

1.2 Synthetic Routes Toward Functionalization of Norbornene

Cycloalkenes containing 3-, 4-, 8-, and larger membered rings, undergo ring-opening polymerization based upon thermodynamic considerations of the molecule.[1-4] In contrast, reactions involving 5-, 6-, and 7-membered rings are much more dependent on the sign of the free energy (ΔG), which becomes more negative due to increased ring strain in the monomer. This in turn depends on the reaction temperature and pressure, monomer concentration, and the nature and position of the substituents on the ring. In bridged bicyclic systems, ΔG is often more negative due to the high energy caused by increased ring strain. It is this high-energy constraint in bicyclo[2.2.1] hept-2-enes that is the driving force behind irreversible ring-opening metathesis polymerizations. As a result, many novel derivatives of polynorbornene have been prepared possessing variable thermal and mechanical properties.[1-3]

1.2.1 Functionalization of *Exo*, *Endo*-5-Norbornene-2-Methanol

Incorporation of an alcohol functionality pendent to the norbornene framework in 5-norbornene-2-methanol is extremely important in that it provides a reactive site for further functionalization. It is well known that a primary alcohol can readily be converted to an alkyl halide, a carboxylic ester or a carboxyiic acid, to mention a few accessibly reactive functional groups.[24, 25] As a result, many opportunities exist for the functionalization of this norbornene analogue, thus providing various routes towards the synthesis of novel monomeric compounds.

In the past decade, functionalization of 5-norbornene-2-methanol has led to the formation of polymeric materials suitable for a wide variety of applications.[8, 26-30] These include the preparation of redox-active polymers, materials with both photoconducting and physiological properties as well as polymers suitable for electroluminescence. Schrock and coworkers incorporated ferrocene pendent to the polynorbornene backbone in an attempt to construct polymeric materials capable of possessing redox activity.[26] Ferrocene, a metal-sandwich complex, possesses the potential for electrochemical activity due to the ease with which the iron center undergoes oxidation and reduction.[31] Preparation of the monomer, detailed in Scheme 1.2, involved the initial formation of (chlorocarbonyl)ferrocene which was prepared by the reaction of ferrocenecarboxylic acid with PCl_5 Subsequent reaction of the acid chloride with 5-norbornene-2-methanol in THF and pyridine resulted in the formation of 5-norbornenyl-(*endo,exo*)-2-(methoxycarbonyl)ferrocene.

Several years later, Schrock turned his attention towards the preparation of norbornene monomers containing a blue-light-emitting molecule known as diphenylanthracene (Scheme 1.3), called (norbornene)diphenylanthracene or NBDPA, which has found significant application in chemiluminescence technology.[8] Since the first polymer-based electroluminescent devices constructed from poly(phenylenevinylene) were prepared almost ten years ago, this methodology utilizing polymeric materials as a basis for these devices has sparked significant interest.[8] This is because of the greater ease of processability of these polymers relative to traditional solid-state inorganic materials, which are more difficult to mold.

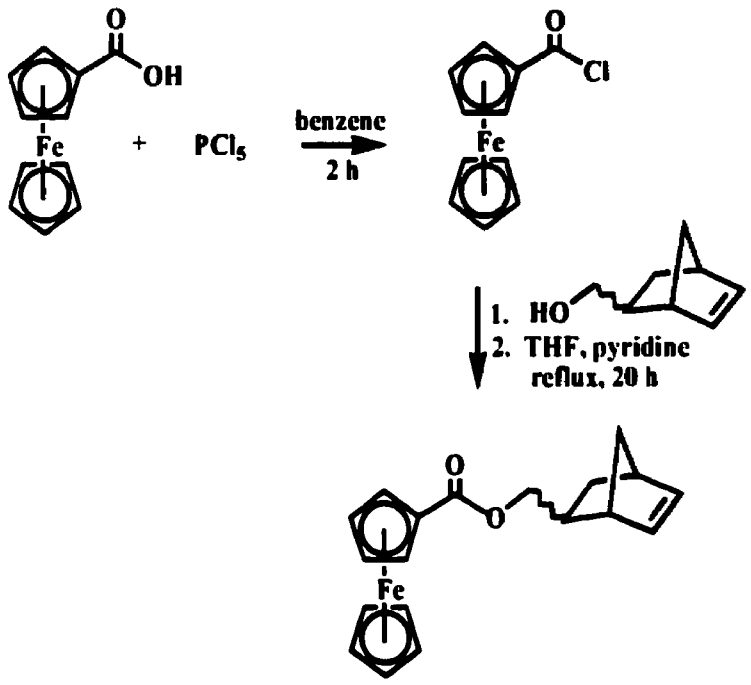
O
OH
Fe
+
PCl5
benzene
2 h
O
Cl
Fe
1. HO
2. THF, pyridine
reflux, 20 h
O
O
Fe

Scheme 1.2

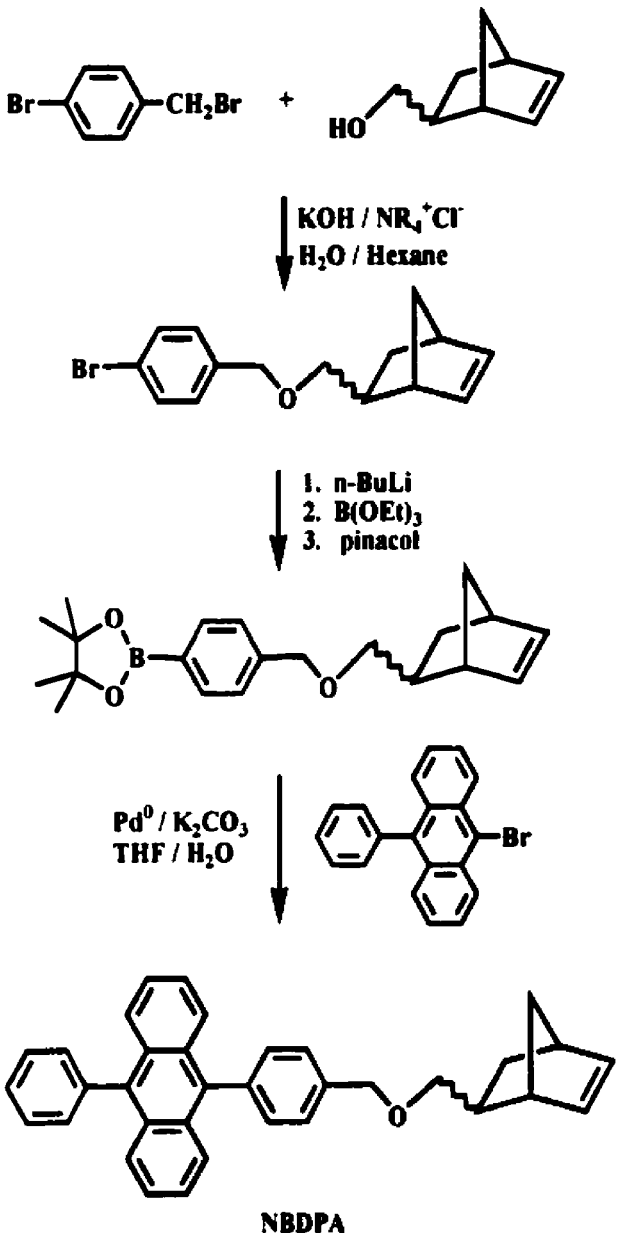

NBDPA

Scheme 1.3

1.2.2 Functionalization of *Exo,Endo*-5-Norbornene-2-Carboxylic acid

Like 5-norbornene-2-methanol, the carboxylic acid derivative of 5-norbornene is also a reactive precursor for a variety of functionalized norbornenes. The reactive carboxylic acid group in 5-norbornene-2-carboxylic acid, can be used to synthesize many new organic compounds.[24, 25] Most often, 5-norbornene-2-carboxylic acid is converted to the acid halide which demonstrates greater reactivity in condensation reactions. Furthermore, this acid halide can be synthesized quite easily making this methodology advantageous.

Living ROMPs involving derivatives of 5-norbornene-2-carboxylic acid have been accomplished and have found application in the preparation of side chain liquid crystalline polymers (SCLCPs) and in the synthesis of various glycopolymers.[5, 32-34] For example, Schrock and coworkers prepared novel SCLCPs containing a rigid mesogen bridged to the norbornene molecule via a flexible aliphatic spacer.[5, 32] Synthesis of the monomer commenced with the initial preparation of the alkylated diphenyl compounds 7-[((4'-methoxy-4-biphenyl)yl)oxy]-1-heptanol or 11-[((4'-cyano-4-biphenyl)yl)oxy]-1-undecanol via the nucleophilic substitution reaction of the haloalkan-1-ol with the 4'-hydroxydiphenyl compound. Subsequent reaction with 5-norbornene-2-carbonyl chloride, synthesized via the reaction of 5-norbornene-2-carboxylic acid with PCl_5, in the presence of triethylamine, led to the formation of the norbornene monomers (70-80% yield), as displayed in Scheme 1.4.[5, 32]

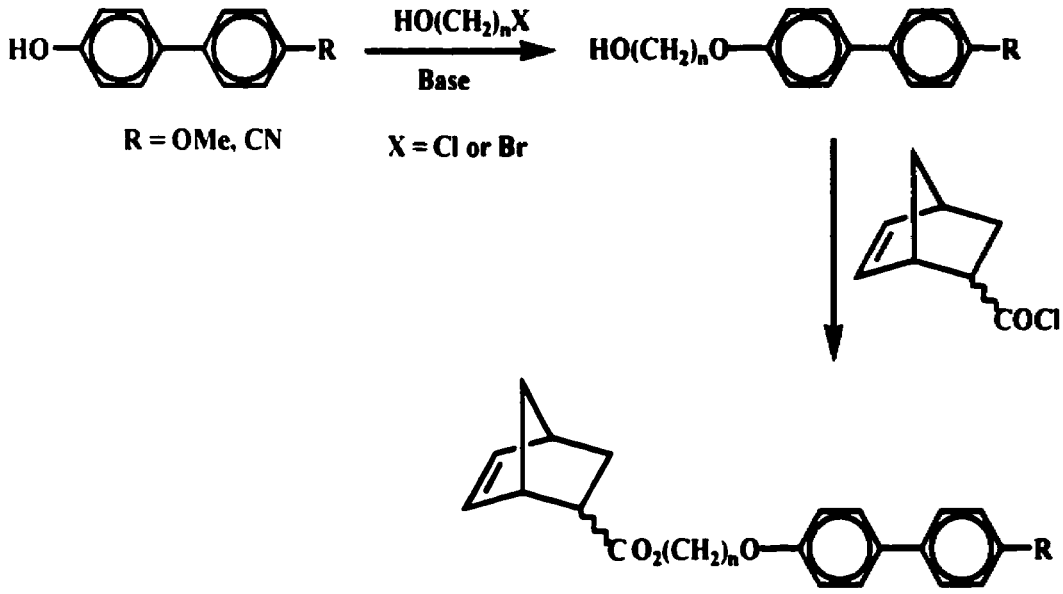

Scheme 1.4

Syntheses of glycopolymers are of vast importance due to the wide range of applications these materials find in biotechnology.[34] Various glycopolymers have found use as binding assays, as chromatographic supports for the separation of proteins demonstrating preference for specific sugar residues, or as cell culture matrices.[34] Most of the carbohydrate-containing polymers prepared thus far have been synthesized via radical polymerization of olefin or acrylamide units that are connected to sugar residues via flexible spacers. Grubbs and Fraser were successful in isolating a glucose-substituted norbornene monomer that was able to undergo ROMP.[34] Their approach towards synthesizing this novel carbohydrate monomer involved the condensation of (±)-*exo*-5-norbornene-2-carbonyl chloride with glucosamine in the presence of triethylamine, shown in Scheme 1.5. This methodology gave the monomeric unit in a 51% yield.

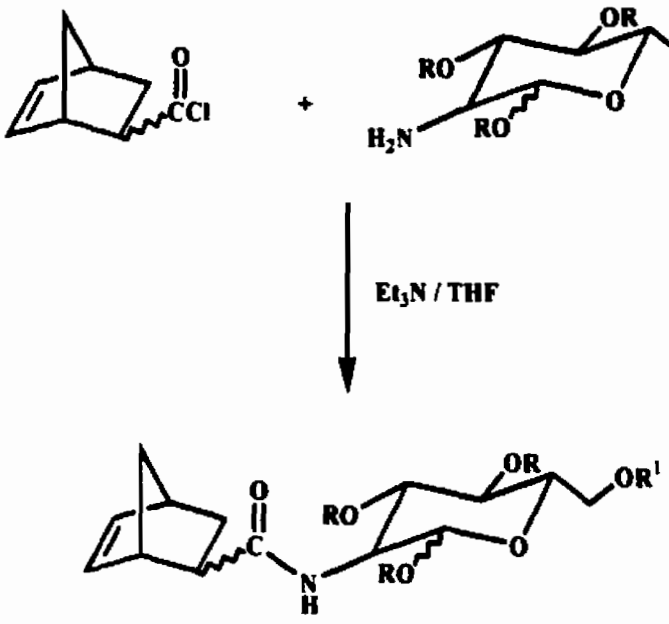

RR^1 = H
$COCH_3$
CH_2Ph
$SiEt_3$
R = H; R^1 = CPh_3

Scheme 1.5

1.2.3 Norbornene Monomers Containing Heterocycles

Limitations of classical metathesis catalysts exist due to their poor ability to polymerize norbornene derivatives containing heteroatoms.[1-3] The main reason for this limitation is that side reactions occur between the heteroatom in the monomer and the ROMP initiator.[35] One of the common side reactions observed involves the cationic ring-opening of the heterocycle. However, since the recent development of more functional-group-tolerant transition metal metathesis catalysts, it is now possible to polymerize norbornene monomers containing various heteroatoms.

Since the late 1970's, numerous reports have detailed attempts to synthesize and polymerize norbornenes functionalized with various heterocycles.[36-44] Norbornene compounds containing oxygen heterocycles were the first monomers to be investigated.[45] Preparation of 5-norbornene-2,3-dicarboxylic anhydride initially by Matsumoto[45] and later by Castner and Calderon,[36] was accomplished by performing a Diels-Alder reaction of cyclopentadiene and maleic anhydride. An interesting finding was that upon attempts to ring-open polymerize this isomeric mixture, only the *exo* isomer was capable of undergoing successful polymerization.[36] Subsequent investigations revealed that the *endo* isomer was completely inert towards metathetic conversion. This selectivity may have been due to deactivation of the catalyst caused by the close proximity of the heteroatom to the site of olefin metathesis and/or by steric restrictions at this location. Using a similar methodology, the *exo* analogue of the dicarboxylic anhydride based upon 7-oxanorbornene was also achieved.[37]

Within the past decade, conversion of the oxygen-containing norbornene heterocycles to their corresponding nitrogen analogues has been achieved. Today, many norbornene monomers exist as variations of functionalized nitrogen heterocycles. Grubbs and coworkers investigated the incorporation of *exo*-*N*-octyl-7-oxabicyclo[2.2.1]hept-5-ene-2,3-dicarboximide as a unit within a triblock copolymer.[39] This monomer was selected due to its hydrophilicity, and was prepared via the reaction of *exo*-7-oxabicyclo[2.2.1]hept-5-ene-2,3-dicarboximide with bromooctane, as shown in Equation 1.2. Isolation of the monomer was achieved in 68% yield.

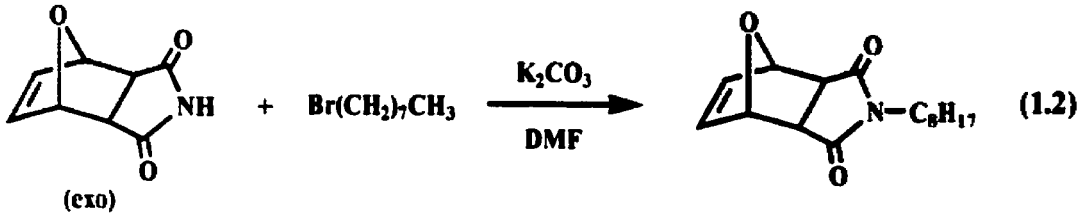

(1.2)

Among the nitrogen-containing norbornene monomers available, one of interest is the product resulting from the reaction of 5-norbornene-2,3-dicarboxylic anhydride with (+) or (-)-alanine methyl ester, as portrayed in Equation 1.3. This work, communicated earlier by Coles *et al* in 1994, is quite remarkable in that the monomer contains a chiral substituent.[46] As a result, polymers prepared from this monomer may eventually find application as templates in the control of polymer design for chiral and molecular recognition applications.

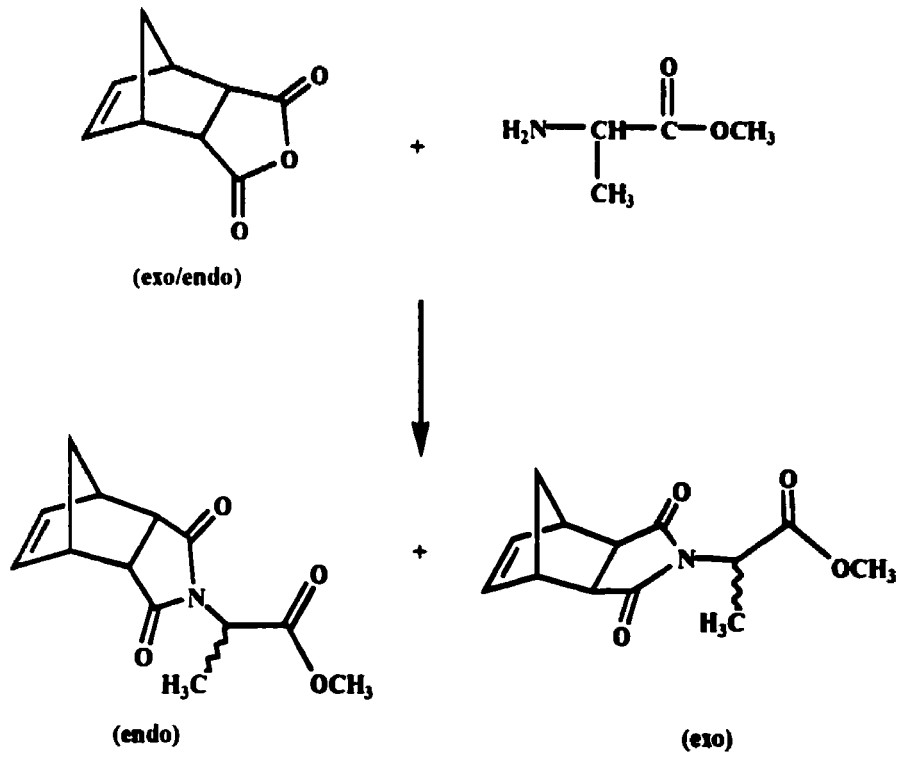

(1.3)

1.3 Overview of ROMP Organotransition Metal Catalysts

There are a number of catalytic systems suitable for initiating ROMP.[1, 2, 19] These may exist as either single component systems or multi-component systems. Of the transition metal initiators capable of facilitating ROMP, W-, Mo- and Re-based systems have proven to be the most active.[1] How a particular catalyst responds to a monomer highly depends on the overall thermodynamics of the reaction as well as on the nature and concentration of the active species. Highly strained monomers, such as norbornene or cyclobutene, release a significant amount of energy upon ring opening. This surge of energy, which is the major thermodynamic driving force behind the reaction, allows for the usage of a wider variety of catalysts with differing reactivity to facilitate ROMP. In contrast, molecules with less ring strain, such as cyclopentene, require a much more reactive catalyst due to the lower amount of energy driving the reaction to completion.

Since many transition metal-based catalysts are available for ROMP, it is impossible to discuss each of them in detail. Four metals have been selected as topics for discussion; Ti, Mo, W and Ru. Other information concerning different catalyst systems can be located within select references listed at the end of this manuscript.[1-4]

1.3.1 Group IVA: Organotitanium Catalysts

As mentioned previously for the ROMP of norbornene, one of the first catalytic systems used to accomplish this synthesis was $TiCl_4/LiAl(n\text{-}C_7H_{15})_4$.[10] With the introduction of the Tebbe reagent to olefin metathesis, (see Equation 1.4), a fundamental

step in the progress of ring-opening polymerizations was made. This was the first catalyst to contain a well-defined metal carbene center.[47] As this carbene center is not readily apparent in the molecular structure, it can be thought as being constructed of two parts; a titanium carbene unit $Cp_2Ti{=}CH_2$ ($Cp = C_5H_5$) and a coordinating Me_2AlCl unit.

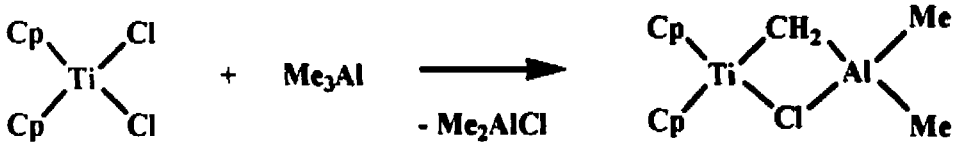

(1.4)

It was not until 1984 that Grubbs and Gilliom reported the very first living ROMP of norbornene using a titanacyclobutane catalyst as shown in Equation 1.5.[48, 49] This was of interest since previous methods for attaining living systems were by cationic, anionic and group-transfer polymerizations.[47]

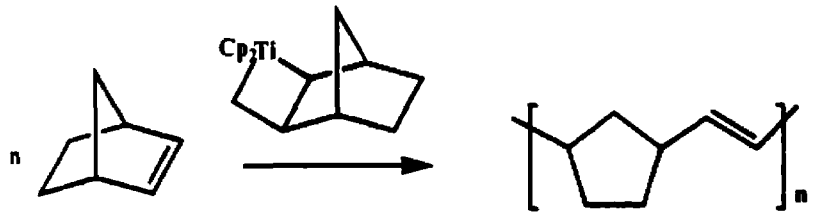

(1.5)

Since a living polymerization had never been previously observed in the ROMP of a bicycloalkene, efforts were made to confirm the living nature of this Ti-initiated polymerization. Results from kinetic studies revealed that the initial step of the reaction involved the ring-opening of the starting metallacycle complex to its corresponding substituted alkylidene.[47, 50] Propagation then followed by reaction of this active precursor with norbornene, as shown in Scheme 1.6. The polymerization indicated a lag or

induction period, displaying a zero-order dependence with respect to the amount of monomer present. This temporary cessation period resulted from the rapid, reversible cleavage of the titanacycle back to norbornene and the titanium methylene complex, termed a non-productive cleavage (**A**). Productive cleavage (**B**), on the other hand, produced a highly unstable diene that readily underwent reaction with available norbornene (**C**). This newly formed trisubstituted titanacycle could further cleave resulting in polymer formation (**D**). Analysis of the mechanism verified the initial ring-opening of the titanacycle as being the rate determining step. This mechanistic pathway was confirmed by an in situ investigation using NMR spectroscopic techniques.

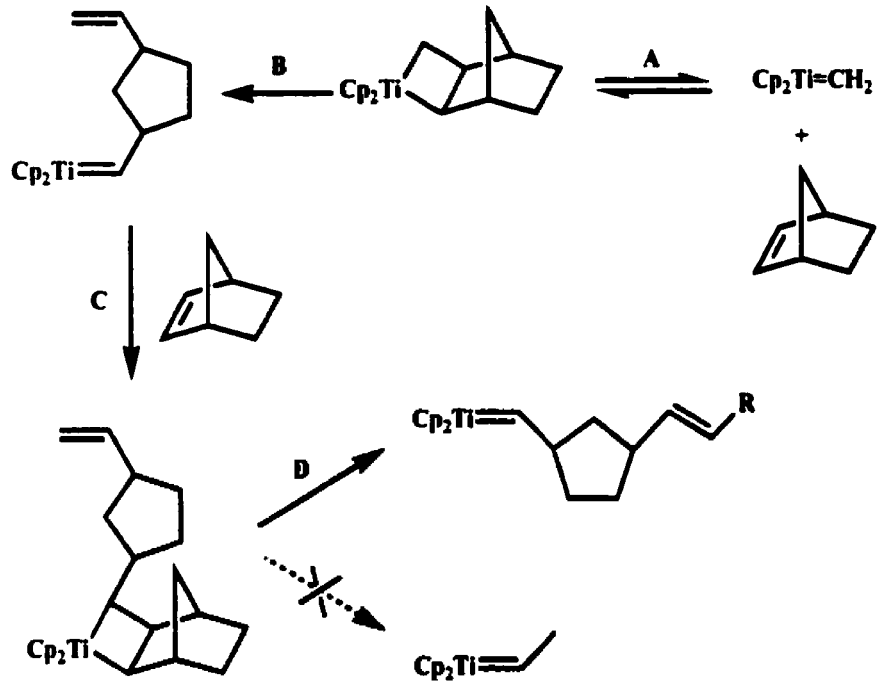

Scheme 1.6

The living nature of these titanocyclobutane catalysts allowed for the preparation of various block copolymers. Cannizzo and Grubbs were successful in preparing an

ABA type triblock copolymer using a series of temperature-controlled initiation, propagation and termination steps. Using this methodology, a triblock copolymer consisting of norbornene (A), cyclopentene functionalized norbornene (B) and norbornene (A) was prepared, as shown in Scheme 1.7.[47, 50, 51] This work was extended to include monomers of the type *endo*, *exo*-dicyclopentadiene, benzonorbornadiene and 6-methylbenzonorbornadiene giving block copolymers having well-defined structures and molecular weights.

Extension of this work involved the incorporation of pre-made polymers into the polynorbornene backbone, through linking at reactive sites within the other polymer. Risse and Grubbs investigated the Wittig-type reaction of polynorbornene capped with titanacyclobutane with various known polymers containing terminal ketones. Scheme 1.8 illustrates an example of such a "graft copolymer," containing a poly(ether ketone) in the backbone of the chain with pendent polynorbornene side chains.

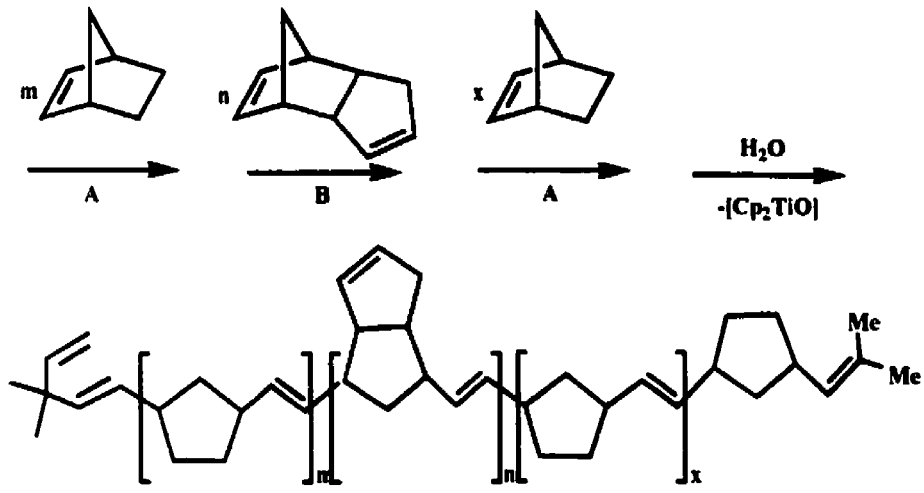

Scheme 1.7

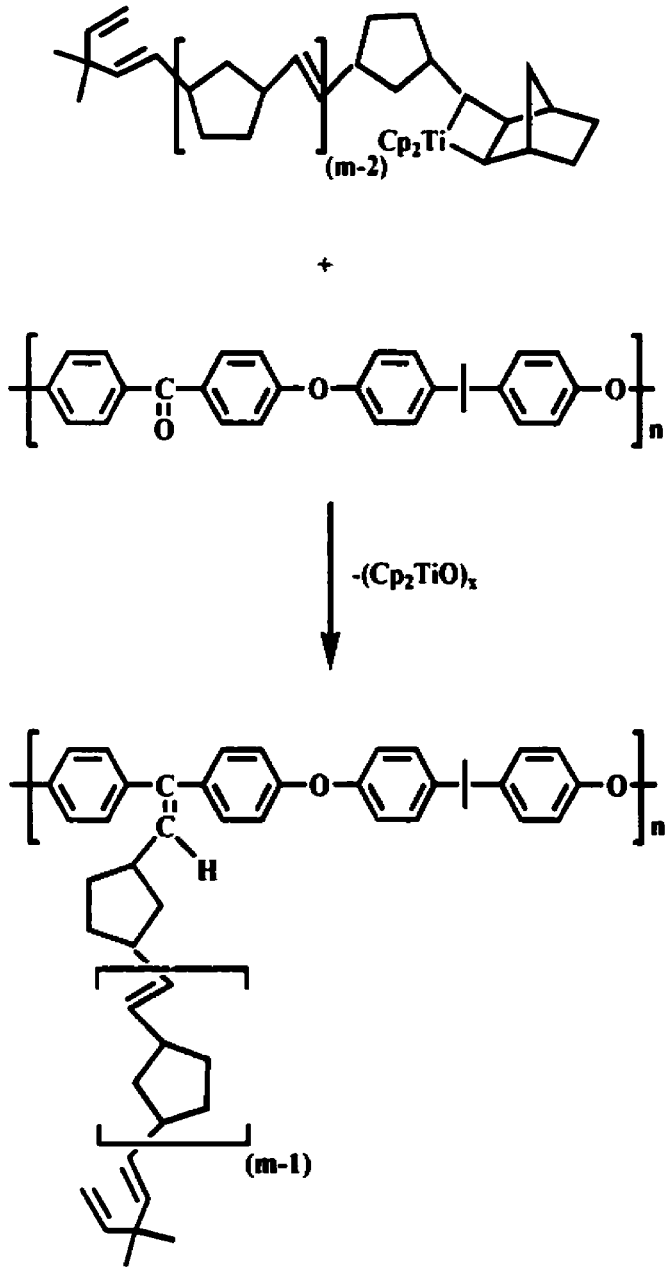

Scheme 1.8

1.3.2 Group VIA: Molybdenum and Tungsten Catalysts

1.3.2.1 Molybdenum Alkylidene ROMP Initiators

Recent advances in the design of ROMP initiators have led to the discovery of several highly active metathesis catalysts based on molybdenum and tungsten.[1] In comparison to tungsten, molybdenum demonstrates superior functional group tolerance due to its less oxophilic nature, and in general, has been found to have higher reactivity.[1] Intermediate Mo alkylidenes also seem to demonstrate greater resistance towards decomposition and side reactions than the W analogues.

Schrock has made significant contributions to olefin metathesis with his work on the synthesis of molybdenum and tungsten alkylidene catalysts.[38, 52-55] In the early 1990's, he established one of the first molybdenum alkylidene catalysts suitable for the living ROMP of ester, cyano, acetate and other functionalized norbornenes and norbornadienes.[52] This complex, $Mo(CH\text{-}t\text{-}Bu)(NAr)(OR)_2$ [Ar = 2,6-diisopropylphenyl], initiates living polymerization such that the resulting polymeric material is essentially monodisperse (PDI=1) and highly stereoregular. Changing the alkoxide ligands has shown to greatly influence the overall activity of the catalyst.[38, 52] When R is *t*-butyl, the catalyst not only demonstrates enhanced functional group tolerance, but also becomes more selective, allowing the metathesis reaction to occur only at the olefinic region in the monomer and not at the polynorbornene backbone.[52] This is advantageous in that no chain transfer or termination steps occur, resulting in the formation of a living polymer.

Several other molybdenum-based catalysts synthesized by Schrock and coworkers of the type $Mo(CHCMe_2R)(NAr)(O\text{-}t\text{-}Bu)_2$ where Ar = 2,6-C_6H_3-*i*-Pr_2 and R = CH_3, C_6H_5 revealed that when R = C_6H_5, the catalyst is more active.[53] As with the previously described Mo catalyst,[38, 52] these initiators are capable of producing high stereoregularity in polymers with narrow polydispersities. Interest in these initiators resulted from the desire to polymerize various analogues of 7-oxanorbornadiene. Initial attempts to polymerize these monomers were unsuccessful, however, they were able to isolate the intermediate metallacycle, which proved to be incredibly stable (see Scheme 1.9). Since there was no evidence indicating stabilization through a direct interaction between the metal and the oxygen atom contained within the norbornadiene bridge, it was proposed that this stabilization resulted from the ability of 7-oxanorbornadiene metallacycles to stabilize themselves through inductive effects. Furthermore, as the intermediate species had not been isolated in other Mo alkylidene systems, part of this stability was attributed to the influence of the ligands on the catalyst. Previous investigations indicated that large groups in close proximity to the metal center lead to stabilization of the intermediate.[38] Since the initiator used in this study contained a bulky dimethylphenylmethyl alkylidene, this could have contributed to the metallacycle stabilization. Full characterization of these intermediate metallacycles was accomplished using NMR and X-ray crystallographic techniques.

Successful polymerization of these monomers, without isolation of the intermediate metallacycle was eventually accomplished by changing the catalyst to $Mo(CHCMe_2Ph)(NAr)(OCMeCF_3)_2$. It was proposed that the better electron-withdrawing ability of the fluorine containing alkoxide ligands greatly reduced the

stability of the intermediate metallacycle, thus allowing a facile conversion from monomer to polymer.

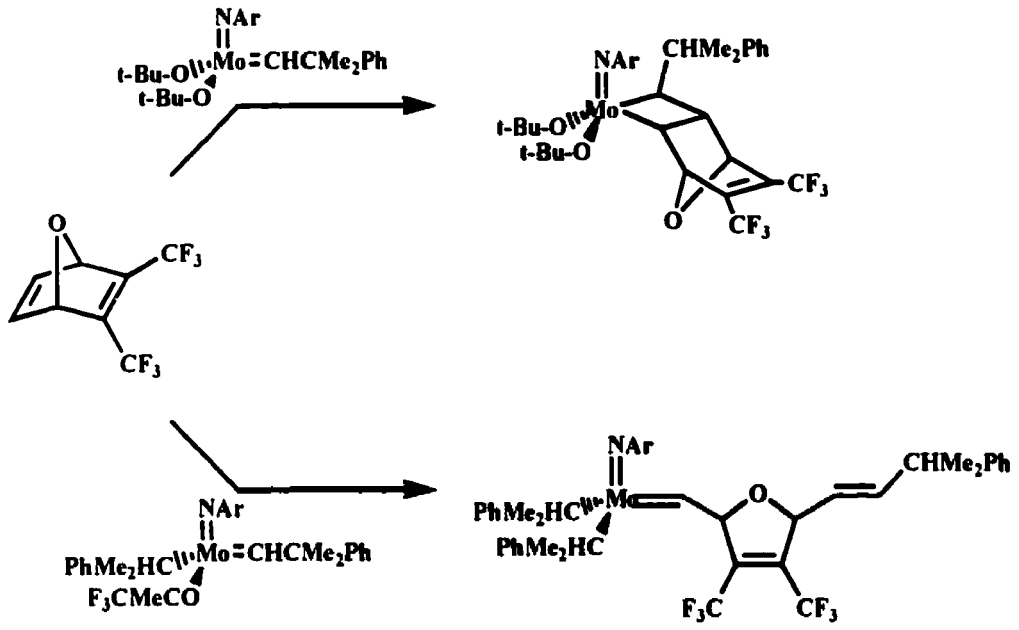

Scheme 1.9

It has only been within the past five years that the mechanism of ROMP involving Mo alkylidene systems has begun to be understood. This has proven to be crucial as it allows for the prediction of the polymer microstructure; cis/trans geometry and tacticity. Previous studies have shown that polymerizations of 2,3-bis(trifluoromethyl)norbornadiene (NBDF6) and 2,3-dicarbomethoxynorbornadiene (DCMNBD), initiated by $Mo(CHCMe_2R')(NAr)(OR)_2$, (R' = Me, Ph; Ar = 2,6-*i*-Pr_2-C_6H_5), yields polymeric materials which have a controlled tacticity and are highly trans when OR = O-*t*-Bu. In contrast, when OR = $OCMe(CF_3)_2$, the polymers demonstrated high cis stereoregularity with only a 75% tacticity bias. It can be concluded that cis/trans

selectivity of these Mo initiators is highly dependent on the nature of the coordinating ligands.[54-56]

Another factor influencing the structural features of the resulting polymer arises from the two conformers of the catalysts, which have previously been reported as the *syn* and *anti* rotamers. The appearance of this rotameric conformation may not be obvious upon immediate examination of the catalyst. Although the two faces of the Mo=C bond are equivalent in the initiator, they are not equivalent during propagation as a result of the chiral carbon present in the alkylidene ligand. Therefore, each rotamer causes differences in propagation, thus playing an important role in defining the polymer microstructure.

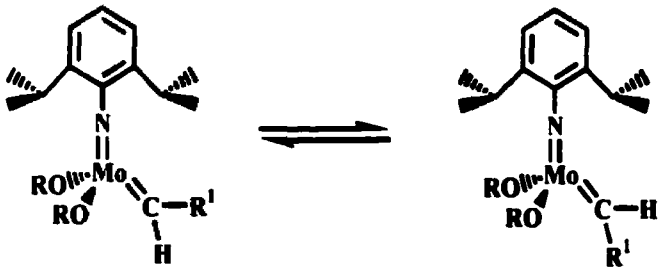

syn **anti**

It has been proposed that a high cis content results when OR = $OCMe(CF_3)_2$, occurring from the systematic propagation of the *syn* rotamer as shown in Scheme 1.10. This corresponds to the facial approach of the monomer to the CNO side of the pseudotetrahedral catalyst such that the methylene group in the monomeric bridge is oriented over the arylimido position, thus aligning the C=C and Mo=C bonds. Ring-opening of the resulting cis metallacycle would then give the cis structural geometry within the polymer as a *syn* insertion product. In contrast, the *anti* rotamer, which is at least two orders of magnitude more reactive than the *syn* rotamer, yields the *syn* insertion product giving the trans geometry.[54, 55]

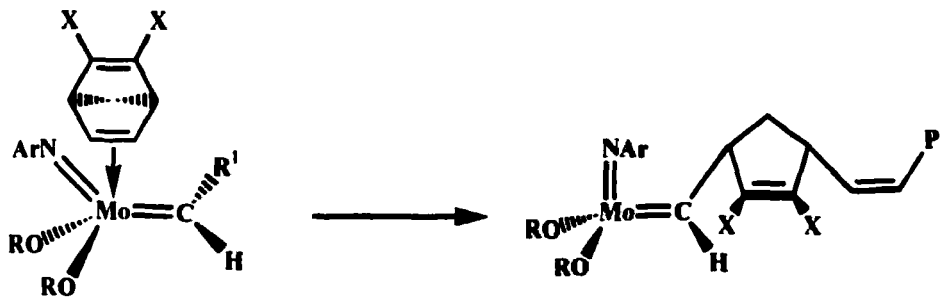

syn

syn + 1

OR = $OCMe(CF_3)_2$
R^1 = CMe_3; CMe_2Ph

Scheme 1.10

1.3.2.2 Tungsten Catalysts: Classical and Alkylidene

Of all the known catalysts, tungsten-based systems comprise the majority due to their high reactivity.[1] Of these initiators, most are classical systems, however, WCl_6 is still widely used due to its high reactivity and functional group tolerance.[57, 58] In the presence of a cocatalyst, which is an organometallic reagent, this initiator forms a stable metal-carbene simply by exchange of ligands and loss of HCl, as illustrated in Equations 1.6 and 1.7. It was not until 1970, however, that this metal-carbene complex, generated from the catalyst-cocatalyst system, was identified as being the reactive component in ROMP.[50, 59]

$$WCl_6 + (CH_3)_4Sn \longrightarrow CH_3WCl_5 + (CH_3)_3SnCl \qquad \textbf{(1.6)}$$

$$CH_3WCl_5 \longrightarrow CH_2{=}WCl_4 + HCl \qquad \textbf{(1.7)}$$

Schrock has reported the synthesis of a series of tungsten alkylidene complexes suitable for living ROMP.[52, 54, 60-64] Scheme 1.11 shows the reaction of 50-200 equivalents of norbornene with W(CH-*t*-Bu)(NAr)(O-*t*-Bu)$_2$ where Ar = 2,6-diisopropylphenyl, which upon termination with benzaldehyde, yields a polymer prepared from the full conversion of the monomer to the polymer.[61] Gel-permeation chromatographic (GPC) analysis revealed that the polymer was essentially monodisperse, having a narrow molecular weight distribution of 1.05. Characterization of the catalyst revealed its high selectivity towards unhindered olefins and its disregard for internal olefinic bonds, or those present within the polynorbornene backbone.

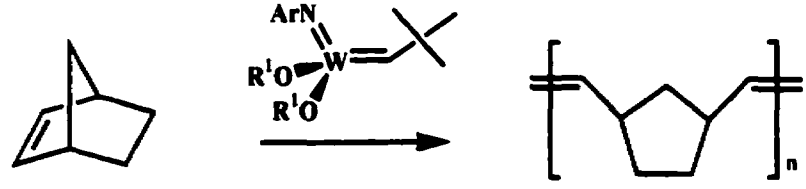

Ar = 2,6-diisopropylphenyl
R^1 = t-Bu; $C(CH_3)_2CF_3$; $CCH_3(CF_3)_2$

Scheme 1.11

As observed for the molybdenum alkylidene systems, changing the coordinating ligands significantly influences the properties of a catalyst.[64] Recalling the tungsten catalyst W(CH-*t*-Bu)(NAr)(OR^1) described earlier, it was observed that upon modification of the alkoxide ligands to more electron-withdrawing groups such as –$OC(CH_3)_2CF_3$ or –$OCCH_3(CF_3)_2$ there was a significant increase in the activity of the catalyst.[50] In fact when –$OCCH_3(CF_3)_2$ was the ligand, the catalyst became so active that

it was able to polymerize acyclic dienes at a rate of over 1000 turnovers per minute. An offset of this was the observed decrease in selectivity for olefin metathesis between the polymeric backbone and the monomer.

An in situ ^1H NMR study of the activity of the initiator containing OR = $-OCCH_3(CF_3)_2$ at -60 °C showed that over the course of the polymerization (several hours), the catalyst slowly broke down until it reached 100% decomposition.[61] Examination of the catalyst stability was then investigated revealing that it decomposed ~10 % a day even while isolated from atmospheric conditions. These results were rather puzzling since the structural conformation of the polymer underwent a dramatic change from originally having a 95% cis geometry to a highly trans geometry when allowed to sit at room temperature for several days. This was attributed to a secondary metathesis of the C=C bonds within the polymer chain, which was explained by the subsequent increase in polydispersity. Based on these results, utilization of this particular W-based catalyst has been limited.

1.3.3 Group VIII: Ruthenium Catalysts

Only recently have group VIII transition metals been used as catalysts for initiating ROMP. A major factor hindering their usage was slow initiation rates resulting in considerably longer reaction times.[35] Of the late transition metal catalysts, those containing ruthenium have demonstrated the most promise as ROMP initiators. Although tungsten and molybdenum catalysts have been found to be more active than the ruthenium systems, they suffer due to their inability to facilitate polymerizations in

aqueous, protic or oxygenated environments. Thus, ruthenium initiators are advantageous in that they have greater applications industrially due to more favorable reaction conditions. Ruthenium-based systems also exhibit greater functional group tolerance, allowing the polymerization of a wider variety of substituted cyclo- and bicycloalkenes.

1.3.3.1 Ruthenium Trichloride (Hydrate)

In 1988, Novak and Grubbs reported the first aqueous polymerization of 7-oxanorbornene derivatives using $RuCl_3$·(hydrate) in the presence of air.[65] This was a remarkable contribution towards olefin metathesis in that polymerizations until that time generally required the presence of an inert atmosphere. In an attempt to reduce initiation periods from the 22-24 h period, as was observed in the organic reactions, water was added to the organic solvent system, which rapidly decreased the initiation period to 35 min. Rather than deactivating the catalyst, the water behaved as a cocatalyst, significantly decreasing the time required for initiation. In addition, it was noticed that product yields increased substantially. Polymerizations in purely aqueous environments also demonstrated a high conversion of the monomer to the polymer, with even faster initiation periods. Analogous findings using aqueous/organic media to facilitate ROMP of other cyclic olefins with $RuCl_3$·(hydrate) have been reported which are in agreement with these results.[66]

As a means to make a particular methodology favorable towards industrial standards, it is important to make it as cost-efficient as possible. With this in mind,

Novak and Grubbs recovered the $RuCl_3$·(hydrate) from the aqueous polymerization reaction and used it in a subsequent reaction. During the second ROMP reaction, initiation times were notably shorter, and when used again in a third polymerization, initiation rates decreased from 35 minutes to 10-12 seconds. Reports have shown that recycled $RuCl_3$·(hydrate) maintains its degree of activity when used up to 14 consecutive times.[45]

Although $RuCl_3$·(hydrate) is still used in ROMP,[27] as with most classical systems, it is unable to produce living polymerizations. It was not until the contributions of Grubbs and coworkers that the successful preparation of a variety of well-defined ruthenium carbene catalysts capable of facilitating the living ROMP of cyclo- and bicycloalkenes was achieved.

1.3.3.2 Ruthenium Alkylidene and Benzylidene Catalysts

In 1992, Grubbs and coworkers reported the preparation of a ruthenium alkylidene complex capable of polymerizing norbornene in both organic media and aqueous solvent systems.[67] This catalyst, identified as $(PPh_3)_2Cl_2Ru{=}C{=}CPh_2$, is stable for several weeks in organic media under an inert atmosphere, however, upon exposure to air, its lifetime rapidly reduces to a few minutes. Interestingly, this initiator is stable in a CH_2Cl_2/C_6H_6 solution in the presence of water, alcohol, or a diethyl ether solution of HCl. It was then established that this initiator had a greater tolerance towards opening a wider variety of functionalized monomers than other known alkylidene systems. Further

investigations revealed its ability to undergo reactions with ketones and aldehydes, of which the Mo and W alkylidene catalysts are incapable of tolerating.[67]

A year later, two analogues of this Ru alkylidene catalyst were reported having greater metathesis activity than $(PPh_3)_2Cl_2Ru{=}C{=}CPh_2$.[68] These were similar in structure to the original complex, differing only by the type of phosphine ligands attached to the ruthenium center. One was the tricyclohexylphosphine (Cy_3P) derivative whereas the other contained triisopropylphosphine [(i-Pr)$_3$P] ligands. Both analogues of this ruthenium alkylidene complex demonstrated similar stabilities toward functional groups and solvent systems as previously described for $[(Ph_3P)_2Cl_2Ru{=}CHCH{=}CPh_2]$. A significant difference existed for the individual reactivities of these initiators. Although the tricyclohexylphosphine derivative exhibited greater activity than the triphenylphosphine derivative, it suffered from relatively long initiation periods, which was identified in the broad molecular weight distribution of the resulting polymer.[68] Despite the high PDI's, this catalyst warranted further investigation since it demonstrated superior activity in the polymerization of cycloalkenes with low ring strain.

Based upon these findings, it was of interest to determine how the nature of the phosphine ligands influenced activation at the carbene site. As these phosphine ligands are bulky and good electron-donating groups, it was proposed that their influence could be steric and/or electronic. Steric effects were readily discarded based upon findings that the differing cone angle between the (Cy_3P) and [(i-Pr$_3$)P] ligands of 10 ° did not influence catalytic activities at all. Therefore, it was concluded that carbene activation was mostly based upon the electron-donating ability of the phosphine ligands in the catalyst structure.[68]

A study done in 1997 by Dias, Nguyen and Grubbs compared and contrasted the unique features of Ru alkylidene catalysts based on the structure $(PR_3)_2X_2Ru{=}CHCH{=}CPh_2$.[69] The general trend observed for increasing catalytic activity for PR_3 groups was: $PPh_3 << P^iPr_2Ph < PCy_2Ph < P^iPr_3 < PCy_3$. Furthermore, when the halide (X) was Cl, the catalyst demonstrated much greater activity than if it were Br or I. It was concluded from this investigation that greater catalytic activity is achieved when larger, better electron-donating phosphine groups are used in conjunction with smaller, more electron-withdrawing halogens. Although the above ruthenium initiators demonstrated a high level of olefin metathesis activity, they faced limitations due to their slow rates of initiation, resulting in broad PDI's.

Around the same time that these alkylidene complexes were being investigated, the construction of what is now one of the most widely used catalyst systems for ROMP was taking place.[70] Ruthenium catalysts of the type $(PR_3)_2Cl_2Ru{=}CHPhX$ were being developed with R = Ph; Cy and X = H; Cl. Through a series of investigations, it was determined that bis(tricyclohexylphosphine)benzylidene ruthenium(IV) dichloride, $(PCy_3)_2Cl_2Ru{=}CHPh$, demonstrated remarkable activity as a ROMP initiator, proving to be even greater than the vinylcarbene complexes. In a subsequent study, the corresponding triphenylphospine system was compared to the tricyclohexylphosphine derivative.[71] The former was found to polymerize at a rapid rate of ~150 equivalents per hour in dichloromethane at room temperature yielding almost exclusively the trans polymer (90%) and giving narrow PDI's (1.04 – 1.10).[70] Tricyclohexylphosphine benzylidene catalysts demonstrated similar characteristics to those of the triphenylphosphine derivatives with the exception of displaying better catalytic activity,

being air-stable in the solid state, and showing no signs of decomposition in organic solvents at 60 °C, or in the presence of protic solvents.

Aqueous polymerizations of functionalized norbornene monomers employing the more active Ru[PCy_3] benzylidene catalyst, required fairly strict reaction conditions in order for successful ROMP to be achieved.[43] Polymerizations were carried out in the presence of an emulsifying agent, dodecyltrimethylammonium bromide (DTAB), which served to deoxygenate the water that the monomer was dispersed in. Polymerization began upon the addition of catalyst dissolved in a minimal amount of organic solvent, either dichloromethane or dichloroethane. Solvent mixtures of 5:1 water:organic media were used as dictated by the solubility of the catalyst in the organic solvent. This method enabled the controlled initiation and isolation of well-defined polymers. In comparison to polymerizations done in purely organic environments, this methodology suffered from lower molecular weights and yields, with no change in the PDI. Increased reaction times, however, enabled for complete monomer consumption thus significantly improving molecular weights and polymer yields comparable to the organic reactions, while maintaining narrow PDI's.

The living nature of this initiator in aqueous environments was explored and confirmed via the successful preparation of homopolymers and copolymers, as illustrated in Scheme 1.12. Since this report, another study performed by Grubbs and coworkers detailed the homogeneous living ROMP in water of a water soluble analogue of the Ru[PCy_3] initiator.[72]

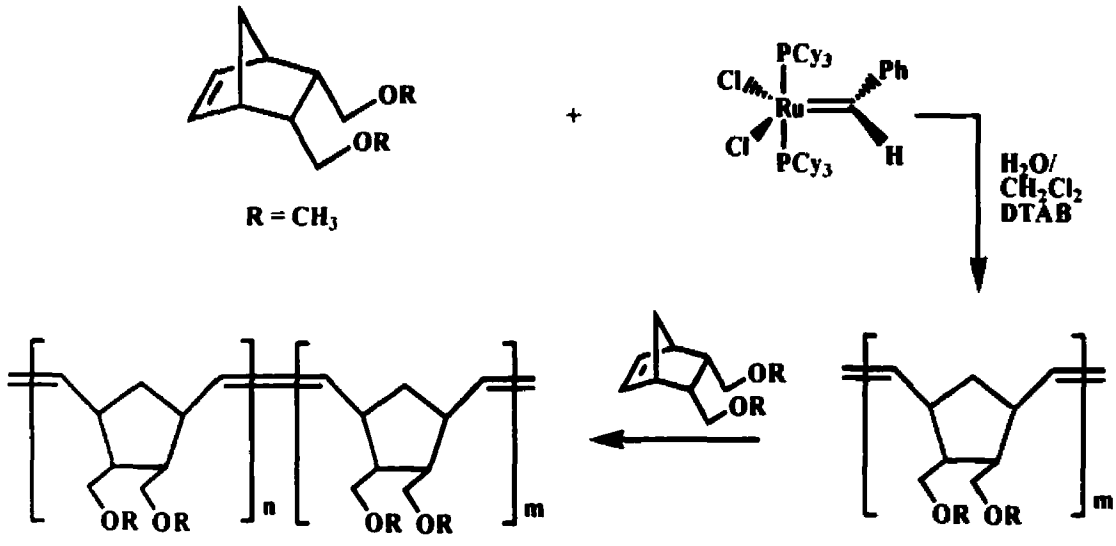

Scheme 1.12

Various binuclear ruthenium bisalkylidenes have also been prepared as catalysts suitable for initiating ROMP, of the structure $(PR_3)_2Cl_2Ru{=}CPhCH{=}RuCl_2(PR_3)_2$, where R = Ph, Cy or Cyp (cylopentyl).[39] It was found that when R = Ph, the system was ineffective in the polymerization of functionalized 7-oxanorbornenes. However, when R = Cy or Cyp, a wide variety of functionalized norbornene and 7-oxanorbornene derivatives could be polymerized in a living fashion in greater than 98% yield. Of these systems, the complex containing the cyclopentyl groups demonstrated superior ability in attaining narrow molecular weight distributions. No studies have yet been reported indicating the effectiveness of these complexes in aqueous or oxygenated environments.

A final related topic of interest is the recent report by Dias and Grubbs detailing the synthesis and characterization of several homo- and heterobimetallic ruthenium complexes, which have been reported to improve ROMP activity.[73] This study was

initiated upon careful examination of the ROMP mechanism which involves a preequilibrium step consisting of olefin binding and phosphine dissociation (Scheme 1.13). This step is so slow that it hinders the metathesis reactivity of the catalyst. CuCl, which is a phosphine scavenger, was employed as a means to enhance reaction conditions, however, its poor solubility in organic solvents has limited its use. Therefore, Dias and Grubbs focused on building catalysts containing only one phosphine ligand as well as a labile group that would ease the dissociation process. These systems, shown in Figure 1.0, have relative rates (k_{rel}) reported for the ROMP of 1,5-cyclooctadiene.[73] The general trend observed for catalytic activity was an increase in the order of Ru < Ru-Ru < Ru-Os < Ru-Rh, with the benzylidene derivatives demonstrating greater initiation than the vinyl alkylidenes. Although the Ru-Ru system has been reported to be effective in the ROMP of 7-oxanorbornene derivatives, no detailed information has yet been reported.

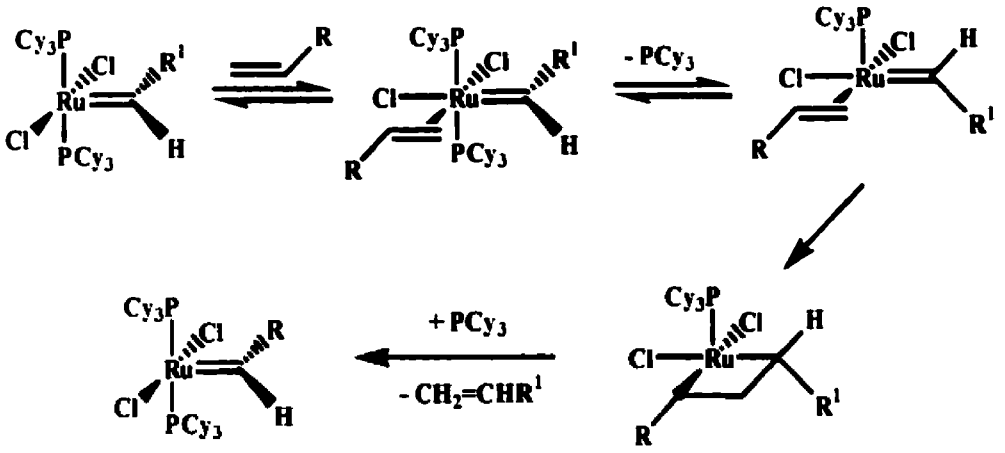

Scheme 1.13

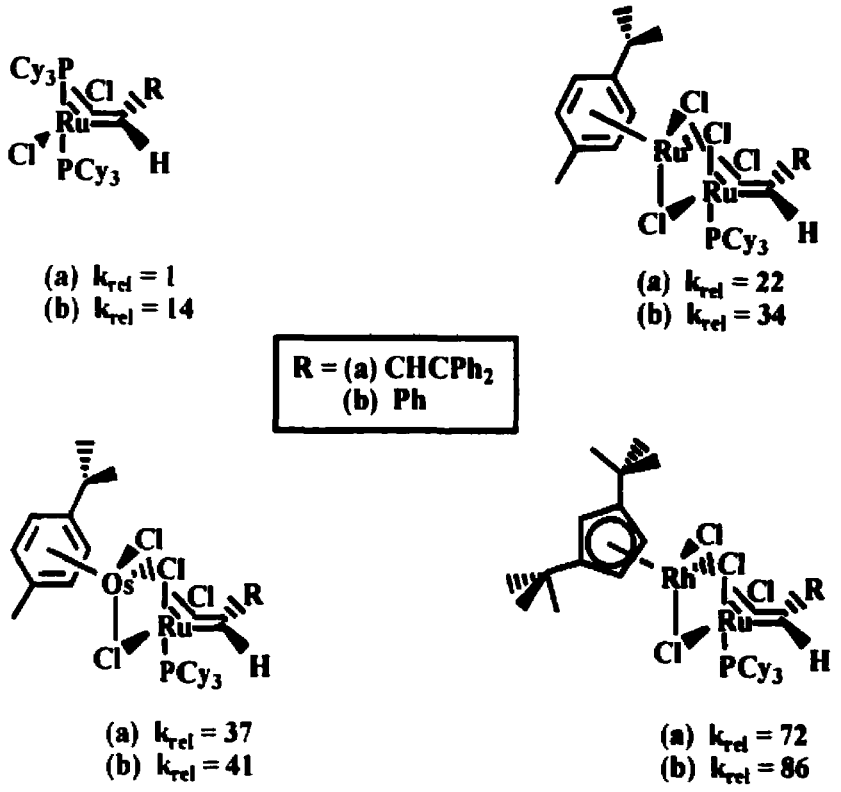

Figure 1.0: Rates of olefin metathesis for various homo- and heteronuclear ruthenium catalysts based on ROMP of 1,5-cyclooctadiene.

1.4 Reactivity of Complexed Arenes

Temporary complexation of a metal moiety to aromatic compounds has allowed for considerable advancements to be made in the role organometallic chemistry has in the production of novel aromatic compounds.[74-78] Upon complexation of a metal moiety, its ability to behave as an electron-withdrawing group allows the ring to become activated towards several modes of functionalization.[74-77] Of these pathways, nucleophilic addition and substitution reactions are the most common. Oxidation of a methyl substituent(s) on

the aromatic ring to its corresponding carboxylic acid is another possible route towards functionalization, however, this route has been much less explored.

Coordination of a metal to an arene allows activation of the organic compound through the π-coordinated electron-withdrawing ability of the transition metal.[74] Studies have shown that arenes coordinated to $(CO)_3Cr$, $CpFe^+$ (Cp = cyclopentadienyl), $CpRu^+$ or $(CO)_3Mn^+$ suppresses the ring's ability to undergo reactions with electrophiles and encourages nucleophilic attack.[76] Kinetic studies on the rate of nucleophilic aromatic substitution determined that $(CO)_3Mn^+ > CpRu^+ \equiv CpFe^+ >> (CO)_3Cr$.[79, 80] Despite the higher activation obtained when using $(CO)_3Mn^+$, its use is somewhat limited due to its high cost and degree of toxicity. As $CpRu^+$ and $CpFe^+$ behave quite similarly in terms of their arene activating abilities, selection of iron over ruthenium resulted from its lower cost and ability to readily undergo complexation and decomplexation under mild reaction conditions.

The first documented synthesis detailing the coordination of an arene to the cyclopentadienyliron moiety ($CpFe^+$) was achieved by Coffield and coworkers in the late 1950's whereby they reacted cyclopentadienyliron dicarbonyl chloride with mesitylene to give the η^6-mesitylene-η^5-cyclopentadienyliron(II) salt.[81] This methodology has seen only limited application, however, due to poor product yields and the inability of the metal moiety to coordinate to some arenes. In 1963, Nesmeyanov and coworkers reported the first synthesis of a cyclopentadienyliron complexed arene via the replacement of one of the cyclopentadienyl rings of ferrocene by an arene.[82-85] This ligand exchange reaction liberated an arene cyclopentadienyliron cation as its

tetrafluoroborate, hexafluorophosphate or tetraphenylborate salt, as described in Equation 1.8.[86-89]

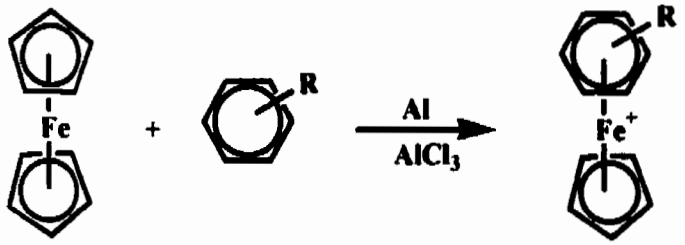

(1.8)

Several years ago, a report was published detailing the novel synthesis of (arene)$CpFe^+$ complexes utilizing microwave dielectric heating.[90, 91] Advantages of using this new methodology include higher product yields (53-99%) and shorter reaction times (from 4-6 h to 4 min). Unlike the conventional methods, this route allows the preparation of various halogenated arenes and arylamines in exceptional yields.

It is well known that electron-withdrawing groups on an arene activates the ring towards nucleophilic attack. This was first demonstrated by Nicholls and Whiting in their investigations of the S_NAr of chloroarene $Cr(CO)_3$ complexes with various methoxy nucleophiles.[92] It was not until 1967 that Nesmeyanov and coworkers reported the use of the $CpFe^+$ moiety as an electron withdrawing group in the activation of haloarenes towards a variety of nucleophiles.[93] It was observed that for complexes of the type $[XC_6H_5Fe^+Cp]$ where X = F or Cl, attack by various O, S and N nucleophiles was possible. Subsequent kinetic investigations revealed that when X = Cl, the complex demonstrated almost equal activity as the 2,4-dinitrochlorobenzene derivatives.[94]

2.0 Design of Polynorbornenes Containing Pendent Aryl Ether Side Chains

2.1 Introduction

Over the last several years, significant interest has developed in polynorbornenes as materials for high temperature applications. Polynorbornenes fused to heterocycles, especially those being dicarboxyimides, offer some of the highest thermal stabilities for these types of materials.[41, 42, 44, 58] Since functionalization of the polynorbornene backbone is known to influence the thermal behavior of the resulting polymer, a large number of polynorbornenes are being investigated, with much attention being focused on their thermal properties.[6, 7, 32, 42] Current investigations are also exploring the incorporation of nitrile and ester functionalities into the monomeric design, as these have been reported to improve the overall thermal properties of the resulting polymers.[1-3, 32, 33]

Among the most thermally stable polymers available are poly(aromatic ethers) which constitute a class of polymers known as "engineering thermoplastics".[95-97] Therefore, it was of interest to functionalize the polynorbornene backbone with these groups in an attempt to improve the thermal properties. In addition, polymers were designed containing an ester bridge linking the pendent aromatic chain to the norbornene unit since the incorporation of an ester group leads to enhanced thermal stability.[1-3]

2.1.1 Preparative Methods of Poly(aromatic ethers)

A number of different routes exist for synthesizing both long and short chain aromatic ethers. These consist of the Ullman polymerization,[95, 96] conventional nucleophilic aromatic substitution reactions,[97, 98] coupling reactions [99, 100] and metal-mediated nucleophilic aromatic substitution reactions.[101-108] As this body of work utilizes metal-mediated complexation for the preparation of aromatic ether side chains, this section will be discussed in greatest detail.

2.1.1.1 Ullman Polymerization

In 1904, the Ullman ether synthesis was reported detailing the formation of diaryl ethers with the assistance of a copper salt.[96] A typical Ullman condensation involves the reaction of a sodium or potassium phenoxide salt with an unactivated aryl halide at 100-300 °C. Addition of a copper salt to the reaction vessel (copper halide or copper oxide) has been shown to catalyze the reaction. Of these, copper oxide demonstrates the greatest degree of reactivity.[95, 96]

A slight modification of this methodology has lead to the formation of longer chain aromatic ethers, which was not possible using conventional Ullman reaction conditions.[95] Equation 2.1 illustrates the synthesis of a poly(1,4-phenylene oxide) derivative prepared via the reaction of the sodium salt of bisphenol-A and 4,4'-dibromobiphenyl in the presence of a copper catalyst. A cuprous chloride – pyridine catalyst works best in these reactions.

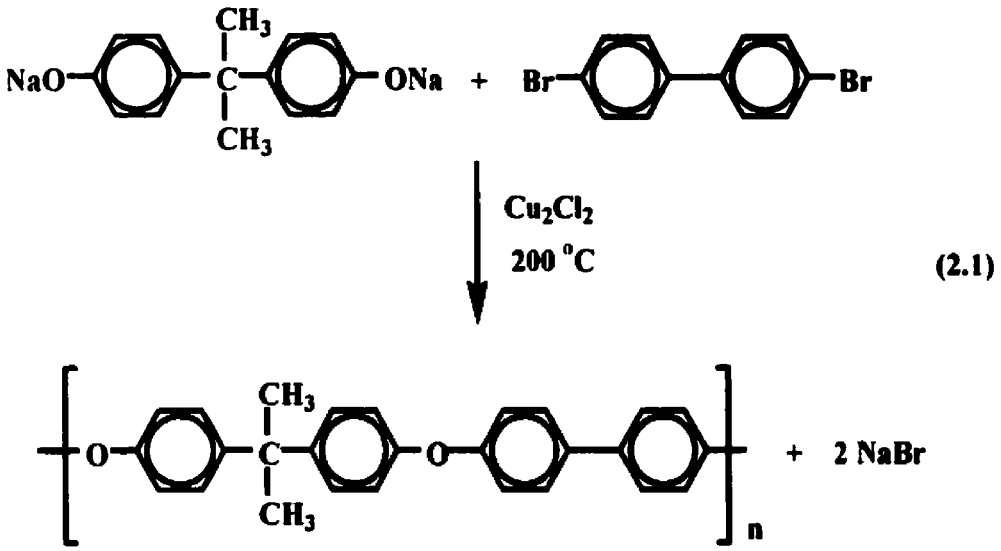

(2.1)

2.1.1.2 Nucleophilic Aromatic Substitution

Poly(aryletherketones) (PAEKs) constitute a class of thermally stable engineering thermoplastics.[95] These materials have found potential application as electrical insulators for high-performance wiring, in the production of flame, hydrolytic and solvent resistant materials and in the construction of films, fibers, moldings and coatings.[95] One common, commercially available PAEK is PEK, or poly(etherketone), which can be synthesized by reacting the potassium salt of 4,4'-dihydroxybenzophenone with 4,4'-difluorobenzophenone in the presence of dimethyl sulfoxide or sulflane, as shown in Equation 2.2. These polymerizations are now performed in diphenyl sulfone at 300 °C, yielding polymers with much higher molecular weights.

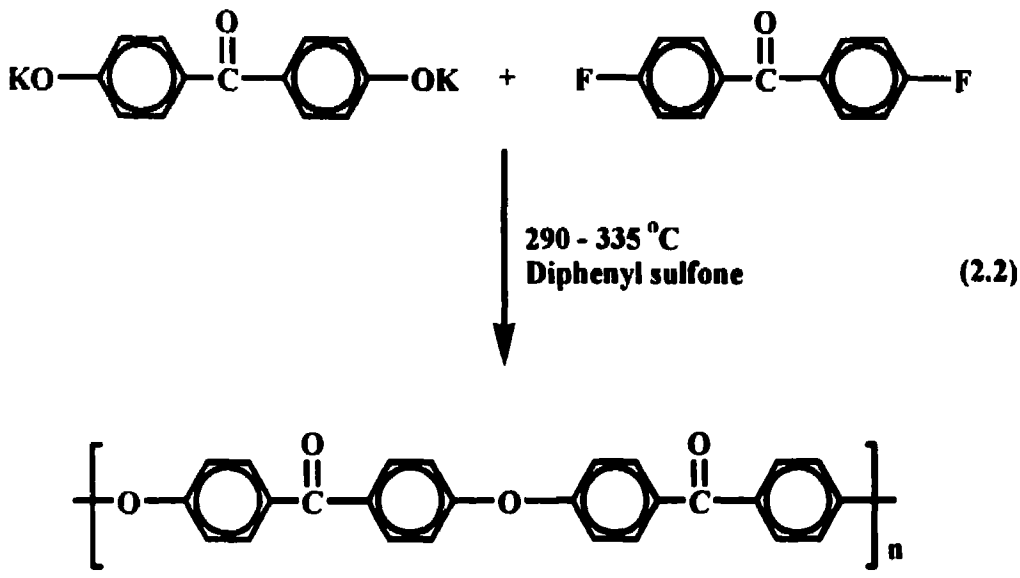

The reactivity of a S_NAr polymerization is highly dependent upon the nature of the alkali metal used in the preparation of the phenate and the nature of the halide contained in the halogenated monomer as well as on the strength of the electron-withdrawing group.[95] The following trend has been reported for alkali metal influence on reactivity; Cs > K > Na > Li. Generally, potassium is used as it is less expensive than Cs, while maintaining a high reactivity. Aryl halide reactivity is observed in the order of F >>> Cl > Br > I.[95] This substantial increase in reactivity upon changing the halogen from chlorine to fluorine, was demonstrated by the reaction of two different aryl halides with phenoxide, in which the aryl fluoride proved to be one hundred times more reactive than the aryl chloride when both were activated by a keto group.[95] As a result, fluorinated arenes are commonly used in the preparation of PAEKs, which is attributed to the greater leaving ability of the fluoride ion. The activating ability of the electron-withdrawing groups used to prepare various aromatic ethers decreases in the order of $NO_2 \sim SO_2 > CO > N{=}N$.[95] In the preparation of PAEKs, fluorine atoms must be present on the aromatic

ring in order to promote the reaction since the keto group is only a mild electron-withdrawing group.

Over the past few years, many derivatives of PAEKs have been prepared.[95] Most of the modifications made in these systems, have involved the reaction of 4,4'-difluorobenzophenone with various dinucleophiles, especially analogues of bisphenol.[97] Wang and coworkers have recently reported the synthesis of various phenylene- and mixed phenylene-naphthalene-containing poly(etherketones), as shown in Figure 2.0.[97, 98] Thermal studies of these mixed systems demonstrated reduced crystallinity, and glass transition temperatures (Tg) 20 - 45 °C higher than the phenylene derivates.[97] This methodology was later used to incorporate two naphthylene units for every repeat unit within the polymer chain.[98]

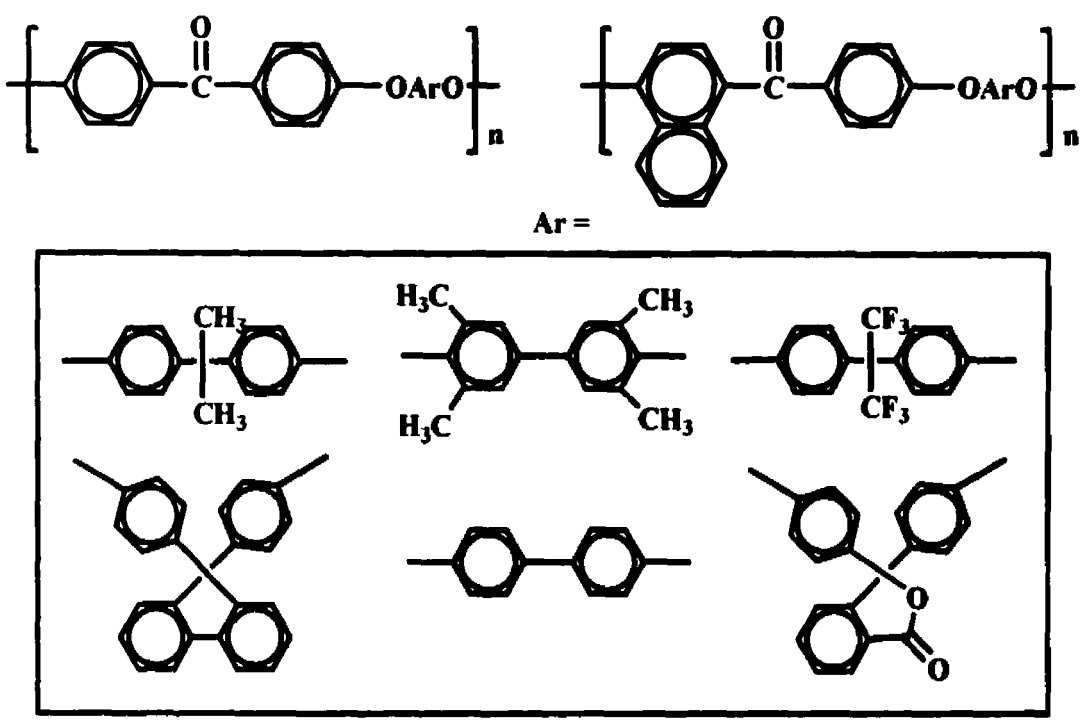

Figure 2.0: Phenylene- and mixed phenylene-naphthylene derivatives of PAEKS.

2.1.1.3 Nickel-Catalyzed Coupling

Another useful method for preparing poly(aromatic ethers) and PAEKs involves the nickel(0) catalyzed coupling of aryl dichlorides. This synthesis involves the elimination of two halogens resulting in the formation of an aryl-aryl linkage.[99, 100] The zero-valent nickel, which is required for this reaction, is prepared from a mixture composed of a nickel salt, triphenylphosphine and an excess of a reducing metal (Mg, Mn or Zn).[99] Of the types of nickel salts capable of attaining this zero-valency nickel chloride and bromide are the most effective.

A typical nickel-catalyzed coupling reaction for the preparation of a PAEK (Equation 2.3) requires the polymer to have a low crystalline nature so that it will remain soluble, which significantly limits the scope of this methodology. Another requirement for these polymerizations involves the selection of monomers containing electron-withdrawing groups, as these tend to improve product yields (with the exception of NO_2 and protic groups), whereas electron-donating groups encourage side reactions.

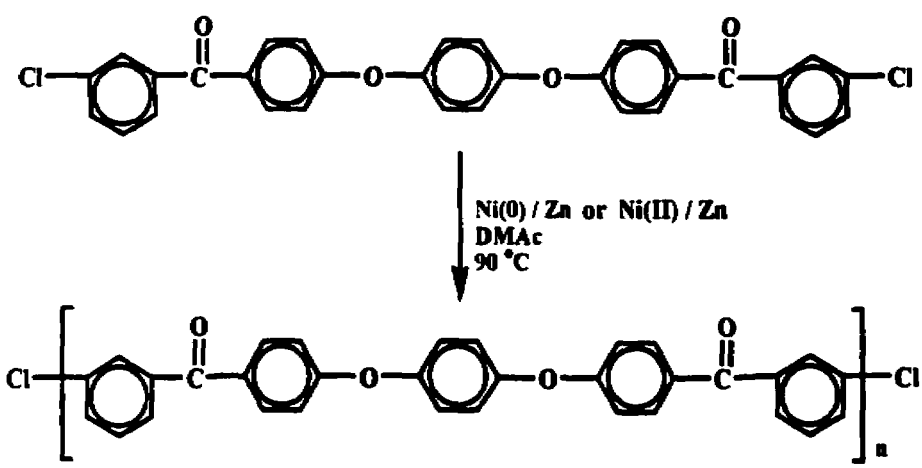

(2.3)

2.1.1.4 Metal-Mediated Nucleophilic Aromatic Substitution

Synthesis of both short and long chain aromatic ethers is possible via $CpFe^+$ mediated S_NAr. Initial, comprehensive studies involving the preparation of symmetric bimetallic aromatic ethers via S_NAr reactions was reported in 1992 by Abd-El-Aziz.[101] This investigation involved the reaction of η^6-chlorobenzene-η^5-cyclopentadienyliron hexafluorophosphate with various aromatic dioxygen nucleophiles [1,2; 1,3; 1,4-dihydroxybenzene and 2,2'; 4,4'-biphenol]. Yields typically ranged from 70-95%. In 1994, a new route towards the preparation and functionalization of these bimetallic diaryl ether complexes was reported using milder reaction conditions, while maintaining high product yields.[102] Scheme 2.1 denotes the wide range of symmetric complexes prepared using this methodology.

This method was extended to prepare asymmetric bis(cyclopentadienyliron)arene complexes.[102, 103] This two step synthesis required the initial preparation of the substituted monometallic complex via the reaction of a substituted chlorobenzene complex with an excess of hydroquinone. The resulting hydroxy monoarylether complex was further reacted in a subsequent step with an equimolar amount of *p*-dichlorobenzene $CpFe^+$ to give the desired asymmetric complexes. This synthesis is illustrated in Scheme 2.2.

Several years ago, Abd-El-Aziz reported the first synthesis of poly(aromatic ethers) containing pendent $CpFe^+$ moieties.[104, 105] Preparation of these novel polymeric materials proceeded by a series of nucleophilic aromatic substitution reactions of both symmetric and asymmetric complexes. Numerous metallated oligomers and polymers

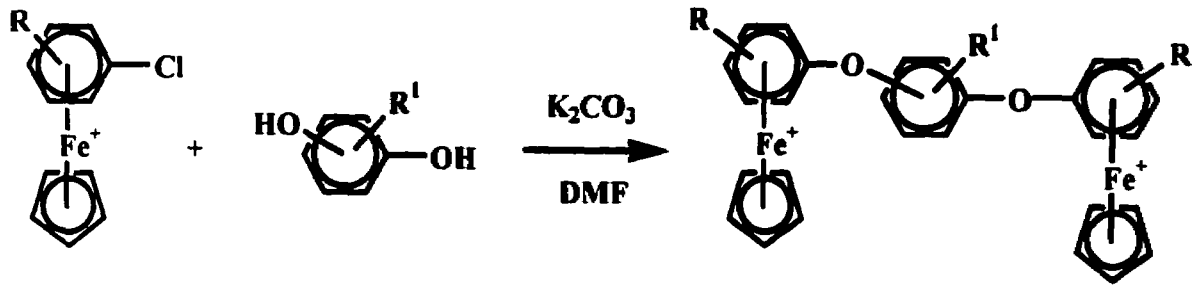

R	R^1
H	H
2-CH_3	H
3-CH_3	H
4-CH_3	H
2-Cl	H
3-Cl	H
4-Cl	H
2,6-$(CH_3)_2$	H; 1,4
H	2-CH_3; 1,3
H	4-C_2H_5; 1,3
H	2-C_6H_5; 1,4
2,6-$(CH_3)_2$	2-C_6H_5; 1,4
H	2-CH_3; 1,4

Scheme 2.1

have been prepared using this stepwise approach, the largest of which contained thirty-five metals pendent to the polymer backbone. An advantage of this method is the increased solubility of the metallated systems, relative to organic poly(aromatic ethers). Due to this increased solubility, these metallated analogues may find potential use due to their greater processability.

Recently, a one-pot synthesis was reported on the synthesis of metallated poly(aromatic ethers), as a direct approach which allows the synthesis of a large variety of polymeric materials complexed to the $CpFe^+$ moiety.[106, 107] The synthesis involves the reaction of the *p*-dichlorobenzene $CpFe^+$ complex with an equimolar amount of the dihydroxy nucleophile, as illustrated in Scheme 2.3. Bisphenol-A or 4,4'-biphenol were used as the dinucleophiles which resulted in isolation of the polymers in 83 and 81% yields, respectively.

Due to the effectiveness of the $CpFe^+$ moiety to facilitate S_NAr reactions, a wide variety of monomeric materials, which cannot be prepared using traditional organic methods, were prepared.[95, 108] Abd-El-Aziz and coworkers recently investigated the synthesis of a variety of metallated compounds capped with naphthoxy groups.[108] Removal of the metal moieties using photolytic techniques liberated the organic building blocks as precursors for polymer synthesis (Scheme 2.4).

These monomers could then be used in the Scholl polymerization, shown in Scheme 2.4, which is another method used for preparing poly(aromatic ethers).[95] This reaction, which proceeds in the presence of a Friedel-Crafts catalyst, can be described as the elimination of two aryl hydrogen atoms at the C-4 positions of terminal naphthoxy groups followed by the formation of an aryl-aryl bond.

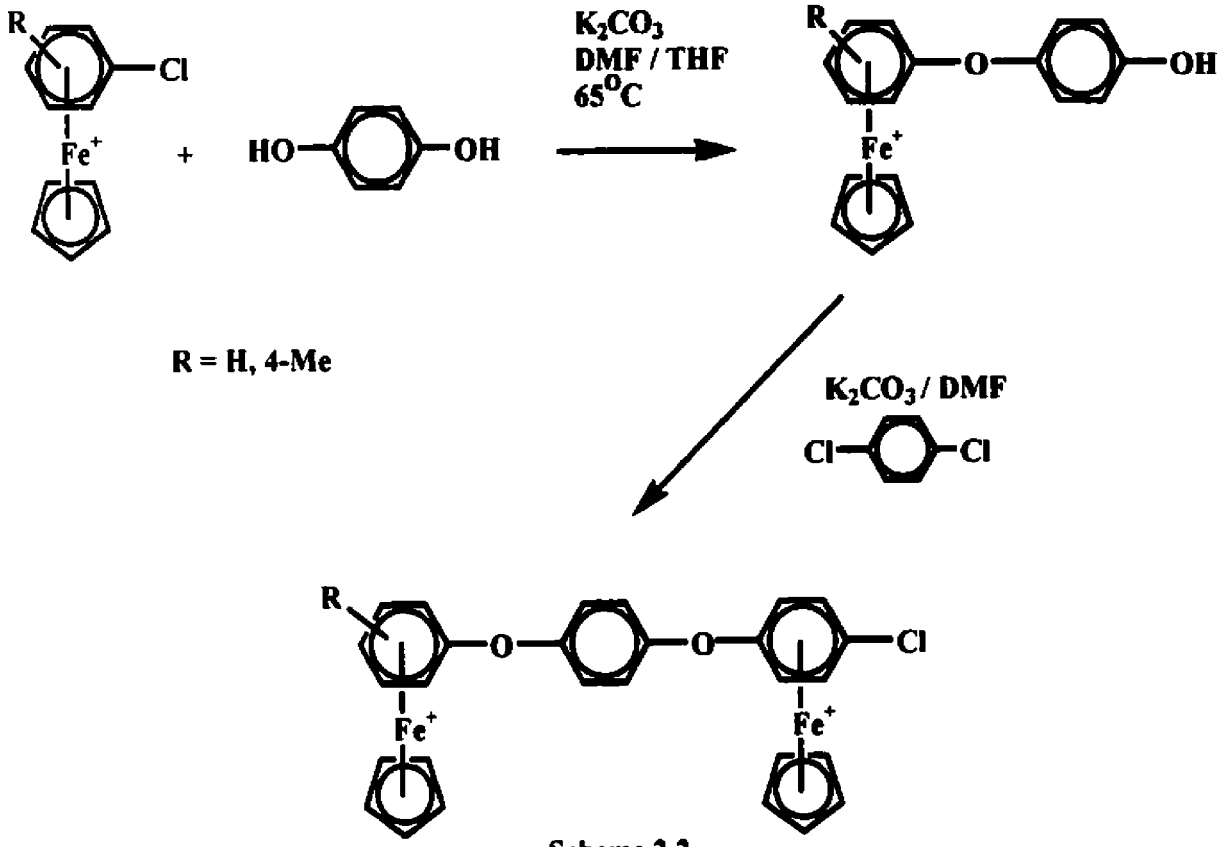

Scheme 2.2

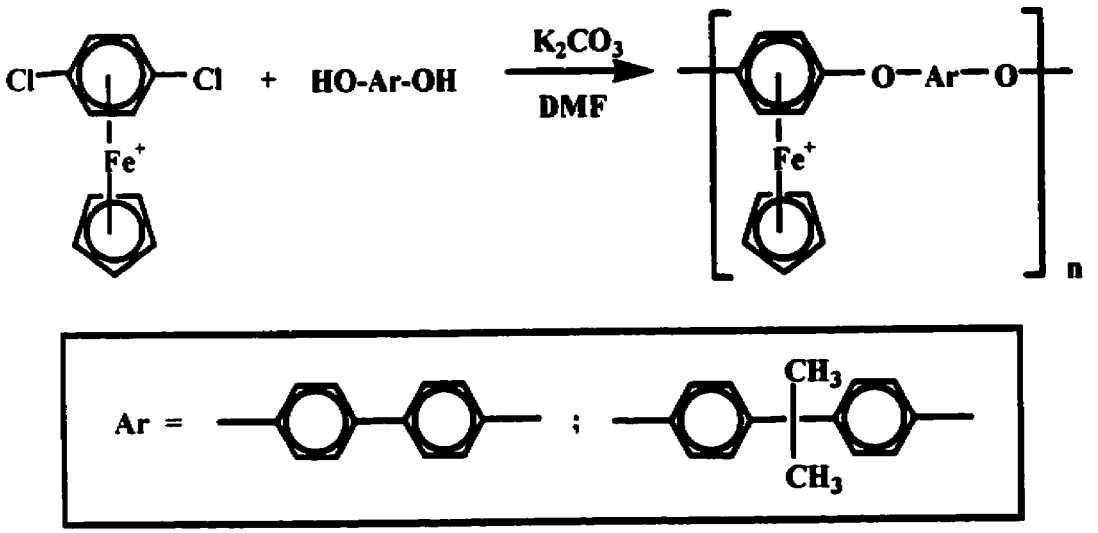

Scheme 2.3

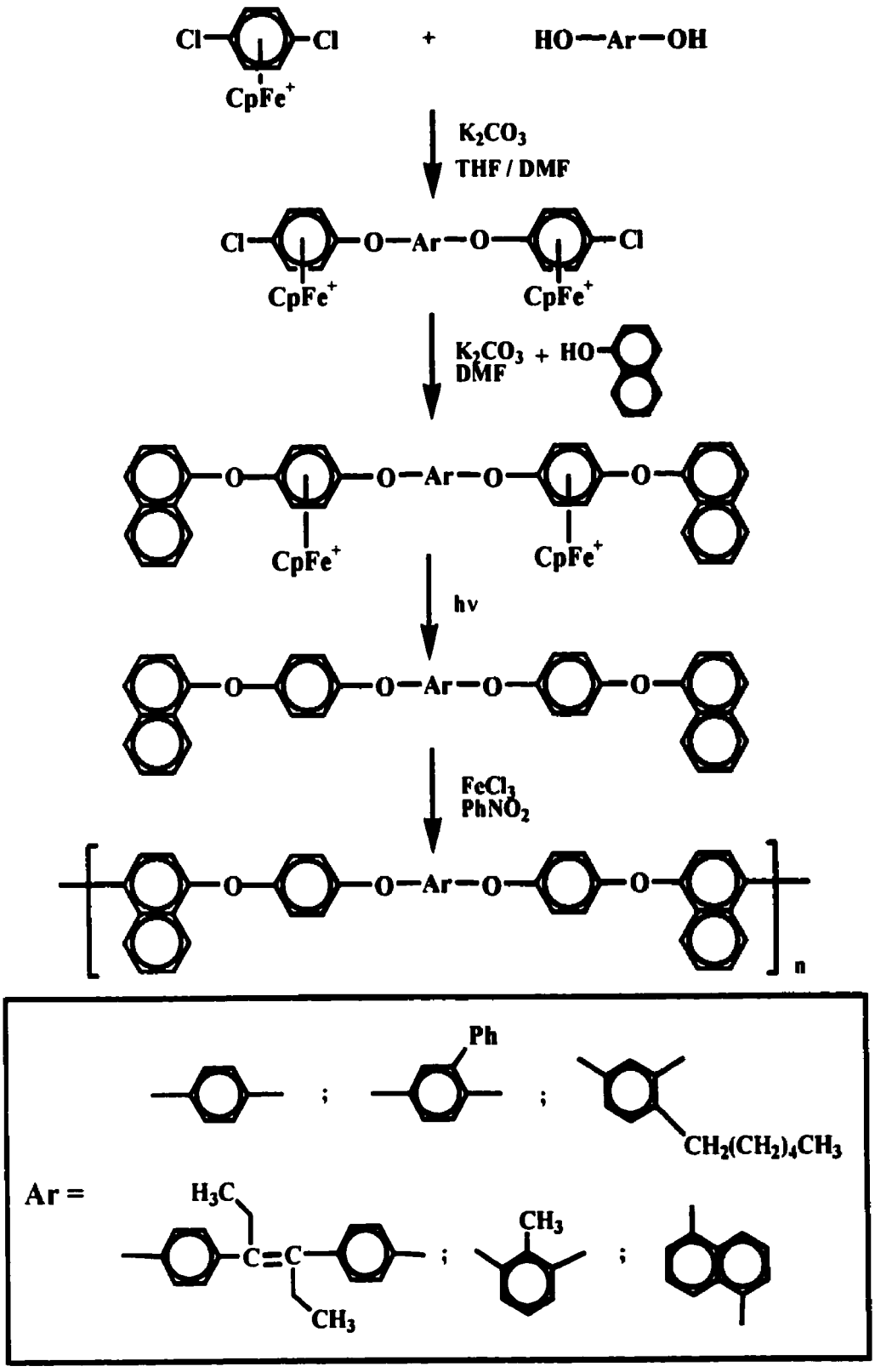
Cl
Cl
CpFe+
+
HO—Ar—OH
K2CO3
THF / DMF
O—Ar—O
K2CO3 + HO
DMF
hv
FeCl3
PhNO2
n
Ar =
Ph
CH2(CH2)4CH3
H3C
CH3
CH3

Scheme 2.4

2.1.1.4.1 Methods for Removal of the Metal Moiety – Liberation of the Organic Compound

Isolation of the organic compound from its metallic moiety can be accomplished using either of the following three methods; pyrolysis,[109, 110] electrolysis[111, 112] and photolysis.[113-117] In 1970, Nesmeyanov reported the removal of the $CpFe^{+}$ moiety using photolytic techniques.[117] This method involves dissolution of the complexed material in a coordinating solvent followed by irradiation under UV light rays leading to the liberation of the modified arene, an Fe(II) salt and ferrocene.[117] Selection of solvent is critical for this method as it has been determined that in the presence of a coordinating solvent there is an increase in product yield.[116] Therefore, acetonitrile is most predominantly used due to its good solvating ability and the ease with which the organic compound may be isolated from it.

2.1.2 Scope of Present Work

With the intention of preparing derivatives of polynorbornene with improved thermal stability, we investigated the design of monomeric units containing pendent oligomeric aryl ether chains. As discussed above, poly(aromatic ethers) offer unusually high thermal stability which was a desired property of the aryl ether functionalized polynorbornenes. To further improve the thermal properties of polynorbornene, the objective was to design polymers that contained an ester bridge between the pendent aromatic chain and the polynorbornene backbone.

2.2 Results and Discussion

2.2.1 Preparation of Aryl Ether Functionalized Norbornene Monomers

2.2.1.1 Synthetic Approach Towards the Preparation of Monoaryl Ester Building Blocks

Complexed toluene (**2.1**) and chlorotoluene (**2.2**) were readily synthesized by the previously established ligand exchange reaction.[82-85] Nesmeyanov has previously described the conversion of these complexes to their corresponding carboxylic acids (**2.3**, **2.4**) in the presence of a strong oxidizing agent, as shown in Scheme 2.5.[118-120] However, since it proved to be extremely difficult to prepare the more reactive acid halides of these complexes, another route was explored involving dicyclohexylcarbodiimide (DCC) mediated-coupling.

Since *exo*, *endo*-5-norbornene-2-methanol (**2.5**) readily undergoes functionalization at its hydroxyl group, capping of this group with various monoaryl acids was explored. This was accomplished by reacting either complexed benzoic acid (**2.3**) or *p*-chlorobenzoic acid (**2.4**) with a slight excess of **2.5** in the presence of DCC, a catalytic amount of pyridine, and dichloromethane at room temperature for either 7 h (**2.6**) or 3 h (**2.7**). This reaction, which is outlined in Scheme 2.5, yielded the metallated monomers **2.6** and **2.7** in 62 and 70 %, respectively. Structural characterization of these metallated monomers was carried out using 1-D and 2-D NMR techniques, infrared spectroscopy and elemental analysis. The complex NMR spectra of these metallated

compounds, resulting from the presence of *exo* and *endo* isomers, will be described in Section 2.2.2.

There have been reports detailing the advantages of using stronger bases, such as 4-dialkylaminopyridines, as acylation catalysts to facilitate these coupling reactions.[121-126] In the DCC-mediated conversion of methylcyclohexanol to its acetate derivative, dimethylaminopyridine (DMAP), a highly basic acylation catalyst (pKa = 9.7), has been reported to give yields as high as 86% relative to the 5% obtained when using pyridine (pKa = 5.2).[126] Substantially faster reaction times are routinely observed using this "super acylation" initiator.[121] Therefore, in an attempt to improve product yields of **2.6** and **2.7**, a reaction of **2.3** with **2.5** was investigated. In contrast to the reported findings, substantially lower product yields were obtained, as well as an inseparable product mixture. Temporary coordination of DMAP to the electrophilic Fe^{+} center may inhibit the desired reaction, thus limiting its usage in the preparation of complexes **2.6** and **2.7**. This proposal is based upon previous findings that DMAP readily undergoes reaction with electrophiles.[124]

The high product yields (62 and 70%) achieved when using pyridine and DCC in the synthesis of the ester complexes **2.6** and **2.7** suggests that the electron-withdrawing ability of the $CpFe^{+}$ moiety promoted this product formation. This is in agreement with literature reports for the preparation of organic phenolic esters using a similar method, which indicates increased product yields (40 – 90 %) when electron-withdrawing nitro substituents are present on the arene.[127] Additional studies determined that optimum yields were obtained for these DCC-pyridine reactions when the nitro group was in the *para* position.

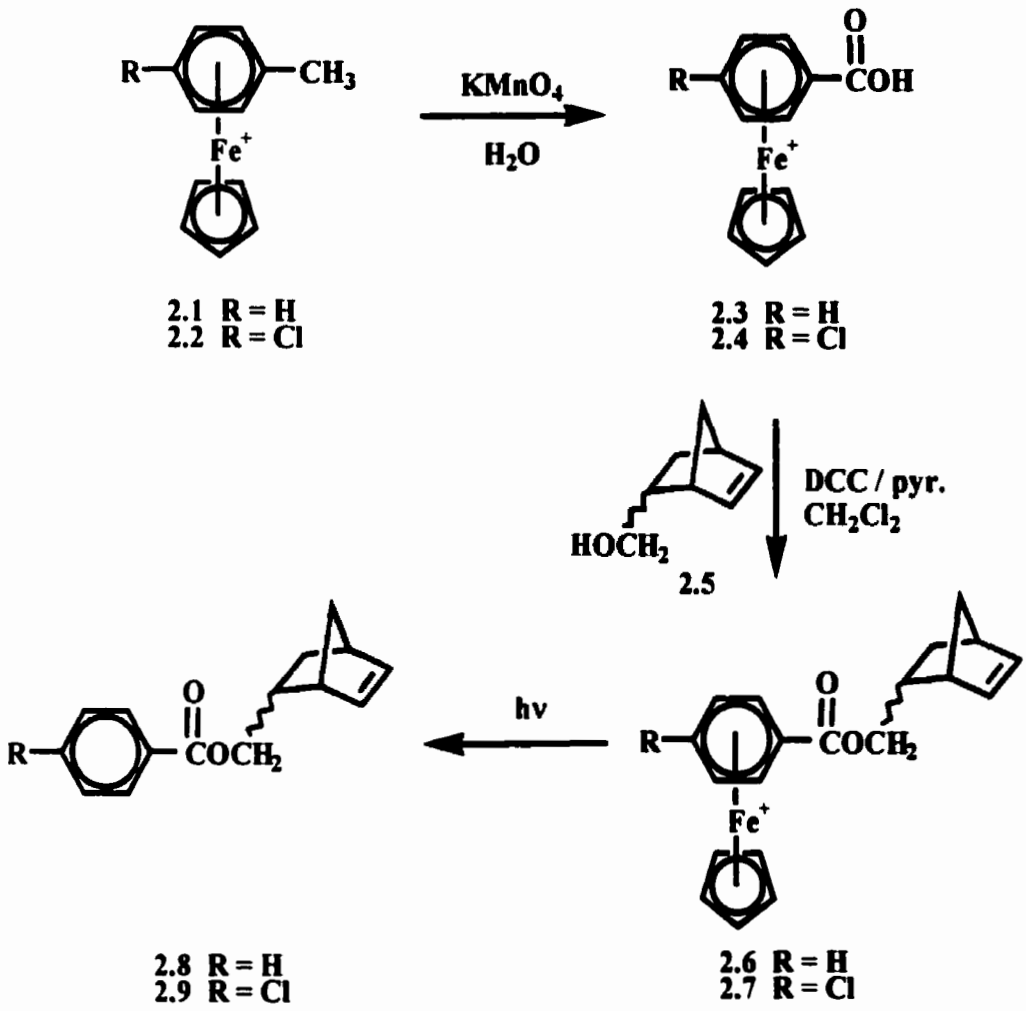

Scheme 2.5

This increased reactivity resulting from incorporation of an electron-withdrawing substituent on the ring also explains the faster reaction times achieved in synthesizing the chlorine substituted derivative **2.7** relative to the nonsubstituted complex **2.6**. Synthesis of **2.6** containing only one electron-withdrawing group required 7 h, however, **2.7** containing both a chlorine substituent and a $CpFe^+$ moiety required only 3 h. In summary, this synthesis offers mild reaction conditions, shorter reaction times and a cost-

efficient route towards the preparation of monoaryl ester derivatives of arene(cyclopentadienyl)iron hexafluorophosphate complexes.

Isolation of the organic monomers **2.8** and **2.9** (Scheme 2.5) was accomplished using the previously outlined photolytic demetallation technique.[113-117] This methodology involved photolysis of a 1:3 (v/v) acetonitrile/dichloromethane solution of the metallated species. Irradiation of the solution for 4 h resulted in decomplexation of the $CpFe^+$ moiety from the modified arene. Purification of the sample via column chromatography liberated the organic norbornene monomers as viscous oils in 64-70% yield.

Since it was of interest to investigate the properties of the *p*-methylated analogues of norbornene for comparison purposes, the initial synthesis of complexed toluic acid was explored. Attempts to isolate this complex from the $KMnO_4$ oxidations of both *p*-xylene(cyclopentadienyl)iron and *p*-isopropyltoluene(cyclopentadienyl)iron were unsuccessful due to the formation of the diacid complex in the oxidation of the *p*-xylene derivative, as previously reported by Nesmeyanov.[117] Instead, these monomeric syntheses were performed using commercially available toluic acid and benzoic acid, carried out in the absence of the iron moiety, and accordingly, the stronger acylation catalyst DMAP was employed. These coupling reactions were typically accomplished using 2.0 mmol of **2.12** or **2.13** in the presence of a 2.4 mmol excess of **2.5**, DCC and DMAP in a dichloromethane solution at room temperature (Scheme 2.6). Isolation of the viscous products was achieved via column chromatography liberating monomers **2.8** and **2.14** in 85-91% yield.

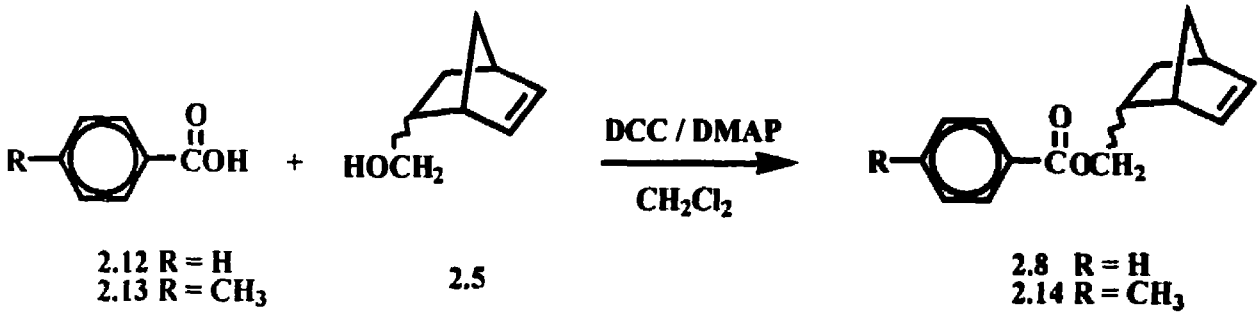

2.12 R = H
2.13 R = CH_3

2.5

2.8 R = H
2.14 R = CH_3

Scheme 2.6

2.2.1.2 Synthesis of Norbornenes Containing Pendent Aromatic Ether Side Chains

Expansion of the monoaryl ester monomers to those containing tri- and penta-aryl ether side chains was the next step in this synthetic strategy. The initial preparation of the aryl ether chains was conducted using a similar method to that established by Abd-El-Aziz for the design of asymmetric, aromatic ethers containing a terminal chloro-substituent.[102, 103] The terminal hydroxy derivatives of these complexes were prepared and then subjected to nucleophilic aromatic substitution with complex **2.7**. Demetallation gave the novel norbornene monomers containing pendent aryl ether chains linked to the norbornene unit through an ester bridge.

2.2.1.2.1 Isolation of Oligoether $CpFe^+$ Complexes

Scheme 2.7 illustrates the syntheses of terminal phenoxy complexes using S_NAr. This methodology was adapted from the previously reported synthesis of the nonmethylated and methylated monometallics, **2.20** and **2.21**, respectively.[102] Synthesis of complexes **2.22** and **2.23** was accomplished by reacting the asymmetrical terminal chloroarene complexes (**2.17** and **2.18**, respectively) with an excess of hydroquinone (**2.19**) in a THF/DMF solvent mixture under a nitrogen atmosphere at 65 °C. The metallated products were obtained as yellow precipitates in 90-92% yield.

NMR spectral data were used to characterize these complexes. In the ^1H NMR spectrum of the asymmetric bimetallic complex **2.23** (Figure 2.1), there are two distinct resonances at 5.18 and 5.27 ppm representative of the cyclopentadienyl protons. The appearance of a single resonance for each of these Cp rings is characteristic of the rapid rotation of the rings at room temperature.[128, 129] Each proton in each of the Cp rings is magnetically equivalent, thus appearing as two well-defined singlets. This spectrum differs from that of its starting chlorinated precursor **2.18** by the appearance of a collapsed singlet at 7.51 ppm integrating to four protons, which is attributed to the uncomplexed aromatic protons in the terminal phenoxy ring. In addition, the small broad resonance at 8.70 ppm showing an integration of one for the alcohol functionality verifies the presence of the terminal hydroxy group in this complex. A final identifying feature was the single methyl resonance appearing at 2.48 ppm.

^{13}C NMR spectroscopy further confirmed the structural features of this bimetallic species. All ^{13}C NMR were performed as Attached Proton Tests (APT) which allowed

differentiation between carbon atoms. This technique displays methyl and methine carbon resonances below the baseline, whereas methylene and quaternary carbons appear above it. Figure 2.2 illustrates the ^{13}C NMR spectrum for **2.23**. Two distinct resonances at 78.08 and 78.33 ppm confirmed the presence of two Cp rings in this complex. Further structural confirmation was provided by the absence of a quaternary carbon signal at 104.94 ppm, which is the characteristic shift for the carbon bonded to the chlorine atom in the complexed starting material. Loss of this resonance indicated that successful substitution had occurred at this site. Finally, the two additional uncomplexed aromatic resonances at 117.41 and 122.49 ppm indicate the presence of the terminal phenoxy ring. A full representation of the NMR data is provided in Tables 2.1 and 2.2.

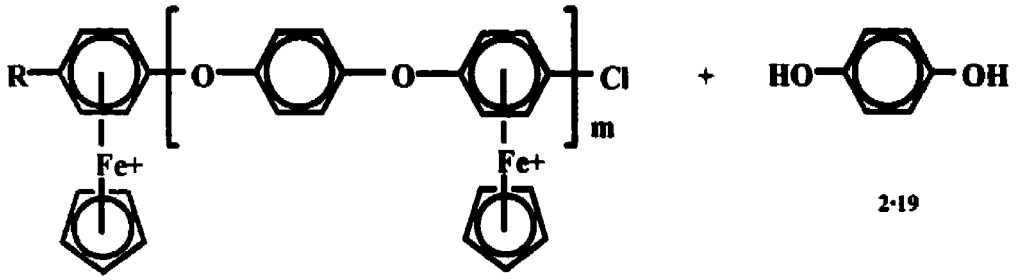

2·19

m	R = H	CH_3
0	2.15	2.16
1	2.17	2.18

K_2CO_3
THF / DMF

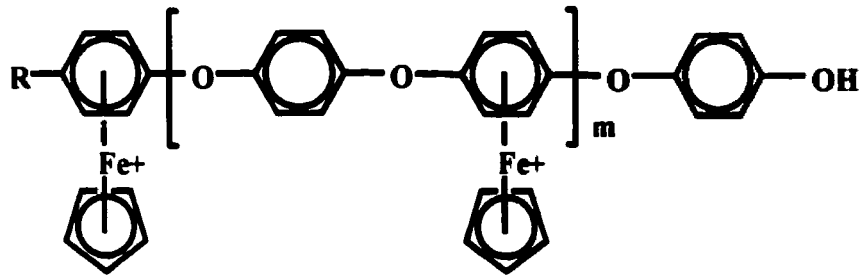

m	R = H	CH_3
0	2.20	2.21
1	2.22	2.23

Scheme 2.7

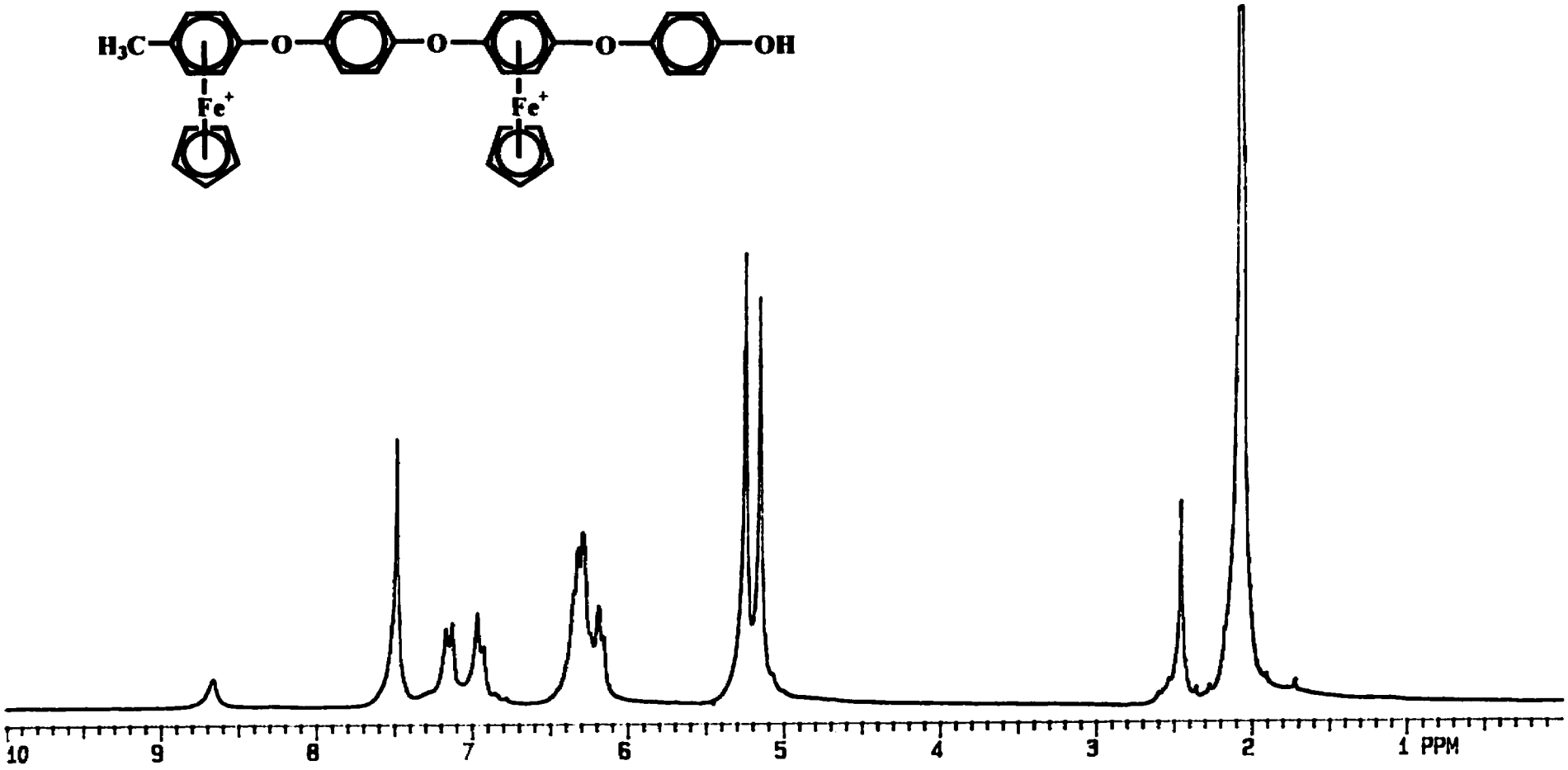

Figure 2.1: ^{1}H NMR of complex **2.23** in acetone-d_6.

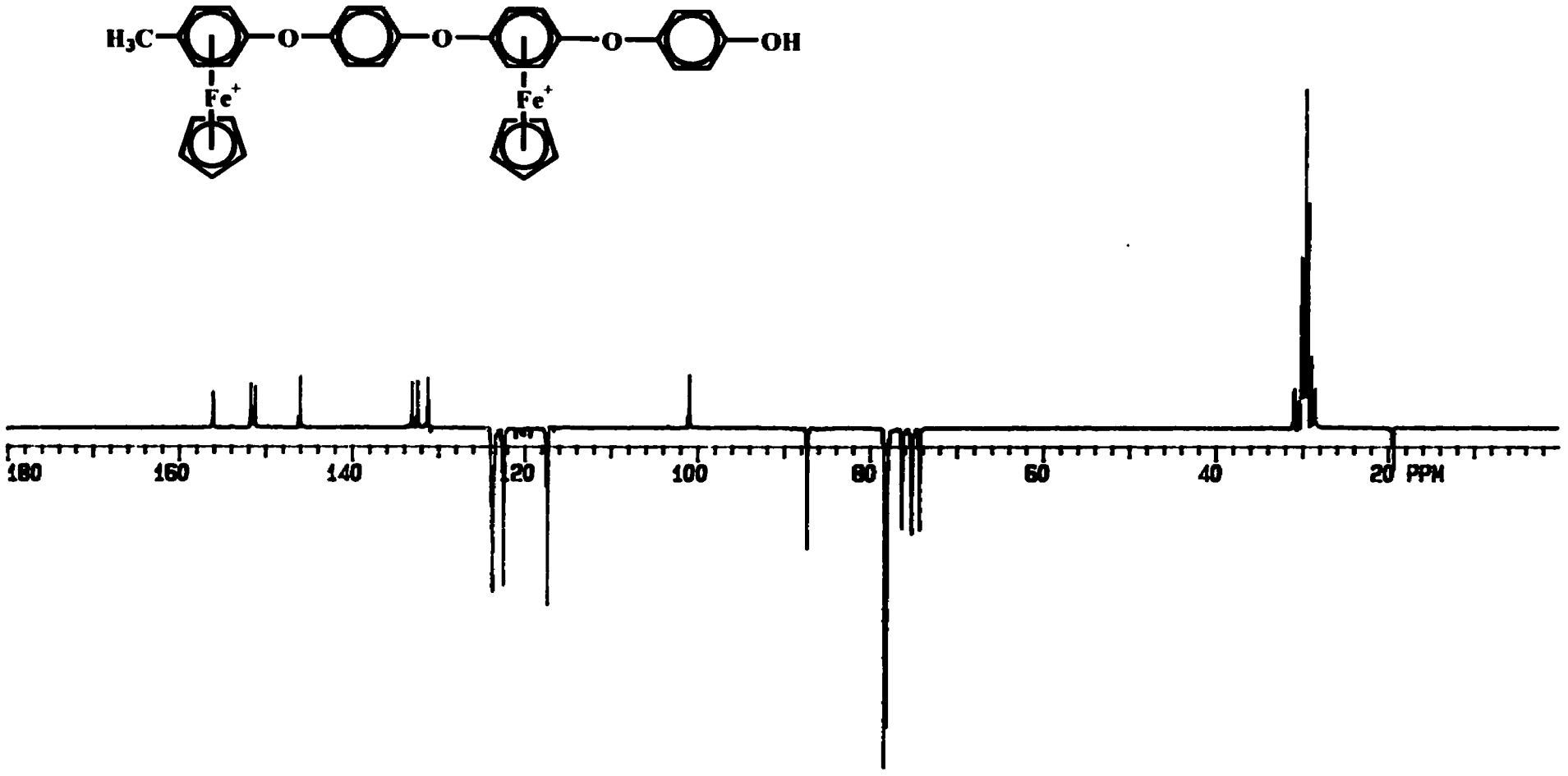

Figure 2.2: ^{13}C NMR of complex **2.23** in acetone-d_6.

2.2.1.2.2 Metal-Mediated Synthesis of Oligomeric Aryl Ether Functionalized Norbornenes

To prepare monomers for our target functionalized polynorbornenes, S_NAr reactions were carried out with the oligomeric aryl ether nucleophiles, **2.20-2.23**. As complex **2.7** contains a chlorine substituent, it was a suitable precursor for facilitating S_NAr. Therefore, capping of the terminal phenoxy complexes with **2.7** allowed for the synthesis of metallated aromatic ether complexes bridged by an ester linkage to the norbornene molecule.

Scheme 2.8 displays the synthetic pathway used to prepare these norbornene monomers. A typical reaction, using complex **2.20** as an example, involved one equivalent of **2.7** in the presence of excess K_2CO_3 in *N,N*-dimethylformamide (DMF) at room temperature under a deoxygenated environment. Work-up required the subsequent addition of the reaction mixture to a 10% (v/v) HCl solution, which liberated the metallated oligomer **2.24** as a yellow precipitate in 81% yield. Characterization of these norbornene derivatives will be described in detail in the next section (2.2.2).

Isolation of the uncomplexed monomers was achieved as previously described for the monoaryl esters, differing only in the amount of time the complexed materials remained in the photolysis chamber. In general, longer irradiation times were employed as the number of metals increased: when only two metals were present, photolysis times were commonly 4-5 h, increasing to 6 h for the cleavage of three metals. Isolation of the organic monomers was accomplished using column chromatography giving compounds

2.28–2.31 in 46-51% yield. The resulting molecular structures were analyzed using a combination of NMR, IR, MS and elemental analysis.

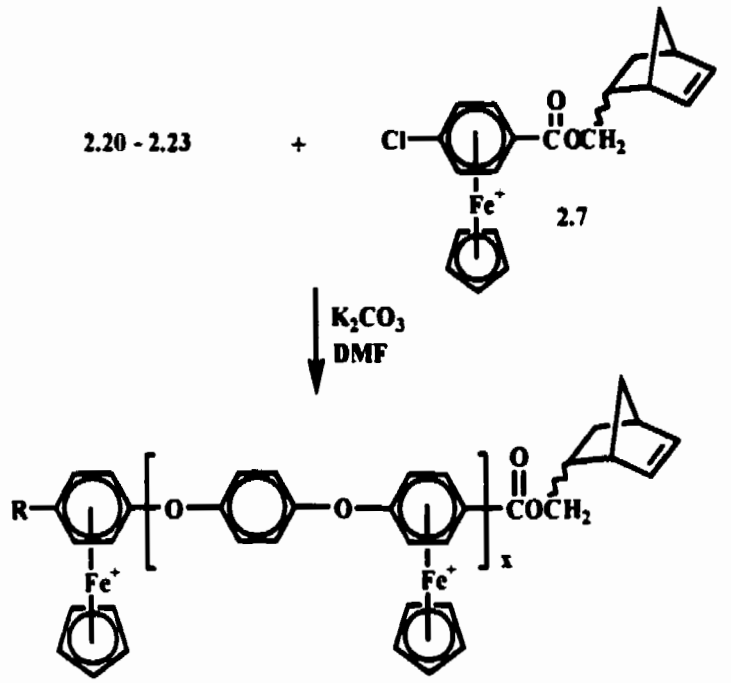

x	R = H	CH_3
1	2.24	2.25
2	2.26	2.27

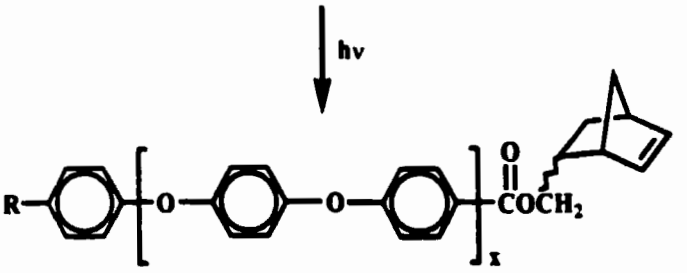

x	R = H	CH_3
1	2.28	2.29
2	2.30	2.31

Scheme 2.8

2.2.2 One- and Two-Dimensional NMR Spectroscopic Characterization of Norbornenes

Since the commercial availability of high-resolution nuclear magnetic resonance (NMR) spectrometers in 1953, this instrument has become an extremely valuable tool for scientists worldwide.[130-132] Technological advances have led to the design of better superconducting magnets, pulse techniques[130-132] and Fourier transformations[130-132] resulting in the development of higher resolution instruments.[130] From these remarkable advances in instrument design, NMR is now highly recognized as a valuable tool for analytical analyses as sample sizes in the microgram range can finally be detected.

In contrast to the 1-D NMR spectrum, which involves a series of single pulses immediately followed by signal acquisition and Fourier transformation of the free induction decay (FID),[130, 132] the 2-D spectrum involves multipulse sequences. The 2-D spectrum is essentially a 3-D spectrum composed of a cross-section of a series of "stacked peaks", that are representative of peak intensities, as identified in Figure 2.3. Of the 2-D NMR techniques available, homonuclear ^{1}H-^{1}H correlation spectroscopy (COSY) and ^{1}H-^{13}C heteronuclear correlation spectroscopy (HETCOR) are the most common.

An ^{1}H-^{1}H COSY spectrum provides information about proton-proton connectivities.[130, 132] As protons are not directly connected to each other, this technique is more accurately defined as C-C connectivities which can be traced through the couplings of the protons to which they are bonded. The actual proton spectrum in an ^{1}H-^{1}H COSY NMR appears along the diagonal of the plot as contours which are representative of peak intensities. Contours appearing off of this diagonal are called

crosspeaks. Based upon the appearance of symmetrical crosspeaks on both sides of the diagonal, ^{1}H-^{1}H connectivites can be elucidated. This is accomplished by drawing both a horizontal and vertical line 90 ° to one another through the same crosspeak. Each of the contours they bisect on the diagonal are said to be coupled or "connected" to one another.

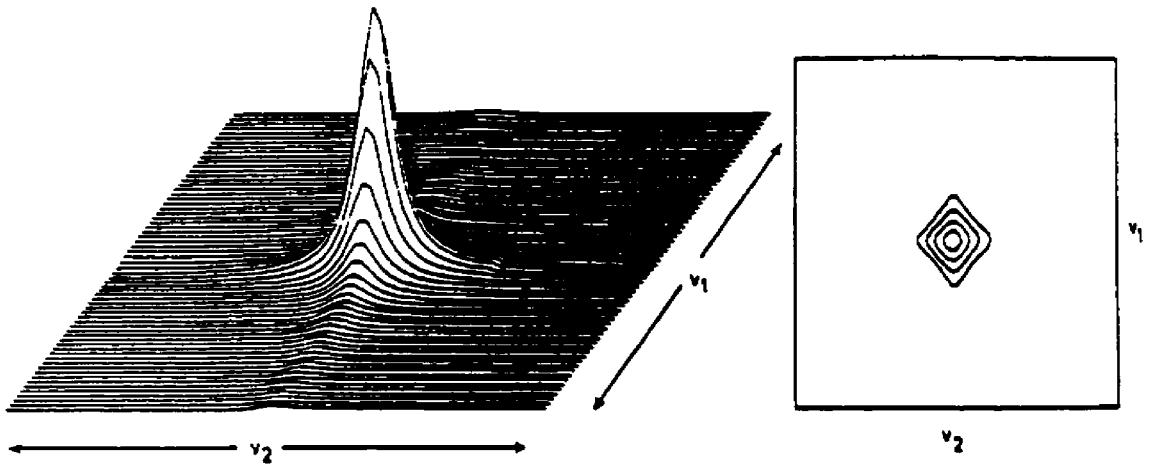

Figure 2.3: Frequency-domain spectrum showing both the peak resulting from the FT of a series of FID's and its contour.

Heteronuclear correlation spectroscopy, or HETCOR, is a technique useful for identifying proton – carbon connectivities. This is achieved through the correlation of peaks in the ^{1}H NMR spectrum with peaks in the ^{13}C NMR spectrum.[130, 132] A typical ^{1}H-^{13}C correlation spectrum consists of the ^{1}H spectrum along the horizontal axis with the ^{13}C broadband-decoupled spectrum along the vertical axis. H-C correlation is identified through the intersection of a horizontal and vertical line at a contour indicating that the respective proton and carbon atoms are connected. The information provided from both

the 2-D heteronuclear and homonuclear COSY NMR techniques, when used in conjunction with one another, is generally sufficient for the elucidation of complicated molecular structure assignments.

2.2.2.1 NMR Identification of Substituted Norbornenes

Synthesis of substituted bicyclo[2.2.1]heptenes via the well-known Diels-Alder reaction, leads to the isolation of a pair of isomers. Structural analysis of these *endo* and *exo* derivatives of norbornene has proven to be quite difficult using traditional chemical methods.[133] However, with advances in NMR technology, characterization of these derivatives can now be accomplished because of several characteristic features of these compounds. Figure 2.4 has been included as a means to identify relative proton and carbon atoms in the norbornene structure and will be vital towards comprehending the remainder of this discussion.

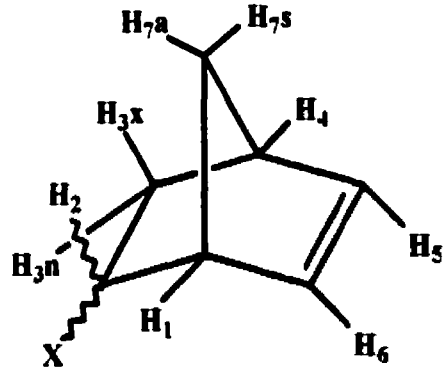

Figure 2.4: Proton schematic of a substituted norbornene.

Extensive NMR studies of bridged ring systems have been performed,[133-142] however, it was not until the work of Musher in the early 1960's on bicyclo[2.2.1]heptanols that any substantial contributions to this field were made.[136] A major observation in this study by Musher detailed the significantly different magnetic shieldings observed for each of the *endo* and *exo* isomers comprising the diastereomeric mixture. These differences were attributed to differing ring-currents and/or the long-range influences of intramolecular electric fields. Another characteristic of these diastereomers was the difference in coupling constants observed for the *endo-endo* coupling relative to the *exo-exo* coupling. Despite having identical dihedral angles, Musher attributed this coupling dissimilarity to the unique electrostatic environments each set of protons had within the molecule. A final observation made from this investigation involved the presence of large long-range couplings in the order of four bond lengths (^4J).

A study done by Fraser in 1962 detailed the influence that the anisotropic double bond had on the relative chemical shifts of *exo* and *endo* protons.[133] It was proposed that all protons in a bicyclo[2.2.1]heptene would be shielded to some extent by the anisotropic nature of the double bond and that the degree of shielding depended upon the orientation and position of these protons relative to the vinylic carbons. To confirm this theory, Fraser examined the hydrogenation of the double bond assessing the effects this would have on the relative chemical shifts of the isomers. In norbornene derivatives, the *exo* proton lies in the plane of the double bond and is thus deshielded by the double bond anisotropy, resulting in a more downfield appearance of this resonance. Upon hydrogenation of the double bond, a notable upfield shift of the *exo* protons was

observed, confirming the influence of the double bond anisotropy on relative proton chemical shifts. Similarly, as the *endo* protons lie above the plane of the double bond, they are shielded, experiencing an upfield shift. Subsequent hydrogenation of the double bond showed a notable downfield shift of the proton, which further confirmed this theory. Similar investigations using this methodology verified these findings.[137, 138, 140, 141]

Proton couplings in norbornene compounds are unique for the *endo* and *exo* isomers. In 1964, Laszlo and von Ragué Schleyer examined the ^{1}H NMR spectra of a wide variety of norbornene derivatives and were able to assign all proton resonances as well as measure all chemical shifts and coupling constants.[141] A defining feature when identifying both isomers was the differences in proton couplings between H_2 and H_3 with the bridgehead protons, H_1 and H_4, which can be identified by referring back to Figure 2.4. Analysis of the ^{1}H NMR spectra indicated that the *exo* H_2 and H_{3x} protons could couple with the bridgehead H_1 and H_4 protons, respectively, indicating the presence of the *endo* isomer. In contrast, the *exo* isomer could be characterized by the lack of coupling observed for the *endo* H_2 and H_{3n} protons with H_1 and H_4. Another defining feature allowing for the differentiation of isomers involved the very strong coupling observed for the *exo-exo* H_2 and H_{3x} protons ranging from 8.9-11.4 Hz differing from the weaker *endo-endo* H_2 and H_{3n} protons (5.8-7.7 Hz) as determined from a norbornane compound. Similar findings distinguishing these significantly different couplings for the *endo-endo* and *exo-exo* protons have been reported.[136] Although a transoidal coupling of 2.1-5.8 Hz exists for the *endo* H_2 proton and H_{3x} as well as for the *exo* H_2 proton and H_{3n}, it does not allow any differentiation between the diastereomers.

Geminal couplings in the molecule were quite large for the H_{3x} and H_{3n} protons as well as for the H_{7a} and H_{7s} bridge protons. Coupling for the H_{3x} and H_{3n} protons, observed as 12.3-13.2 Hz, was considerably larger than for the bridge protons having a J value of 8.5-9.5 Hz. This is consistent with the varying size of the H-C-H angle, which is known to influence geminal coupling constants.[141] Vicinal couplings were also quite significant for protons H_5 and H_6 which had values in the range of 5.0-6.0 Hz. As these protons are also capable of coupling with the bridgehead protons (H_1 and H_4), an additional coupling constant of 2.4-3.0 Hz was observed representing the $J_{4,5}$ and $J_{1,6}$ couplings.

Of all the protons examined within the norbornene and norbornadiene frameworks, the bridge protons, H_{7a} and H_{7s}, referring to the *anti* and *syn* orientations of the protons with respect to the double bond, proved the most difficult to assign. It was not until the investigation of 7-substituted norbornadienes and norbornenes that the assignment of the *anti* and *syn* protons could be accomplished.[139, 141] These findings revealed that the H_{7s} proton is more shielded than H_{7a} which accounts for the fact that H_{7a} appears more downfield than H_{7s}. Another interesting observation is the different coupling constants observed between H_{7a} and the bridgehead protons relative to H_{7s}. As both dihedral angles are the same and as both bridgehead protons (H_1 and H_4) are the same, a larger coupling was observed for $J_{7s,1}$ and $J_{7s,4}$ (1.5-2.0 Hz) which was attributed to the shielding effects of the vinylic carbons. Essentially no coupling was observed for H_{7a} with either H_1 or H_4.

An interesting feature of these bicyclo[2.2.1]heptenes is with their ability to long-range couple with protons four bonds away.[136, 138, 139, 141] Figure 2.5 illustrates four

examples of possible long-range couplings that are observable in these types of structures. Of the bridge protons, it has been observed that H_{7a} can weakly couple with either of the olefinic protons, H_5 and H_6 giving a coupling constant of approximately 0.5 Hz or less. This olefinic coupling is not detected with H_{7s}, however, it demonstrates a relatively moderate transoidal coupling with the *endo* protons H_2 and H_{3n} with a value ranging from 2.0-3.1 Hz. Further long-range coupling has been identified between the bridgehead protons giving a value of 1.5 Hz as well as an allylic coupling between the bridgehead and olefinic protons (0.5-1.0 Hz).

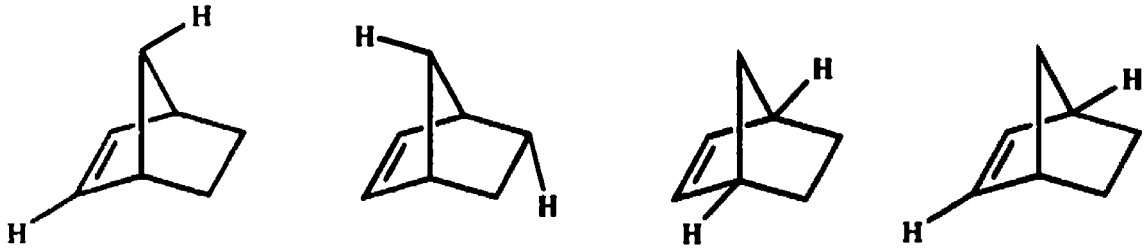

Figure 2.5: Long-range couplings observable in bicyclo[2.2.1]heptenes.

2.2.2.2 NMR Analyses of Metallated Aryl Ether Functionalized Norbornenes

NMR spectroscopic analysis of these functionalized bicyclo[2.2.1]heptenes was quite complicated due to the usage of 98%-*exo*,*endo*-5-norbornene-2-methanol in their synthesis. As a result, a mixture of *exo* and *endo* diastereoisomers was present for each of the monomers, making their NMR spectra rather difficult to assign. However, this complication was readily overcome using the 2-D NMR techniques ^1H-^1H COSY and HETCOR.

Figure 2.6 is a representation of the ^{1}H NMR spectrum of complex **2.7**. The metallated nature of this complex was identified by the single strong resonance at 5.36 ppm, due to the protons on the Fe^+ coordinated Cp. Since this molecule exists as *endo/exo* diastereomers, it was surprising that only a single Cp resonance was observed instead of the expected two. This was attributed to the large separation distance between the norbornene unit and the Cp ring. This distance provided sufficient spacing between the two groups such that the electronic environment of the Cp protons was unaffected by the differing magnetic environments of the *endo* and *exo* isomeric protons contained in norbornene. This was confirmed in the ^{13}C NMR spectrum (Figure 2.7), which also displayed a single resonance at 81.47 ppm for the Cp carbon atoms.

The ^{1}H NMR spectrum of *exo,endo*-5-norbornene-2-methanol shows four resonances from 3.24-3.60 ppm, due to the *endo* and *exo* isomers of the methylene protons in the alcohol functionality (nor-CH_2OH).[142] Each isomer contains two peaks consisting of a doublet of doublets and a triplet, due to the presence of the chiral carbon at C_2. These resonances were observable in the ^{1}H NMR spectrum of **2.7** appearing from 4.03 – 4.53 ppm. The considerable downfield shift of these resonances for the modified norbornene monomer relative to the commercially available one, results from the presence of the highly electron-withdrawing carbonyl group, which deshields the methylene protons.

^{1}H-^{1}H connectivites were used to identify which proton resonances belonged to each isomer. For complex **2.7**, it can be seen that the methylene protons, comprising the ester functionality, strongly couple to the proton on C_2 designated as H_2. Examination of the 2-D HH COSY NMR spectrum illustrated in Figures 2.8 (a and b) revealed a distinct

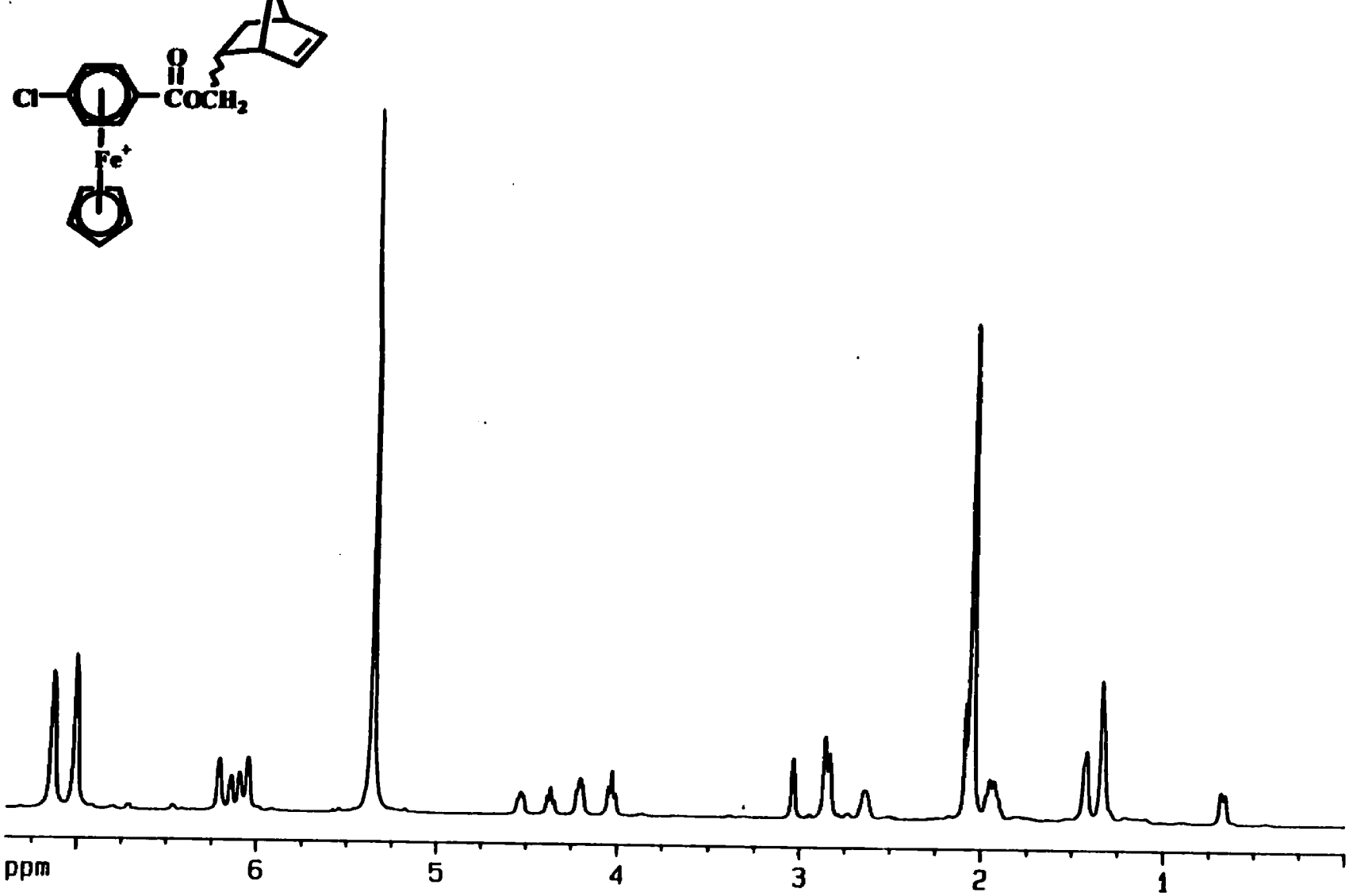

Figure 2.6: ^{1}H NMR of complex **2.7** in acetone-d_6.

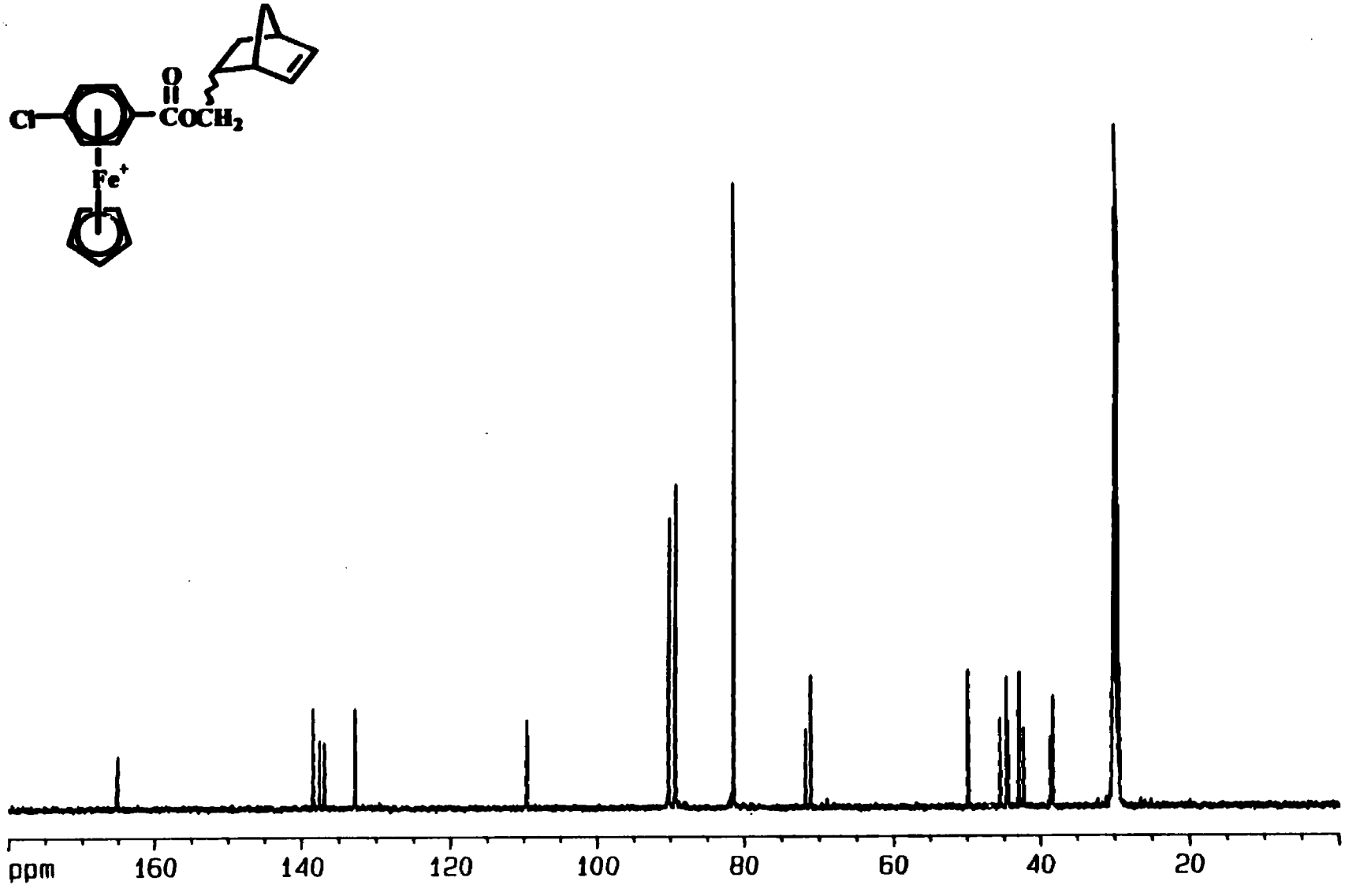

Figure 2.7: ^{13}C NMR of complex **2.7** in acetone-d_6.

coupling between the methylene resonances at 4.03 and 4.20 ppm with a broad peak at 2.64 ppm, which was attributed to an H_2 proton for one of the isomers. Due to the broad nature of the H_2 resonance, proton – proton couplings could not be determined thus requiring the use of a further connectivity to aid in isomer identification. A fundamental concept for distinguishing between the two isomers is that the bridgehead H_1 proton will only couple to H_2 when it is in the *exo* position. From the HH COSY spectrum a coupling between H_2 and a proton more downfield at 3.04 ppm can be observed. Since the bridgehead H_1 proton appears farther downfield than the H_2 protons, due to the anisotropic affect of the double bond, this proton can be assigned as H_1. Due to peak broadness, however, a coupling constant could not be measured, however, a moderately strong coupling was observable with respect to the size of the contours on either side of the diagonal, which is consistent with literature findings for this coupling.[141] As a result of these findings, it was determined that the methylene proton resonances appearing at 4.03 and 4.20 ppm as well as resonances at 2.64 (H_2) and at 3.04 (H_1) ppm all belonged to the *endo* isomer.

Once the position of the bridgehead H_1 proton for the *endo* isomer was identified the assignment of the olefinic protons H_5 and H_6 could be accomplished. Studies have shown that a moderate coupling exists between H_1 and H_6,[141] which was determined to be 2.6 Hz. Of the four distinct olefinic resonances appearing from 6.05-6.21 ppm, the peak furthest upfield at 6.05 ppm was representative of the *endo* H_6 isomer. Location of the *endo* H_5 isomer at 6.21 ppm could then be achieved because of the moderately strong coupling that it had to the H_6 proton, being $J_{(5,6)} = 5.5$ Hz. Another identifying feature of the olefinic protons was their expected doublet of doublets and triplet appearance.[8]

Extracted from these splittings were the characteristic spin-spin couplings for $J_{(1,6)}$ = 2.6 Hz, $J_{(5,6)}$ = 5.5 Hz and a coupling of 3.1 Hz which was identified as the $J_{(4,5)}$ coupling for the *endo* isomer. This latter coupling was then used to identify the bridgehead H_4 proton at 2.84 ppm which also belonged to the *endo* isomer.

Differentiation of the *exo* and *endo* isomers of H_{3x} ($_x \equiv$ *exo* orientation) and H_{3n} ($_n \equiv$ *endo* orientation) could now be accomplished knowing that H_4 can only couple to H_{3x}. Having already located the *endo* H_4 isomer, a connectivity was identified to a proton more upfield at 1.96 ppm. A coupling constant of 3.7 Hz was measured from this peak which is characteristic of $J_{(3x,4)}$ for the *endo* isomer. Musher had previously established that different magnetic environments exist for the *exo-exo* H_2 and H_{3x} protons relative to the *endo-endo* H_2 and H_{3n} protons, where the *exo-exo* show a much stronger coupling.[136] Examination of the splitting for the H_{3x} proton of the *endo* isomer allowed for the determination of $J_{(2,3x)}$ = 8.9 Hz . Location of the H_{3n} proton in the *endo* isomer was determined by a strong geminal coupling of 11.7 Hz to a proton at 0.67 ppm. Since this coupling is characteristic of the $J_{(3x,3n)}$ coupling, the assignment could be made with confidence. Furthermore, since this peak also contained the transoidal coupling of 4.0 Hz for $J_{(2,3n)}$, H_2 being the *exo* proton, this confirmed the orientation of H_{3n} in the *endo* isomer.

Spectroscopic characterization of the bridge protons, H_{7a} and H_{7s}, has previously been studied by examining isomeric 7-substituted norbornene derivatives and assessing the nature of their coupling.[138, 139, 141] Chemical shift differences for these two protons arise from different magnetic environments caused by their orientation with respect to the

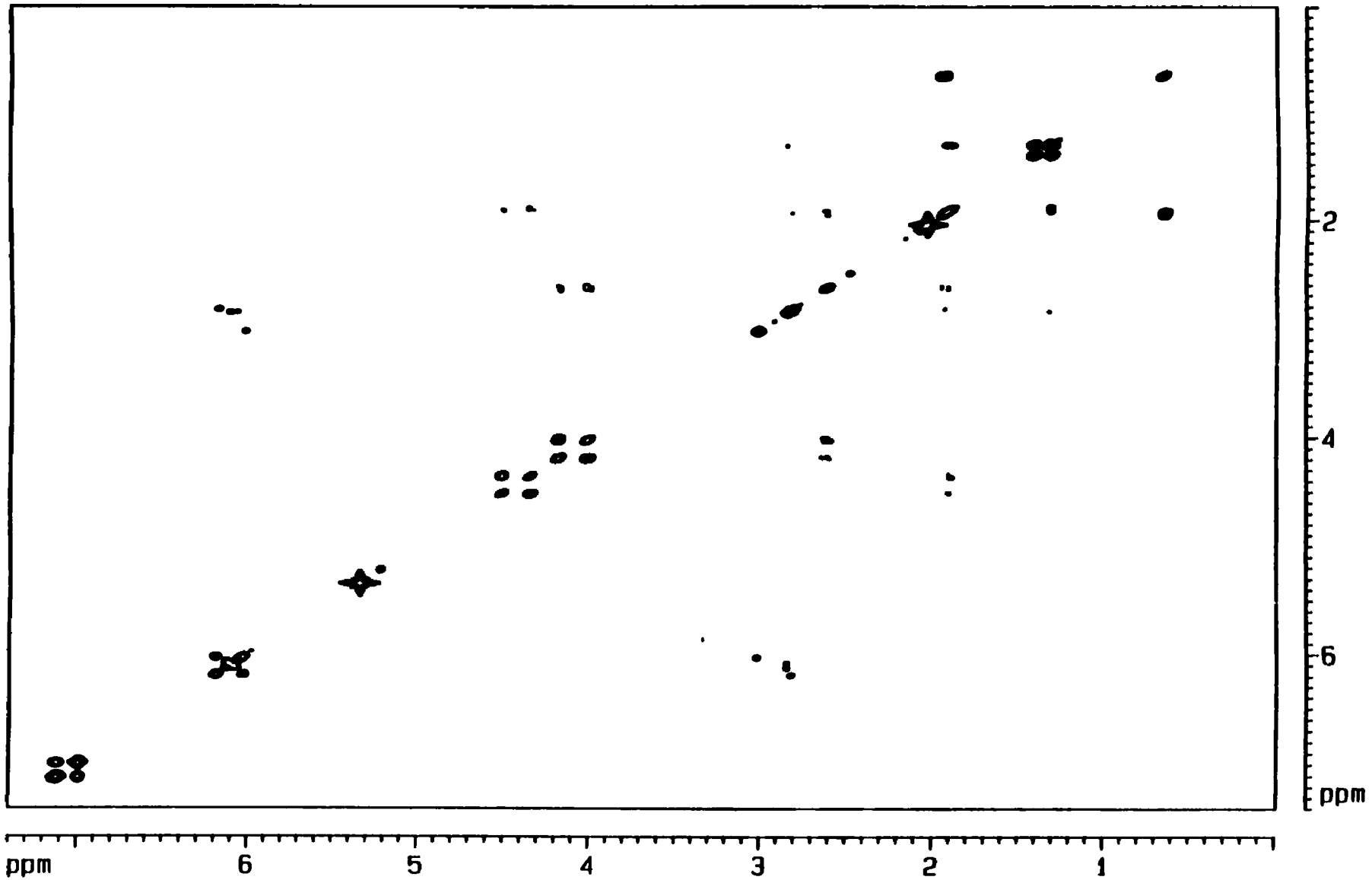

Figure 2.8 (a): HH COSY of complex 2.7 in acetone-d_6.

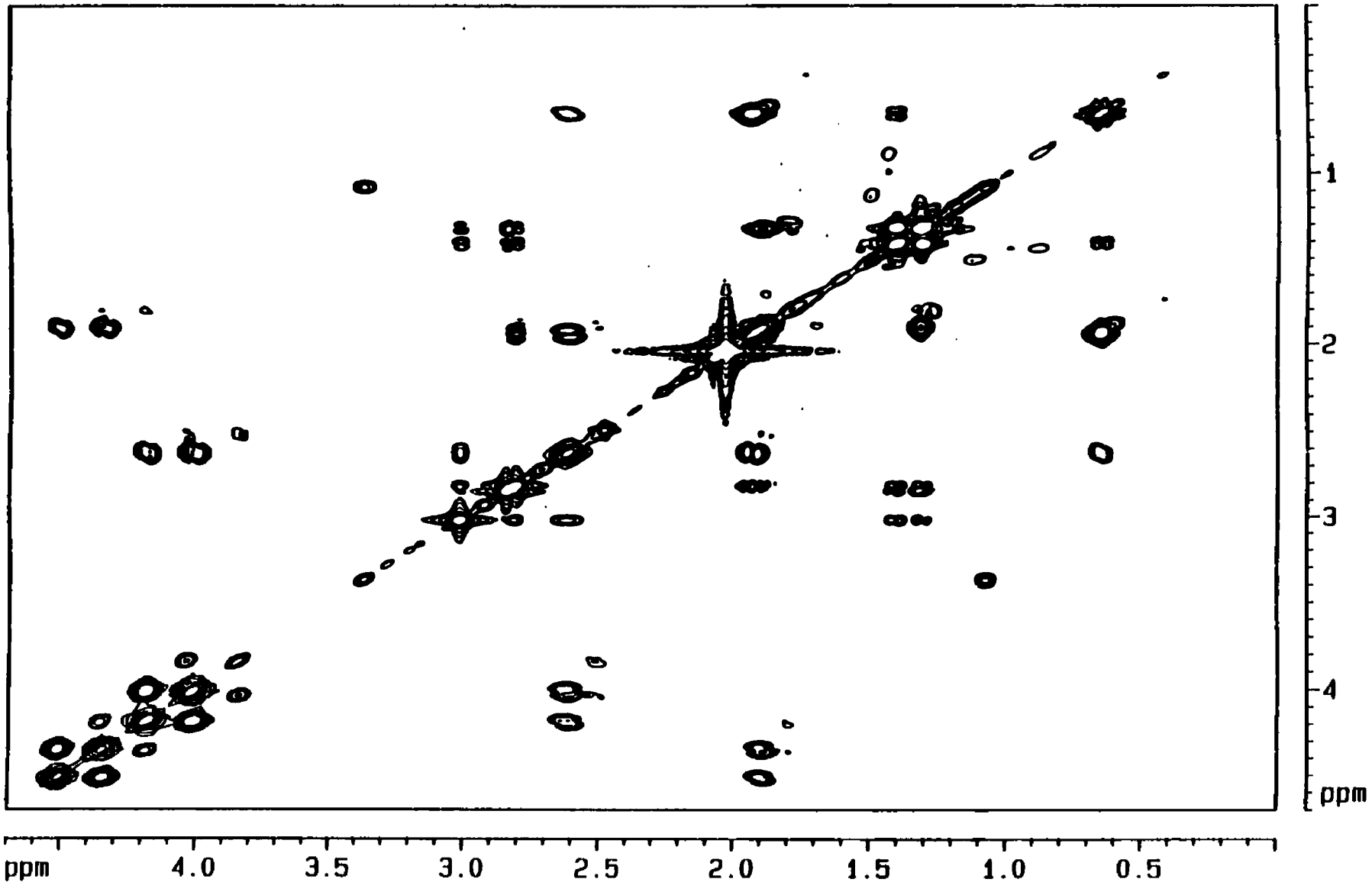

Figure 2.8 (b): Expanded HH COSY of complex **2.7** in acetone-d_6

double bond. In complex **2.7**, the chemical shifts of H_{7a} and H_{7s} were assigned because of their coupling or lack of coupling to the bridgehead protons. Examination of the HH COSY spectrum indicated a moderate coupling between H_{7s} with H_1 and H_4. As H_{7a} only weakly couples to H_1 and H_4, this crosspeak was unobservable in the 2-D spectrum, which is in agreement with previous findings for H_{7a}.[138, 139, 141] Therefore, the presence of a resonance at 1.42 ppm indicated the H_{7s} proton in the *endo* isomer. This was further verified by the long-range coupling observed between H_{7s} and H_{3n}. Location of the *endo* H_{7a} proton was made through the long-range coupling observed between itself and each of the olefinic protons. This resonance appeared at 1.32 ppm for the *endo* isomer. Determination of the protons representative of the *exo* isomer was then determined using this same stepwise methodology. Table 2.3 contains the respective *exo* and *endo* ^1H NMR data for this complex.

Identification of carbon-hydrogen correlations was obtained through analysis of the ^1H-^{13}C HETCOR NMR spectrum, which is shown in Figure 2.9 (a and b). Drawing a vertical line from the center of a proton resonance to the center of its contour followed by a 90° horizontal line to its corresponding carbon resonance allowed for determination of the respective *exo* and *endo* carbon atoms. Completion of this task allowed for full spectral analysis of **2.7**. For a full list of ^1H and ^{13}C NMR data for complexes **2.6** and **2.7**, Tables 2.3 - 2.5 have been included.

As similar spectral patterns existed for each of the *endo* and *exo* isomers in the monoaryl and bi- and tri-metallic aryl ether complexes (**2.24-2.27**), NMR analyses of **2.24-2.27** could be accomplished quite readily. Differentiating the bimetallic

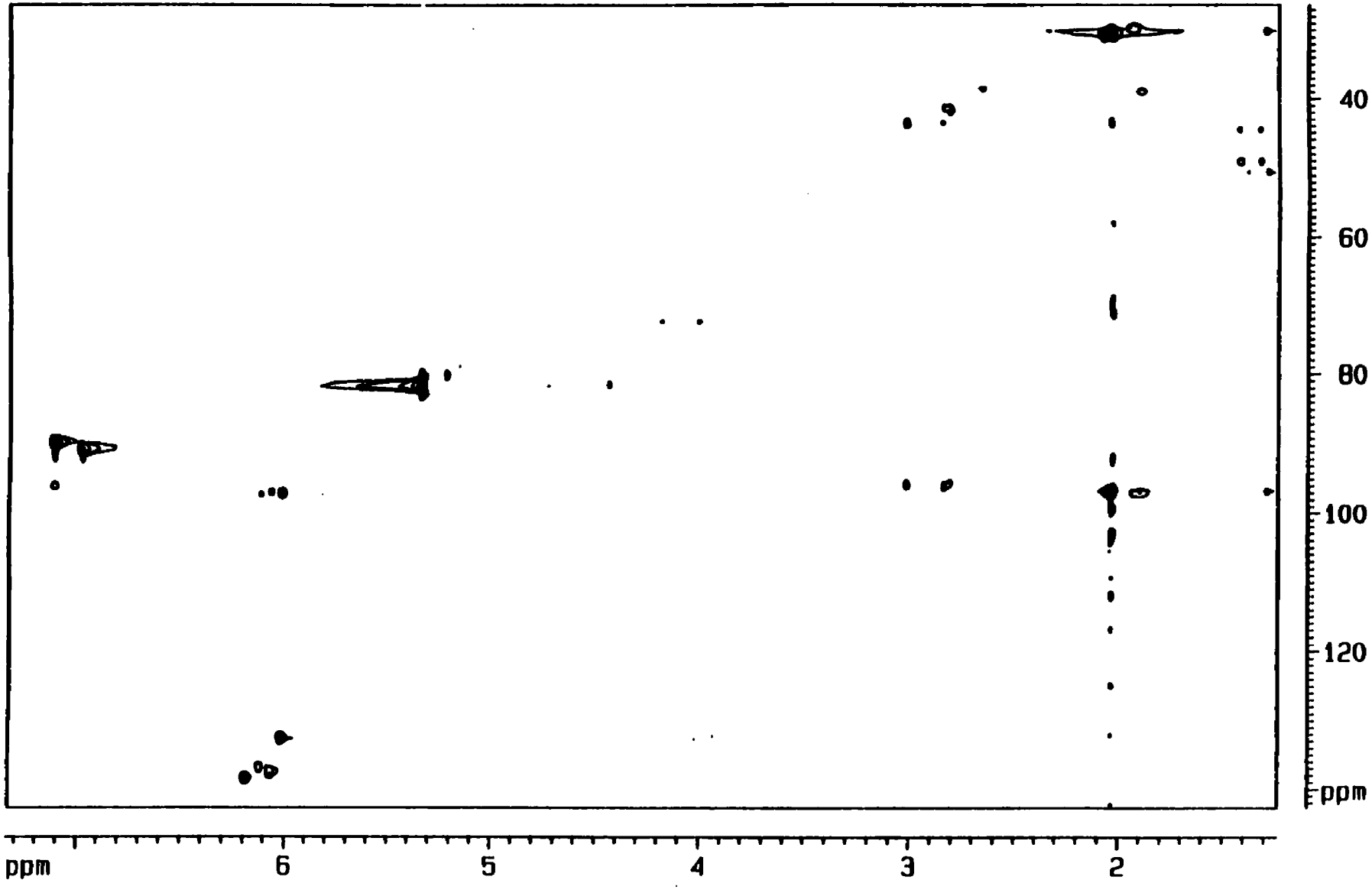

Figure 2.9 (a): CH COSY of complex **2.7** in acetone-d_6.

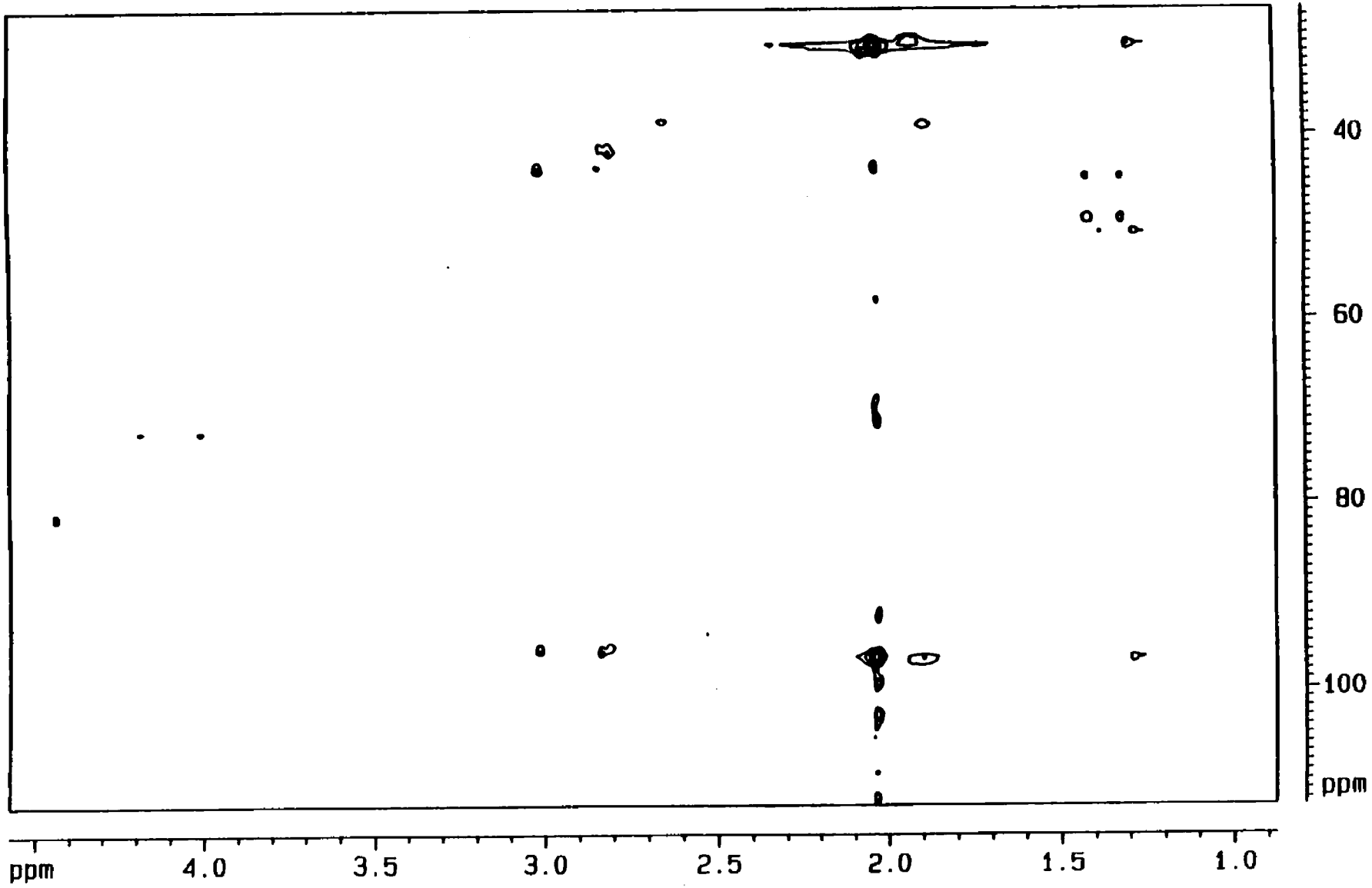

Figure 2.9 (b): Expanded CH COSY of complex 2.7 in acetone-d_6.

complex **2.24** from its parent complex **2.7**, as an example, allowed for some interesting spectral evidence to be obtained. A characteristic number of Cp resonances confirmed the bimetallic nature of this complex. Analysis of the ^{1}H NMR spectrum, as displayed in Figure 2.10, showed two strong singlets at 5.26 and 5.33 ppm. Further confirmation was gained upon examination of the ^{13}C NMR spectrum (Figure 2.11), that shows these same two groups as two strong resonances at 78.19 and 79.71 ppm. In the ^{1}H NMR of complex **2.7** (Figure 2.6), the single Cp resonance is now replaced with two different Cp resonances due to the different magnetic environments of each of the Cp ring protons. Further confirmation was obtained from the aromatic region of the ^{1}H NMR spectra: in contrast to the two sets of doublets that appeared in Figure 2.6 for the complexed aromatic protons, a new resonance at 7.55 ppm was present in Figure 2.10 which is characteristic of the uncomplexed aromatic protons within the central ring of complex **2.24**. An additional complexed aromatic peak at 6.46 ppm indicated the presence of the terminal benzene ring.

Supplementary evidence from the ^{13}C NMR spectrum was used to identify the structure of **2.24**. Peaks due to three additional complexed aromatic carbons at 77.67, 77.99 and 85.87 ppm were assigned to the terminal aryl carbons in this newly modified complex. Further confirmation for the tri-aryl ring system came from two resonances in the uncomplexed aromatic region of the ^{13}C NMR spectrum, appearing at 124.56 and 124.67 ppm. Loss of the resonance at 109.58 ppm (Figure 2.7), representative of the C-Cl quaternary carbon, was fundamental in confirming that nucleophilic aromatic substitution had occurred. The presence of peaks due to two uncomplexed and two complexed aromatic quaternary carbons, further verified the tri-aryl ring system.

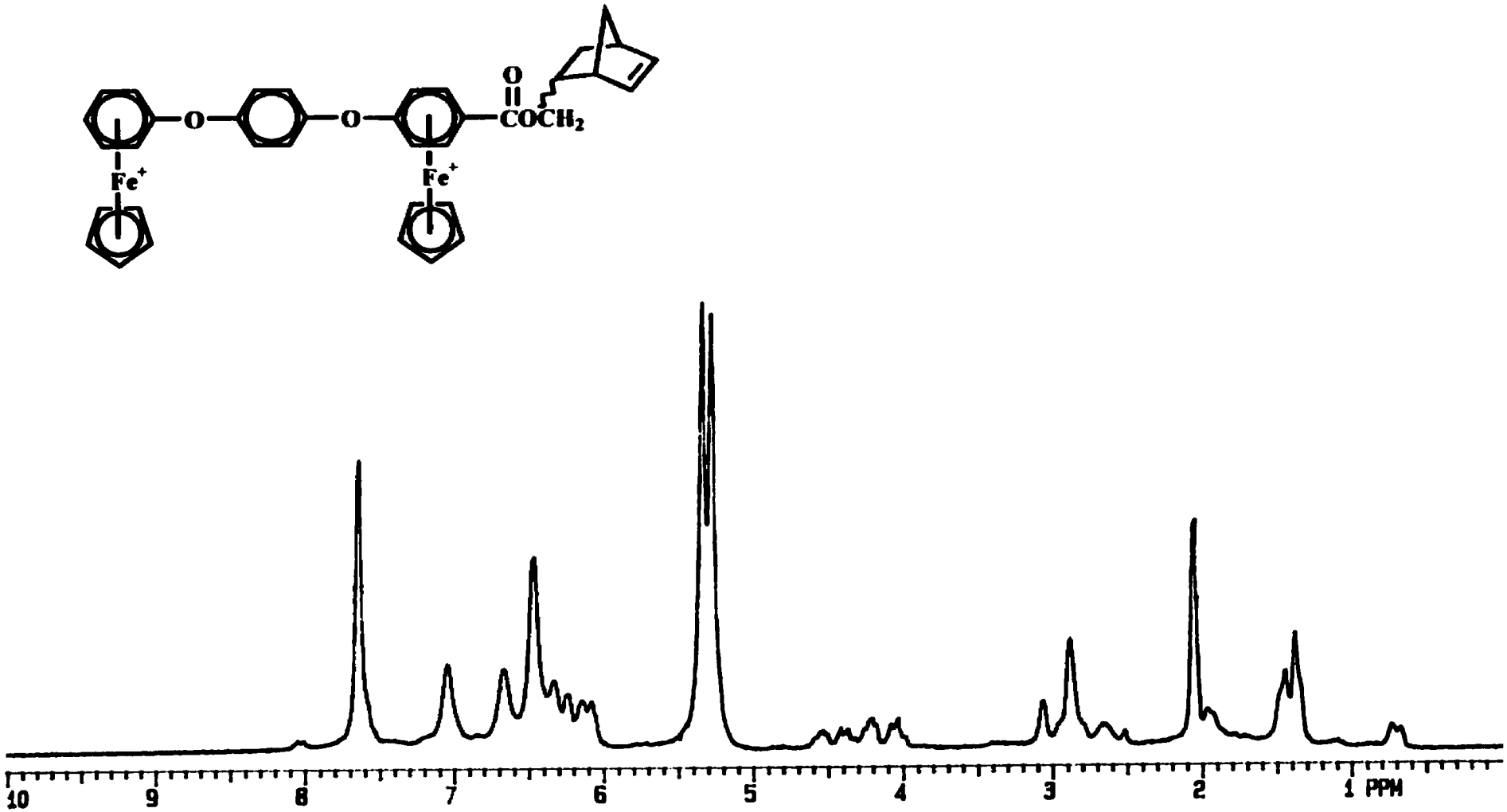

Figure 2.10: ^{1}H NMR of complex **2.24** in acetone-d_6.

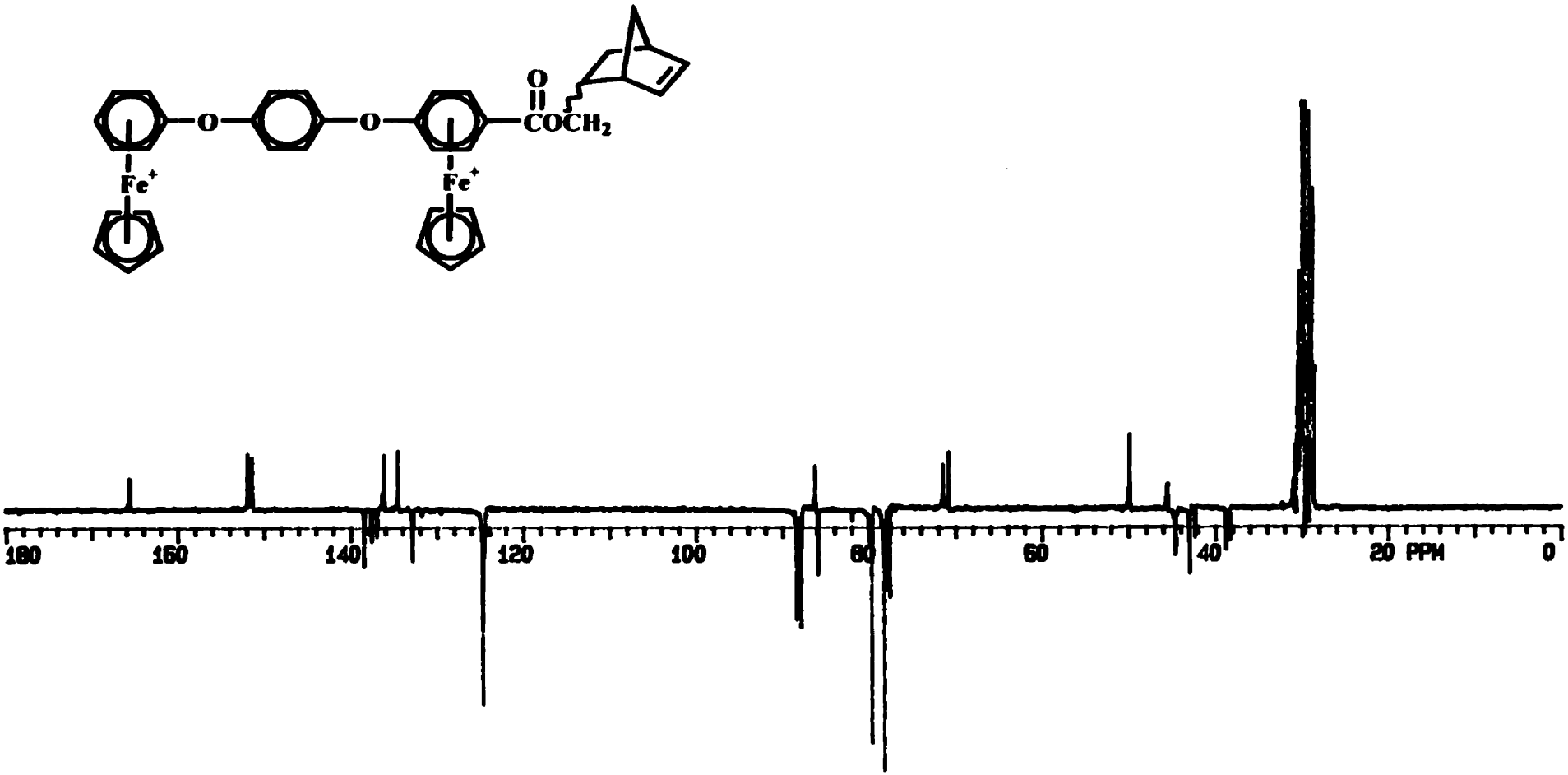

Figure 2.11: ^{13}C NMR of complex **2.24** in acetone-d_6.

Of the quaternary carbon peaks, the one adjacent to the carbonyl group is absent in the NMR spectrum presumably due to overlap by other aromatic carbon resonances. The absence of this peak is in agreement with previous ^{13}C NMR studies of functionalized benzoic acid complexes.[128] Tables 2.6 to 2.9 contain all of the NMR spectral data for complexes **2.24** to **2.27**. All of the analytical data for each of these complexes can also be located in Table 2.10.

2.2.2.3 NMR Spectral Investigations of Uncomplexed Aryl Ether Norbornene Monomers

Isolation of the organic monomer by removal of the $CpFe^+$ moiety was accomplished by photolytic demetallation. The organic nature of compound **2.8** was confirmed by the loss of the Cp resonance in the ^1H NMR (Figure 2.12), which previously appeared at 5.28 ppm in the spectrum of complex **2.6**. This is further verified by the ^{13}C NMR spectrum (Figure 2.13) which shows no signal in the range of 77-80 ppm, the characteristic region for Cp carbon resonances.[129] Another identifying feature is the downfield shift of the aromatic protons from 6.72-7.05 ppm in the complexed monomer to 7.44-8.07 ppm in the demetallated compound, which is in agreement with previous findings for loss of the metallic moiety.[128] The ^{13}C NMR spectrum provided substantial evidence for the uncomplexed nature of the aromatic ring. This was confirmed by the loss of aromatic resonances in the complexed region of the spectrum (89.40, 89.96 and 90.94 ppm) which normally appear significantly more upfield than those due to the uncomplexed aromatic carbons (128.26, 129.50 and 132.73 ppm).

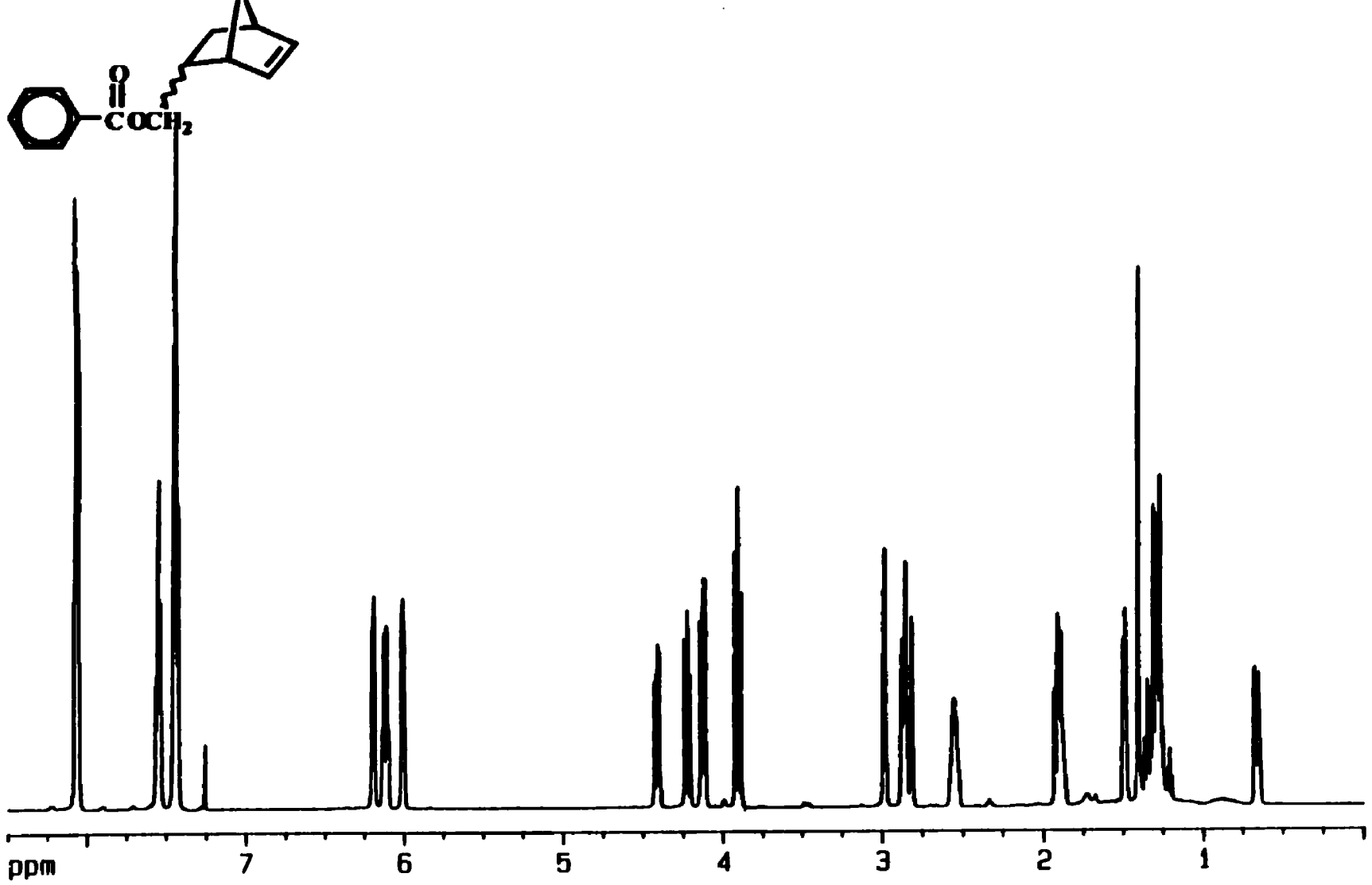

Figure 2.12: ^{1}H NMR of monomer **2.8** in $CDCl_3$.

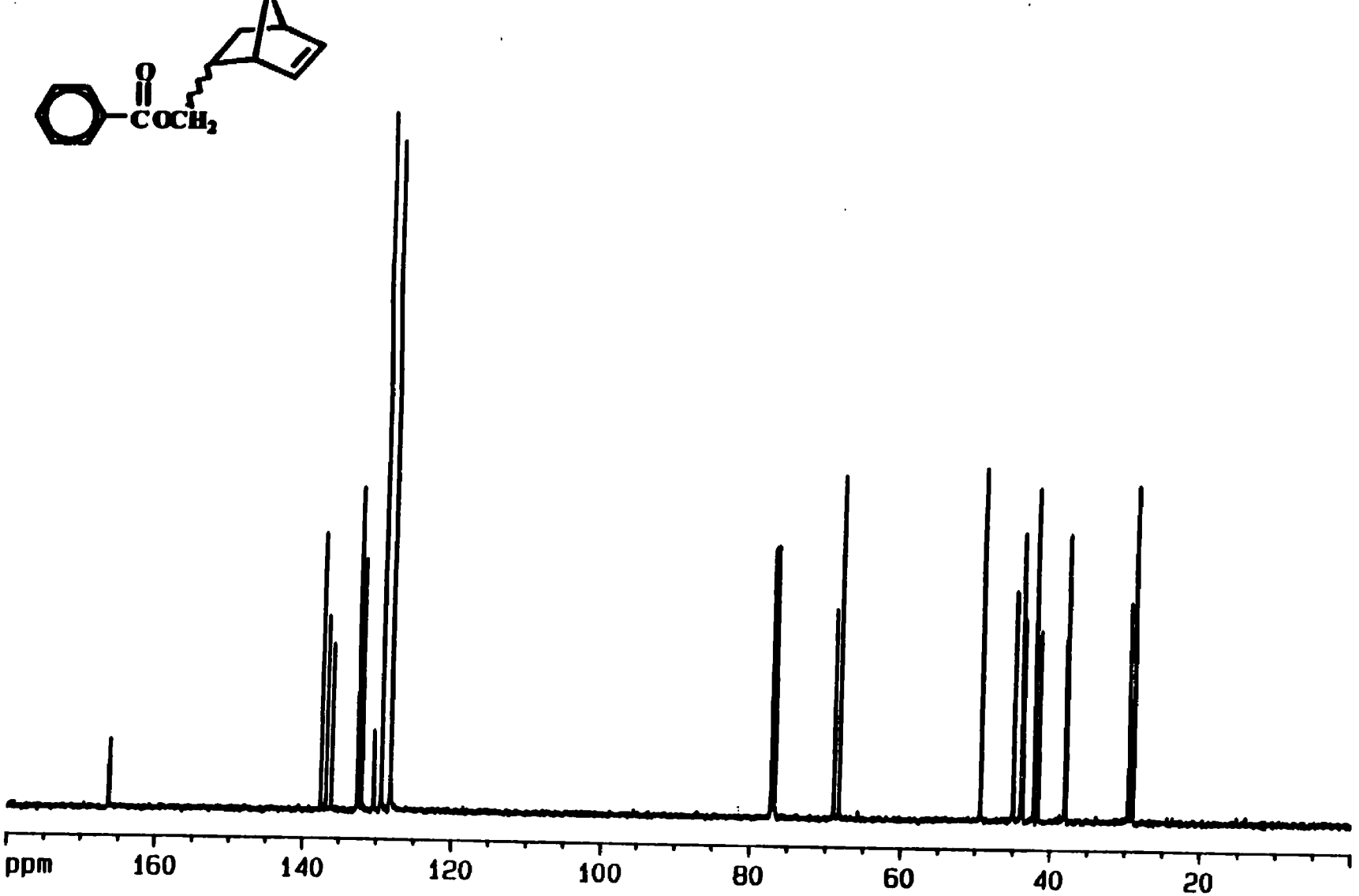

Figure 2.13: ^{13}C NMR of monomer **2.8** in $CDCl_3$.

As well, a slight upfield shift of the bridge methylene proton resonances was observed moving from 4.05 – 4.56 ppm in the ^{1}H NMR spectrum of **2.6** up to 3.91 – 4.42 ppm in **2.8**.

2-D NMR techniques coupled with 1-D spectral information were used to distinguish each of the *exo* and *endo* isomers of **2.8**. Location of signals due to the characteristic methylene protons contained in the ester-bridge gave a useful starting point for the analysis. Based on previous studies of the metallated norbornene complexes, tentative assignment of the two most upfield methylene resonances (3.91 and 4.13 ppm) in the ^{1}H NMR spectrum were attributed to the *endo* isomer. The HH COSY NMR spectrum shown in Figures 2.14 (a and b) revealed a connectivity between these methylene protons and a broad multiplet at 2.99 ppm. Since this proton was coupled to another proton at 2.55 ppm (the region of the bridgehead protons) it was concluded that this latter peak was H_1 and the broad multiplet was the *exo* H_2 proton. As described previously for the metallated monomers, no coupling is observed between the *endo* H_2 proton and the bridgehead H_1 proton. This confirmed that the observed H_2-H_1 connectivity was representative of the *endo* isomer. Analysis of the H_1 proton resonance in the HH COSY spectrum showed a crosspeak intersecting with a contour in the olefinic region of the spectrum. Since H_1 will couple with H_6 and not H_5, this coupling allowed for identification of the H_6 olefinic proton within the *endo* isomer at 6.01 ppm [$J_{(1,6)}$ = 2.8 Hz]. Identification of H_5 at 6.20 ppm was accomplished by the moderately strong vicinal coupling it displayed to H_6 [$J_{(5,6)}$ = 5.7 Hz]. This enabled the identification of the bridgehead H_4 proton based on an observed coupling constant of 3.0

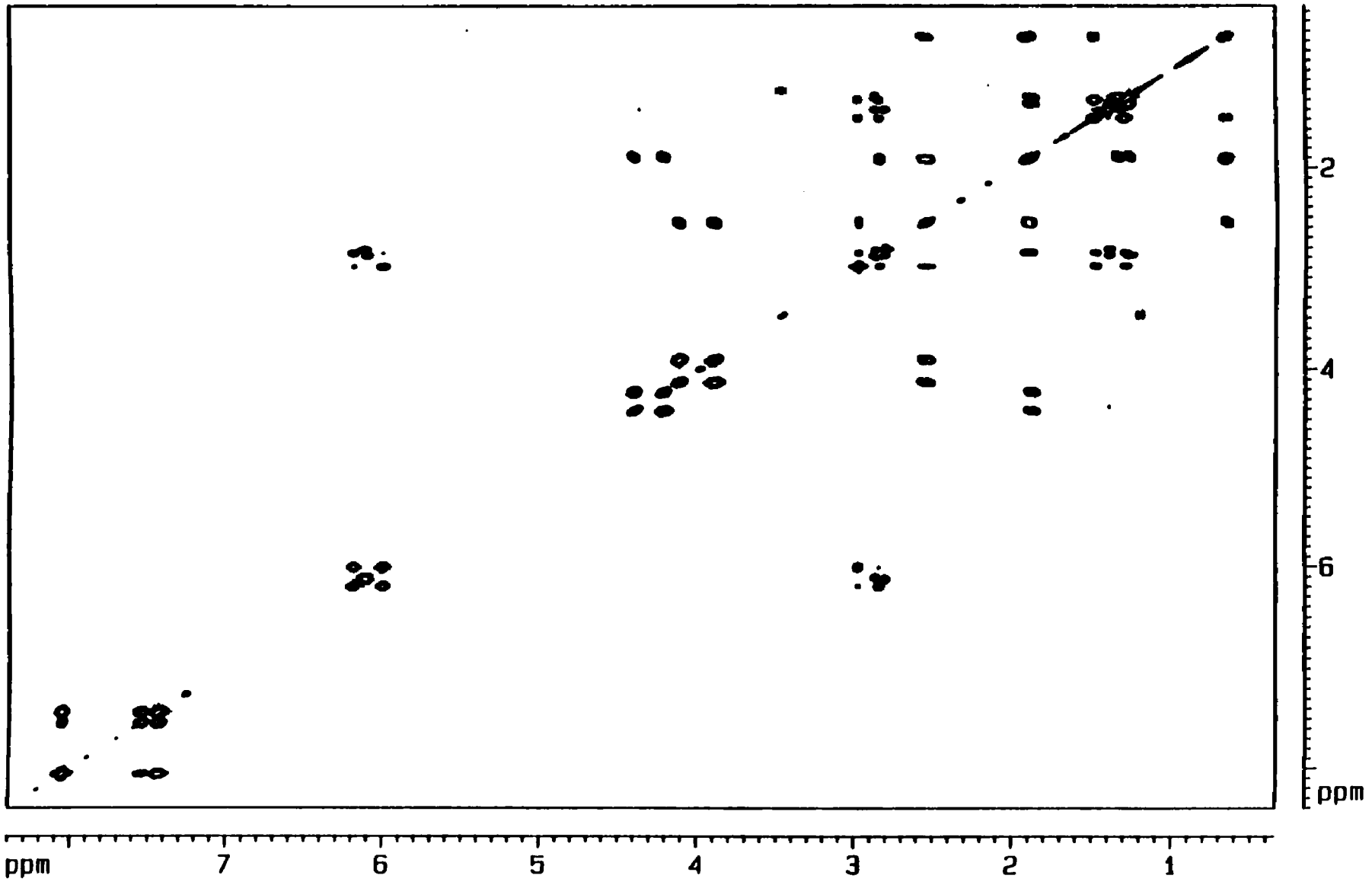

Figure 2.14 (a): HH COSY of monomer **2.8** in $CDCl_3$.

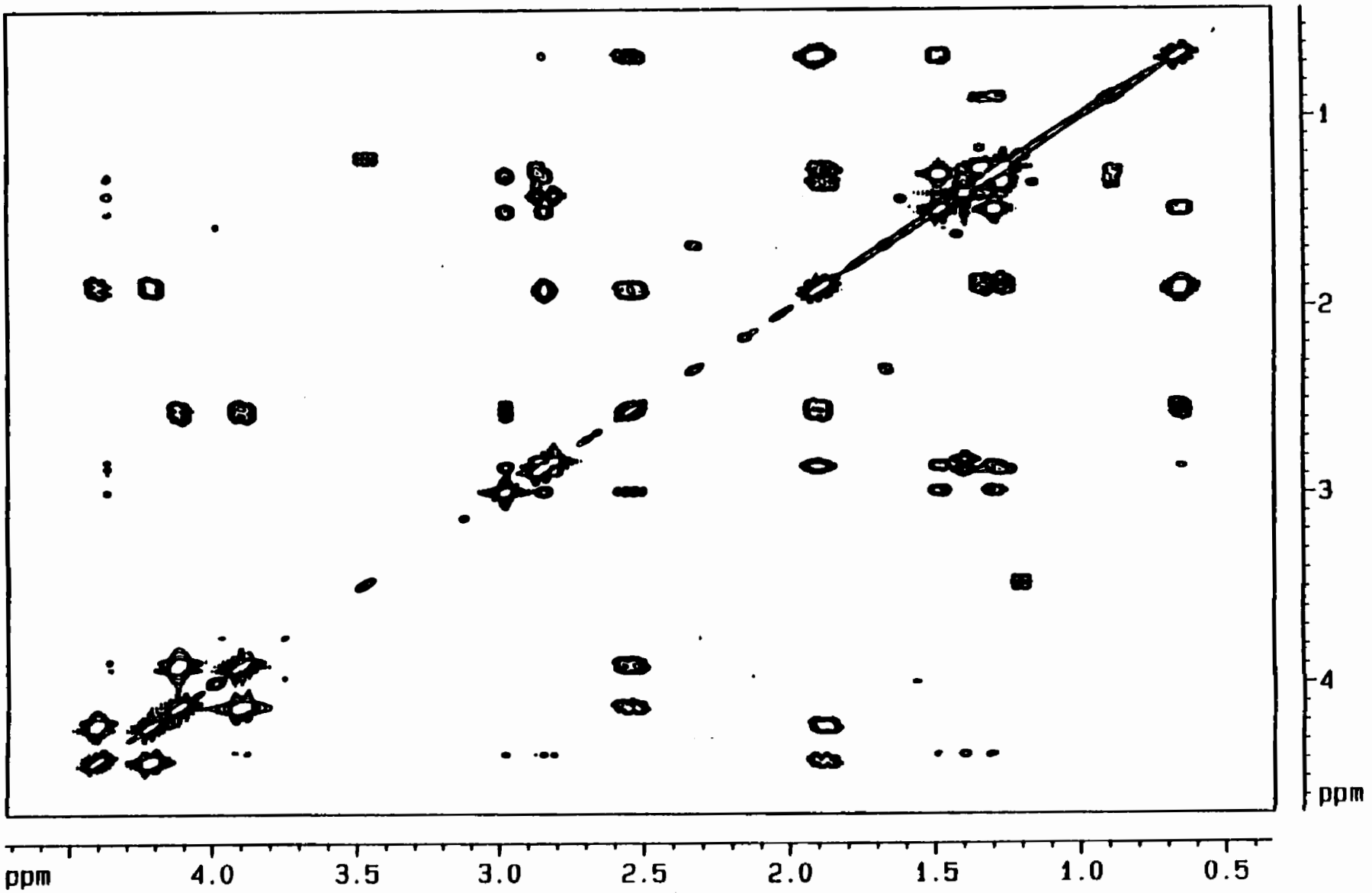

Figure 2.14 (b): Expanded HH COSY of monomer **2.8** in $CDCl_3$.

Hz [$J_{(4,5)}$]. As with the coupling for the *exo* H_2 proton to H_1, H_4 displayed only a coupling with H_{3x}, the signal which appeared at 1.90 ppm and had a $J_{(3x,4)}$ coupling of 3.8 Hz. The signal for H_{3n} was identified because of its strong geminal coupling with H_{3x}. The HH COSY NMR spectrum displayed a rather large contour as a crosspeak to H_{3n}, which intersected the diagonal at 0.67 ppm. Measurement of the coupling constant for this proton was 11.7 Hz for $J_{(3x,3n)}$, which is a typical geminal coupling. Further verification that this proton signal at 0.67 ppm arose from the *endo* isomer was due to its connectivity to the *exo* H_2 proton, which was already assigned to the *endo* isomer. The transoidal coupling constant for these two protons was calculated as 4.2 Hz, which is in agreement with previous findings for compounds of similar nature.[141]

Assignment of the carbon atom NMR signals was accomplished using the 2-D NMR technique previously described as HETCOR. This was achieved based upon the proton-carbon connectivities that could be extracted from this heteronuclear correlation spectrum, which is shown in Figures 2.15 (a and b). For a complete review of all the NMR data for the mono-aryl compounds **2.8**, **2.9** and **2.14**, Tables 2.11 - 2.15 have been included. Analytical characterization has also been included and is shown in Table 2.23.

Using this analysis of the monoaryl compounds, the tri- and penta-aryl norbornene monomers were much simpler to characterize. For compound **2.31**, it can be seen in the ^1H NMR spectrum, in Figure 2.16, that three Cp resonances originally present at 5.22, 5.34 and 5.42 ppm are absent. This was further confirmed using ^{13}C NMR analysis, which verified the absence of the Cp resonances originally appearing at 78.60, 79.08 and 79.73 ppm (Figure 2.17). Further proof of decomplexation was the upfield shift of the methyl group resonance; appearing at 2.52 ppm in complex

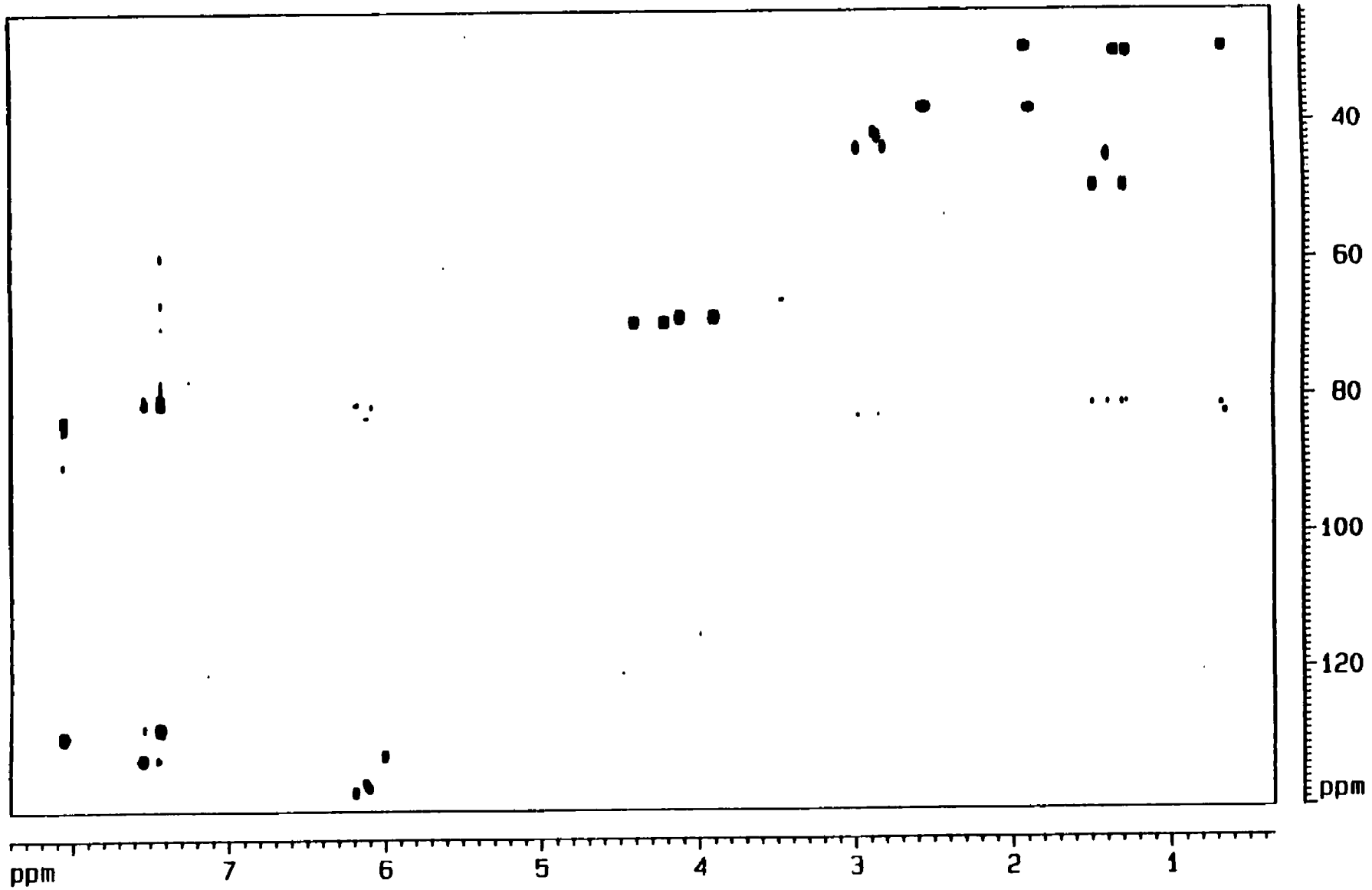

Figure 2.15 (a): CH COSY of monomer **2.8** in $CDCl_3$.

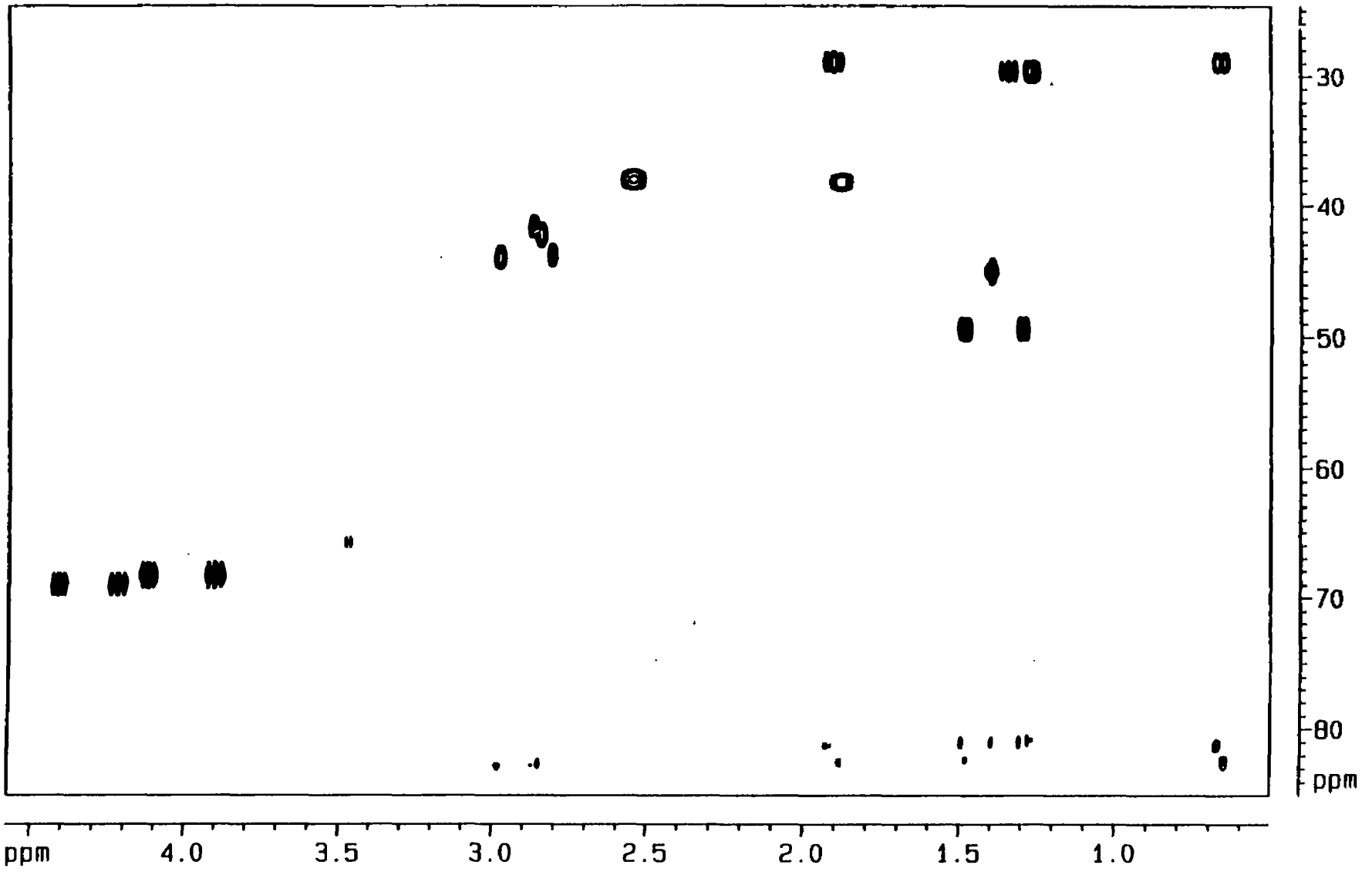

Figure 2.15 (b): Expanded CH COSY of monomer **2.8** in $CDCl_3$.

2.27, this peak shifts to 2.33 ppm in the organic monomer. As previously observed for the monoaryl derivatives, a downfield shift of the aromatic protons was observed, allowing for an unhindered view of the olefinic proton resonances. Further NMR spectral information can be obtained in Tables 2.16 to 2.22 for compounds **2.28** to **2.31**. All other analytical data has been compiled in Table 2.23, which can be used to further characterize these aromatic ether functionalized norbornene monomers.

2.2.3 Synthesis of Aryl Ether Functionalized Polynorbornenes

ROMP of these aromatic ether functionalized norbornene monomers was accomplished using bis(tricyclohexylphosphine)benzylidene ruthenium (IV) dichloride otherwise known as "Grubbs' catalyst". Initial studies of the ROMP reaction focused on optimizing the reaction conditions in an attempt to achieve high molecular weight polymers with narrow polydispersities. This was accomplished by investigating the influence that various monomer to initiator ratios ([M]:[I]) had on the polymeric materials. All polymerizations were carried out using dichloromethane as the solvent, since previous findings reported the highest degree of polymerization in this medium.[33] A series of polymerizations were carried out using monomer **2.8** while varying the ratios of [M]:[I] by 25-, 50-, 100- and 150:1. Weight average molecular weights (Mw) and number average molecular weights (Mn) were determined using gel permeation chromatography (GPC). Calibration of the instrument versus polystyrene standards determined that when using ratios of 25:1 and 50:1, low Mw's of 8, 400

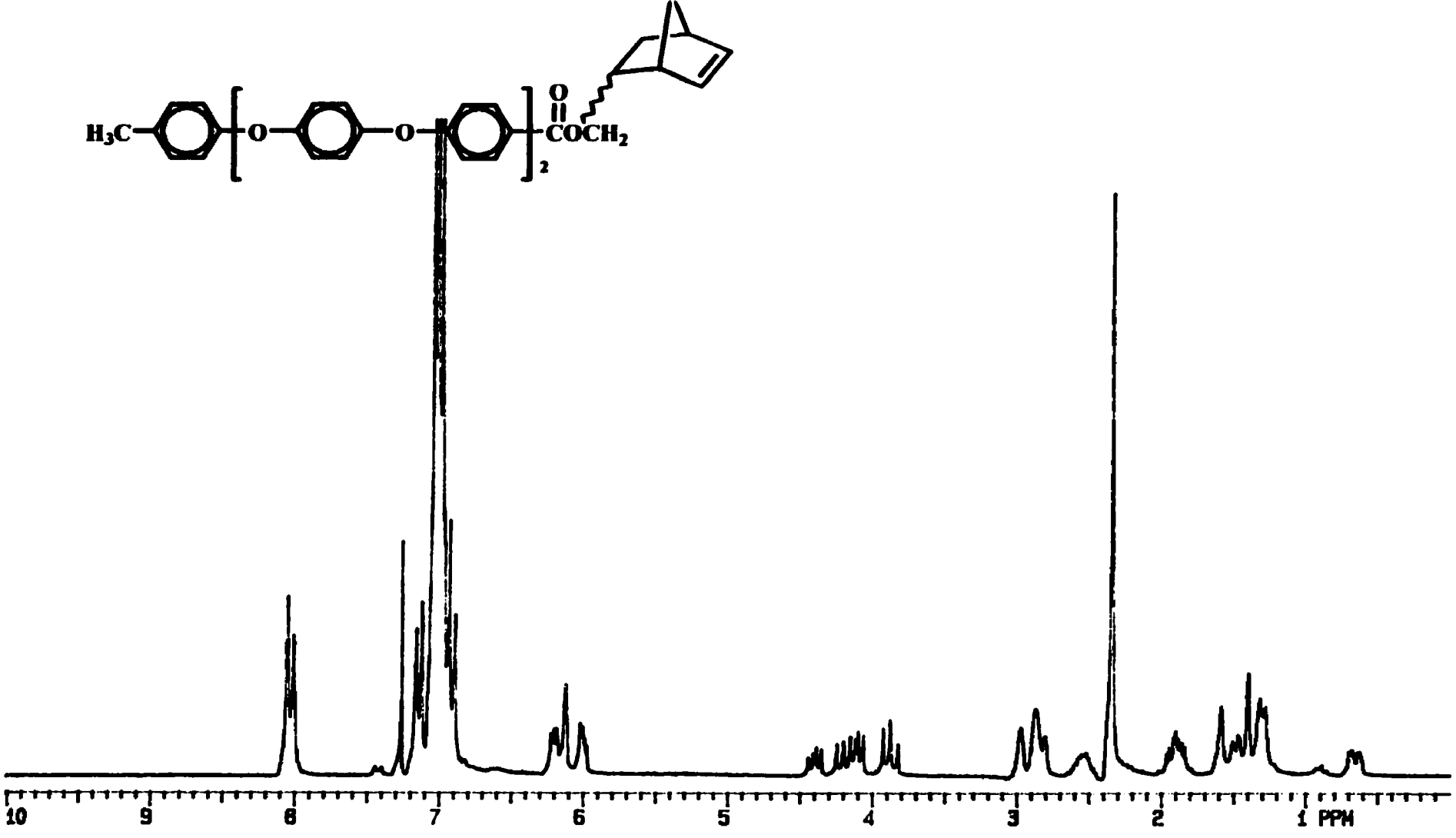

Figure 2.16: ^{1}H NMR of monomer **2.31** in $CDCl_3$.

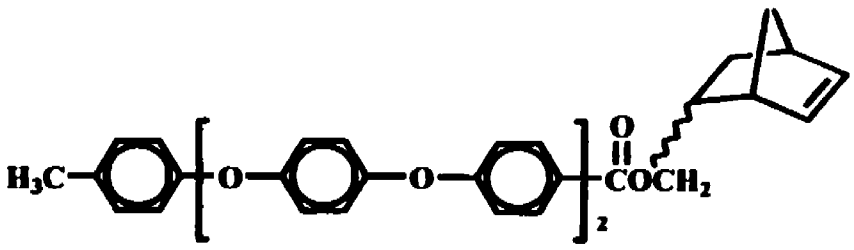

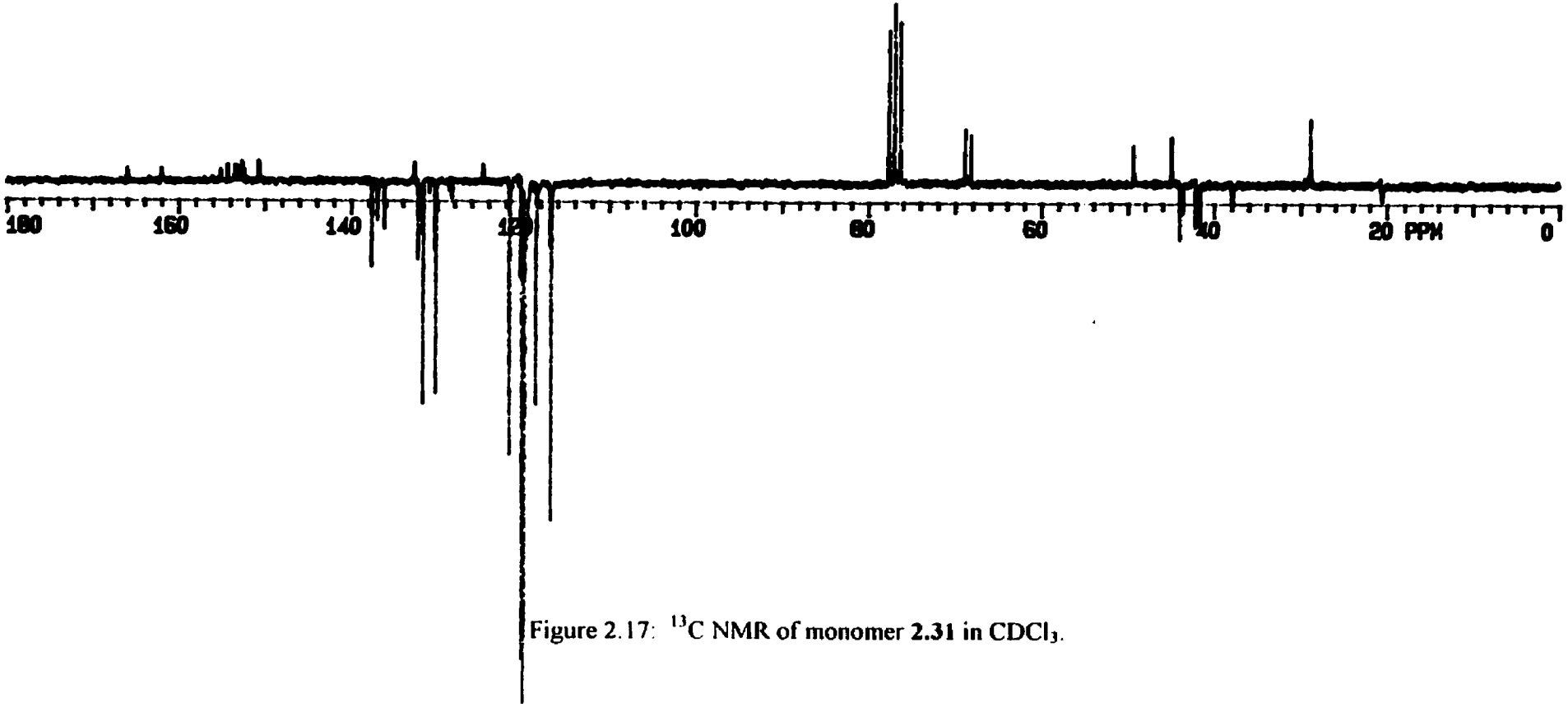

Figure 2.17: ^{13}C NMR of monomer **2.31** in $CDCl_3$.

and 16 000 g/mol with PDI's of 2.4 and 2.7, respectively, were obtained. Next, using a substrate:catalyst ratio of 100:1, a polymer having an Mw of 108,000 g/mol and a PDI of 1.9 was prepared. These results were quite promising as a much larger Mw was obtained with a reduction of the PDI. In an attempt to improve these conditions, a larger 150:1 ratio was investigated. Significantly higher Mw's were obtained (511,000), but this was accompanied with a much higher PDI (3.0). Therefore, as a means to maintain high molecular weights with narrow polydispersities, ratios of 100:1 were used in subsequent experiments. Table 2.24 can be referred to for comparison of these GPC data.

A typical synthesis of the polymeric materials, as shown in Scheme 2.9, was accomplished by weighing out the appropriate amount of catalyst in a glove box such that a ratio of 100:1 of monomer to initiator was used. The catalyst was then dissolved in an amount equivalent to 0.5 mL of dichloromethane per each 100 mg of monomer used in the ROMP reaction. Polymerization was initiated by subsequent addition of the catalyst to a solution of the monomer in dichloromethane, using an airtight syringe. The reaction was then stirred under an inert nitrogen atmosphere at room temperature until a gelatinous material formed. Polymers **2.32 – 2.34** generally formed within 1 – 2.5 h, however, polymers **2.35 – 2.38** formed within 5 min. An excess of ethyl vinyl ether was then used to cleave the catalyst from the polymer chain. The resulting white material was then purified upon dissolution in a minimum amount of dichloromethane or chloroform and finally precipitated into cold methanol. Isolation of the off-white, fibrous materials yielded polymers **2.32 – 2.38** in yields ranging from 66 – 90%, which are typical of conversion rates of monomer to polymer when using Grubbs' catalyst.[143] GPC analysis of polymers **2.32 – 2.38** showed Mw's ranging from 63 000 to 462 000 g/mol and Mn's

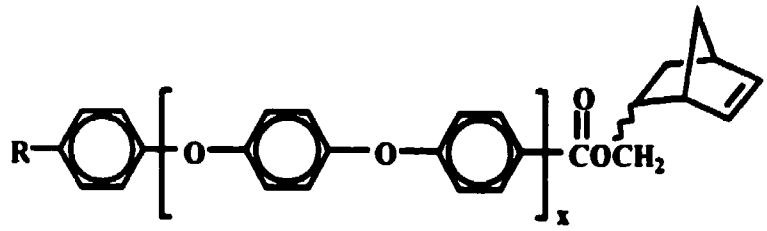

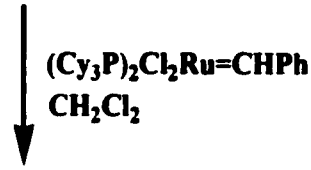

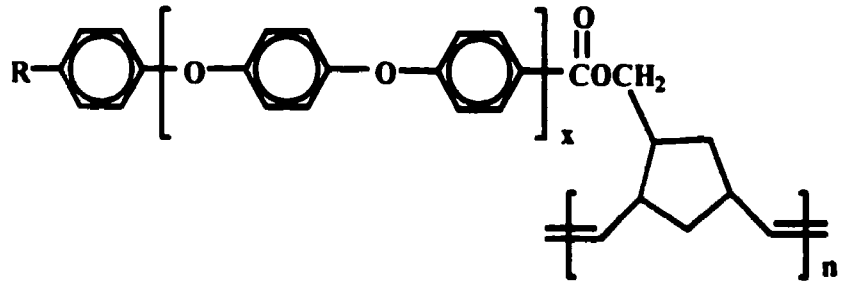

monomer	R	polymer	x
2.8	H	2.32	0
2.9	Cl	2.33	0
2.14	CH_3	2.34	0
2.28	H	2.35	1
2.29	CH_3	2.36	1
2.30	H	2.37	2
2.31	CH_3	2.38	2

Scheme 2.9

ranging from 44 000 to 195 000 g/mol. Polydispersities ranged from 1.1 to 2.4. Table 2.25 provides a detailed overview of the respective Mn's, Mw's, PDI's and yields for each of these polymers.

Assessment of the living nature of the above-mentioned polymerizations was accomplished upon the preparation of a homopolymer (**2.39**) of monomer **2.8**. As described in chapter one, for a polymerization to be considered living, consumption of the monomer must proceed such that initiation is faster than propagation. Preparation of the homopolymer proceeded in a two step synthesis involving the initial preparation of polymer **2.32**. Knowing that monomer **2.8** would polymerize to completion in 1 h, an aliquot of polymer solution was removed at this time and worked up using ethyl vinyl ether and methanol. At the same time this aliquot was removed, another aliquot of monomer was added to the stirring polymer solution. If the polymerization was a living system, the added monomer should continue to be used up in chain propagation without increasing the polydispersity index from that obtained for the first aliquot of polymer.[23]

GPC analysis of the two polymers prepared using this methodology revealed that the second polymer displayed a much higher Mw than that of the polymer removed after 1 h of reacting. Analysis of the GPC trace revealed a Mw of 22,600 g/mol for the first polymer whereas the second polymer had a much higher Mw of 108,000 g/mol. Another exciting result was the decrease in the PDI from polymer one (PDI = 2.8) to polymer two (PDI = 1.9). This decrease in molecular weight distribution indicates that the molecular weight of the polymer did not increase from back-biting within the polymer chain, but from additional monomer initiation and propagation. Therefore, it is this gain in Mw and decrease in the PDI that establishes the living nature of this polymerization.

Investigation of the solubilities for each of these polymeric materials was essential for determining their potential processibility. Each of the polymers had their solubilities examined in chloroform ($CHCl_3$), dimethylacetamide (DMAc), dimethylformamide (DMF) and dimethylsulfoxide (DMSO). Polymers **2.32 – 2.34** demonstrated excellent solubility in $CHCl_3$ and DMAc at room temperature, however, only minimal solubility in DMF and DMSO was observed. With regards to the longer aromatic ether functionalized polynorbornenes (**2.35 – 2.38**), only $CHCl_3$ gave minimal dissolution of the polymer at room temperature. Increased solubility of these polymers was noted upon refluxing in $CHCl_3$ for several hours.

Identification of the structural features of the polymers was accomplished primarily using ^{1}H NMR spectroscopy. For polymer **2.32**, indication that polymerization had successfully taken place was identifiable by the loss of the olefinic resonances from 6.01 – 6.20 ppm in the monomer (**2.8**). The appearance of new olefinic resonances at 5.20 - 5.40 ppm in the polymer was indicative of the unsaturated polynorbornene backbone. Examination of this single broad peak implied that the polymer microstructure existed in the trans geometry. Further evidence for this stereochemistry was achieved based upon previous studies detailing the favored orientation of the *trans* mictrostructure when using Grubbs' catalyst, $(Cy_3P)_2Cl_2Ru{=}CHPh$.[71, 143] Therefore, it can be said with confidence that the vinylene units exist in the trans configuration. Further analysis of the ROMP spectrum denoted the collapsed broad peaks of the methylene bridge protons appearing from 4.05 - 4.40 ppm for **2.32**. Since all of the peaks were quite broad, it can be concluded that the polymer did in fact form as peak broadening is characteristic of polymer formation. For the purpose of comparing the ^{1}H NMR spectra for monomer **2.8**

and its polymer **2.32**, Figure 2.18 has been included. Further ^{1}H NMR data for each of the polymers can be found in Table 2.26.

Analysis of the ^{13}C NMR spectrum, shown in Figure 2.19, provided minimal structural characterization features due to the complicated spectra arising from the contributions of head-head, head-tail and tail-tail conformations in the polymer microstructure. Also, due to the chiral nature of the C_2 bond to the methylene-bridged carbons, this further complicated the spectral analysis rendering the investigation futile. Of the information obtained in the spectrum for **2.32** were the aromatic carbons at 128.27, 129.51 and 132.76 ppm and the quaternary carbon at 130.42 ppm. Further information extracted from this spectrum were the carbonyl resonances at 166.61 and 166.47 ppm as well as the methylene bridge carbons at 66.56 and 67.72 ppm. Identification of the extreme upfield cyclopentane resonances, which normally discloses information concerning the syndiotactic, isotactic or atactic nature of the polymer chain,[1-3] was not possible due to the congested aliphatic carbon resonances that were present in this region.

Further confirmation of the structural features of the modified polynorbornenes was obtained via FT-IR spectroscopy. The carbonyl absorptions in the IR spectrum were observed in the region of 1712 to 1718 cm^{-1}. Table 2.26 contains a listing of the individual CO absorptions for each of the polymers. Spectral verification of the *trans* geometry of the double bond in the unsaturated polymer backbone was also apparent using this technique. This was accomplished by looking at the regions where *cis* and *trans* absorptions should appear. Previous studies involving analysis of the polynorbornene microstructure using IR techniques have detailed that the *cis* in-plane

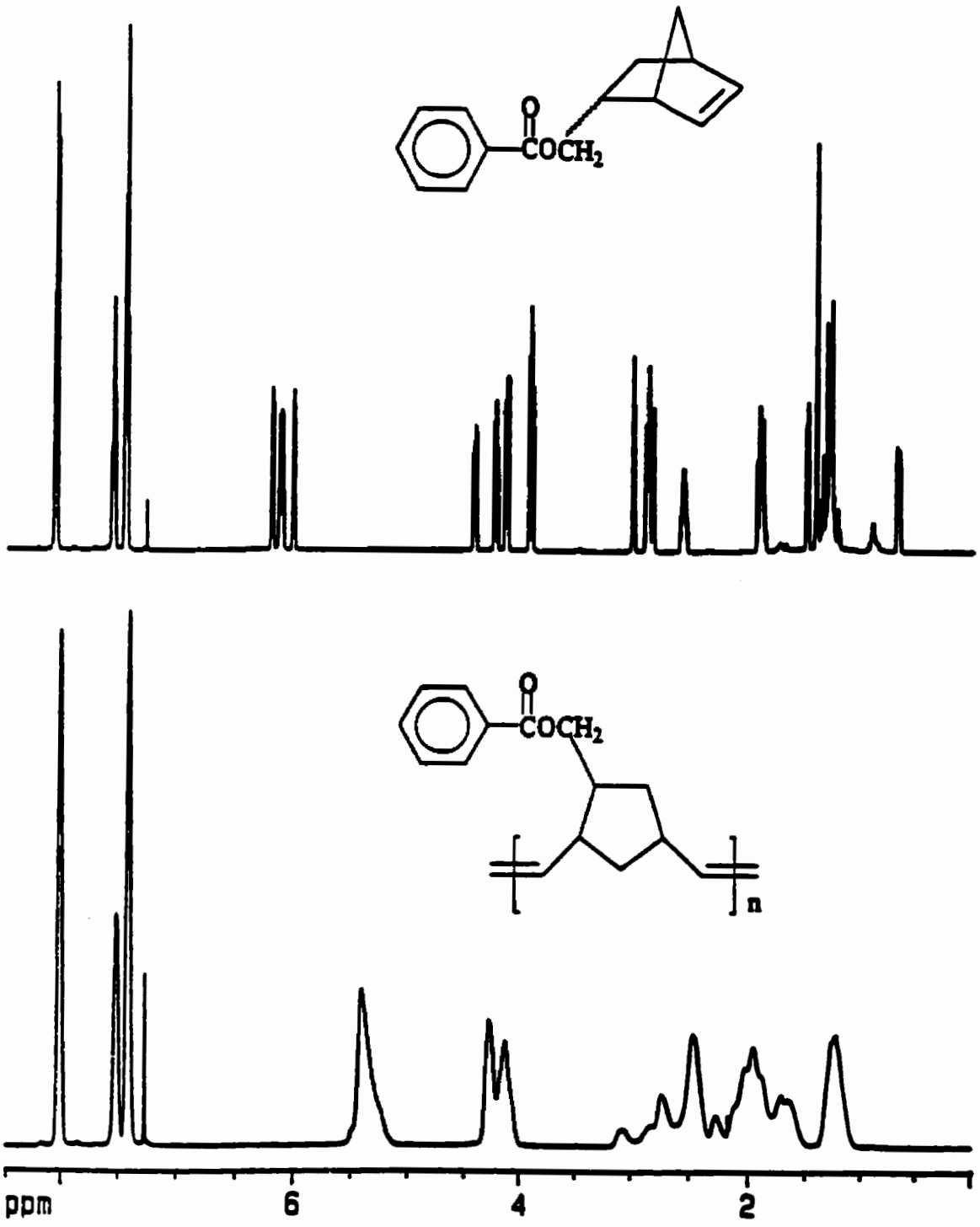

Figure 2.18: ^{1}H NMR of monomer **2.8** and polymer **2.32** in $CDCl_3$.

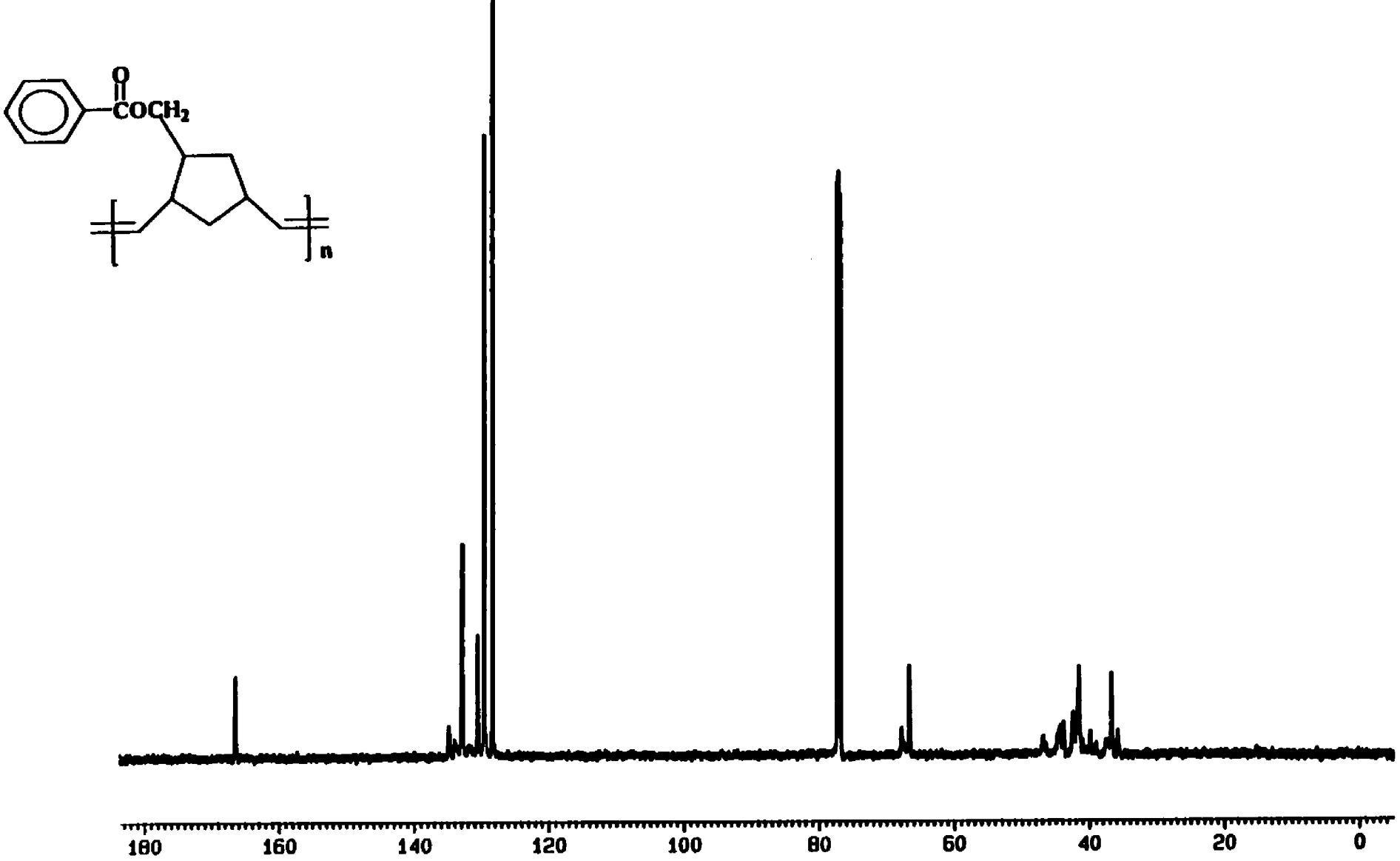

Figure 2.19: ^{13}C NMR of Polymer **2.32** in $CDCl_3$.

=C-H bending occurs at 1404 cm^{-1} and 740 cm^{-1}, where as the *trans* appears at 960 cm^{-1}.[144] Upon comparison of the IR spectra of monomer **2.8** and polymer **2.32** a noticeable absorption at 969 cm^{-1} was observed in the polymer spectrum. In addition, the absence of absorptions in the regions of 1404 and 740 cm^{-1} indicated the lack of *cis* conformer in the polymer. Table 2.26 contains a complete listing of *trans* absorptions for polymers **2.32 - 2.38**. As a result of the combined IR and ^1H NMR spectral data each of the polymers were found to contain a high percentage of *trans* geometry within their structural conformation.

Thermal analysis of each of the polymers was accomplished using differential scanning calorimetry (DSC) and thermogravimetric analysis (TGA). Polynorbornene has a very low glass transition (Tg) of 35 °C,[144] which is defined as the temperature at which the polymers amorphous regions become somewhat glassy, meaning brittle, stiff and rigid.[145, 146] This value is highly reflective of the mechanical motion within the polymer, known as segmental motion. Therefore, the value for a Tg defines how the polymer will respond mechanically at a specified temperature and thus is a variable useful in assigning how the material will be processed and used.[145, 146] A similar trend was observed for the aryl ether functionalized polynorbornenes such that as the length of the aromatic ether chain increased, so did the Tg's. For polymer **2.32** containing a single aryl group in every repeat unit, a well-defined Tg was present at 54.7 °C. Increasing the number of aromatic groups, the Tg in the tri-aryl ring system (**2.35**) was found to dramatically increase to 67.6°C and reached as high as 73.3 °C for the penta-aryl derivative (**2.37**), as can be seen in Table 2.27 and in the DSC thermogram shown in Figure 2.20. These results clearly show a correlation between the length of the aryl ether chain and the glass

transition temperature such that as the length of the aryl ether chain increases, an increase in the overall thermal stability of the functionalized polynorbornenes is also observed.

A similar response was observed with the *p*-methylated derivatives displaying higher Tg's as the length of the pendent aryl ether chain increased. The effects of incorporating a methyl substituent were difficult to measure due to the small temperature differences that existed between the methylated and nonmethylated polymers. The expected increase in the glass transition temperature upon incorporating the more bulky methyl group was proposed based upon the reduced segemental motion that was anticipated. This improved thermal behavior was observed only for polymers **2.32** and **2.34** which displayed well defined Tg's at 54.7 °C and 61.8 °C, respectively. However, as only slight variations existed between **2.35** and **2.36** as well as between **2.37** and **2.38**, it was difficult to attribute these temperature differences solely to the methyl group. Since it is well known that differences in Mw can also influence the appearance of the Tg, these temperature variations were likely due to a contribution of both the methyl group and Mw differences.

TGA was employed to assess the decomposition temperatures of the resulting polymers. As from the DSC analyses, it was further confirmed that as the number of aryl ether linkages increased so did the thermal stability of the polymers. Polymer **2.32** displayed a decomposition at 417.0 °C as shown in Figure 2.21 which increased to 422.4 °C for the tri-aryl ether system (**2.35**) and up to 460.2 °C for the penta-aryl ether containing polymers (**2.37**). These results were expected due to previous findings for industrially prepared engineering thermoplastics such as PEEK or PAEKs, which demonstrate increased thermal properties as the number of aromatic ether units in the

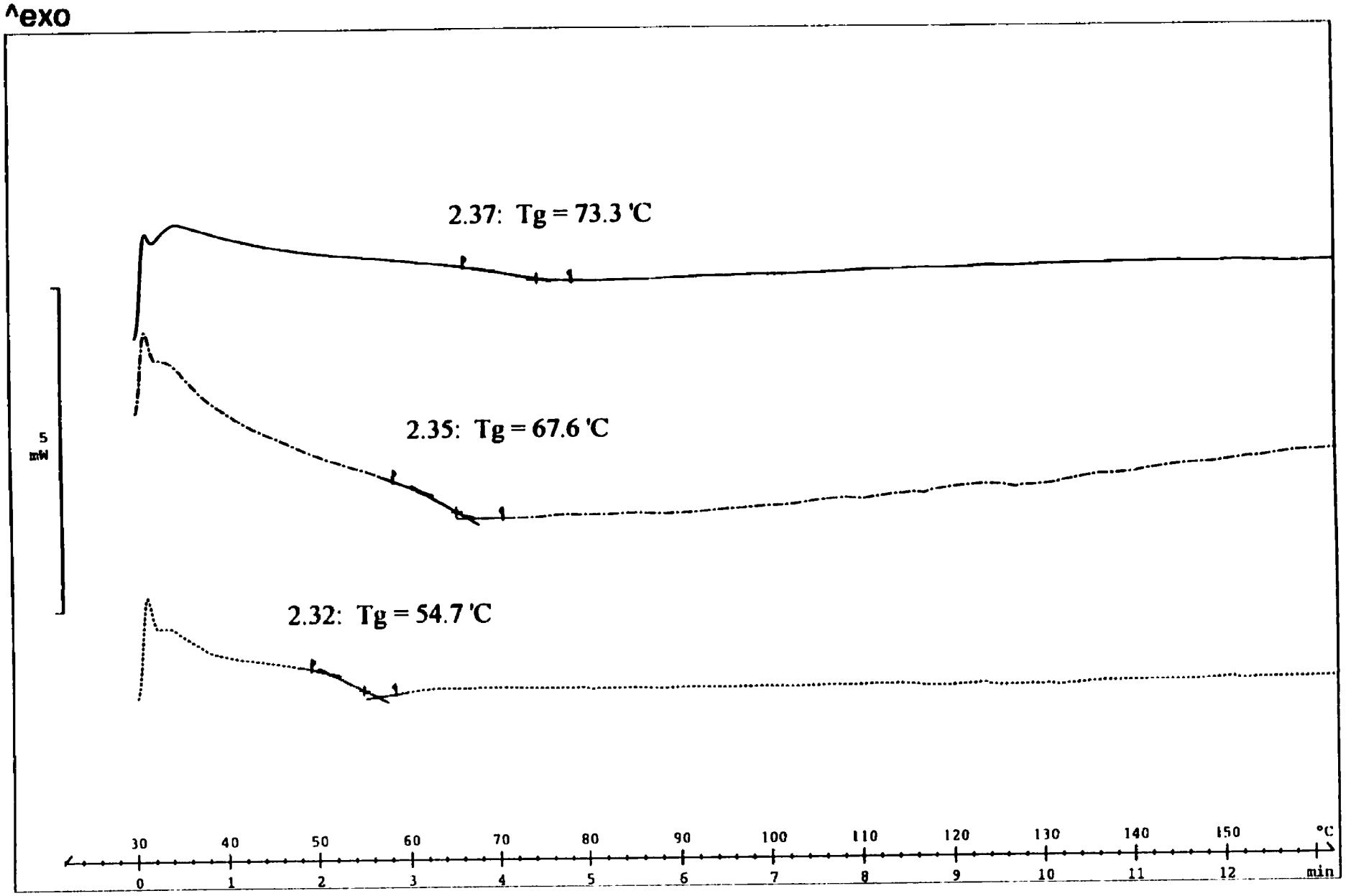

Figure 2.20: DSC Thermogram of Polymers **2.32, 2.35** and **2.37**.

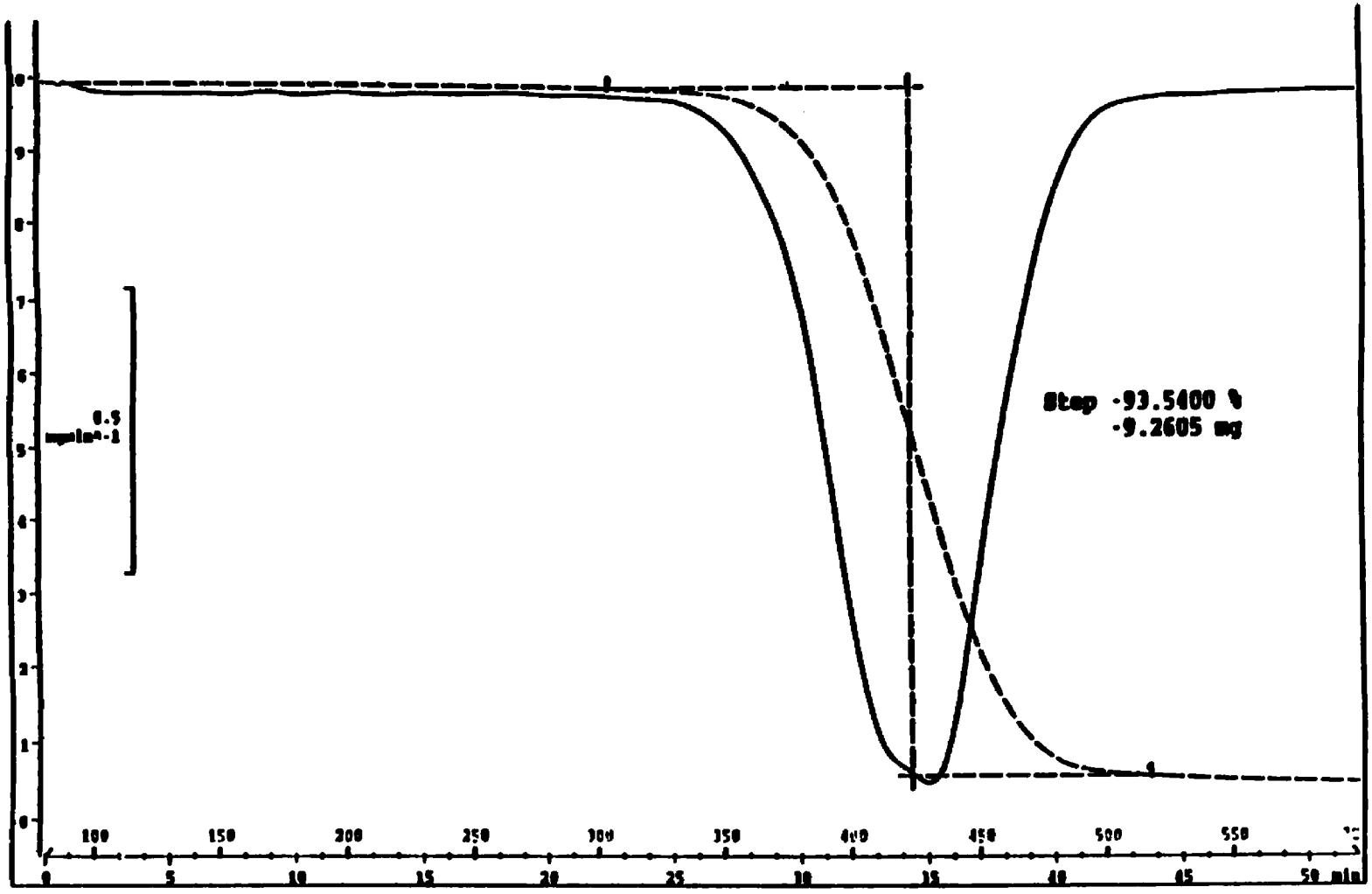

Figure 2.21: TGA Thermogram of Polymer **2.32**.

polymer backbone increases.[77] A full list of thermal data is provided in Table 2.27 for each of the polymers prepared during this investigation.

2.3 Conclusion

In summary, it has been shown that metal-mediated S_NAr and DCC-mediated coupling reactions have lead to the formation of novel aromatic ether functionalized norbornenes in very good yield. Subsequent ROMP in the presence of bis(tricyclohexylphosphine)benzylidene ruthenium (IV) dichloride allowed for the synthesis of high molecular weight polymers with low to narrow polydispersities. Thermal investigations of the resulting polymeric materials revealed that as the length of the aryl ether chain pendent to the polynorbornene backbone increased, a subsequent increase in the Tg's and decomposition temperatures was observed. These results revealed a significant increase in the thermal stability relative to polynorbornene which decomposes at 400 °C. As such, these materials may one-day find use in high temperature applications.

2.4 Experimental

2.4.1 General Methods

^{1}H and ^{13}C NMR spectra were recorded either at 200 and 50 MHz on a Gemini 200 NMR spectrometer or at 500 and 125 MHz on a Bruker 500 spectrometer, respectively. Chemical shifts were referenced to the deuterated solvent that the spectrum was run in and coupling constants were calculated in Hz. A Bomem FT-IR spectrophotometer was used to record the IR spectra. Mass spectra were obtained on a Hewlett-Packard 5890 Series II mass spectrometer as well as on a Hewlett-Packard 5989A mass spectrometer. Molecular weight determinations by GPC analysis were performed using a BL-gel mixed D column (Phenomenex) equipped with a CH-30 column heater (Eppendorf) and a PL-DCU (Polymer Laboratories) detection system, with $CHCl_3$ as the eluent at a flow rate of 0.7 mL/min. Calibration of the instrument was performed versus polystyrene standards. Glass transition temperatures were obtained using DSC performed on a Mettler DSC 25 at a heating rate of 10 °C/min, taking the midpoint of the transition from the second heating. TGA's were recorded on a Mettler Toledo TGA/SDTA851 with a heating rate of 10 °C/min under a constant flow of nitrogen (20 mL/min). Elemental analyses were performed at Guelph Chemical Laboratories Ltd.

2.4.2 Starting Materials

Anhydrous aluminum chloride, aluminum powder, ferrocene, chloroarenes, ammonium hexafluorophosphate, dicyclohexylcarbodiimide, dimethylaminopyridine, hydroquinone, 98%-*exo,endo*-5-norbornene-2-methanol and bis(tricyclohexylphosphine)-benzylidene ruthenium (IV) dichloride are all commercially available and were used without further purification. Pyridine was vacuum distilled over calcium chloride and dried over 4-Å molecular sieves. All solvents (reagent grade) were used without further purification, with the exception of THF, which was distilled over sodium metal and benzophenone under nitrogen gas. Silica gel 60-100 mesh, was used in the column chromatographic purification of the modified norbornenes. Prior to polymerization, dichloromethane was dried over calcium chloride, distilled and then degassed by several freeze-pump-thaw repetitions.

2.4.3 Ligand Exchange Reaction

Preparation of starting complexes **2.1**, **2.2**, **2.15** and **2.16** was accomplished according to previously described ligand exchange reactions.[82-85] The general method used in synthesizing these complexes involved the addition of 27.9 g (150 mmol) ferrocene, 40.0 g (300 mmol) aluminum chloride, 4.0 g (150 mmol) aluminum powder and a four-fold excess of the arene to a 500 mL 3-necked round bottom flask. The reaction was then heated to 135 °C for 5 h under a nitrogen atmosphere. Cooling of the reaction mixture to 60 °C and pouring into a 200 mL ice-water mixture yielded a

greenish-brown solution. The resulting mixture was then filtered through sand to remove the aluminum and then washed with 3 x 50 mL of diethyl ether. Addition of 13.9 g (75 mmol) of ammonium hexafluorophosphate produced a yellow-green precipitate which was redissolved in a dichloromethane/acetone mixture (4:1). Extraction of the water layer was performed until the aqueous layer was virtually colorless. The resulting organic layer was dried over $MgSO_4$, filtered and concentrated under reduced pressure until approximately 25 mL of solvent remained. Addition of diethyl ether yielded the complexed arenes as yellow-green solids, which were then collected by suction filtration, rinsed again with diethyl ether and dried under vacuum.

2.4.4 Complexed Alkylbenzene Oxidations

Synthesis of the complexed acids of **2.3** and **2.4** was performed using the methodology established by Nesmeyanov and coworkers,[118-120] with the exception of **2.3** which was scaled up. Preparation of **2.3** proceeded by the addition of 2.83 g (8.00 mmol) of **2.1** and 12.64 g (80.00 mmol) of $KMnO_4$ to a 250 mL round bottom flask. In contrast, synthesis of **2.4** involved the reaction of 2.00 g (5.10 mmol) of **2.2** with 5.68 g (35.94 mmol) of $KMnO_4$ in a 250 mL round bottom flask. From this point on, both reactions proceeded in an identical fashion to one another. To each of the round bottom flasks, 100 mL of distilled water were added and the resulting solutions were refluxed at 100 °C for 24 h. After the reaction flasks had cooled to room temperature, oxalic acid was added until effervescence ceased. Suction filtration of the resulting solutions gave yellow aqueous mixtures, which were subsequently acidified to a pH = 1 using concentrated

HCl. Formation of the hexafluorophosphate salt was accomplished by the addition of 1.30 g (8.00 mmol) of ammonium hexafluorophosphate to **2.3** and 0.83 g (5.10 mmol) to **2.4**. The resulting yellow aqueous solutions were extracted with a nitromethane/dichloromethane mixture (1:1) until the aqueous layer was clear. Subsequent drying of the organic layer over $MgSO_4$, filtration and concentrating via rotary evaporation gave the yellow powders in 85 % (**2.3**) and 95 % (**2.4**) yields.

2.4.5. DCC Condensation Reactions

2.4.5.1 Preparation of Metallated Mono-Aryl Norbornenes 2.6 and 2.7

Into a 25 mL round bottom flask 0.422 g (1.00 mmol) of **2.3** or **2.4**, 0.206 g (1.00 mmol) DCC and 0.20 mL (1.654 mmol) 5-norbornene-2-methanol (**2.5**) were placed. To this was added 10 mL of dichloromethane and 4 drops of pyridine. The reaction mixture was then gently stirred for 7 h (**2.6**) or 3 h (**2.7**), resulting in the formation of a yellow, heterogeneous mixture. The white precipitate that formed due to the formation of dicyclohexylurea (DCU) during the reaction process was filtered off, and the reaction flask was subsequently rinsed with 2 x 10 mL aliquots of dichloromethane. Rotary evaporation of the resulting yellow solution liberated a yellow viscous material, which was further purified by dissolving in a minimal amount of acetone and filtered once again to remove any remaining DCU. Subsequent precipitation of the crude product into cold diethyl ether and cooling in the freezer overnight yielded the pure complexes as yellow semi-crystalline materials.

2.4.5.2 Direct Synthesis of Organic Mono-Aryl Monomers 2.8 and 2.14

Typically, (2.00 mmol) of **2.12** or **2.13**, 0.29 mL (2.40 mmol) of **2.5** and 0.292 g (2.40 mmol) DMAP, were placed into a 50 mL round bottom flask to which 9 mL of dichloromethane was added. The reaction flasks were then cooled on ice while slowly stirring. Subsequent addition of 0.496 g (2.40 mmol) of DCC dissolved in 1 mL of dichloromethane to the reaction flask at 0 °C commenced the reaction. Upon completion of the addition of DCC, the reaction flask remained on ice for an additional 5 min after which it was allowed to stir at room temperature for 8 h. During the reaction process, the homogeneous clear solution turned white and heterogeneous as the DCU began to precipitate out. After 8 h, the reaction mixture was poured into a 10 mL ice-water slurry and then transferred to a separatory funnel using dichloromethane. The resulting organic solution was washed with brine (NaCl) (3 x 25 mL) to remove any excess DMAP. Drying of the organic layer was achieved using $MgSO_4$, which was then removed by filtration. Subsequent rotary evaporation yielded the clear, oily crude product. Dissolution into a minimal amount of acetone and an additional filtration removed the remaining DCU and once again the product was dried under reduced pressure. Separation of the compound from the excess 5-norbornene-2-methanol was accomplished using a silica gel column. Elution of **2.8** and **2.14** as clear, viscous monomers was achieved using a 3:1 chloroform/hexane solution.

2.4.6 Nucleophilic Aromatic Substitution Reactions.

2.4.6.1 Synthesis of Metallated Complexes Capped with Terminal Phenoxy Groups (2.20 – 2.23)

Into a 50 mL round bottom flask, 1.00 mmol of **2.17** or **2.18** was added to 0.881 g (8.00 mmol) of hydroquinone (**2.19**) and 0.276 g (2.00 mmol) of potassium carbonate using 4 mL of DMF and 16 mL of THF. The flask was fitted with a reflux condenser and the contents were stirred at 65 °C under a nitrogen atmosphere for 16 h. Isolation of the products was achieved by pouring the cooled reaction mixture into a 10 % (v/v) HCl solution. Precipitation of the yellow solid was accomplished by adding an aqueous solution of 2.00 mmol of ammonium hexafluorophosphate. The products were then collected by suction filtration, washed with distilled water and rinsed with diethyl ether to remove the excess hydroquinone.

2.4.6.2 Preparation of Oligomeric Aryl Ether Functionalized Norbornenes 2.24 – 2.27

Typically, 1.00 mmol of the terminal phenolic complex (**2.20** - **2.23**) was added to 0.528 g (1.00 mmol) of **2.7** along with 0.346 g (2.50 mmol) of potassium carbonate in a 50 mL round bottom flask. Addition of 10 mL of DMF yielded a dark brown solution, which was stirred under nitrogen for 16 h at room temperature. A standard work-up procedure involved pouring the reaction mixture into a 10% (v/v) HCl solution followed

by the addition of 1.00 mmol of an aqueous NH_4PF_6 solution. The resulting yellow precipitates **2.24-2.27** were collected via suction filtration, washed with distilled water, rinsed with diethyl ether and dried prior to analysis.

2.4.7 Photolytic Demetallation

Isolation of monomers **2.8**, **2.9** and **2.28 – 2.31** from their metallated precursors was accomplished by dissolving each of the complexes in a 3:1 (v/v) dichloromethane/acetonitrile solution and placing then in a pyrex tube. These were then fitted into a photochemical apparatus equipped with a Xenon lamp and were irradiated for 4 – 6 h, the time increasing as the number of metal moieties increased. After this time, the solvent was removed under reduced pressure and the crude product dissolved in chloroform. The resulting organic layer was washed with 3 x 50 mL of distilled water to remove the iron salts produced during the photolysis reaction and then dried over $MgSO_4$, filtered and dried under vacuum. Using a minimal amount of chloroform, the crude product was then transferred to a silica gel column made in hexane. Eluting first with hexane removed the ferrocene followed by the elution with chloroform to obtain the product. Once again, the solvent was removed by rotary evaporation liberating the organic norbornene derivatives as off-white, viscous compounds.

2.4.8 Experimental Procedure for ROMP Yielding Polymers 2.32 – 2.38

ROMP reactions were routinely carried out using [M]:[I] ratios of 100:1. In a glove box, the catalyst was weighed out and transferred to a 10 mL round bottom flask. To this flask was added 0.5 mL of dichloromethane for every 100 mg of monomer used. Outside of the glovebox, the monomer contained in another 10 mL round bottom flask was dissolved in an equivalent amount of dry dichloromethane and stirred under nitrogen for 20 min. To the vigorously stirring monomer was added the catalyst solution using an airtight syringe. The ROMP reaction was allowed to progress until the formation of a gelatinous material was observed. This usually occurred in 1 - 2.5 h for the mono-aryl systems whereas required only minutes for the norbornene monomers with longer aromatic ether chains. Termination of the polymerization was achieved via the addition of an excess of ethyl vinyl ether which was necessary for cleaving the catalyst from the polymer chain. The polymer was then dissolved in either dichloromethane or chloroform and precipitated into methanol yielding the material as a fibrous, off-white solid.

Table 2.1: ^{1}H NMR Data of Bimetallic Aryl Ether Complexes **2.22** and **2.23**.

δ (acetone-d_6), ppm				
Complex	**Cp**	**Complexed Aromatic**	**Uncomplexed Aromatics**	**Others**
2.22	5.25 (s, 5H) 5.31 (s, 5H)	6.23 – 6.45 (m, 9H)	7.00 (d, 2H, J = 7.4) 7.19 (d, 2H, J = 6.9) 7.55 (s, 4H)	8.72 (br s, 1H, OH)
2.23	5.18 5.27	6.19 – 6.38 (m, 8H)	6.98 (d, 2H, J = 8.1) 7.18 (d, 2H, J = 8.2) 7.51 (br. s, 4H)	2.48 (s, 3H, CH_3) 8.70 (br. s, 1H, OH)

Coupling constants are reported in Hz.

Table 2.2: ^{13}C NMR Data of Bimetallic Aryl Ether Complexes **2.22** and **2.23**.

δ (acetone-d_6), ppm					
Complex	**Cp**	**Complexed Aromatic**	**Uncomplexed Aromatics**	**Others**	**% Yield**
2.22	78.13 78.70	74.79, 75.71 77.58, 85.81 87.80, 131.70* 132.98,* 134.51*	117.87, 122.90 124.11, 124.42 146.45,* 151.57* 152.32,* 156.75*	---	90
2.23	78.08 78.33	74.33, 75.21 76.35, 87.30 101.04,* 131.25* 132.48*, 133.08*	117.41, 122.49 123.61, 123.82 146.08*, 151.30* 151.77*, 156.14*	19.49 (CH_3)	92

* Denotes a quaternary aromatic carbon.

Table 2.3: ^{1}H NMR Data of Monoiron Complexes **2.6** and **2.7**.

δ (acetone-d_6), ppm; (200 & 500 MHz NMR)													
Monomer	**Endo/ Exo**	**H-1**	**H-2**	**H-3x**	**H-3n**	**H-4**	**H-5**	**H-6**	**H-7a**	**H-7s**	**CH_2O**	**Cp**	**ArH**
2.6	**Endo**	3.07 (br s)	2.66 (m)	1.97 (br m)	0.73 (br m)	2.84 (br s)	6.23 (dd)	6.08 (dd)	1.34 (br d)	1.46 (br s)	4.05 (t, 1H, J = 9.2), 4.23 (dd, 1H, J = 6.8)	5.28 (s, 5H)	6.72 (m, 3H), 7.05 (d, 2H)
	Exo	2.89 (br s)	1.93 (br m)	2.13 (br m)	1.31 (br m)	2.89 (br s)	6.15 (m)	6.14 (m)	1.37 (br d)	1.45 (br s)	4.39 (t, 1H, J = 9.0), 4.56 (dd, 1H, J = 6.8)	5.28 (s, 5H)	6.72 (m, 3H), 7.05 (d, 2H)
[a]**2.7**	**Endo**	3.04 (br s)	2.64 (m)	1.96 (m)	0.67 (m)	2.84 (br s)	6.21 (dd)	6.05 (dd)	1.32 (d)	1.42 (d)	4.03 (t, 1H), 4.20 (dd, 1H)	5.36 (s, 5H)	7.01 (d, 2H, J = 6.6), 7.14 (d, 2H, J = 6.8)
	Exo	2.86 (br s)	1.92 (m)	2.15 (br m)	1.30 (m)	2.86 (br s)	6.14 (m)	6.10 (m)	1.33 (br d)	1.41 (br d)	4.36 (t, 1H), 4.53 (dd, 1H)	5.36 (s, 5H)	7.01 (d, 2H, J = 6.6), 7.14 (d, 2H, J = 6.8)

Coupling constants (J) are recorded in Hz.

[a] Refer to Table 2.4 for the observed coupling constants.

Table 2.4: Measured Coupling Constants (Hz) for the *Endo* and *Exo* Isomers of Complex **2.7**

Couplings	*Endo*	*Exo*
$J_{(1,6)}$	2.6	2.3
$J_{(2,3x)}$	8.9	---
$J_{(2,3n)}$	4.0	---
$J_{(2,CH)}$	6.8	6.8
$J_{(3x,3n)}$	11.7	---
$J_{(3x,4)}$	3.7	---
$J_{(3n,7s)}$	2.4	---
$J_{(4,5)}$	3.1	2.3
$J_{(5,6)}$	5.5	---
$J_{(CH2)}$	10.5; 9.5	10.8; 9.11

--- Refers to unobtainable values due to peak broadness and overlap.

Table 2.5: ^{13}C NMR Data for Monoiron Complexes **2.6** and **2.7**.

δ (acetone-d_6), ppm; (50 and 125 MHz NMR)												
Monomer	**Endo/ Exo**	**C-1**	**C-2**	**C-3**	**C-4**	**C-5**	**C-6**	**C-7**	**CH_2O**	**Cp**	**ArC**	**CO**
2.6	**Endo**	44.64	38.36	29.79	42.94	138.50	132.78	49.91	70.83[n]	79.21	89.40, 89.96, 90.94	165.96
	Exo	44.39	38.73	29.40	42.35	136.87	137.69	45.52	71.51[x]	79.21	89.40, 89.96, 90.94	166.02
2.7	**Endo**	44.59	38.26	29.77	42.90	138.45	132.79	49.92	71.12[n],	81.47	89.28, 90.19, 109.58[•]	165.09
	Exo	44.37	38.60	29.46	42.31	136.93	137.57	45.50	71.78[x]	81.47	89.28, 90.19, 109.58[•]	165.19

[•] Denotes a quaternary aromatic carbon.

- Aromatic quaternary carbon adjacent to the carbonyl group does not appear in either of the ^{13}C NMR spectra.

Table 2.6: ^{1}H NMR Data of Diiron Complexes **2.24** and **2.25** Prepared via S_NAr.

δ (acetone-d_6), ppm; (200 & 500 MHz NMR)															
M	**Endo /Exo**	**H-1**	**H-2**	**H-3x**	**H-3n**	**H-4**	**H-5**	**H-6**	**H-7a**	**H-7s**	**CH_2O**	**Cp**	**Complexed ArH**	**UC ArH**	**Other**
2.24	**Endo**	3.06 (br s)	2.66 (m)	1.97 (m)	0.73 (m)	2.82 (br s)	6.33 (m)	6.08 (m)	1.36 (br d)	1.46 (br d)	4.07 (br t, 1H), 4.23 (br dd, 1H)	5.26 (s, 5H), 5.33 (s, 5H)	6.46 (br s, 5H), 6.67 (br s, 2H), 7.05 (br s, 2H)	7.55 (br s, 4H)	---
	Exo	2.88 (br s)	1.95 (m)	2.15 (br m)	1.30 (m)	2.88 (br s)	6.24 (m)	6.14 (m)	1.38 (br d)	1.44 (br d)	4.42 (br t, 1H), 4.55 (br dd, 1H)	5.26 (s, 5H), 5.33 (s, 5H)	6.46 (br s, 5H), 6.67 (br s, 2H), 7.05 (br s, 2H)	7.55 (br s, 4H)	---
2.25	**Endo**	3.06 (br s)	2.62 (m)	1.97 (m)	0.73 (m)	2.84 (br s)	6.33 (m)	6.08 (m)	1.34 (br d)	1.48 (br d)	4.09 (br t, 1H), 4.21 (br dd, 1H)	5.22 (s, 5H), 5.32 (s, 5H)	6.37 (br s, 4H), 6.66 (br s, 2H), 7.04 (br s, 2H)	7.60 (br s, 4H)	2.52 (s, 3H) (CH_3)
	Exo	2.88 (br s)	1.95 (m)	2.15 (br m)	1.30 (m)	2.88 (br s)	6.23 (m)	6.14 (m)	1.38 (br d)	1.44 (br d)	4.42 (br t, 1H), 4.56 (br dd, 1H)	5.22 (s, 5H), 5.32 (s, 5H)	6.37 (br s, 4H), 6.66 (br s, 2H), 7.04 (br s, 2H)	7.60 (br s, 4H)	2.52 (s, 3H) (CH_3)

M = Monomer
UC = Uncomplexed Aromatic Proton.

Table 2.7: ^{13}C NMR Data for Diiron Complexes **2.24** and **2.25** Prepared via S_NAr.

δ (acetone-d_6), ppm; (50 MHz NMR)														
M	**Endo /Exo**	**C-1**	**C-2**	**C-3**	**C-4**	**C-5**	**C-6**	**C-7**	**CH_2O**	**Cp**	**Complexed ArC**	**UC ArC**	**CO**	**Other**
2.24	**Endo**	44.69	38.36	29.81	42.92	138.46	132.85	49.94	70.86	78.19 79.71	77.67, 77.99, 85.87, 87.87, 88.34, 134.65*, 136.25*	124.56, 124.67, 151.40*, 151.92*	165.62	---
	Exo	44.45	38.74	29.42	42.35	136.99	137.59	45.56	71.52	78.19 79.71	77.67, 77.99, 85.87, 87.87, 88.34, 134.65*, 136.25*	124.56, 124.67, 151.40*, 151.92*	165.71	---
2.25	**Endo**	44.62	38.28	29.79	42.83	138.38	132.79	49.87	70.79	78.56 79.69	76.89, 77.92, 87.78, 88.26, 101.32*, 133.35*, 136.13*	124.45 (4C), 151.15*, 151.98*	165.57	20.00 (CH_3)
	Exo	44.38	38.53	29.41	42.26	136.95	137.50	45.48	71.44	78.56 79.69	76.89, 77.92, 87.78, 88.26, 101.32*, 133.35*, 136.13*	124.45 (4C), 151.15*, 151.98*	165.61	20.00 (CH_3)

* Denotes a quaternary aromatic carbon. (Aromatic quaternary carbon adjacent to the carbonyl group does not appear in either of the ^{13}C NMR spectra).

M = Monomer; UC = Uncomplexed Aromatic Carbon.

Table 2.8: ^{1}H NMR Data of Triiron Complexes **2.26** and **2.27** Prepared via S_NAr.

δ (acetone-d_6), ppm; (200 MHz NMR)															
M	**Endo /Exo**	**H-1**	**H-2**	**H-3x**	**H-3n**	**H-4**	**H-5**	**H-6**	**H-7a**	**H-7s**	**CH_2O**	**Cp**	**Complexed ArH**	**UC Ar**	**Other**
2.26	**Endo**	3.08 (br s)	2.76 (br m)	2.00 (m)	0.71 (m)	2.81 (br s)	6.28 (m)	6.13 (m)	1.35 (br d)	1.53 (br d)	4.01 (br t, 1H), 4.24 (br dd, 1H)	5.26 (s, 5H), 5.32 (s, 5H), 5.34 (s, 5H)	6.68-6.31 (br s, 9H), 7.05 (br s, 2H), 7.18 (br s, 2H)	7.61 (br s, 4H), 7.64 (br s, 4H)	---
	Exo	2.87 (br s)	1.93 (br m)	2.04-2.13 (br m)	1.34 (br m)	2.87 (br s)	6.22 (m)	6.20 (m)	1.37 (br d)	1.44 (br d)	4.37 (br t, 1H), 4.56 (br dd, 1H)	5.26 (s, 5H), 5.32 (s, 5H), 5.34 (s, 5H)	6.68-6.31 (br s, 9H), 7.05 (br s, 2H), 7.18 (br s, 2H)	7.61 (br s, 4H), 7.64 (br s, 4H)	---
2.27	**Endo**	3.09 (br s)	2.70 (br m)	1.99 (m)	0.71 (m)	2.80 (br s)	6.25 (m)	6.10 (m)	1.35 (br d)	1.52 (br d)	4.03 (br t, 1H), 4.22 (m, 1H)	5.22 (s, 5H), 5.34 (s, 5H), 5.42 (s, 5H)	6.30-6.61 (br m, 8H), 7.07 (br s, 2H), 7.18 (br s, 2H)	7.59 (br d, 8H)	2.52 (s, 3H) (CH_3)
	Exo	2.88 (br s)	1.94 (br m)	2.04-2.13 (br m)	1.31 (br m)	2.87 (br s)	6.22 (m)	6.19 (m)	1.37 (br d)	1.42 (br d)	4.38 (br t, 1H), 4.55 (m, 1H)	5.22 (s, 5H), 5.34 (s, 5H), 5.42 (s, 5H)	6.30-6.61 (br m, 8H), 7.07 (br s, 2H), 7.18 (br s, 2H)	7.59 (br d, 8H)	2.52 (s, 3H) (CH_3)

M = Monomer; UC = Uncomplexed

Table 2.9: ^{13}C NMR Data for Triiron Complexes **2.26** and **2.27** Prepared via S_NAr.

δ (acetone-d_6), ppm; (50 MHz NMR)														
M	**Endo /Exo**	**C-1**	**C-2**	**C-3**	**C-4**	**C-5**	**C-6**	**C-7**	**CH_2O**	**Cp**	**Complexed ArC**	**UC ArC**	**CO**	**Other**
2.26	**Endo**	44.64	38.35	29.81	42.94	138.47	132.88	49.95	70.81	78.08, 78.97, 79.60	75.34, 75.36, 77.39, 77.71, 85.77, 87.76, 88.26, 132.25* (2C), 134.68*, 136.64*	124.46, 124.50, 124.62, 124.68, 151.36*, 151.61*, 152.03*, 152.30*	165.59	---
	Exo	44.42	38.75	29.42	42.36	136.99	137.53	46.56	71.47	78.08, 78.97, 79.60	75.34, 75.36, 77.39, 77.71, 85.77, 87.76, 88.26, 132.25* (2C), 134.68*, 136.64*	124.46, 124.50, 124.62, 124.68, 151.36*, 151.61*, 152.03*, 152.30*	165.69	---
2.27	**Endo**	44.68	38.35	29.79	42.88	138.44	132.15	49.94	70.82	78.60, 79.08, 79.73	75.56, 76.88, 81.64 (4C), 87.87, 88.36, 101.36* 132.15* (2C), 133.54*, 136.29*	124.49, 124.53, 124.57, 124.75, 151.29*, 151.75*, 151.88*, 152.26*	165.55	20.08 (CH_3)
	Exo	44.44	38.73	29.40	42.32	137.03	137.60	45.54	71.47	78.60, 79.08, 79.73	75.56, 76.88, 81.64 (4C), 87.87, 88.36, 101.36* 132.15* (2C), 133.54*, 136.29*	124.49, 124.53, 124.57, 124.75, 151.29*, 151.75*, 151.88*, 152.26*	165.63	20.08 (CH_3)

* Denotes a quaternary aromatic carbon. (Aromatic quaternary carbon adjacent to the carbonyl group does not appear in either of the ^{13}C NMR spectra). M = Monomer; UC = Uncomplexed.

Table 2.10: Yields, IR and C, H Elemental Analysis for Complexes **2.6**, **2.7**, **2.24** – **2.27** Prepared via the S_NAr substitution of **2.7** with Various Terminal Phenoxy Oligomeric Ethers.

Complex	% Yield	IR (cm^{-1}) (CO)	Elemental Analysis [Calculated (Found)]	
			C	H
2.6	62	1733	48.61 (48.37)	4.28 (4.33)
2.7	70	1733	45.44 (45.70)	3.81 (4.00)
2.24	81	1732	47.06 (47.34)	3.63 (3.61)
2.25	80	1729	47.63 (47.98)	3.79 (3.86)
2.26	86	1732	46.51 (46.49)	3.40 (3.56)
2.27	83	1730	---	---

--- Denotes that the C, H - analysis was not obtained.

Table 2.11: ^{1}H NMR Data of Monoaryl Monomers **2.8**, **2.9** and **2.14**.

δ ($CDCl_3$), ppm; (500 MHz NMR)													
M	**Endo /Exo**	**H-1**	**H-2**	**H-3x**	**H-3n**	**H-4**	**H-5**	**H-6**	**H-7a**	**H-7s**	**CH_2O**	**ArH**	**Other**
2.8	**Endo**	2.99 (br s)	2.55 (m)	1.90 (m)	0.67 (m)	2.85 (br s)	6.20 (dd)	6.01 (dd)	1.30 (br d)	1.49 (br d)	3.91 (t, 1H), 4.13 (dd,1H)	7.44 (t, 2H, J = 8.1), 7.55 (t, 1H, J = 7.2), 8.07 (d, 2H, J = 8.0)	---
	Exo	2.82 (br s)	1.90 (m)	1.26 (m)	1.34 (m)	2.88 (br s)	6.13 (dd)	6.11 (dd)	1.40 (br s)	1.40 (br s)	4.22 (t, 1H), 4.42 (dd, 1H)	7.44 (t, 2H, J = 8.1), 7.55 (t, 1H, J = 7.2), 8.07 (d, 2H, J = 8.0)	---
2.9	**Endo**	2.94 (br s)	2.52 (m)	1.89 (m)	0.63 (m)	2.83 (br s)	6.17 (dd)	5.98 (dd)	1.28 (br s)	1.46 (br s)	3.88 (t, 1H), 4.09 (dd, 1H)	7.39 (d, 2H, J = 8.7), 7.97 (d, 2H, J = 8.6)	---
	Exo	2.77 (br s)	1.86 (m)	1.27 (m)	1.32 (m)	2.85 (br s)	6.11 (m)	6.10 (m)	1.37 (br s)	1.37 (br s)	4.20 (t, 1H), 4.38 (dd, 1H)	7.39 (d, 2H, J = 8.7), 7.97 (d, 2H, J = 8.6)	---
2.14	**Endo**	2.98 (br s)	2.54 (m)	1.90 (m)	0.65 (m)	2.84 (br s)	6.19 (dd)	6.00 (dd)	1.29 (br s)	1.48 (br s)	3.89 (t, 1H), 4.11 (dd, 1H)	7.23 (d, 2H, J = 7.8), 7.96 (d, 2H, J = 8.0)	2.40 (s, 3H) (CH_3)
	Exo	2.81 (br s)	1.88 (m)	1.27 (m)	1.33 (m)	2.87 (br s)	6.13 (dd)	6.10 (dd)	1.40 (br s)	1.40 (br s)	4.20 (t, 1H), 4.39 (dd, 1H)	7.23 (d, 2H, J = 7.8), 7.96 (d, 2H, J = 8.0)	2.40 (s, 3H) (CH_3)

(---) Denotes a hidden peak. Coupling constants are in Hz. Refer to Tables 2.12 - 2.14 for the observed coupling constants.

Table 2.12: Measured Coupling Constants (Hz) for the *Endo* and *Exo* Isomers of Monomer **2.8**.

Couplings	*Endo*	*Exo*
$J_{(1, 6)}$	2.8	2.9
$J_{(2, 3x)}$	8.8	---
$J_{(2, 3n)}$	4.2	---
$J_{(2, CH)}$	6.6	6.5
$J_{(3x, 3n)}$	11.7	11.7
$J_{(3x, 4)}$	3.8	---
$J_{(3n, 7s)}$	2.6	---
$J_{(4, 5)}$	3.0	3.1
$J_{(5, 6)}$	5.7	5.6
$J_{(7a, 7s)}$	8.2	8.4
$J_{(CH2)}$	10.8; 9.6	10.9; 9.2

--- Refers to unobtainable values due to peak broadness and overlap.

Table 2.13: Measured Coupling Constants (Hz) for the *Endo* and *Exo* Isomers of Monomer **2.9**.

Couplings	*Endo*	*Exo*
$J_{(1,6)}$	2.8	---
$J_{(2,3x)}$	9.3	---
$J_{(2,3n)}$	5.8	---
$J_{(2,CH)}$	6.6	6.6
$J_{(3x,3n)}$	11.7	---
$J_{(3x,4)}$	3.8	---
$J_{(3n,7s)}$	2.8	---
$J_{(4,5)}$	3.0	---
$J_{(5,6)}$	5.8	---
$J_{(7a,7s)}$	8.1	---
$J_{(CH2)}$	10.7; 9.3	10.9; 9.1

--- Refers to unobtainable values due to peak broadness and overlap.

Table 2.14: Measured Coupling Constants (Hz) for the *Endo* and *Exo* Isomers of Monomer **2.14**.

Couplings	*Endo*	*Exo*
$J_{(1, 6)}$	2.9	2.8
$J_{(2, 3x)}$	8.8	---
$J_{(2, 3n)}$	4.0	---
$J_{(2, CH)}$	6.6	6.5
$J_{(3x, 3n)}$	11.7	11.6
$J_{(3x, 4)}$	3.8	4.0
$J_{(3n, 7s)}$	2.7	---
$J_{(4, 5)}$	2.9	---
$J_{(5, 6)}$	5.4	5.6
$J_{(7n, 7s)}$	8.0	8.4
$J_{(CH2)}$	10.7; 9.8	10.9; 9.3
$J_{(7s, 4)}$	1.2	---
$J_{(7s, 1)}$	1.2	---

--- Refers to unobtainable values due to peak broadness and overlap.

Table 2.15: ^{13}C NMR Data for Monoaryl Monomers **2.8**, **2.9** and **2.14**.

δ ($CDCl_3$), ppm; (125 MHz NMR)												
M	**Endo /Exo**	**C-1**	**C-2**	**C-3**	**C-4**	**C-5**	**C-6**	**C-7**	**CH_2O**	**ArC**	**CO**	**Other**
2.8	**Endo**	43.95	37.88	28.93	42.19	137.57	132.16	49.35	68.26	128.26, 129.50, 132.73, 130.54*	166.45	---
	Exo	43.71	38.08	29.56	41.59	136.19	136.92	44.97	68.94	128.26, 129.50, 132.73, 130.54*	166.55	---
2.9	**Endo**	43.86	37.77	28.85	42.11	137.56	131.99	49.28	68.40	128.50, 130.80, 129.91*, 139.05*	165.42	---
	Exo	43.60	37.96	29.48	41.50	136.04	136.86	44.88	69.09	128.50, 130.80, 129.91*, 139.05*	165.52	---
2.14	**Endo**	43.91	37.84	28.88	42.14	137.48	132.15	49.30	68.03	127.74*, 128.93, 129.48, 143.28*	166.48	21.56 (CH_3)
	Exo	43.64	38.38	28.88	41.55	136.16	136.84	44.93	68.70	127.74*, 128.93, 129.48, 143.28*	166.56	21.56 (CH_3)

* Denotes a quaternary aromatic carbon.
M = Monomer

Table 2.16: ^{1}H NMR Data for Triaryl Ether Monomers **2.28** and **2.29**.

δ ($CDCl_3$), ppm; (200 MHz NMR)													
M	**Endo /Exo**	**H-1**	**H-2**	**H-3x**	**H-3n**	**H-4**	**H-5**	**H-6**	**H-7a**	**H-7s**	**CH_2O**	**ArH**	**Other**
2.28	**Endo**	2.98 (br s)	2.55 (m)	1.91 (br m)	0.64 (m)	2.87 (br s)	6.21 (dd)	6.02 (dd)	1.32 (br s)	1.50 (br d)	3.90 (t, 1H), 4.10 (dd, 1H)	6.98 – 7.15 (br s, 9H), 7.38 (br d, 2H), 8.05 (br d, 2H)	---
	Exo	2.82 (br s)	1.84 (br m)	1.25 (br m)	1.34 (br m)	2.89 (br s)	6.13 (m)	6.11 (m)	1.40 (br s)	1.40 (br s)	4.21 (t, 1H), 4.40 (dd, 1H)	6.98 – 7.15 (br s, 9H), 7.38 (br d, 2H), 8.05 (br d, 2H)	---
2.29	**Endo**	2.97 (br s)	2.55 (m)	1.90 (br m)	0.69 (m)	2.86 (br s)	6.19 (dd)	6.00 (dd)	1.32 (br s)	1.47 (br d)	3.88 (t, 1H), 4.10 (dd, 1H)	6.85 – 7.10 (br s, 8H), 7.15 (br d, 2H), 8.02 (br d, 2H)	2.34 (s, 3H) (CH_3)
	Exo	2.81 (br s)	1.84 (br m)	1.28 (br m)	1.34 (br m)	2.86 (br s)	6.12 (m)	6.08 (m)	1.40 (br s)	1.40 (br s)	4.20 (t, 1H), 4.40 (dd, 1H)	6.85 – 7.10 (br s, 8H), 7.15 (br d, 2H), 8.02 (br d, 2H)	2.34 (s, 3H) (CH_3)

Coupling constants are recorded in Hz.
Refer to Tables 2.17 and 2.18 for the observed coupling constants.
M = Complexed.

Table 2.17: Measured Coupling Constants (Hz) for the *Endo* and *Exo* Isomers of Monomer **2.28**.

Couplings	*Endo*	*Exo*
$J_{(1, 6)}$	2.9	---
$J_{(2, 3x)}$	8.7	---
$J_{(2, 3n)}$	4.3	---
$J_{(2, CH)}$	6.7	6.5
$J_{(3x, 3n)}$	11.2	---
$J_{(3x, 4)}$	3.7	---
$J_{(3n, 7s)}$	2.5	---
$J_{(4, 5)}$	2.9	---
$J_{(5, 6)}$	5.8	---
$J_{(7a, 7s)}$	---	---
$J_{(CH2)}$	10.8	10.9

--- Refers to unobtainable values due to peak broadness and overlap.

Table 2.18: Measured Coupling Constants (Hz) for the *Endo* and *Exo* Isomers of Monomer **2.29**.

Couplings	*Endo*	*Exo*
$J_{(1, 6)}$	2.7	---
$J_{(2, 3x)}$	8.5	---
$J_{(2, 3n)}$	4.1	---
$J_{(2, CH)}$	6.6	6.5
$J_{(3x, 3n)}$	11.6	---
$J_{(3x, 4)}$	3.9	---
$J_{(3n, 7s)}$	2.5	---
$J_{(4, 5)}$	2.9	---
$J_{(5, 6)}$	5.7	---
$J_{(7a, 7s)}$	8.0	---
$J_{(CH2)}$	10.7; 9.5	10.8; 9.2
$J_{(7s, 4)}$	1.8	

--- Refers to unobtainable values due to peak broadness and overlap.

Table 2.19: ^{13}C NMR Data for Triaryl Ether Monomers **2.28** and **2.29**.

δ ($CDCl_3$), ppm; (50 MHz NMR)												
M	**Endo /Exo**	**C-1**	**C-2**	**C-3**	**C-4**	**C-5**	**C-6**	**C-7**	**CH_2O**	**ArC**	**CO**	**Other**
2.28	**Endo**	43.95	37.89	28.92	42.19	137.61	132.19	49.35	68.17	116.79, 118.56, 120.36, 121.51, 123.18, 124.62*, 129.79, 131.66, 150.93*, 153.75*, 157.36*, 162.05*	165.98	---
	Exo	43.69	37.89	28.92	41.60	136.22	136.96	44.99	68.84	116.79, 118.56, 120.36, 121.51, 123.18, 124.62*, 129.79, 131.66, 150.93*, 153.75*, 157.36*, 162.05*	166.04	---
2.29	**Endo**	43.96	37.91	28.94	42.20	137.61	132.20	49.37	68.18	116.72, 118.83, 119.76, 121.48, 124.67*, 130.29, 131.64, 132.99*, 150.57*, 154.41*, 154.85*, 162.15*	166.02	20.66 (CH_3)
	Exo	43.71	37.91	28.94	41.61	136.23	136.96	45.00	68.85	116.72, 118.83, 119.76, 121.48, 124.67*, 130.29, 131.64, 132.99*, 150.57*, 154.41*, 154.85*, 162.15*	166.14	20.66 (CH_3)

* Denotes a quaternary aromatic carbon.
M = Monomer.

Table 2.20: ^{1}H NMR Data for Pentaaryl Ether Monomers **2.30** and **2.31**.

δ ($CDCl_3$), ppm; (200 MHz NMR)													
M	**Endo /Exo**	**H-1**	**H-2**	**H-3x**	**H-3n**	**H-4**	**H-5**	**H-6**	**H-7a**	**H-7s**	**CH_2O**	**ArH**	**Other**
2.30	**Endo**	2.97 (br s)	2.54 (m)	1.90 (br m)	0.66 (m)	2.86 (br s)	6.20 (m)	6.00 (m)	1.30 (br s)	1.48 (br d)	3.89 (t, 1H, J = 10), 4.10 (dd, 1H, J = 10 and J = 6.5)	6.92 – 7.09 (br s, 17H), 7.33 (br d, 2H), 8.02 (br d, 2H)	---
	Exo	2.80 (br s)	1.88 (br m)	1.27 (br m)	1.34 (br m)	2.88 (br s)	6.12 (m)	6.12 (m)	1.40 (br s)	1.40 (br s)	4.21 (t, 1H, J = 10), 4.39 (dd, 1H, J = 10 and J = 6.5)	6.92 – 7.09 (br s, 17H), 7.33 (br d, 2H), 8.02 (br d, 2H)	---
[a]2.31	**Endo**	2.97 (br s)	2.52 (m)	1.90 (m)	0.64 (m)	2.86 (br s)	6.19 (dd)	6.00 (dd)	1.30 (br s)	1.49 (br d)	3.87 (t, 1H), 4.14 (dd, 1H)	6.88 – 7.03 (br s, 16H), 7.12 (br d, 2H), 8.03 (br d, 2H)	2.33 (s, 3H) (CH_3)
	Exo	2.80 (br s)	1.84 (br m)	1.26 (br m)	1.34 (br m)	2.88 (br s)	6.12 (m)	6.12 (m)	1.39 (br s)	1.39 (br s)	4.20 (t, 1H), 4.38 (dd, 1H)	6.88 – 7.03 (br s, 16H), 7.12 (br d, 2H), 8.03 (br d, 2H)	2.33 (s, 3H) (CH_3)

Coupling constants are recorded in Hz.

[a] Observable coupling is located in Table 2.21.

M = Monomer.

Table 2.21: Measured Coupling Constants (Hz) for the *Endo* and *Exo* Isomers of Monomer **2.31.**

Couplings	*Endo*	*Exo*
$J_{(1, 6)}$	2.8	---
$J_{(2, 3x)}$	9.3	---
$J_{(2, 3n)}$	4.3	---
$J_{(2, CH)}$	6.5	6.6
$J_{(3x, 3n)}$	11.5	---
$J_{(3x, 4)}$	3.8	---
$J_{(3n, 7s)}$	2.6	---
$J_{(4, 5)}$	2.9	---
$J_{(5, 6)}$	5.7	---
$J_{(7a, 7s)}$	8.1	---
$J_{(CH2)}$	10.7; 9.4	10.9; 9.1
$J_{(7s, 4)}$	2.0	

--- Refers to unobtainable values due to peak broadness and overlap.

Table 2.22: ^{13}C NMR Data for Pentaaryl Ether Monomers **2.30** and **2.31**.

δ ($CDCl_3$), ppm; (50 MHz NMR)												
M	**Endo /Exo**	**C-1**	**C-2**	**C-3**	**C-4**	**C-5**	**C-6**	**C-7**	**CH_2O**	**ArC**	**CO**	**Other**
2.30	**Endo**	43.94	37.87	28.92	42.19	137.61	132.18	49.35	68.18	116.74, 118.20, 119.69, 119.83, 119.86, 120.21, 120.45, 121.63, 122.86, 124.62*, 129.70, 131.63, 150.72*, 152.58*, 153.11*, 153.33*, 154.34*, 157.72*, 162.06*, 162.08*	165.98	---
	Exo	43.69	37.87	28.92	41.59	136.21	136.95	44.98	68.84	116.74, 118.20, 119.69, 119.83, 119.86, 120.21, 120.45, 121.63, 122.86, 124.62*, 129.70, 131.63, 150.72*, 152.58*, 153.11*, 153.33*, 154.34*, 157.72*, 162.06*, 162.08*	166.04	---
2.31	**Endo**	43.98	37.92	28.95	42.22	137.62	132.20	49.39	68.21	116.77, 118.49, 119.68, 119.73, 119.76, 119.91, 120.22, 121.54, 124.72*, 130.22, 131.64, 132.68*, 150.73*, 152.51*, 152.74*, 153.21*, 153.51* 154.40*, 155.24*, 162.10*	166.01	20.65 (CH_3)
	Exo	43.73	37.92	28.95	41.62	136.22	136.97	45.02	68.87	116.77, 118.49, 119.68, 119.73, 119.76, 119.91, 120.22, 121.54, 124.72*, 130.22, 131.64, 132.68*, 150.73*, 152.51*, 152.74*, 153.21*, 153.51* 154.40*, 155.24*, 162.10*	(---)	20.65 (CH_3)

* Denotes a quaternary aromatic carbon. M = Monomer

Table 2.23: Yields, IR, MS and C, H Elemental Analysis for Monomers **2.8**, **2.9**, **2.14** and **2.28 – 2.31**.

Complex	% Yield	IR (cm^{-1}) (CO)	Elemental Analysis [Calculated (Found)]		MS M^+ (m/z)
			C	H	
2.8	91	1714	78.92 (78.54)	7.06 (7.12)	228
2.9	64	1715	68.57 (68.23)	5.75 (5.95)	262
2.14	85	1708	79.31 (79.18)	7.49 (7.71)	242
2.28	51	1707	78.62 (78.84)	5.86 (5.80)	412
2.29	49	1710	---	---	426
2.30	46	1716	78.51 (78.28)	5.41 (5.49)	597
2.31	47	1712	---	---	610

--- Denotes that the C, H analysis was not obtained.

Table 2.24: ROMP of Monomer **2.8** using Varying Ratios of [M]:[I] as a Means to Compare Mw, Mn, PDI and Yield.

[M]:[I]	Mw	Mn	PDI	Yield (%)
25:1	8 400	3 500	2.4	59
50:1	16 000	5 900	2.7	52
100:1	108 000	57 000	1.9	71
150:1	511 000	168 000	3.0	80

Table 2.25: Mw, Mn, PDI and Yield for Aryl Ether Functionalized Polynorbornenes **2.32 – 2.38**.

Polymer	Mw	Mn	PDI	Yield (%)
2.32	108 000	57 000	1.9	71
2.33	462 000	195 000	2.4	74
2.34	63 000	44 000	1.4	90
2.35	145 000	87 000	1.7	73
2.36	110 000	84 000	1.3	85
2.37	74 000	49 000	1.5	66
2.38	104 000	96 000	1.1	89

Table 2.26: ^{1}H NMR Spectral Information and IR for Polymers **2.32 – 2.38**.

δ ($CDCl_3$, ppm)					IR (cm^{-1})
Polymer	**Aromatic H's**	**Vinyl H's**	**Nor-CH_2O-**	**Aliphatic H's**	**(CO) [trans olefin]**
2.32	7.30-7.60 (br, 3H), 7.95-8.05 (br s, 2H)	5.20–5.40 (br s, 2H)	4.05-4.40 (br d, 2H)	1.19-3.10 (br peaks, 7H)	(1714) [969]
2.33	7.35-7.45 (br s, 2H), 7.90-8.01 (br s, 2H)	5.20-5.40 (br s, 2H)	4.05-4.35 (br d, 2H)	1.04-3.09 (br peaks, 7H)	(1715) [969]
2.34	7.17-7.21 (br s, 2H), 7.87-7.90 (br s, 2H)	5.30-5.41 (br s, 2H)	4.08-4.24 (br s, 2H)	1.13-3.05 (br peaks, 10H)	(1718) [966]
2.35	6.75-7.40 (br, 11H), 7.80-8.00 (br s, 2H)	5.25-5.45 (br s, 2H)	4.05-4.35 (br d, 2H)	0.90-3.00 (br peaks, 7H)	(1712) [967]
2.36	6.75-7.35 (br, 10H), 7.80-8.00 (br s, 2H)	5.20-5.45 (br s, 2H)	4.00-4.30 (br d, 2H)	0.85-2.90 (br peaks, 10H)	(1717) [---]
2.37	6.75-7.35 (br, 19H), 7.85-8.00 (br s, 2H)	5.20-5.45 (br s, 2H)	4.10-4.40 (br s, 2H)	0.90-3.00 (br peaks, 7H)	(1714) [964]
2.38	6.70-7.20 (br, 18H), 7.85-8.00 (br s, 2H)	5.20-5.45 (br s, 2H)	4.00-4.35 (br s, 2H)	0.85-2.90 (br peaks, 7H)	(1714) [---]

--- Refers to obscurity within the fingerprint region of the IR spectrum making assignment of the trans IR band difficult.

Table 2.27: Thermal Information of Polymers **2.32-2.38** Obtained from DSC and TGA Analyses.

	DSC (°C)		TGA (°C)	
Polymer	**Tg[a]**	**T_{onset}**	**$T_{midpoint}$**	**T_{endset}**
2.32	54.7	385.3	417.0	450.6
2.33	65.3	354.3	401.9	427.5
2.34	61.8	397.5	413.7	434.4
2.35	67.6	393.9	422.4	456.8
2.36	68.6	387.6	407.3	421.8
2.37	73.3	408.5	460.2	509.6
2.38	71.6	408.0	451.0	492.1

[a]Glass transition temperatures (Tg's) are reported as midpoints.

3.0 Synthesis of Polynorbornenes with Aliphatic Side Chains

3.1 Introduction

It has been of interest to investigate the preparation of monomeric materials containing a rigid mesogen bridged to a highly strained bicyclo[2.2.1]heptene via a flexible aliphatic spacer due to the importance the resulting polymers may exhibit as side chain liquid crystalline polymers or SCLCPs. Monomers used in this study were prepared in a two-step synthesis involving the initial preparation of a monoaryl alcohol and its subsequent reaction with *exo,endo*-5-norbornene-2-carboxylic acid. This final study presents the first example of using the $CpFe^{+}$ moiety as a means to design monomers suitable for the synthesis of novel SCLCPs.

"Liquid crystallinity" refers to the liquid/solid interface or mesophase in which a material exists.[4] Interest in the design of liquid crystals was first investigated in 1888 by Reinitzer who discovered that these types of molecules had the ability to arrange themselves in ordered domains.[147] Molecular ordering in a polymer structure may exist in two different conformations. These have been categorized as nematic or smectic mesophases, with the smectic LCs demonstrating a higher degree of order. Through the aid of optical microscopy, it has been possible to attribute this greater level of ordering in the smectic systems to the linear orientation of the chains, which differs significantly from the highly disordered chain ends observed in nematic systems.[4] It is the highly ordered construction of smectic polymers that is felt to contribute to their higher

viscosities. A visual representation of this supramolecular ordering can be seen in Figure 3.0.

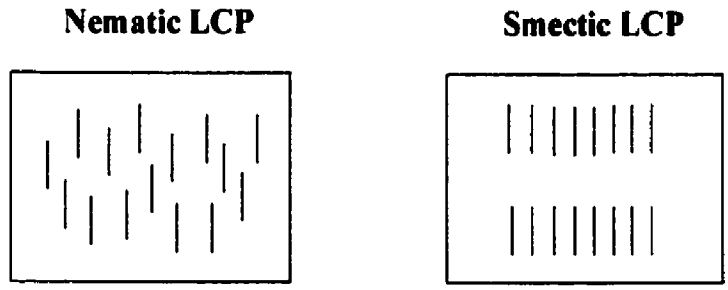

Figure 3.0: Smectic and nematic ordering in LC polymers, where each "|" refers to a polymer.

Studies have shown that liquid crystallinity increase as the molecular weight of a compound increases, which is a primary reason why such a vast amount of effort has been expended into the research of polymeric liquid crystalline materials.[33] Two common types of liquid crystals are those containing the rigid mesogen and aliphatic group pendent to the polymer chain (SCLCPs) and those that contain them within the polymer backbone which are called main chain liquid crystal polymers (MCLCPs), as illustrated in Figure 3.1.[148]

Synthesis of LCPs offers many advantages in terms of their industrial applications. Due to lower melt viscosities and increased ordering in these systems relative to random coiled polymers, there is a much greater ease of processability.[4] More importantly, these materials offer incredible strength and modulus due to their highly crystalline nature.[4] Due to this increased ordering, most LCPs demonstrate high thermal stability.

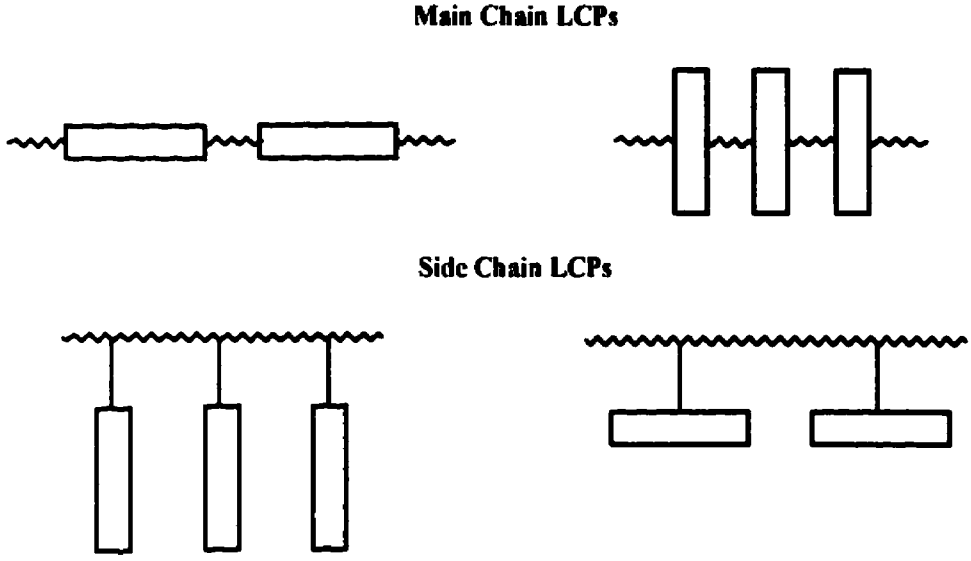

Figure 3.1: Description of SCLCPs and MCLCPs.

In recent years, there has been considerable interest in the preparation of novel SCLCPs due to their potential use in electronic applications such as electro-optics, the production of displays and photoconductors.[5, 29, 33, 148-153] By definition, SCLCPs constitute a class of polymers that consist of a flexible aliphatic spacer between a rigid mesogen and the polymer main chain. This concept of preparing these polymers was proposed by Finkelmann and Ringsdorf in 1978.[154, 155] With this structural design it was hoped that molecular motion between the polymer backbone and the pendent side chains could be decoupled allowing for greater conformational freedom in the polymeric material. This would enable the polymer to arrange itself through its flexible spacer resulting in the formation of a highly ordered system.

Interest in the design of new SCLCPs has focused primarily on the type of rigid mesogen incorporated into the polymeric material. Investigations have revealed that the nature of this group highly influences how the polymer will arrange itself and thus effects

its ordering. Therefore, mesogens of various sizes and shapes have been and are currently being investigated so as to gain an understanding of how these groups effect liquid crystalline behavior. Two classifications of mesogens have been established based upon the different molecular structures each type possesses. These have been defined as being either rod-like or disk-like.[4]

In the past decade, developments in ROMP of highly strained cyclo- and bicyclo-alkenes have permitted the synthesis of novel polynorbornenes with LC behavior. Recently, Grubbs and coworkers reported the synthesis of discotic columnar SCLCPs in which the mesogens were flat, rigid molecules or disks.[149] Synthesis of the monomers involves the reaction of 5-norbornene-2-carbonyl chloride with two different hydroxy-functionalized triphenylene derivatives. Linking these two rigid molecules together is a twelve-membered aliphatic spacer. It is the incorporation of this bridging aliphatic spacer that provides the flexibility that is characteristic of SCLCPs. Living ROMP was achieved using $(Cy_3P)_2Cl_2Ru{=}CHPh$ in the presence of dichloromethane (Scheme 3.1) liberating the LCP with high molecular weights and narrow polydispersities. DSC measurements of the resulting polymeric materials yielded Tg's of –3 °C, characteristic of the nature of these types of polymers.

A similar study investigating the self-assembly of a novel polymeric material containing two tapered monodendritic groups in every repeat unit was recently reported by Percec and Schlueter.[153] This polymeric material, as illustrated in Equation 3.1, was prepared using Grubbs' catalyst. Thermal analysis of the resulting poly(7-oxa-norbornene) derivative by DSC indicated much higher thermal transitions relative to the polynorbornene derivative shown in Scheme 3.1. This is characteristic of the higher

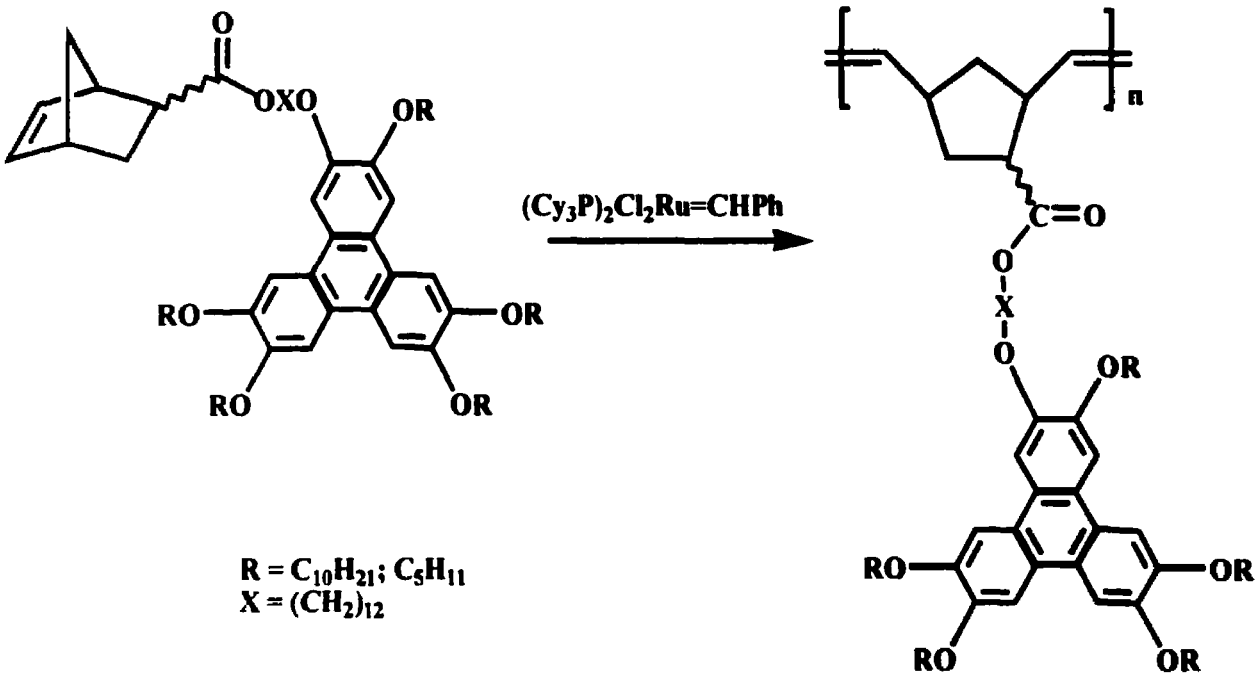

Scheme 3.1

number of aromatic groups present in this dendritic polymer relative to the polymer described by Grubbs. Furthermore, since there are fewer flexible aliphatic spacers incorporated into the dendritic polymer, there is less rotational conformation, thus increasing the overall thermal properties of the resulting polymer. DSC analysis also indicated that this coiled supramolecular material was able to assemble itself into both disk-like and cylindrical structures, which were able to form a column-like structure. Since poly(7-oxa-norbornene) forms a helical-type structure,[35] this confirms the columnar structure observed in this investigation.

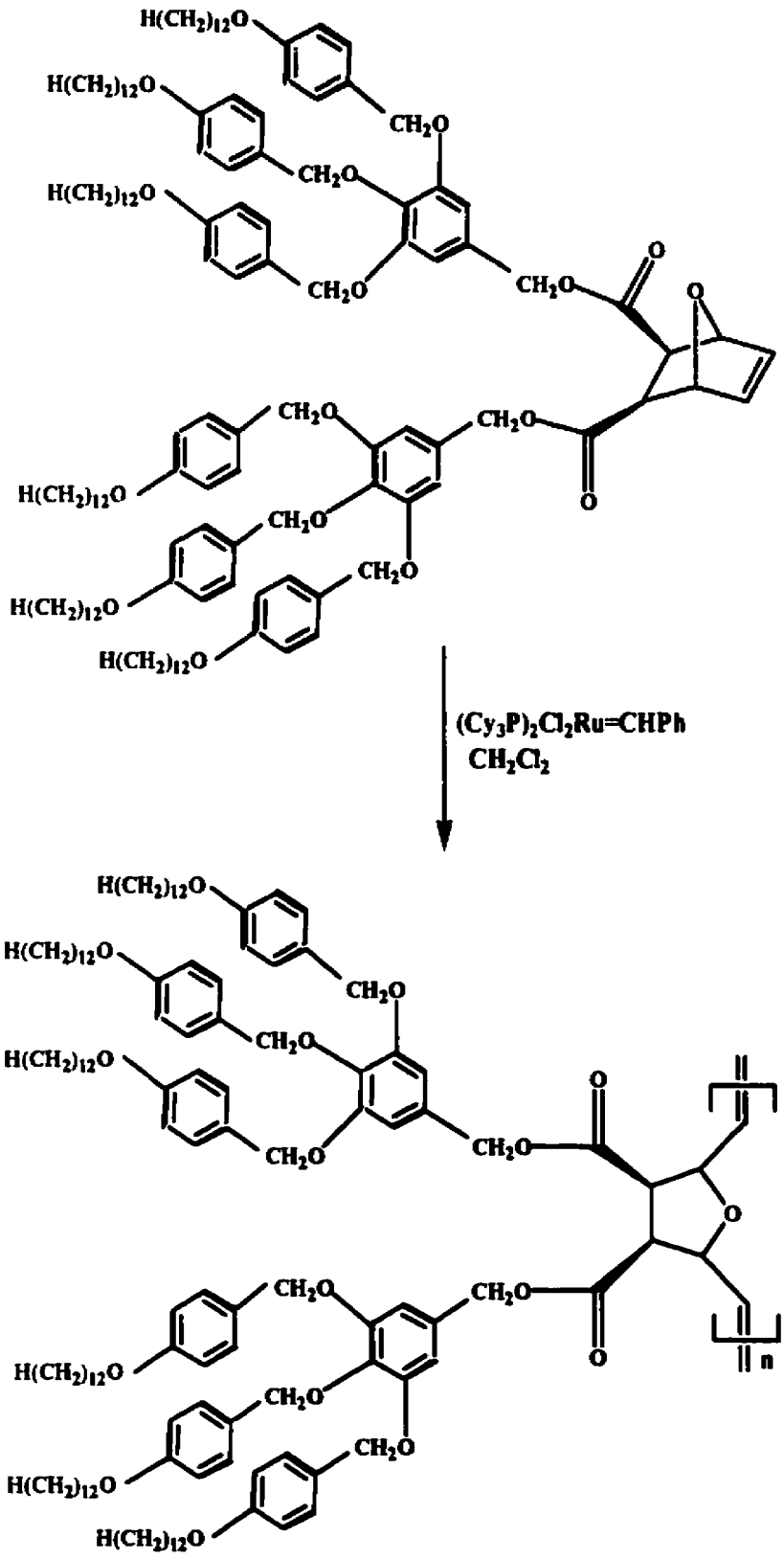

(3.1)

3.1.1 Monoarylation of Aliphatic Diols

3.1.1.1 Organic Pathway

In 1993, Allan and Spreer reported the preparation of a monoaryl alcohol for use as a precursor in the preparation of a water soluble bis(phosphotriester) macrobicyclic polyether cryptand.[156] The starting compound, tri(ethylene glycol) monobenzyl ether, was of interest to this study due to the presence of an aliphatic ether containing a terminal hydroxy group. Synthesis of this particular compound, as seen in Equation 3.2, proceeded by the initial reaction of tri(ethylene glycol) with sodium hydride resulting in the formation of an intermediate glycoxide. This underwent subsequent reaction with benzyl chloride, giving the product in 50% yield. Normally, these types of reactions require an excess of the diol in order to favor monosubstitution, however, with an excess of tri(ethylene glycol), the disubstituted compound was formed in 25% yield.

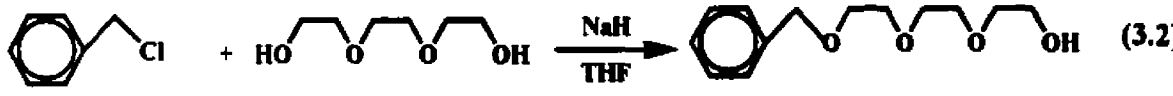

(3.2)

3.1.1.2 Cyclopentadienyliron-Mediated Formation of Monoaryl Alcohols

Several years ago, Pearson and Gelormini reported the synthesis of arene(cyclopentadienyl)iron complexes of monosubstituted diols.[157] When studying the metal-mediated S_NAr reactions of ethylene glycol and 1,4-bis((hydroxyethoxy)ethoxy)benzene with η^6-chlorobenzene(η^5-cyclopentadienyl)iron

hexafluorophosphate (Scheme 3.2) they found that excess diol (2-4 equivalents) gave significant formation of the monoarylated species (62 and 84%, respectively). A typical synthesis involved generation of the intermediate sodium alkoxide by reaction of the diol with NaH in the presence of THF. Subsequent addition of the chlorobenzene complex dissolved in THF, gave a 10:1 ratio of monoarylated to diarylated complex.

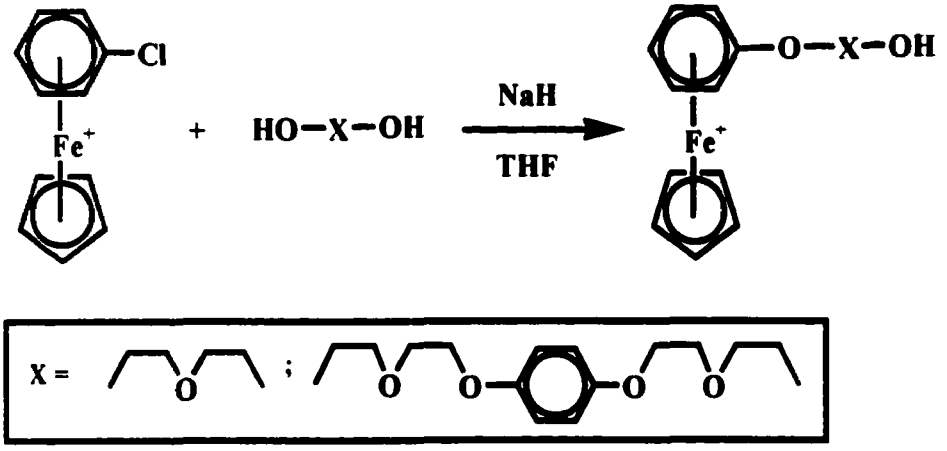

Scheme 3.2

3.2 Results and Discussion

3.2.1 Synthesis of Capped Norbornene Monomers

3.2.1.1 Synthesis of Tri(ethylene glycol) Monobenzyl Norbornene

Initial interest in the design of monomers containing both rigid and flexible components was prompted by the monoaryl alcohol compound discovered by Allan and Spreer whose synthesis was previously described in Equation 3.2.[156] The appearance of this molecule was intriguing due to the presence of the rigid benzyl group as well as the reactive pendent tri(ethylene glycol) linkage, which makes it a suitable precursor for the synthesis of norbornenes containing pendent flexible side chains. Equation 3.3 shows the preparation of tri(ethylene glycol) monobenzyl norbornene. A typical synthesis involved the reaction of tri(ethylene glycol) (**3.1**) with an equivalent amount of *exo,endo*-5-norbornene-2-carboxylic acid (**3.2**) and DMAP in the presence of dichloromethane.

Characterization of the resulting monomer (**3.3**) was accomplished using both 1-D and 2-D NMR spectroscopic techniques (refer to Figure 3.2 for proton and carbon identification), IR and MS. Analysis of the ^{1}H NMR spectrum shown in Figure 3.3 began with identification of the olefinic protons appearing from 5.93 – 6.17 ppm. Since the *endo* H_6 proton appears as the most upfield resonance of the four sets of doublet of doublets, it was assigned the chemical shift at 5.93 ppm. From this well-defined peak, the *endo* H_5 proton could be determined base upon its strong vicinal coupling with H_6 (5.4Hz). Therefore, H_5 belonging to the *endo* isomer was assigned at 6.17 ppm. It is also

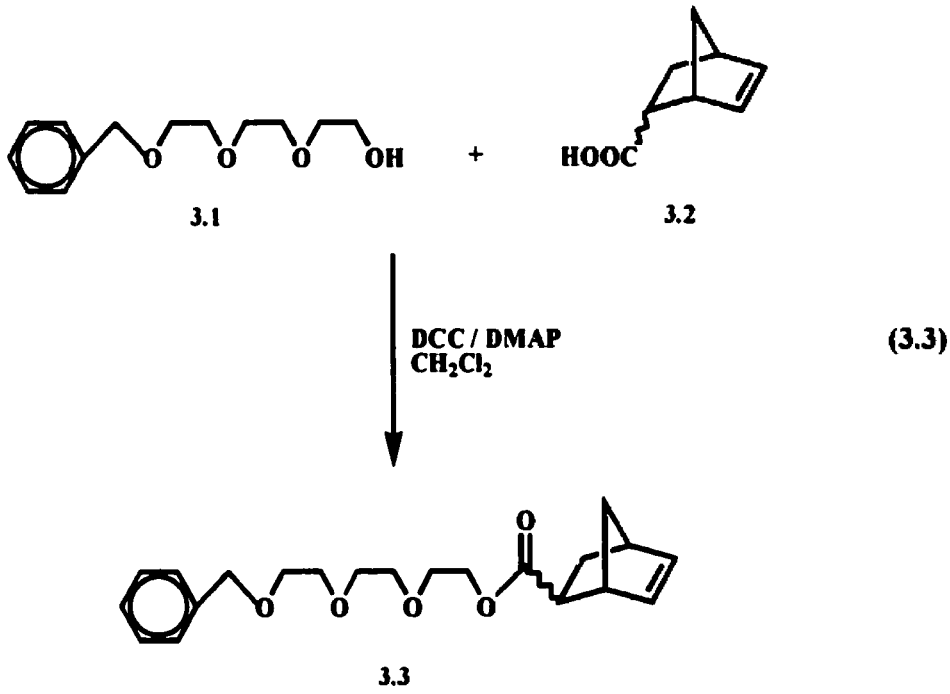

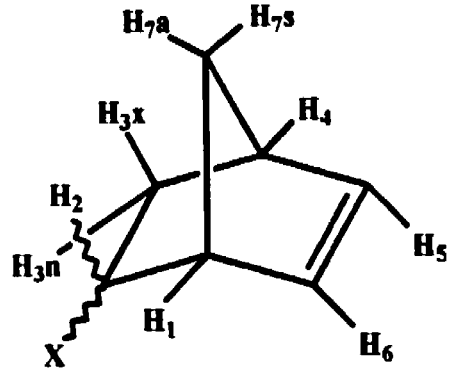

Figure 3.2: Proton schematic of substituted norbornene

understood that H_6 should have a moderate coupling to the bridgehead H_1 proton, whereas H_5 should show a similar coupling with H_4. This coupling is apparent in the HH COSY spectrum in Figure 3.4 as connectivities are observed between H_6 and a proton at 3.20 ppm identified as *endo* H_1 as well as between H_5 and a proton at 2.88 ppm (*endo* H_4). Further confirmation of these crosspeaks was obtained upon measuring the respective couplings [2.7 Hz for $J_{(1,6)}$ and 3.0 Hz for $J_{(4,5)}$], which are in agreement with previous literature findings.[141]

Recall that H_1 can only couple with H_2 when it is in the *exo* position and H_4 can only couple with H_{3x}.[141] Analysis of the HH COSY spectrum revealed a connectivity between H_1 and a broad multiplet at 2.96 ppm which represented the *exo* H_2 proton in the *endo* isomer. Another crosspeak was observed between H_4 and a multiplet at 1.88 ppm which represented the H_{3x} resonance in the *endo* isomer. Due to significant peak broadening, the coupling could not be measured for $J_{(1,2)}$, however, it was calculated as 3.5 Hz for $J_{(3x,4)}$. Confirmation of the assigned chemical shifts for H_2 and H_{3x} belonging to the *endo* isomer was obtained upon measuring their strong *exo-exo* coupling ($J_{(2,3x)}$ = 9.7 Hz), which is typical for this coupling. Location of the *endo* H_{3n} proton was then achieved based upon its strong geminal coupling with H_{3x}. This value of 10.3 Hz provided definitive evidence that the proton resonance present at 1.41 ppm belonged to that of H_{3n}.

Identification of the chemical shifts representative of the bridge H_{7a} and H_{7s} protons was extremely difficult to accomplish. As these proton resonances normally

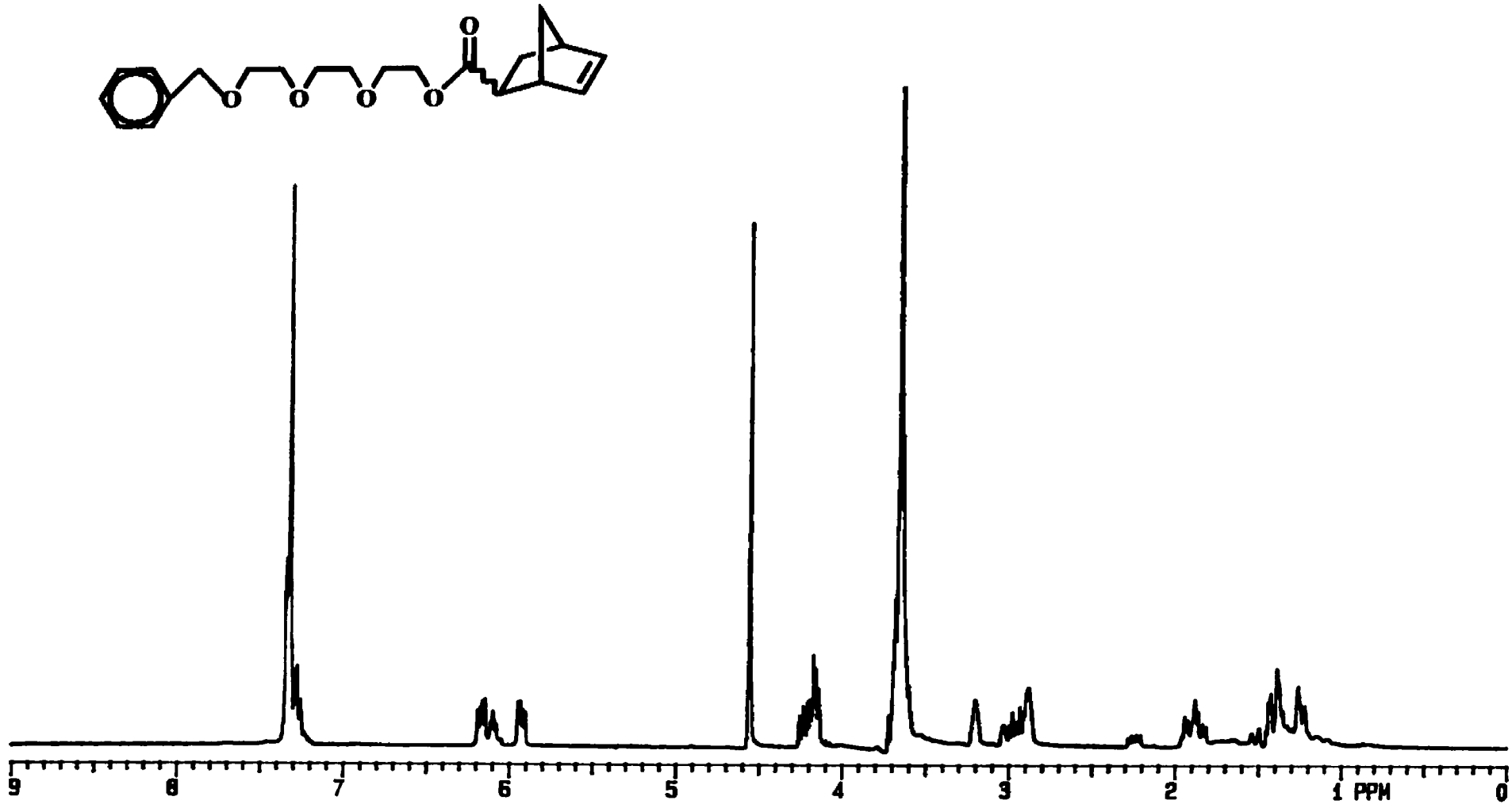

Figure 3.3: ^{1}H NMR of compound **3.3** in $CDCl_3$.

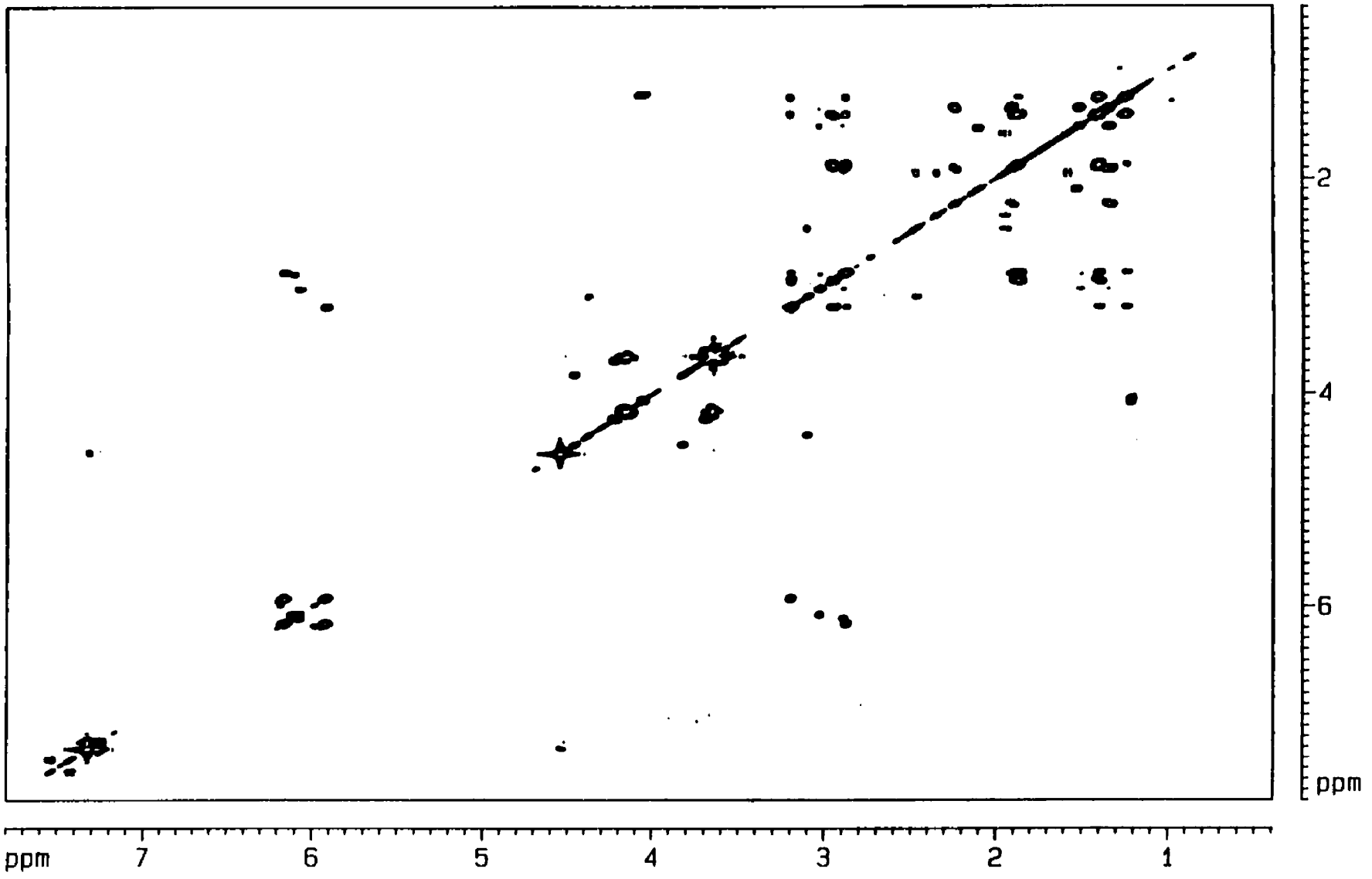

Figure 3.4: HH COSY of compound **3.3** in $CDCl_3$.

appear the most upfield relative to the other protons in norbornene and have a very strong geminal coupling, the general vicinity of these protons can be located.[139, 141] An intense coupling of 9.5 Hz was calculated for two protons present at 1.25 and 1.41 ppm. A tentative assignment of these resonances to the *endo* isomer was made upon the general trend observed in the ^{1}H NMR spectrum where the *endo* isomer protons appear significantly more intense than those belonging to the *exo* isomer. Furthermore, as these were the last two unassigned intense peaks in the ^{1}H NMR spectrum, they were tentatively attributed to the *endo* isomer. Further analysis of the HH COSY spectrum revealed a weak long-range coupling between the signal at 1.25 ppm to the *endo* olefinic protons H_5 and H_6. Previous NMR studies of 7-functionalized norbornenes show that the only proton of the two bridge H_7 protons that can exhibit a coupling with either of the olefinic resonances is H_{7a}.[139, 141] In addition, since it was coupled to the *endo* olefinic protons, it confirmed the *endo* assignment of these protons. Since the other peak present at 1.41 ppm did not demonstrate a connectivity to the olefinic protons, it was assigned as the H_{7s} proton in the *endo* isomer. Once each of the *endo* isomeric protons was assigned, location of the *exo* isomeric protons could then be accomplished.

Characterization of the methylene resonances in the tri(ethylene glycol) bridge was achieved by comparing the ^{1}H NMR spectra of both the monomer and the starting compound 5-norbornene-2-carboxylic acid (**3.2**). The ^{1}H NMR spectrum of **3.3** clearly displays three strong resonances in the range of 3.66 – 4.56 ppm, which are absent in the spectrum of the parent starting material (**3.2**). Since this region is characteristic of aliphatic ether methylene protons, the protons were assigned to these peaks.[132] A strong singlet at 4.56 ppm integrating to two protons was attributed to the methylene protons

alpha to the benzene ring. An interesting feature was the appearance of a multiplet at 4.17 ppm integrating to two protons. These methylene protons were assigned as those neighboring the carbonyl group, as was confirmed using mathematical chemical shift calculations.[132] The appearance of a multiplet for this particular peak was attributed to the nature of these diastereomeric protons. Due to their close proximity to C_2, which is a chiral center, this peak at 4.17 ppm demonstrates similar effects of isomerism. The final broad multiplet appearing at 3.66 ppm was representative of the remaining methylene protons contained in the aliphatic bridge. A final resonance that was originally absent in the ^{1}H NMR spectrum of the parent norbornene compound was that appearing from 7.32 – 7.33 ppm representative of the aromatic protons. A full record of ^{1}H NMR chemical shift data can be found in Table 3.1 and the observed coupling constants in Table 3.3.

Identification of the *endo* and *exo* carbon resonances as observed in the ^{13}C NMR spectrum (Figure 3.5) was achieved using HETCOR spectroscopic techniques, of which the spectrum is illustrated in Figure 3.6. Based upon correlations between the already-identified protons in the ^{1}H NMR spectrum with carbons in the ^{13}C NMR spectrum the chemical shift of each carbon atom could be assigned, as referenced in Table 3.2. Assignment of the methylene carbons in the aliphatic spacer commenced with the peak appearing 73.14 ppm representative of the methylene carbon neighboring the aromatic ring. An interesting feature observed upon assigning the remaining methylene carbons in the aliphatic spacer was that a total of seven peaks remained for the six carbons left unassigned. Examination of the HETCOR spectrum revealed a connectivity from a pair

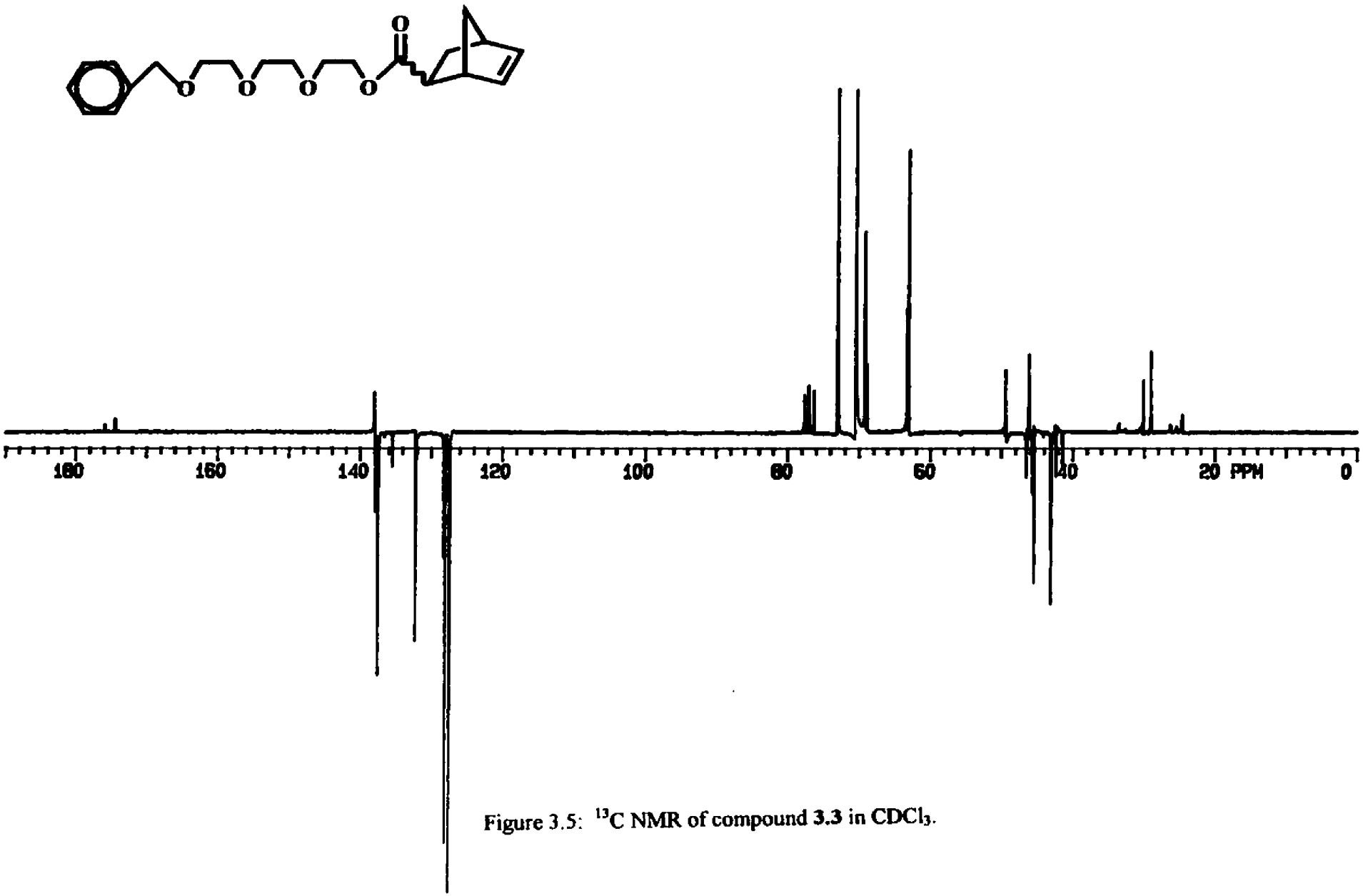

Figure 3.5: ^{13}C NMR of compound **3.3** in $CDCl_3$.

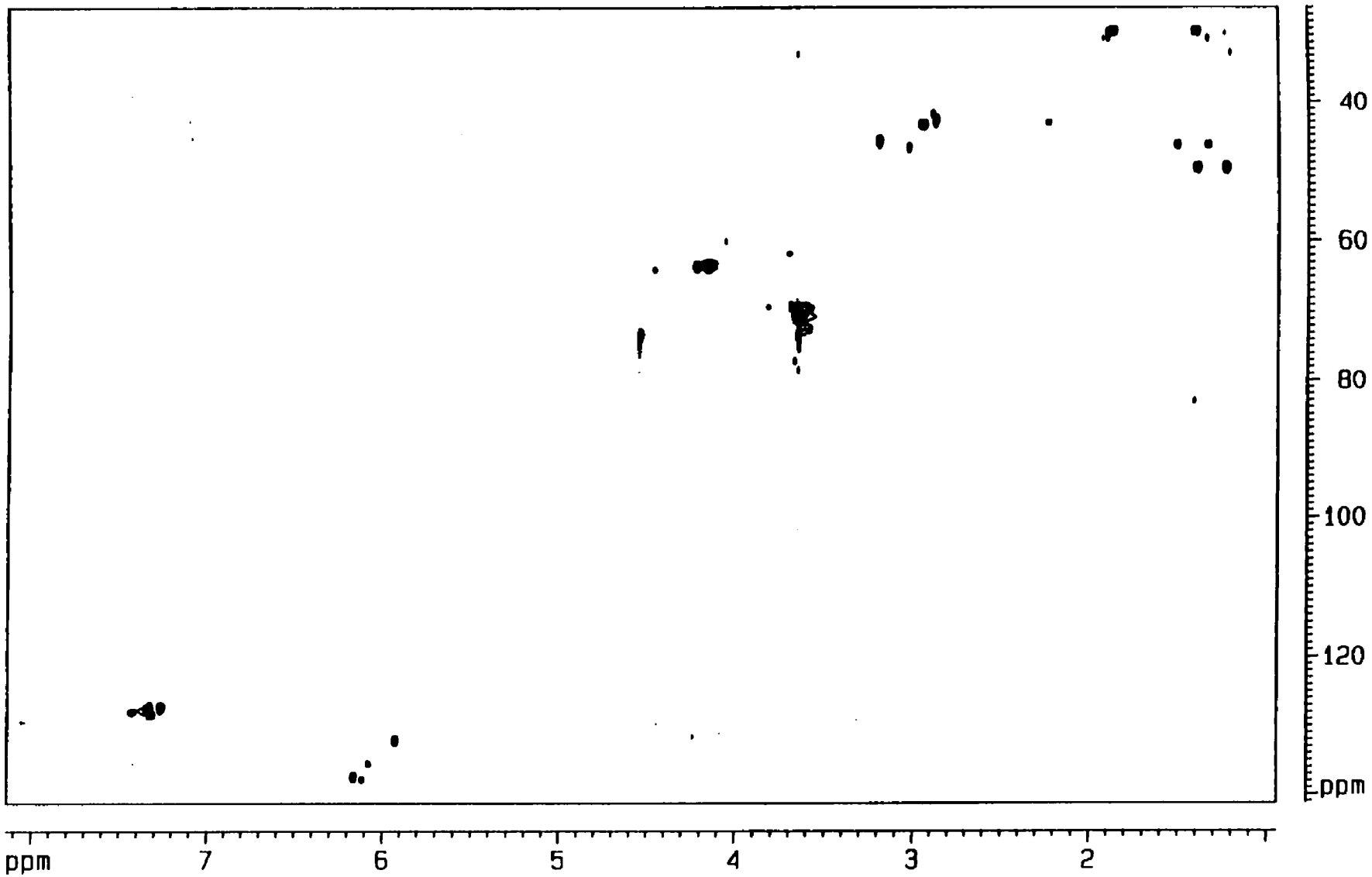

Figure 3.6: CH COSY of compound **3.3** in $CDCl_3$.

of carbon resonances in this region of the spectrum to the proton multiplet appearing at 4.17 ppm in the ^{1}H NMR spectrum that had been previously identified as the methylene protons adjacent to the carbonyl group. As this peak was already described as showing isomerism, the two peaks representative of this correlation at 63.21 and 63.40 ppm were assigned as the *endo* and *exo* isomers of this particular carbon atom, respectively. Other analytical techniques that aided in product identification were MS and IR, which verified the molecular ion peak (M^+) of 360 and the carbonyl group at 1732 cm^{-1}, respectively.

3.2.1.2 Cyclopentadienyliron-Mediated Formation of Norbornene Monomers

3.2.1.2.1 Aliphatic Ether Bridged Monomers: Tri(ethylene glycol)

The role of the $CpFe^+$ moiety in the synthesis of monoaryl alcohols was examined by the ability of chlorobenzene and chlorotoluene complexes to undergo S_NAr with tri(ethylene glycol). Preparation of the benzene analogue (**3.7**) was accomplished via the reaction of chlorobenzene complex (**3.4**) with an excess of tri(ethylene glycol) (**3.6**) as illustrated in Scheme 3.3. The reaction proceeded by the formation of the sodium alkoxide salt, which was generated by the reaction of **3.6** with NaH in THF. Subsequent addition of the complex dissolved in THF and stirring under nitrogen for 6 h gave the complexed monomer **3.7** as a yellow oil in 95 % yield. This metal-mediated methodology routinely gave high yields of the monoarylated products under extremely mild and efficient reaction conditions.

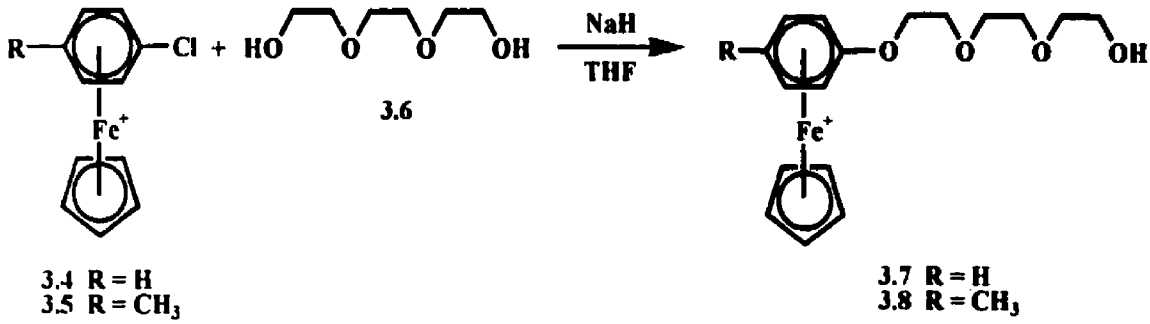

Scheme 3.3

Characterization of complex **3.7** was accomplished by ^{1}H and ^{13}C NMR. Comparison of the ^{1}H NMR spectra between the parent chlorobenzene-(cyclopentadienyl)iron complex **(3.4)** and **3.7** indicated a characteristic upfield shift of the Cp resonance representative of successful S_NAr. The single Cp resonance at 5.31 ppm in the spectrum of the parent complex (Figure 3.7), shifted significantly upfield to 5.19 ppm in the product. As has been previously observed by Pearson in the synthesis of ethylene glycol derivatives of chlorobenzene(cyclopentadienyl)iron complexes,[157] the presence of a 10:1 mixture of monoarylated to diarylated complex was observed as defined by the small Cp resonance appearing at 5.15 ppm in the ^{1}H NMR spectrum. Analysis of the ^{13}C NMR spectrum shown in Figure 3.8 denotes a single Cp carbon resonance at 77.39 ppm, displaying no additional resonance for the diarylated complex.

Presence of the tri(ethylene glycol) substitutent was confirmed through the appearance of strong methylene proton resonances from 3.54 – 4.46 ppm. A strong triplet at 4.46 ppm integrating for two protons and having a coupling constant of 4.3 Hz was representative of the methylene protons alpha to the aromatic ring. The next most downfield resonance (3.90 ppm) was attributed to the methylene protons beta to the aromatic ring which also demonstrate a triplet pattern with J = 4.3 Hz. The rest of the

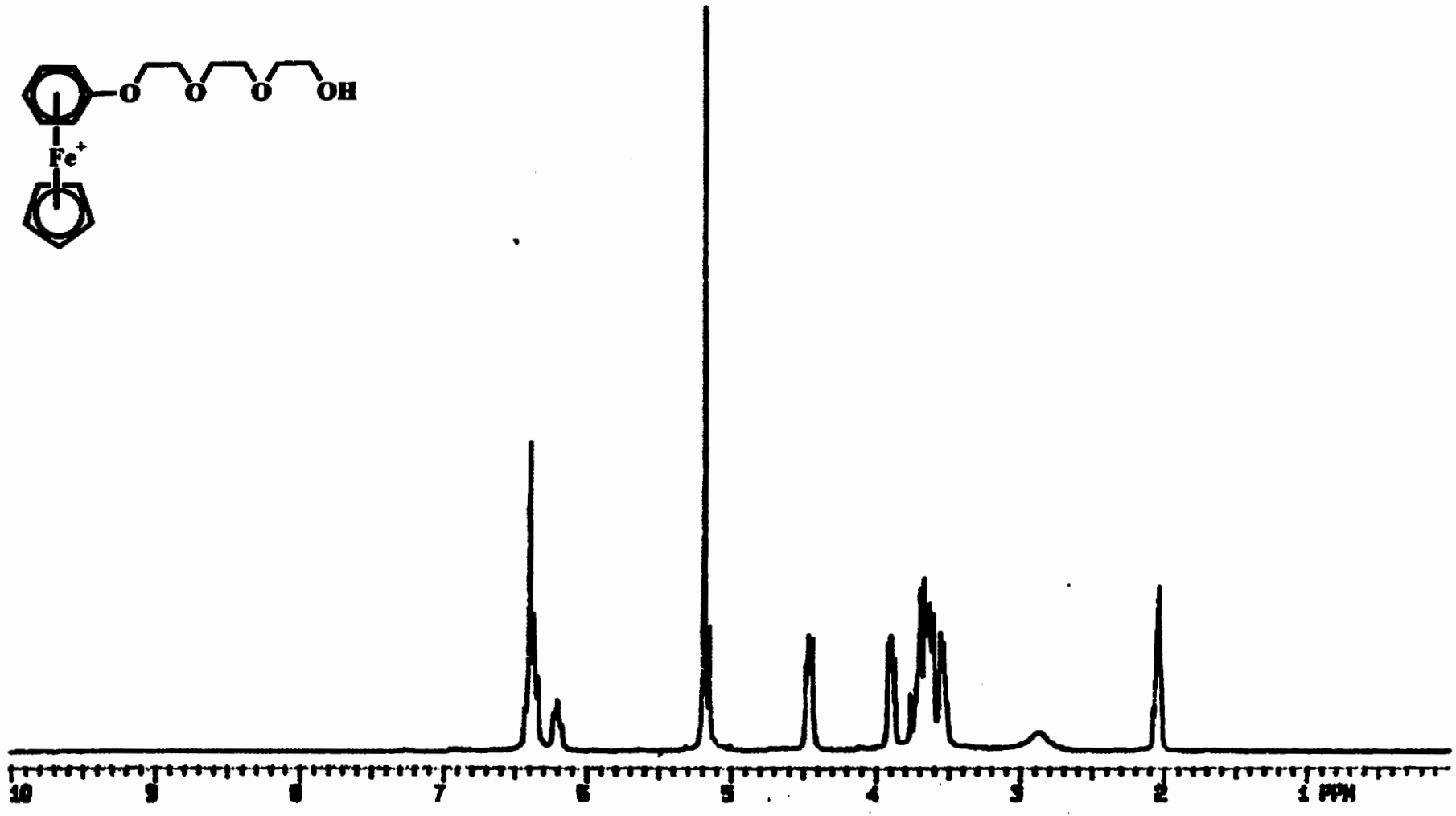

Figure 3.7: ^{1}H NMR of complex **3.7** in acetone-d_6.

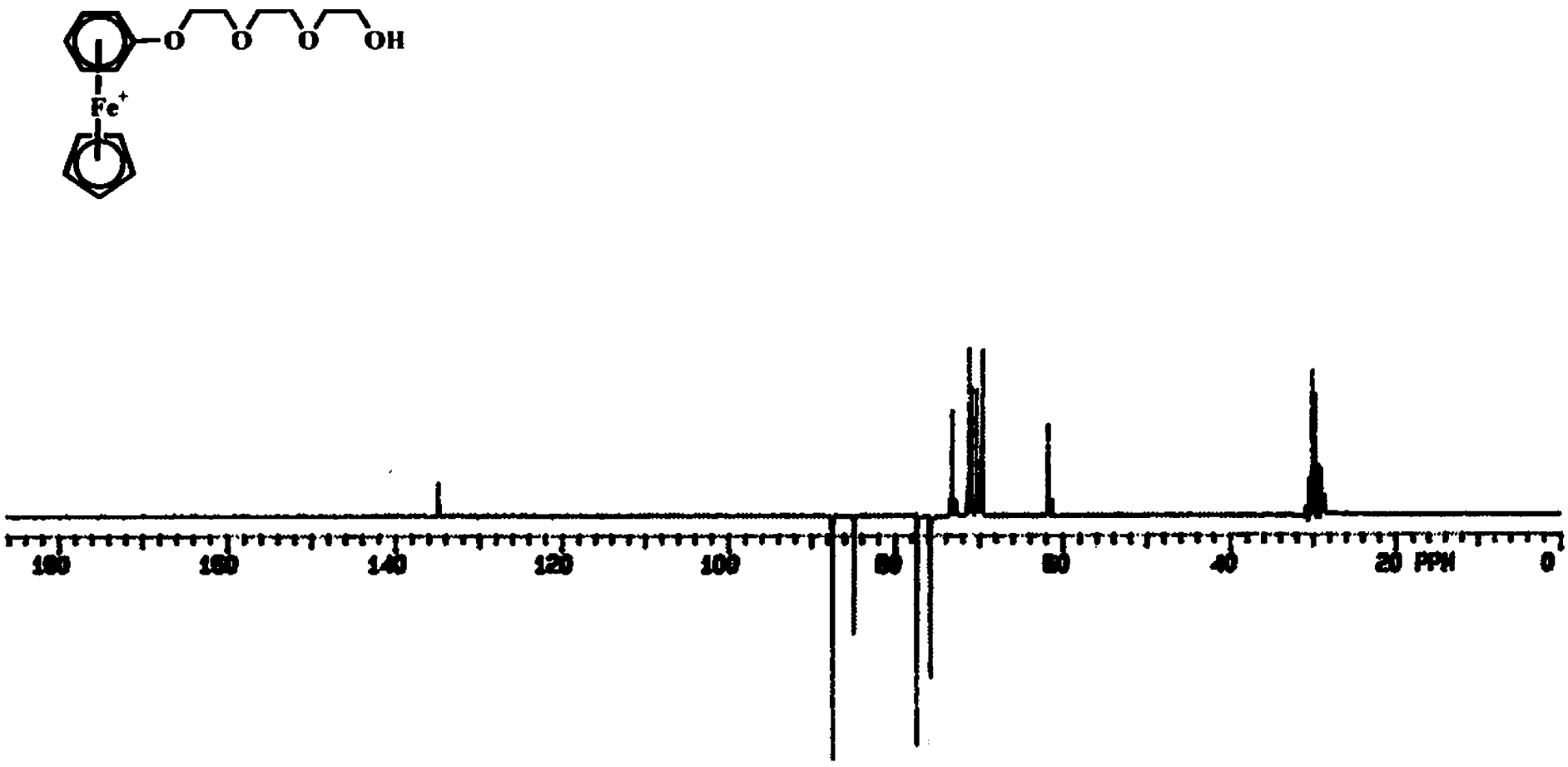

Figure 3.8: ^{13}C NMR of complex **3.7** in acetone-d_6.

methylene protons appeared as a multiplet from 3.54 – 3.77 ppm integrating for the final eight protons. The last peak used to confirm the structural features of this complex was the broad singlet at 2.86 ppm, which represented the terminal hydroxyl group on the pendent aliphatic chain. Table 3.4 contains a full outline of chemical shift data for complexes **3.7** and **3.8**.

Each of the unique methylene carbon atoms in the aliphatic side chain were located as well-defined single resonances appearing in the range of 61.79 – 73.33 ppm in the ^{13}C NMR spectrum. These specific chemical shifts can be observed by referring to Table 3.5 which consists of a complete analysis of the carbon resonances for complexes **3.7** and **3.8**. Conclusive evidence verifying that S_NAr had taken place was denoted by the absence of a resonance at 106.60 ppm which is characteristic of the C-Cl quaternary carbon present in the spectrum for the parent complex **3.4**. A new quaternary resonance at 134.91 ppm represented the newly formed C-O linkage in **3.7**.

Following the synthesis of the tri(ethylene glycol) monoaryl alcohol, condensation with 5-norbornene-2-carboxylic acid allowed for the formation of the metallated monomer. Complex **3.9** was prepared by reacting complex **3.7** in the presence of excess **3.2**, DCC and DMAP using dichloromethane as the solvent, as is represented in Scheme 3.4. The product was isolated as a yellow viscous material in 58 % yield. Decomplexation of **3.9** was accomplished using photolytic demetallation yielding the modified norbornene monomer **3.11** in 77 % yield.

Structural analysis of complexes **3.9**, **3.10** and compounds **3.11** and **3.12** was obtained using ^{1}H and ^{13}C NMR spectroscopy. Tables 3.6 – 3.9 provide all of the NMR spectroscopic data for the ^{1}H and ^{13}C metallated monomers as well as the ^{1}H and ^{13}C

NMR for the organic monomers, respectively. Looking at the structural features of the metallated complex **3.9** as a model for this discussion, a strong singlet at 5.17 ppm in the ^{1}H NMR spectrum (Figure 3.9) and at 77.40 in the ^{13}C NMR spectrum (Figure 3.10), are representative of the Cp resonance. As already observed for the aromatic ether complexed monomers, only a single peak is representative of the Cp in each of the *exo* and *endo* isomers. The appearance of two sets of doublet of doublets separated by a broad multiplet, which is characteristic of the vinylic protons in the ^{1}H NMR spectrum, suggests the presence of two isomers. Further evidence was obtained by the characteristic H_2 *exo* and *endo* resonances. The appearance of a broad multiplet at 2.98 ppm is characteristic of the *exo* H_2 proton in the *endo* isomer, whereas the crown-like doublet of doublet appearance of the *endo* H_2 proton at 2.14 ppm is characteristic of the *exo* isomer. Isomerism can also be identified through a specific chemical shift change denoted in the methylene proton resonances. A broad multiplet at 4.11 ppm is characteristic of the two methylene protons alpha to the carbonyl group. The appearance of a multiplet for these two protons is due to the isomerism present at C_2 in the norbornene structure.

Analysis of the ^{13}C NMR spectrum reveals the presence of two isomers due to the duplicate appearance of norbornene ring carbons in the range of 42.20 – 47.22 ppm, characteristic of the C_1, C_2 and C_4 *endo* and *exo* carbons. Two carbonyl groups at 174.47 and 176.09 also identifies the *endo* and *exo* isomerism, respectively. As each of these unique spectral patterns have also been observed in the analysis of complex **3.10** they can be used as guidelines in the analysis of similar compounds.

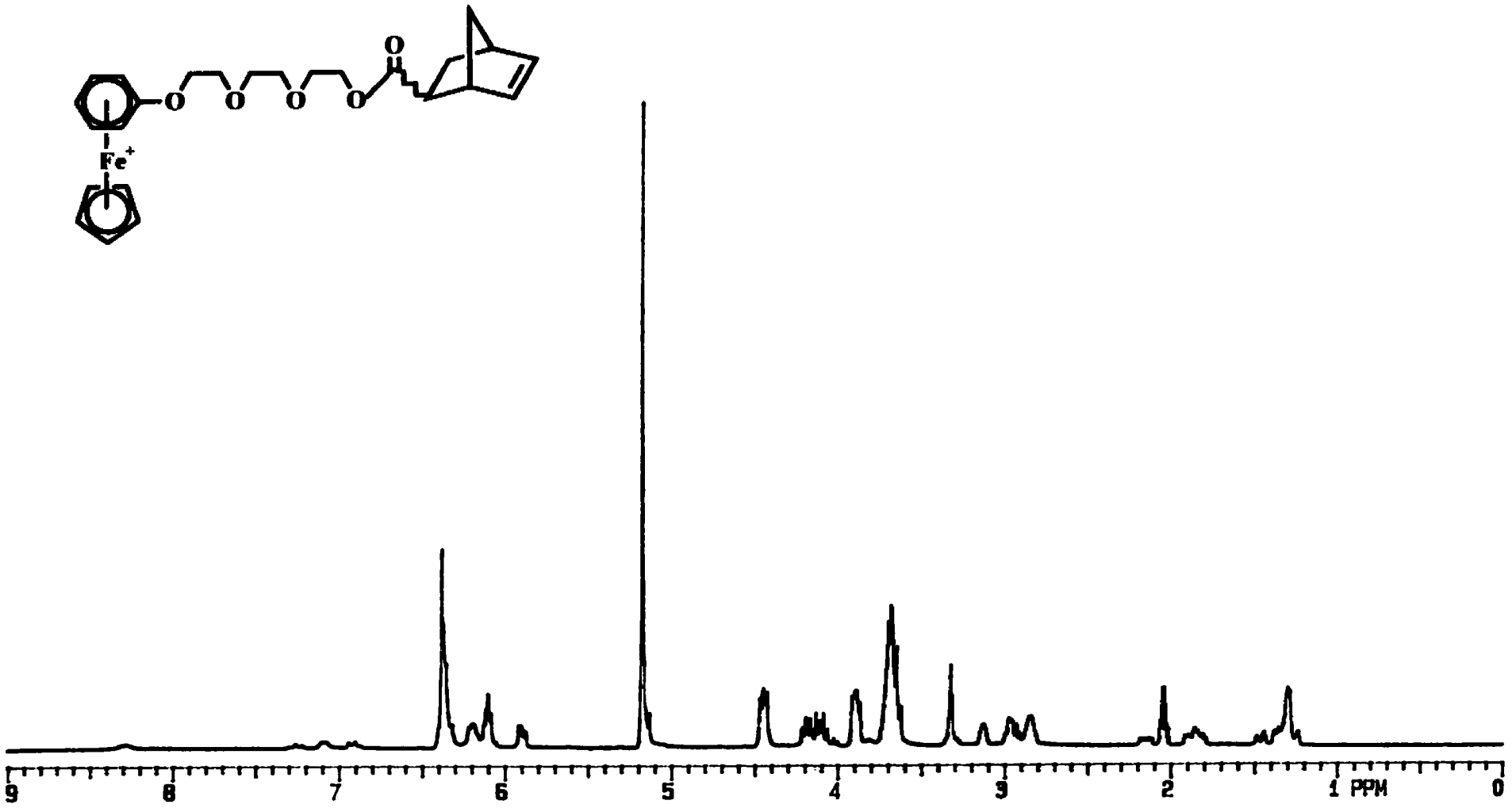

Figure 3.9: ^{1}H NMR of complex **3.9** in acetone-d_6.

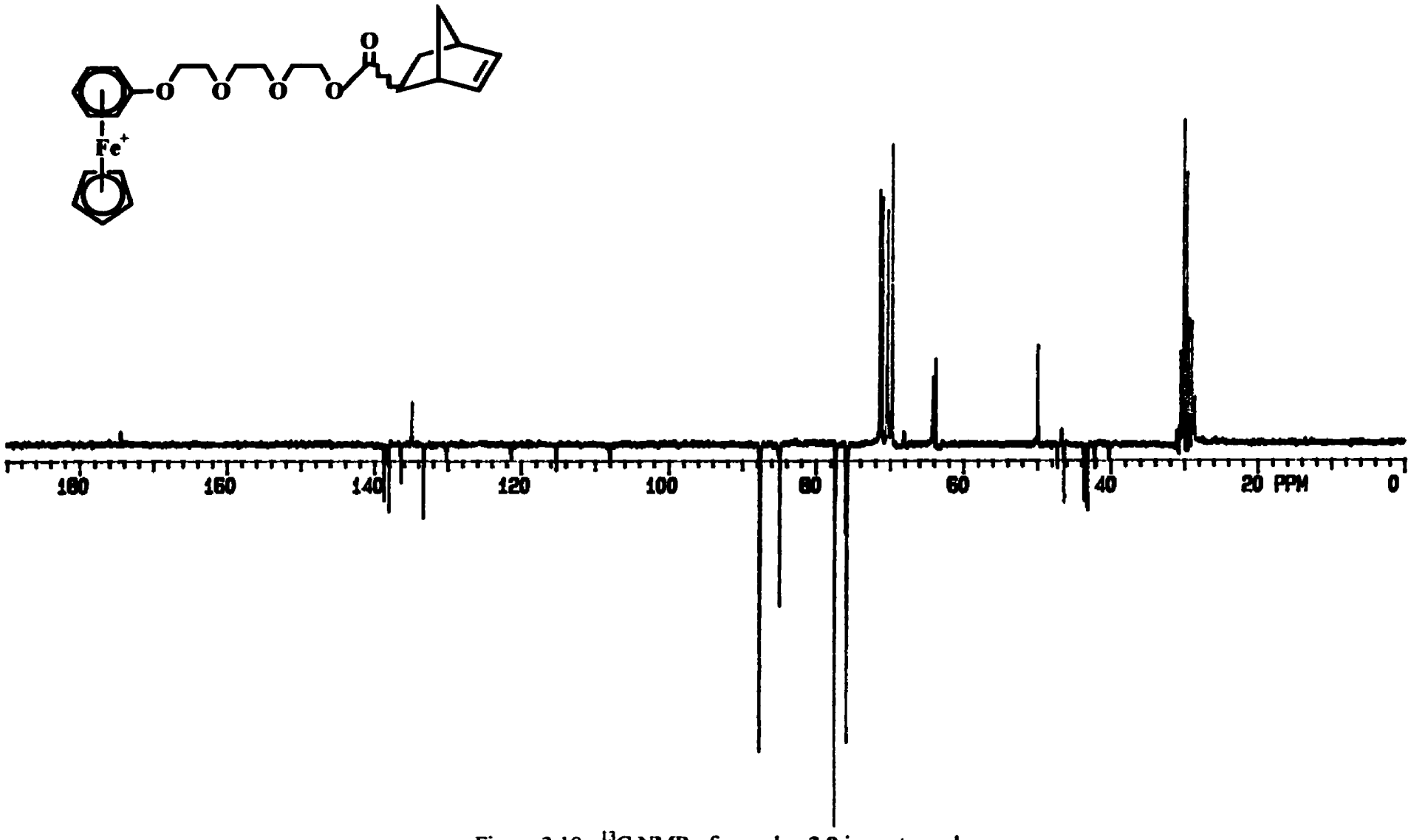

Figure 3.10: ^{13}C NMR of complex **3.9** in acetone-d_6.

Isolation of the organic monomer **3.11** was identified by the absence of the Cp resonance at 5.17 ppm in the ^{1}H NMR spectrum and at 77.40 ppm in the ^{13}C NMR spectrum (Figures 3.11 and 3.12, respectively). Further spectral evidence for loss of the metal moiety was observed by the characteristic downfield shift of the aromatic proton resonances from 6.11 and 6.40 ppm in **3.9** to 6.93 and 7.30 ppm in **3.11**. This shift is more evident in the ^{13}C NMR spectrum which shows three strong uncomplexed aromatic carbon resonances at 114.53, 120.79 and 129.35 ppm which are significantly more downfield than in their original positions in the metallated system (75.85 – 87.54 ppm). The methylene protons alpha to the benzene ring also showed a significant upfield shift upon demetallation such that these protons shifted from 4.45 ppm to 3.86 ppm, as was observed in the ^{1}H NMR spectrum.

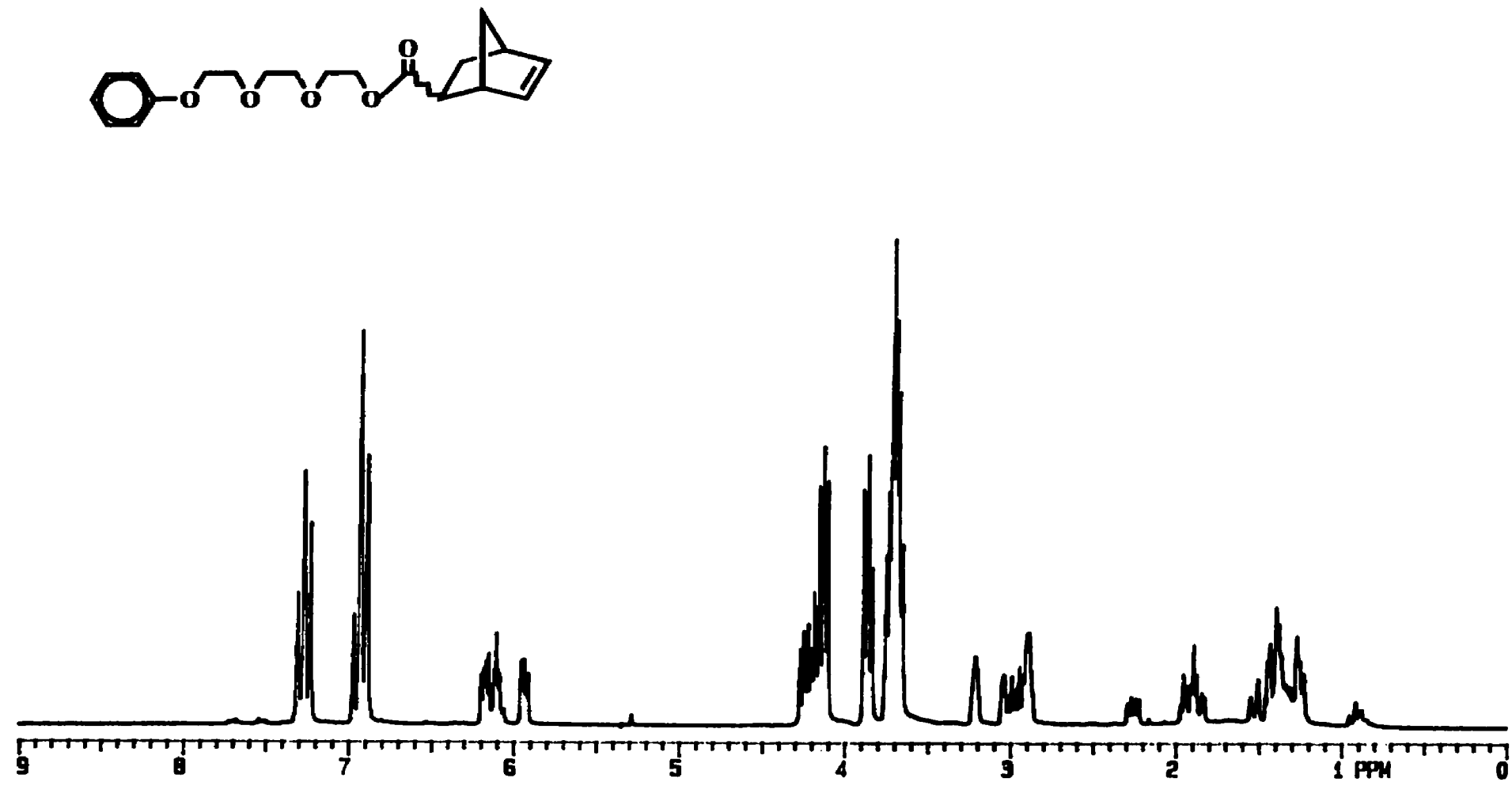

Figure 3.11: ^{1}H NMR of compound **3.11** in $CDCl_3$.

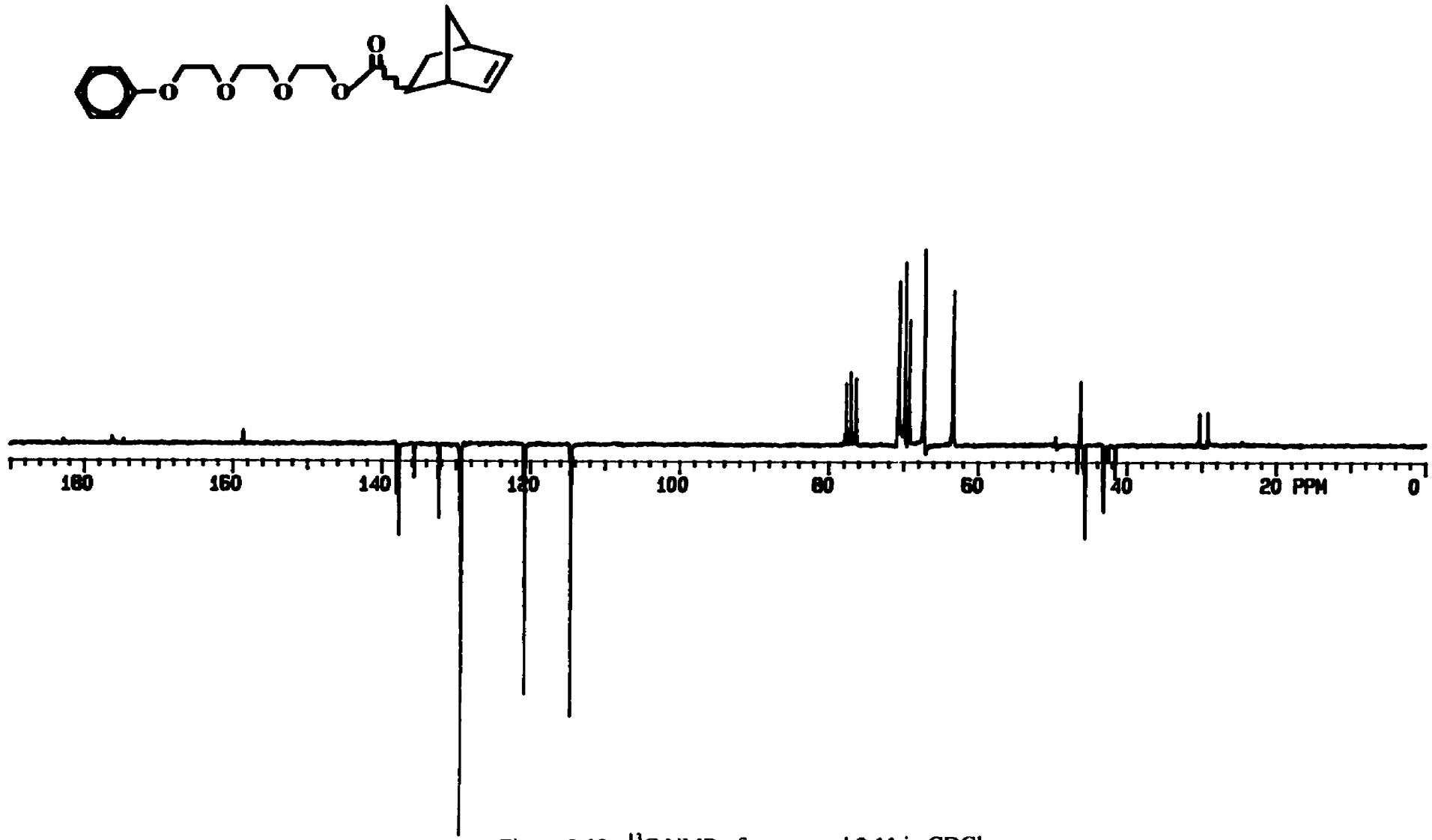

Figure 3.12: ^{13}C NMR of compound **3.11** in $CDCl_3$.

3.2.1.2.2 Aliphatic Bridged Monomers: 1,4-Butanediol and 1,6-Hexanediol

In an attempt to increase chain flexibility between the norbornene unit and the pendent monoarene, new monomers were prepared containing pure methylene bridges. A similar methodology was used for the preparation of these complexes as was previously described for the preparation of the tri(ethylene glycol) monoaryl norbornene derivatives. The first step in this two step synthesis required the initial monoarylation of an aliphatic diol, either 1,4-butanediol or 1,6-hexanediol, which is illustrated in Scheme 3.5. Complex **3.16**, for example, was prepared by the reaction of chlorobenzene(cyclopentadienyl)iron (**3.4**) with an excess of 1,6-hexanediol (**3.14**). Initially, the diol (**3.14**) was reacted with NaH in THF for 15 min. Subsequent addition of the complex dissolved in THF and stirring at room temperature liberated the yellow oil in 83% yield.

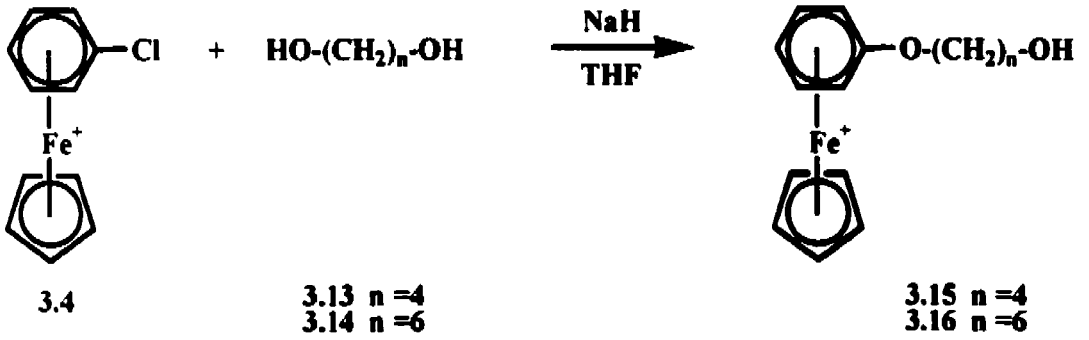

Scheme 3.5

Structural identification of the monoiron complex was obtained by analysis of the ^{1}H and ^{13}C NMR spectra. The ^{1}H NMR spectrum (Figure 3.13) showed a notable upfield

shift in the Cp resonance from its original position of 5.31 ppm in **3.4** to 5.16 ppm in the spectrum of complex **3.16**. This change in the chemical shift of the Cp resonance is significant towards confirming that S_NAr had successfully occurred. Furthermore, the appearance of this resonance as a single peak indicated that only monoarylation had occurred. This was also confirmed in the ^{13}C NMR spectrum shown in Figure 3.14 by the single Cp peak present at 77.12 ppm.

Identification of the aliphatic methylene protons was accomplished by their characteristic chemical shifts and integration patterns. The methylene proton resonances alpha to the benzene complex appeared the furthest downfield as a triplet at 4.30 ppm. The protons neighboring the terminal alcohol functionality also appeared quite far downfield and were located as another triplet at 3.55 ppm. The presence of a multiplet at 1.86 ppm integrating for two protons was determined to be the methylene protons beta to the aromatic group and the large multiplet at 1.50 ppm integrating to six was assigned to the remaining methylene protons. A detailed list of ^1H NMR data can be observed in Table 3.10. Location of each of the methylene resonances could also be identified in the ^{13}C NMR spectrum by the distinct presence of six carbon CH_2 peaks whose chemical shifts are recorded in Table 3.11.

Two final resonances crucial towards verifying the molecular structure of this complex were available in the ^1H and ^{13}C NMR spectra. In the ^1H NMR spectrum, the terminal hydroxyl proton signal was located at 3.13 ppm. Also, successful S_NAr was verified by the absence of the C-Cl quaternary carbon resonance at 106.60 ppm from the parent complex, with the appearance of a new resonance at 135.13 ppm representative of the quaternary carbon belonging to the newly formed C-O bond.

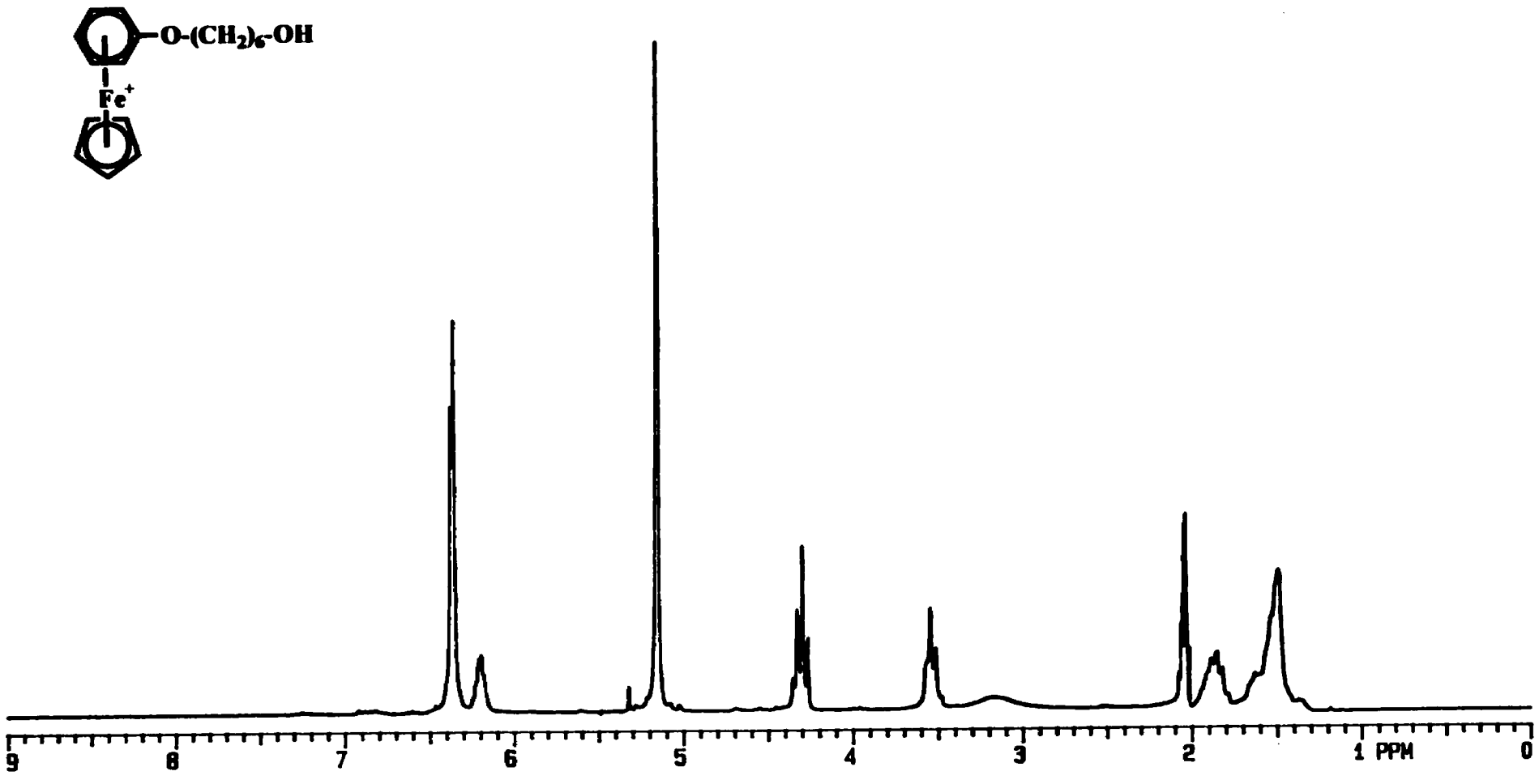

Figure 3.13: ^{1}H NMR of complex **3.16** in acetone-d_6.

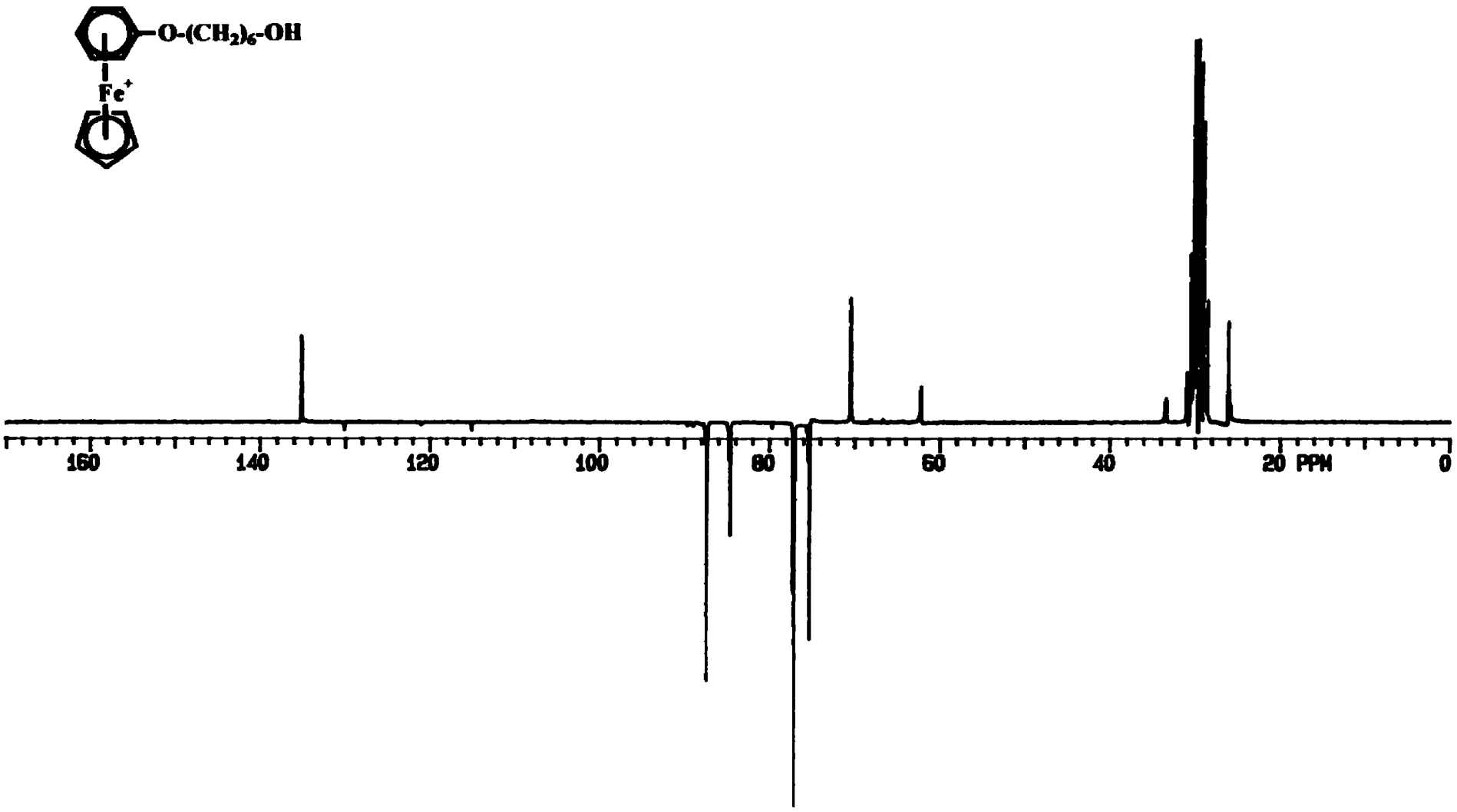

Figure 3.14: ^{13}C NMR of complex **3.16** in acetone-d_6.

Each of these terminal alcohol complexes were then capped with **3.2** as previously described for the tri(ethylene glycol) complexes. Scheme 3.6 describes a typical synthesis of complexes **3.17** and **3.18** that involved the reaction of the monometallic complex (**3.15**; **3.16**) with an excess of **3.2**, DCC and DMAP. The resulting complexed norbornenes were isolated as yellow oils in 63 - 65 % yield. Isolation of the organic monomers **3.19** and **3.20** was achieved once again using photolytic demetallation which liberated the norbornene monomers in 61 – 63 % yield.

Analysis of the structural features of complex **3.18** was accomplished as previously described for **3.9**. A full spectral analysis was used to confirm the *endo* and *exo* isomerism in this complex through the use of one- and two-dimensional NMR (Figures 3.15 – 3.18). Verification of the metallated nature of the complex was achieved upon location of the Cp resonance in both the ^{1}H and ^{13}C NMR spectra. These appeared at 5.14 and 77.21 ppm, respectively. Isomerism was once again identified by the appearance of the characteristic olefinic spectral resonances as well as by the presence of isomerism for the H_1 (C_1), H_2 (C_2) and H_4 (C_4) norbornene ring protons and carbons, respectively. As previously observed in the metallated tri(ethylene glycol) monomers, the methylene protons adjacent to the carbonyl group appeared as a broad multiplet at 4.02 ppm due to the different magnetic environments of the *endo* and *exo* isomers at C_2. This isomerism was further denoted in the ^{13}C NMR spectrum by virtue of the HETCOR spectrum that showed a correlation of this proton resonance to a set of peaks at 64.34 and 64.68 ppm, representative of the *endo* and *exo* methylene carbon atoms. Tables 3.12 and 3.13 contain a detailed overview of the respective ^{1}H and ^{13}C NMR chemical shifts for these complexes.

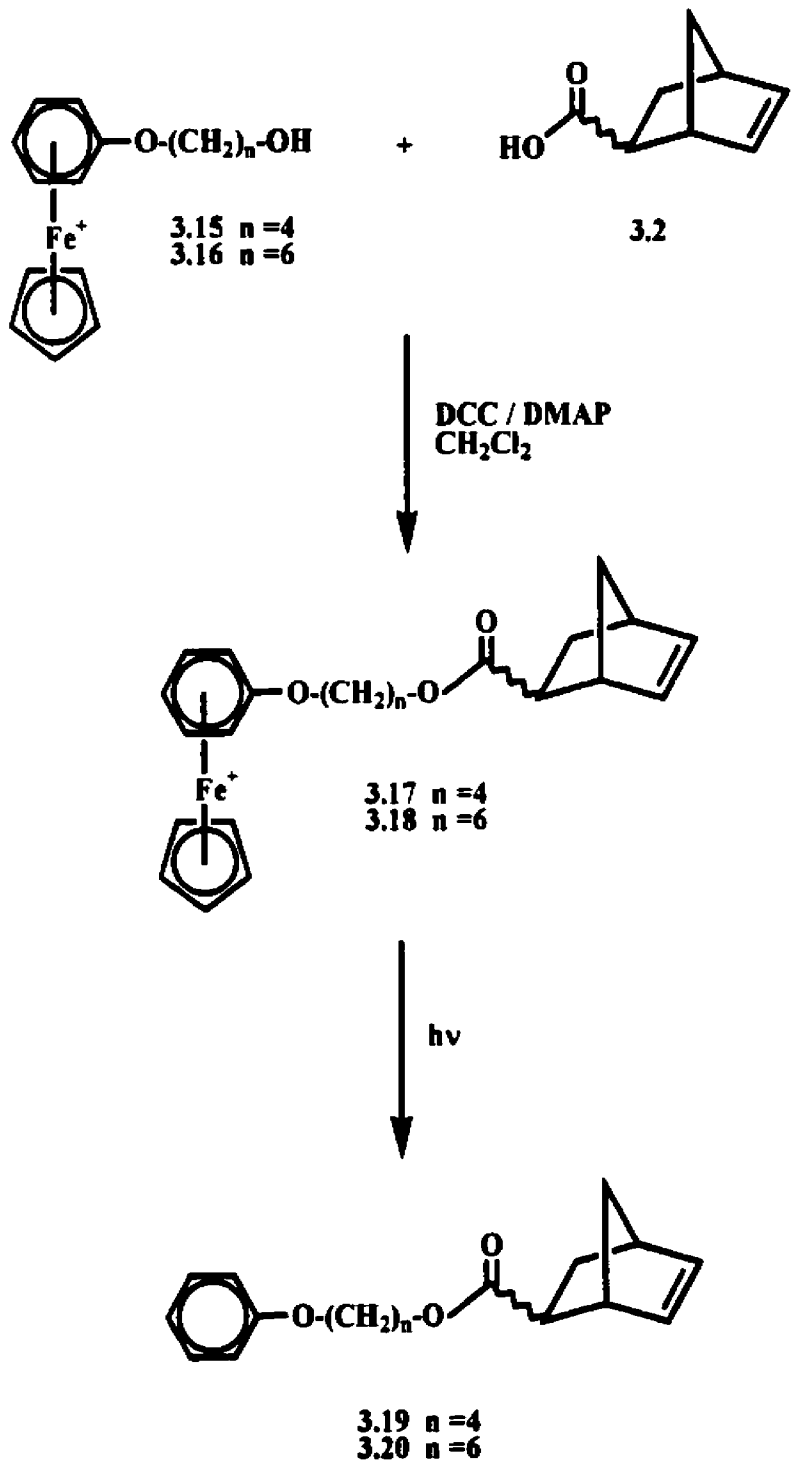
O-(CH2)n-OH
Fe+
3.15 n =4
3.16 n =6
+
HO
O
3.2
DCC / DMAP
CH2Cl2
O-(CH2)n-O
Fe+
3.17 n =4
3.18 n =6
hν
O-(CH2)n-O
3.19 n =4
3.20 n =6

Scheme 3.6

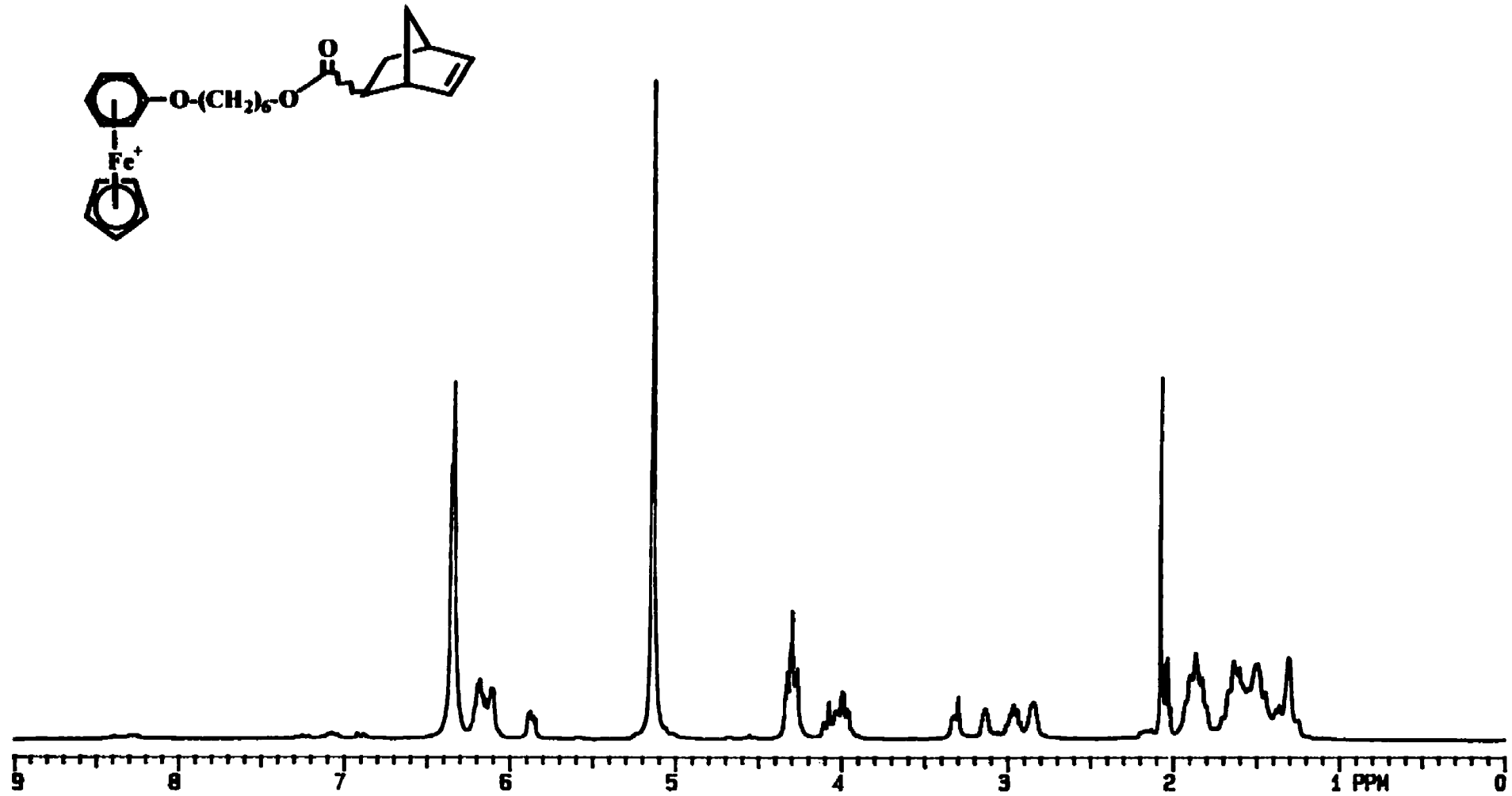

Figure 3.15: ^{1}H NMR of complex **3.18** in acetone-d_6.

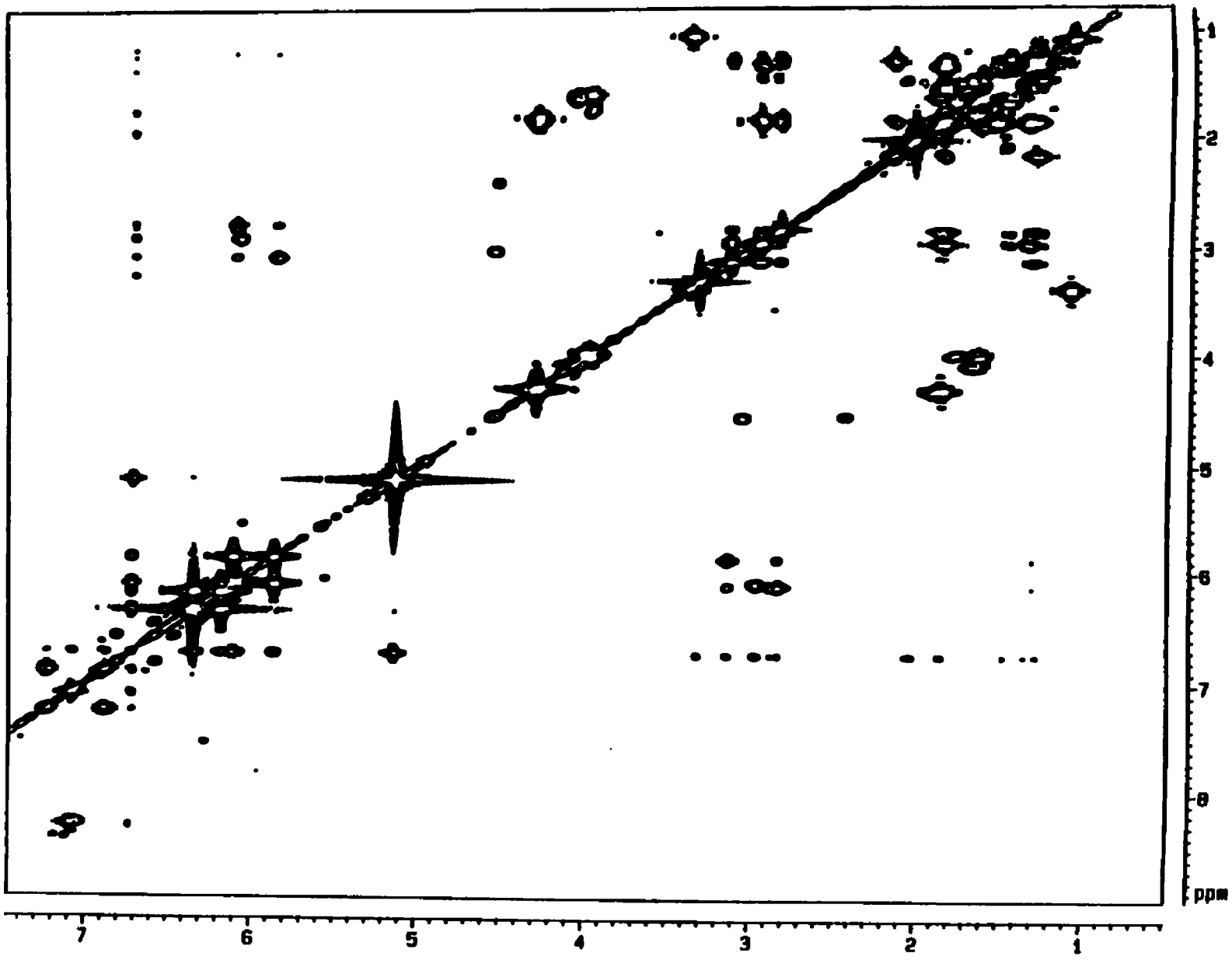

Figure 3.16: HH COSY of complex **3.18** in acetone-d_6.

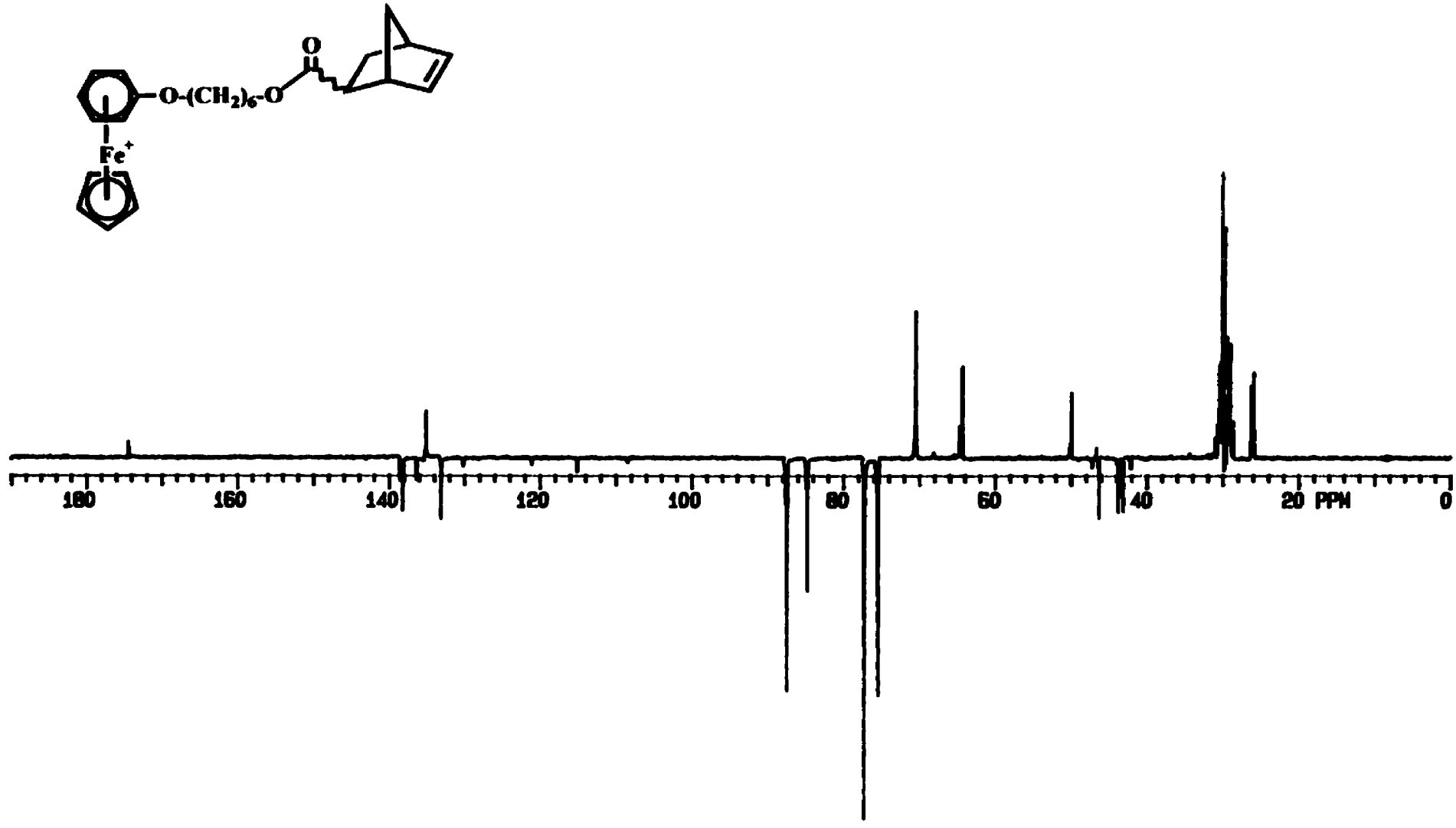

Figure 3.17: ^{13}C NMR of complex **3.18** in acetone-d_6.

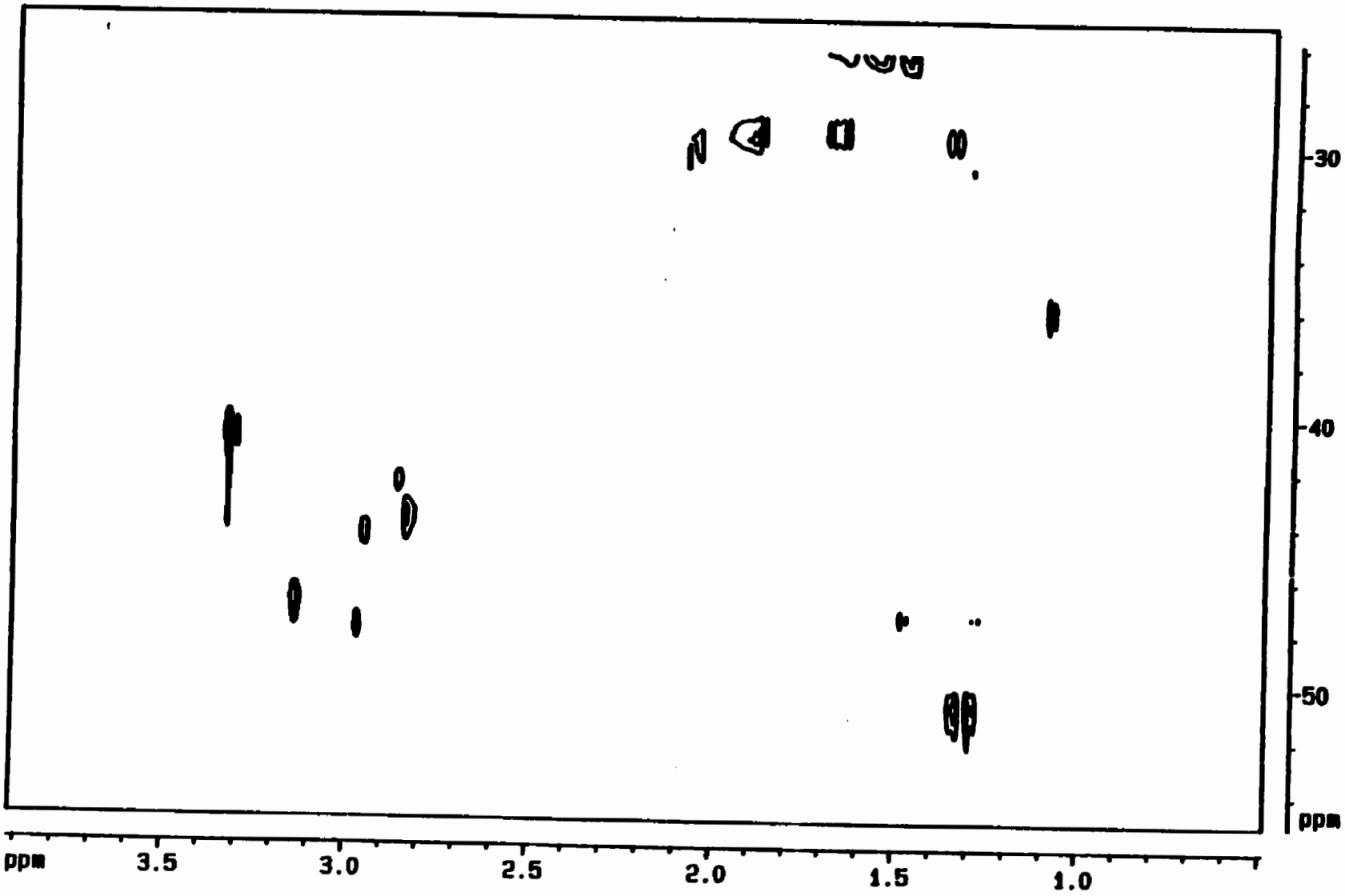

Figure 3.18: Expanded CH COSY of complex **3.18** in acetone-d_6.

Characterization of the uncomplexed monomers **3.19** and **3.20** was achieved using MS, IR, ^{1}H and ^{13}C NMR spectral data. Monomer **3.20** was partially characterized by the molecular ion peak it displayed at 314 in the mass spectrum and by the carbonyl peak at 1720 cm^{-1} in the IR spectrum. As has been previously observed in the NMR spectra of photolyzed compounds, loss of the Cp resonance in the range of 5.0 – 5.5 ppm in the ^{1}H NMR spectrum or 78 – 84 ppm in the ^{13}C NMR spectrum is indicative of successful removal of the $CpFe^{\cdot}$ moiety. Due to the absence of a strong singlet at 5.14 ppm in the ^{1}H NMR spectrum of compound **3.20**, as well as at 77.21 ppm in the ^{13}C NMR spectrum as shown in Figures 3.19 and 3.20, respectively, the organic monomer was proposed to have been isolated. This information used in conjunction with the characteristic downfield shift of the aromatic protons and carbons as well as the collapsed appearance of the methylene resonances in the ^{1}H NMR spectrum, indicate successful isolation of the organic monomer. A compilation of the NMR results for compounds **3.19** and **3.20** are described in Tables 3.14 and 3.15.

3.2.2 Ring-Opening Metathesis Polymerization of Aliphatic Bridged Norbornene Monomers

Living polymerization of these norbornene monomers was accomplished using the same methodology as previously outlined for the ROMP of the aromatic ether norbornenes. These syntheses were performed using the ruthenium benzylidene catalyst, $(Cy_3P)_2Cl_2Ru{=}CHPh$. A typical polymerization, as illustrated in Scheme 3.7, involved a ratio of 100:1 of the monomer to initiator as well as 1 mL of dichloromethane for every

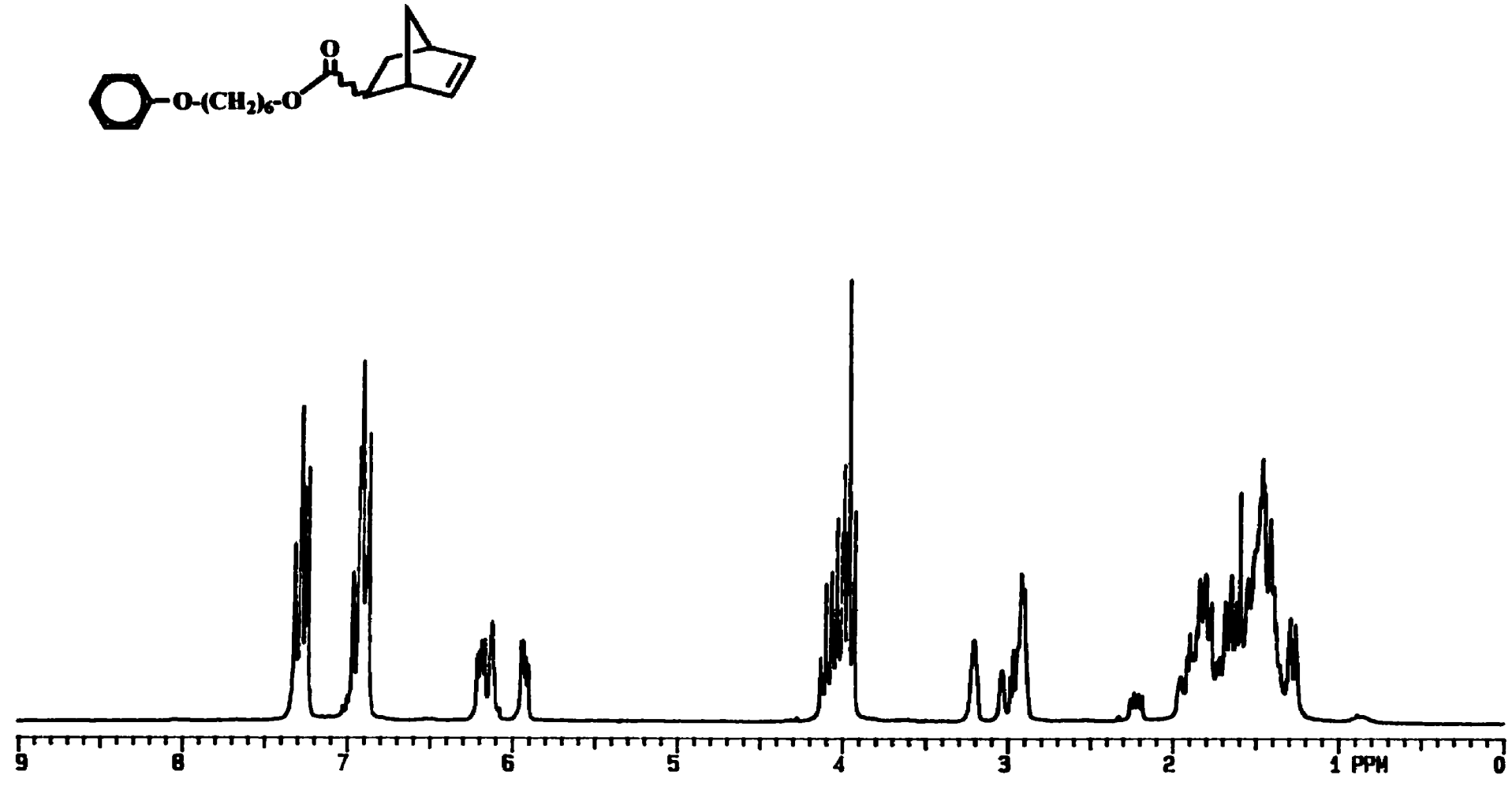

Figure 3.19: ^{1}H NMR of compound **3.20** in $CDCl_3$.

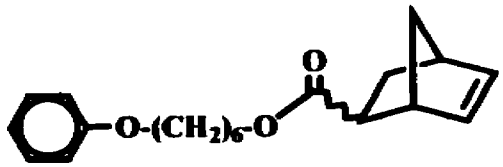

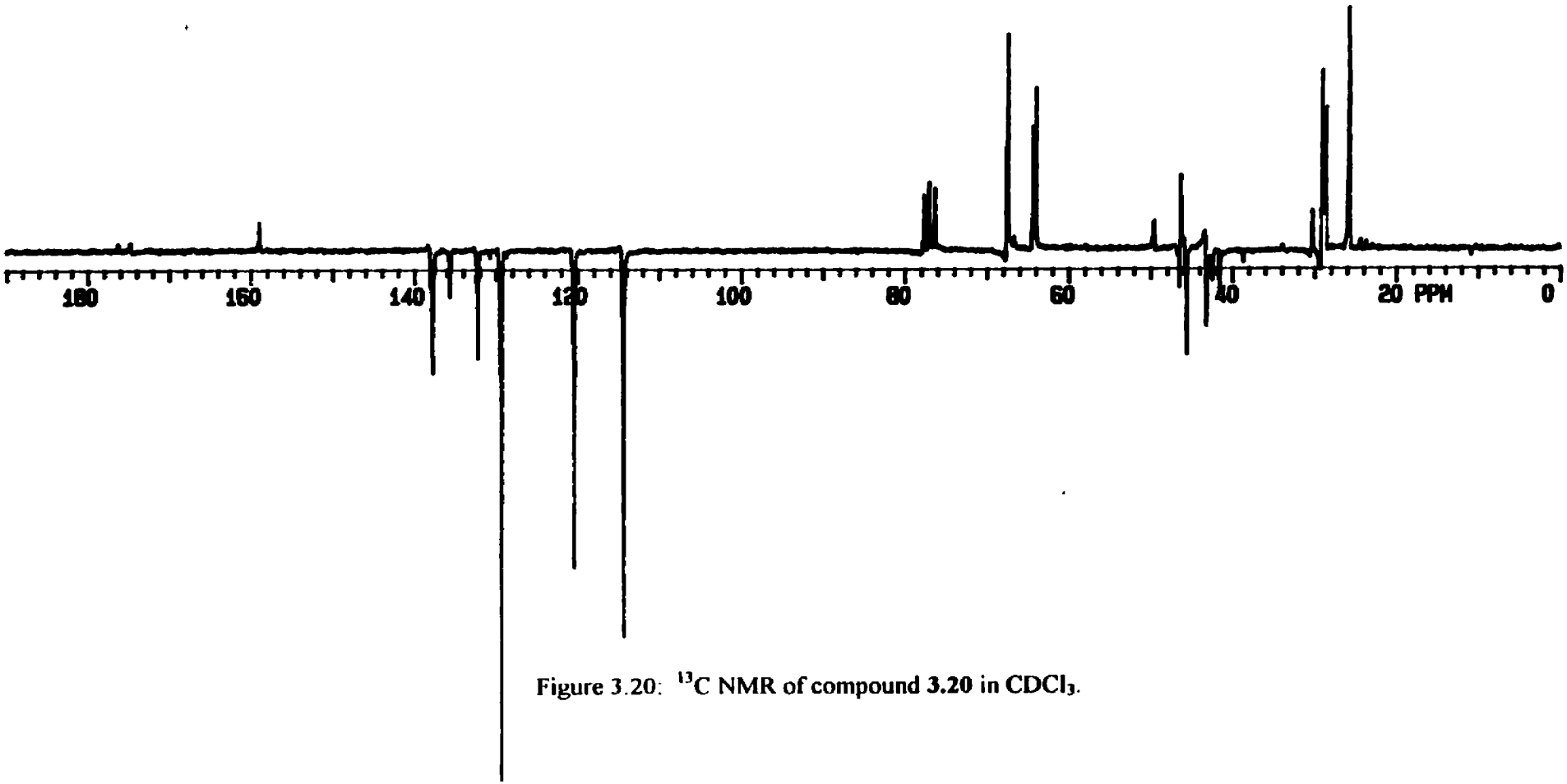

Figure 3.20: ^{13}C NMR of compound **3.20** in $CDCl_3$.

100 mg of monomer. Reaction mixtures were stirred under an inert nitrogen atmosphere until a gelatinous material formed, which generally required 1 – 2 h for the various monomers employed. The flexible off-white polymers **3.21** - **3.25** were obtained in good yield.

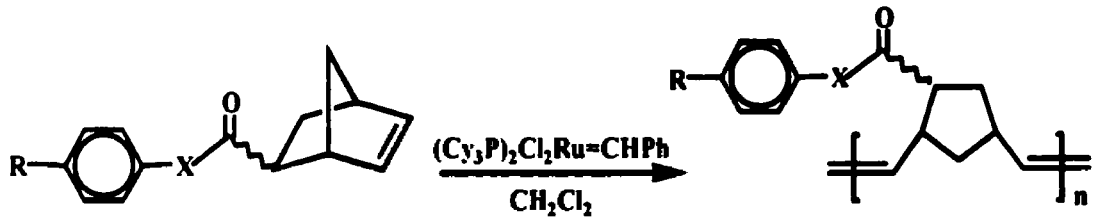

monomer	R	polymer	X
3.3	H	3.21	$CH_2O(CH_2)_2O(CH_2)_2O(CH_2)_2O$
3.11	H	3.22	$O(CH_2)_2O(CH_2)_2O(CH_2)_2O$
3.12	CH_3	3.23	$O(CH_2)_2O(CH_2)_2O(CH_2)_2O$
3.19	H	3.24	$O(CH_2)_4O$
3.20	H	3.25	$O(CH_2)_6O$

Scheme 3.7

Characterization of each of these polymers was done primarily using ^{1}H NMR spectroscopy. Several distinguishing features in the ^{1}H NMR spectrum indicating successful polymerization are peak broadening, loss of the monomeric olefinic resonances and the presence of new vinyl protons for the unsaturated polynorbornene backbone in the region of 5.1 – 5.5 ppm. An interesting feature of the tri(ethylene glycol) bridged polymers (**3.21** – **3.23**) relative to the more flexible, methylene chain polymers (**3.24** and **3.25**) is that in the former, the olefinic resonances appear as two close broad

peaks, one being much larger than the other. The larger of the peaks appearing furthest downfield was attributed to the high trans nature of these polymers (75%), with partial cis geometry occurring as indicated by the smaller more upfield resonance, which is in agreement with previous findings for this structural geometry.[1] A detailed list of the characteristic chemical shifts for polymers **3.21 – 3.25** is contained in Table 3.16.

Due to the high solubilities of each of the polymers in chloroform, GPC analyses were run using this solvent as the mobile phase. From these polymerizations, high Mw's ranging from 66 000 – 390 000 g/mol along with Mn's from 33 000 – 145 000 g/mol were routinely observed. In addition, relatively low PDI's were obtained varying from 1.3 – 2.8. For a complete description of the Mw's, Mn's and PDI's for polymers **3.21 – 3.25**, see Table 3.17.

Thermal decomposition analyses were performed on each of the polynorbornenes. Based upon structural differences between polymers **3.21 – 3.25**, thermal degradation temperatures were found to correlate highly to the varying degrees of flexibility in each system. Polymers **3.21 - 3.23** containing the more rigid tri(ethylene glycol) spacer demonstrated similar decompositions ranging from 428 – 432 °C. However, the influence of the more flexible fully methylene chain in polymers **3.24** and **3.25** decreased the decomposition temperature of the material to 423 – 424 °C, which is in agreement with previous findings for the incorporation of various alkyl chains.[5, 41, 145] Table 3.18 lists the respective onset, midpoint and endset decomposition temperatures for each of the polymers.

3.3 Conclusion

This work has demonstrated the ease with which norbornene monomeric units containing a rigid mesogen and a bridging aliphatic spacer can be prepared. ROMP was accomplished in the presence of Grubbs' ruthenium benzylidene catalyst to form polymeric materials with high molecular weights and low to narrow molecular weight distributions. Subsequent thermal analysis of the polymers revealed the lower decomposition temperatures of the straight chain methylene bridges relative to the more rigid tri(ethylene glycol) spacers.

3.4 Experimental

3.4.1 General Methods

^{1}H and ^{13}C NMR spectra were performed on a 200 and 50 MHz Gemini 200 NMR spectrometer and at 500 and 125 MHz on a Bruker 500 spectrometer. Chemical shifts were referenced to the deuterated solvent that the product was run in with coupling constants measured in Hz. Analysis of polymer molecular weights was accomplished by GPC which was performed using a BL-gel mixed D column (Phenomenex) equipped with a CH-30 column heater (Eppendorf) and a PL-DCU detector (Polymer Laboratories). Chloroform was employed as the mobile phase using a flow rate of 0.7 mL/min. Calibration of the instrument was achieved versus polystyrene standards. TGA was used to determine the decomposition temperatures of the polymers. These were

recorded on a Mettler Toledo TGA/SDTA851 with a heating rate of 10 °C/min under a constant flow of nitrogen (20 mL/min).

3.4.2 Starting Materials

Anhydrous aluminum chloride, aluminum powder, ferrocene, chloroarenes, ammonium hexafluorophosphate, DCC, DMAP, 98%-*exo*,*endo*-5-norbornene-2-carboxylic acid, benzyl chloride, tri(ethylene glycol), 1,4-butanediol, 1,6-hexanediol and bis(tricyclohexylphosphine)benzylidene ruthenium (IV) dichloride are all commercially available and were used without further purification. All solvents (reagent grade) were used without additional purification, except for THF, which was freshly distilled over sodium metal and benzophenone under an inert nitrogen atmosphere. In the column chromatographic purification of the modified norbornenes, silica gel 60-100 mesh was used. Prior to polymerization, dichloromethane was dried over $CaCl_2$, distilled and then degassed by several freeze-pump-thaw-repetitions.

3.4.3 Synthetic Approach for the Monoarylation of Aliphatic Diols

3.4.3.1 Preparation of Tri(ethylene glycol) Monobenzyl Ether (3.1)

This methodology previously established by Allan and Spreer was modified slightly simply by scaling down the reaction. Initially, 0.09 g (2.04 mmol) of sodium

hydride was placed into a 25 mL round bottom flask and to it was added 20 mL of dry THF. The resulting solution was placed under an inert nitrogen atmosphere to which 0.80 mL (6.00 mmol) of tri(ethylene glycol) was added dropwise. After this addition, 0.23 mL (2.00 mmol) of benzyl chloride was added. The resulting reaction mixture was then refluxed for 16 h under nitrogen. Subsequent cooling, filtering and removing of the solvent via rotary evaporation liberated the crude product. This was then redissolved in diethyl ether, washed with 2 x 50 mL of distilled water and once again extracted with diethyl ether (2 x 20 mL). Isolation of the crude product was obtained by drying the organic layer over $MgSO_4$, filtering and rotary evaporating off the solvent. Subsequent purification was obtained by eluting the compound through a hexane silica gel column using ethyl acetate as the mobile phase.

3.4.3.2 Preparation of Metallated Triethylene Glycol Monoaryl Ethers (3.7 and 3.8)

A typical synthesis of **3.7** and **3.8** involved the initial generation of the diol by the preparation of its sodium salt. This was accomplished through the dropwise addition of 0.13 mL (0.8 mmol) of **3.6** to a stirring solution of 0.16 g (0.40 mmol) of sodium hydride in 4 mL of freshly distilled THF within a 25 mL round bottom flask. The resulting solution was then stirred under a nitrogen atmosphere for 15 min. At this time, 0.20 mmol of either complex **3.4** or **3.5**, (whose syntheses were previously outlined in section 2.4.3), dissolved in 6 mL of THF was added to the reaction mixture which was then allowed to stir for an additional 6 h at room temperature under nitrogen. Isolation of the

crude products was achieved by gravity filtration of the solution into a round bottom flask, rinsing with 2 x 25 mL portions of dichloromethane and removing the solvent by reduced pressure. Purification of the crude product by dropwise addition to cold diethyl ether and subsequent cooling in the freezer overnight, yielded the pure monoiron complexes **3.7** and **3.8** as yellow oils in very high yield.

3.4.3.3 Synthesis of Metallated Monoaryl Alcohols 3.15 and 3.16

A similar methodology was used in preparing the 1,4-butanediol and 1,6-hexanediol complexes of **3.15** and **3.16**. Preparation of the sodium alkoxide of the diol was accomplished by the addition of 3.20 mmol of the diol to 0.064 g (1.60 mmol) of sodium hydride dissolved in 6 mL of THF. The resulting solution was stirred under nitrogen for 15 min after which 0.30 g (0.80 mmol) of **3.4** dissolved in 9 mL of THF was added. Continued stirring of the reaction mixture under nitrogen for 6 h liberated the crude product which was isolated by gravity filtering the solution, washing with 2 x 25 mL aliquots of dichloromethane and drying under reduced pressure. Isolation of the pure products was achieved by adding dropwise to diethyl ether and cooling in the freezer overnight, liberating the products as bright yellow oils.

3.4.4 Capping of Terminal Hydroxy Compounds with *Exo*, *Endo*-5-Norbornene-2-Carboxylic Acid

Capping of compound **3.1** and complexes **3.7**, **3.8**, **3.15** and **3.16** was accomplished via condensation with **3.2** in the presence of DCC and DMAP. A general procedure can be described for the syntheses of **3.3**, **3.9**, **3.10**, **3.17** and **3.18**. Into a 25 mL round bottom flask, 0.5 mmol of the monoaryl alcohol was placed along with 0.5 – 0.6 mmol of **3.2**, 0.5 mmol of DMAP and 4 mL of dichloromethane. The resulting mixture was slowly stirred and cooled to 0 °C at which time 0.5 mmol of DCC dissolved in 1 mL of dichoromethane was added dropwise. Continued stirring of the solution was permitted for 7 h at room temperature. After this time, the mixture was hydrolyzed by pouring into approximately 20 mL of ice water. Addition of an aqueous NH_4PF_6 solution was then added to the solutions containing the metallated complexes. Next, the solution was extracted with 2 x 30 mL of dichloromethane, washed with a saturated NaCl solution, dried over $MgSO_4$, filtered and dried by rotary evaporation. Isolation of the organic monomer **3.3** was obtained via column chromatography using a 3:1 chloroform:hexane solvent mixture to elute the product. Purification of the metallated complexes **3.9**, **3.10**, **3.17** and **3.18** was achieved via the subsequent dissolution of the crude products into a minimal amount of acetone and filtering into cold diethyl ether.

3.4.5 Method of Photolytic Demetallation

Isolation of monomers **3.11**, **3.12**, **3.19** and **3.20** was accomplished using a similar methodology as was previously outlined in section 2.4.7. In each of the complexes a time of 4 h was required for removal of the metal moiety. Isolation of compounds **3.11** and **3.12** via column chromatography was accomplished using a 3:1 $CHCl_3$:hexane mobile phase whereas monomers **3.19** and **3.20** required $CHCl_3$.

3.4.6 Experimental Method for ROMP: Synthesis of Polymers 3.21 – 3.25

Polymerizations of monomers **3.3**, **3.11**, **3.12**, **3.19** and **3.20** were carried out under analogous conditions to those employed for the aromatic ether norbornene monomers previously outlined in section 2.4.8.

Table 3.1: ^{1}H NMR Data of Monomer **3.3**.

δ ($CDCl_3$), ppm; (500 MHz NMR)												
M	**Endo /Exo**	**H-1**	**H-2**	**H-3x**	**H-3n**	**H-4**	**H-5**	**H-6**	**H-7a**	**H-7s**	**CH_2 Bridge**	**ArH**
3.3	**Endo**	3.20 (br s)	2.96 (m)	1.88 (m)	1.41 (---)	2.88 (br s)	6.17 (dd)	5.93 (dd)	1.25 (d)	1.41 (dd)	3.66 (m, 10H), 4.17 (m, 2H), 4.56 (s, 2H)	7.32 (m, 1H), 7.33 (m, 4H)
	Exo	3.04 (br s)	2.24 (dd)	1.93 (m)	1.35 (m)	2.89 (br s)	6.12 (dd)	6.08 (dd)	1.35 (m)	1.52 (d)	3.66 (m, 10H), 4.17 (m, 2H), 4.56 (s, 2H)	7.32 (m, 1H), 7.33 (m, 4H)

(---) Denotes a hidden peak.

Table 3.2: ^{13}C NMR Data of Monomer **3.3**.

δ ($CDCl_3$), ppm; (125 MHz NMR)												
M	**Endo /Exo**	**C-1**	**C-2**	**C-3**	**C-4**	**C-5**	**C-6**	**C-7**	**CH_2 Bridge**	**ArC**	**CO**	**% Yield**
3.3	**Endo**	45.63	43.12	29.17	42.44	137.58	132.30	49.49	63.21, 63.40, 69.15, 69.36, 70.30, 70.48, 70.60, 73.14	127.34, 127.47, 128.12, 138.03*	174.40	90
	Exo	46.57	42.96	30.26	41.54	137.95	135.63	46.20	63.21, 63.40, 69.15, 69.36, 70.30, 70.48, 70.60, 73.14	127.34, 127.47, 128.12, 138.03*	175.93	

* Denotes a quaternary aromatic carbon.
M = Monomer.

Table 3.3: Measured Coupling Constants (Hz) for the *Endo* and *Exo* Isomers of Monomer **3.3**.

Couplings	*Endo*	*Exo*
$J_{(1, 6)}$	2.7	2.8
$J_{(2, 3x)}$	9.7	4.3
$J_{(2, 3n)}$	---	9.7
$J_{(3x, 3n)}$	10.3	---
$J_{(3x, 4)}$	3.5	---
$J_{(3n, 7s)}$	3.1	---
$J_{(4, 5)}$	3.0	3.0
$J_{(5, 6)}$	5.4	5.4
$J_{(7a, 7s)}$	9.5	8.4
$J_{(4, 7s)}$	1.7	---

--- Refers to unobtainable values due to peak broadness and overlap.

Table 3.4: ^{1}H NMR Data of Tri(ethylene glycol) Monoaryl Ether Complexes **3.7** and **3.8**.

δ (acetone-d_6), ppm				
Complex	**Cp**	**Complexed Aromatic**	**Methylene Protons**	**Others**
3.7	5.19 (s, 5H)	6.20 (br t, 1H), 6.40 (m, 4H)	3.54 – 3.77 (m, 8H), 3.90 (t, 2H, J = 4.3), 4.46 (t, 2H, J = 4.3)	2.87 (br s, 1H) (OH)
3.8	5.13 (s, 5H)	6.27 (d, 2H, J = 6.8), 6.33 (d, 2H, J = 6.7)	3.56 – 3.75 (br m, 8H), 3.88 (t, 2H, J = 4.2), 4.42 (t, 2H, J = 4.2)	2.90 (br s, 1H), (OH) 2.46 (s, 3H), (CH_3)

Coupling constants are reported in Hz.

Table 3.5: ^{13}C NMR Data and % Yield of Tri(ethylene glycol) Monoaryl Ether Complexes **3.7** and **3.8**.

δ (acetone-d_6), ppm					
Complex	**Cp**	**Complexed Aromatic**	**Methylene Carbons**	**Others**	**% Yield**
3.7	77.39	75.84, 84.87, 87.49, 134.91*	61.79, 69.71, 70.34, 70.91, 71.32, 73.33	---	94
3.8	74.92	77.67, 87.46, 100.24*, 133.76*	69.64, 70.21, 70.33, 70.90, 71.19, 71.52	19.58 (CH_3)	91

* Denotes a quaternary aromatic carbon.

Table 3.6: ^{1}H NMR of Metallated Monomers **3.9** and **3.10**.

δ (acetone-d_6), ppm; (200 MHz NMR)														
M	**Endo /Exo**	**H-1**	**H-2**	**H-3x**	**H-3n**	**H-4**	**H-5**	**H-6**	**H-7a**	**H-7s**	**CH_2 Bridge**	**Cp**	**ArH**	**Other**
3.9	**Endo**	3.32 (br s)	2.98 (m)	1.86 (m)	1.24 (m)	2.85 (br s)	6.19 (br m)	5.90 (dd)	1.29 (br s)	1.29 (br s)	3.68 (m, 6H), 3.89 (t, 2H, J = 4.0), 4.11 (m, 2H), 4.45 (t, 2H, J = 4.0)	5.17 (s, 5H)	6.11 (m, 1H), 6.40 (m, 4H)	---
	Exo	3.13 (br s)	2.14 (dd)	1.90 (m)	1.36 (m)	2.85 (br s)	6.10 (br m)	6.10 (br m)	1.36 (m)	1.46 (br d)	3.68 (m, 6H), 3.89 (t, 2H, J = 4.0), 4.11 (m, 2H), 4.45 (t, 2H, J = 4.0)	5.17 (s, 5H)	6.11 (m, 1H), 6.40 (m, 4H)	---
3.10	**Endo**	3.26 (br s)	2.98 (m)	1.86 (m)	1.25 (m)	2.85 (br s)	6.22 (br m)	5.90 (dd)	1.30 (br s)	1.30 (br s)	3.67 (br m, 6H), 3.89 (br t, 2H), 4.14 (br m, 2H), 4.43 (br t, 2H)	5.13 (s, 5H)	6.31 (m, 4H)	2.46 (s, 3H) (CH_3)
	Exo	3.13 (br s)	2.15 (dd)	1.90 (m)	1.36 (m)	2.85 (br s)	6.11 (m)	6.11 (m)	1.36 (m)	1.45 (br d)	3.67 (br m, 6H), 3.89 (br t, 2H), 4.14 (br m, 2H), 4.43 (br t, 2H)	5.13 (s, 5H)	6.31 (m, 4H)	2.46 (s, 3H) (CH_3)

Coupling constants (J) are recorded in Hz.
Observed Endo Couplings: **3.9**: $J_{(1,6)} = 2.9$, $J_{(5,6)} = 5.6$ and **3.10**: $J_{(1,6)} = 2.8$, $J_{(5,6)} = 5.5$
M = Monomer.

Table 3.7: ^{13}C NMR Data of Metallated Monomers **3.9** and **3.10**.

δ (acetone-d_6), ppm; (50 MHz NMR)														
M	**Endo /Exo**	**C-1**	**C-2**	**C-3**	**C-4**	**C-5**	**C-6**	**C-7**	**CH_2 Bridge**	**Cp**	**ArC**	**CO**	**Other**	**% Yield**
3.9	**Endo**	46.29	43.63	29.49	43.13	138.10	133.25	49.91	63.81, 69.67, 69.74, 70.40, 71.10, 71.36	77.40	75.85, 84.91, 87.54, 134.93*	174.47	---	58
	Exo	47.22	43.54	29.95	42.20	138.65	136.36	46.68	64.08, 69.67, 69.74, 70.40, 71.10, 71.36	77.40	75.85, 84.91, 87.54, 134.93*	176.09	---	
3.10	**Endo**	46.29	43.62	28.80-30.73	43.13	138.11	133.25	49.91	63.83, 69.66, 69.75, 70.43, 71.08, 71.35	77.79	75.02, 87.63, 100.41*, 133.86*	174.47	19.72 (CH_3)	62
	Exo	47.21	43.53	28.80-30.73	42.20	138.66	136.36	46.69	64.09, 69.66, 69.75, 70.43, 71.08, 71.35	77.79	75.02, 87.63, 100.41*, 133.86*	176.09	19.72 (CH_3)	

* Denotes a quaternary aromatic carbon.
M = Monomer.

Table 3.8: ^{1}H NMR Data of Monomers **3.11** and **3.12**.

δ ($CDCl_3$), ppm; (200 MHz NMR)													
M	**Endo /Exo**	**H-1**	**H-2**	**H-3x**	**H-3n**	**H-4**	**H-5**	**H-6**	**H-7a**	**H-7s**	**CH_2 Bridge**	**ArH**	**Other**
3.11	**Endo**	3.21 (br s)	2.94 (m)	1.89 (m)	1.39 (br d)	2.89 (br s)	6.17 (dd)	5.93 (dd)	1.27 (br d)	1.39 (br d)	3.69 (m, 8H), 3.86 (t, 2H, J = 4.8), 4.19 (m, 2H)	6.93 (t, 3H), 7.30 (d, 2H)	---
	Exo	3.04 (br s)	2.25 (dd)	1.97 (m)	1.27-1.35 (---)	2.89 (br s)	6.11 (m)	6.11 (m)	1.27-1.35 (---)	1.52 (br d)	3.69 (m, 8H), 3.86 (t, 2H, J = 4.8), 4.19 (m, 2H)	6.93 (t, 3H), 7.30 (d, 2H)	---
3.12	**Endo**	3.22 (br s)	3.00 (m)	1.90 (m)	1.39 (br d)	2.90 (br s)	6.18 (dd)	5.93 (dd)	1.28 (br d)	1.39 (br d)	3.71 (m, 8H), 3.85 (d, 2H, J = 5.0), 4.19 (m, 2H)	6.81 (d, 2H, J = 8.1), 7.06 (d, 2H, J = 8.1)	2.28 (s, 3H) (CH_3)
	Exo	3.05 (br s)	2.23-2.28 (---)	1.96 (m)	1.28-1.35 (---)	2.90 (br s)	6.10 (m)	6.10 (m)	1.28-1.35 (---)	1.51 (br d)	3.71 (m, 8H), 3.85 (d, 2H, J = 5.0), 4.19 (m, 2H)	6.81 (d, 2H, J = 8.1), 7.06 (d, 2H, J = 8.1)	2.28 (s, 3H) (CH_3)

(---) Denotes a hidden peak.
Coupling constants are recorded in Hz.
Observed *Endo* Coupling: **3.11**: $J_{(1,6)}$=2.7, $J_{(5,6)}$=5.5, $J_{(4,5)}$=2.9 and **3.12**: $J_{(1,6)}$=2.7, $J_{(5,6)}$=5.6
M = monomer

Table 3.9: ^{13}C NMR Data of Monomers **3.11** and **3.12**.

δ ($CDCl_3$), ppm; (50 MHz NMR)													
M	**Endo /Exo**	**C-1**	**C-2**	**C-3**	**C-4**	**C-5**	**C-6**	**C-7**	**CH_2 Bridge**	**ArC**	**CO**	**Other**	**% Yield**
3.11	**Endo**	45.67	43.14	29.20	42.47	137.66	132.31	49.54	63.23, 67.22, 69.22, 69.75, 70.53, 70.77	114.53, 120.79, 129.35, 158.66*	174.68	---	77
	Exo	46.61	42.98	30.30	41.58	137.99	135.66	46.24	63.42, 67.22, 69.22, 69.75, 70.53, 70.77	114.53, 120.79, 129.35, 158.66*	176.17	---	
3.12	**Endo**	45.59	43.06	29.11	42.39	137.56	132.23	49.46	63.17, 67.34, 69.14, 69.73, 70.45, 70.67	114.32, 129.70, 129.89*, 156.47*	174.57	20.33 (CH_3)	79
	Exo	46.52	42.88	30.22	41.49	137.91	135.58	46.15	63.35, 67.34, 69.14, 69.73, 70.45, 70.67	114.32, 129.70, 129.89*, 156.47*	176.09	20.33 (CH_3)	

* Denotes a quaternary aromatic carbon.

M = Monomer.

Table 3.10: ^{1}H NMR Data of Aliphatic Monoaryl Alcohol Complexes **3.15** and **3.16**.

δ (acetone-d_6), ppm				
Complex	**Cp**	**Complexed Aromatic**	**Methylene Protons**	**Others**
3.15	5.17 (s, 5H)	6.21 (br m, 1H), 6.37 (m, 4H)	1.70 (m, 2H), 1.94 (m, 2H), 3.61 (t, 2H, J = 6.0), 4.34 (t, 2H, J = 6.3)	3.21 (br s, 1H), (OH)
3.16	5.16 (s, 5H)	6.22 (br m, 1H), 6.37 (m, 4H)	1.50 (m, 6H), 1.86 (m, 2H), 3.55 (t, 2H, J = 6.2), 4.30 (t, 2H, J = 6.3)	3.13 (br s, 1H), (OH)

Coupling constants are reported in Hz.

Table 3.11: ^{13}C NMR Data and % Yield of Aliphatic Monoaryl Alcohol Complexes **3.15** and **3.16**.

δ (acetone-d_6), ppm				
Complex	**Cp**	**Complexed Aromatic**	**Methylene Carbons**	**% Yield**
3.15	77.27	75.46, 84.81, 87.55, 135.33*	26.38, 29.63, 61.90, 70.69	74
3.16	77.12	75.28, 84.64, 87.37, 135.13*	25.90, 26.13, 29.22, 30.96, 62.20, 70.44	83

*Denotes a quaternary aromatic carbon.

Table 3.12: ^{1}H NMR of Metallated Monomers **3.17** and **3.18**.

δ (acetone-d_6), ppm; (200 & 500 MHz NMR)													
M	**Endo /Exo**	**H-1**	**H-2**	**H-3x**	**H-3n**	**H-4**	**H-5**	**H-6**	**H-7a**	**H-7s**	**CH_2 Bridge**	**Cp**	**ArH**
3.17	**Endo**	3.30 (br s)	2.98 (br m)	1.82-1.90 (---)	1.26 (m)	2.85 (br s)	6.17 (br m)	5.89 (br m)	1.31 (br s)	1.31 (br s)	1.82–1.90 (br m, 4H), 4.09 (br m, 2H), 4.32 (t, 2H, J = 5.5)	5.17 (s, 5H)	6.11 (br s, 1H), 6.37 (br m, 4H)
	Exo	3.14 (br s)	2.17 (dd)	1.82-1.90 (---)	1.37 (m)	2.85 (br s)	6.11 (m)	6.11 (m)	1.37 (m)	1.49 (br d)	1.82–1.90 (br m, 4H), 4.09 (br m, 2H), 4.32 (t, 2H, J = 5.5)	5.17 (s, 5H)	6.11 (br s, 1H), 6.37 (br m, 4H)
3.18	**Endo**	3.30 (br s)	2.96 (br m)	1.80-1.93 (---)	1.25 (m)	2.85 (br s)	6.19 (br m)	5.88 (br m)	1.30 (br s)	1.30 (br s)	1.45-1.67 (br m, 6H), 1.80-1.93 (br m, 2H), 4.02 (br m, 2H), 4.30 (t, 2H, J = 6.3)	5.14 (s, 5H)	6.20 (m, 1H), 6.35 (m, 4H)
	Exo	3.14 (br s)	2.15 (dd)	1.80-1.93 (---)	1.36 (m)	2.85 (br s)	6.11 (m)	6.11 (m)	1.36 (m)	1.45-1.49 (br d)	1.45-1.67 (br m, 6H), 1.80-1.93 (br m, 2H), 4.02 (br m, 2H), 4.30 (t, 2H, J = 6.3)	5.14 (s, 5H)	6.20 (m, 1H), 6.35 (m, 4H)

(---) Denotes a hidden peak. Coupling constants (J) are recorded in Hz.
Observed endo coupling: **3.18**: $J_{(1,6)}$=2.6, $J_{(5,6)}$=5.4.
M = Monomer

Table 3.13: ^{13}C NMR Data of Metallated Monomers **3.17** and **3.18**.

δ (acetone-d_6), ppm; (50 & 125 MHz NMR)													
M	**Endo /Exo**	**C-1**	**C-2**	**C-3**	**C-4**	**C-5**	**C-6**	**C-7**	**CH_2 Bridge**	**Cp**	**ArC**	**CO**	**% Yield**
3.17	**Endo**	46.22	43.64	28.65-30.97	43.07	138.17	133.04	49.93	26.01, 26.26, 63.92, 70.06	77.17	75.31, 84.73, 87.38, 134.88*	174.44	63
	Exo	47.43	43.51	28.65-30.97	42.13	137.97	136.31	46.66	26.01, 26.26, 64.27, 70.06	77.17	75.31, 84.73, 87.38, 134.88*	(---)	
3.18	**Endo**	46.26	43.70	29.03-30.72	43.12	138.17	133.09	49.96	25.99, 26.24, 29.23, 29.34, 64.34, 70.49	77.21	75.39, 84.76, 87.48, 135.19*	174.46	65
	Exo	47.19	43.59	29.03-30.72	42.18	138.58	136.37	46.70	25.99, 26.24, 29.23, 29.34, 64.68, 70.49	77.21	75.39, 84.76, 87.48, 135.19*	(---)	

* Denotes a quaternary aromatic carbon.
(---) Other CO is unobservable.
M = Monomer.

Table 3.14: ^{1}H NMR Data of Monomers **3.19** and **3.20**.

δ ($CDCl_3$), ppm; (200 MHz NMR)												
M	**Endo /Exo**	**H-1**	**H-2**	**H-3x**	**H-3n**	**H-4**	**H-5**	**H-6**	**H-7a**	**H-7s**	**CH_2 Bridge**	**ArH**
3.19	**Endo**	3.23 (br s)	2.99 (m)	1.67-1.90 (---)	1.45 (br d)	2.93 (br s)	6.21 (dd)	5.95 (dd)	1.29 (br d)	1.45 (br d)	1.67-1.90 (m, 4H), 3.98-4.18 (m, 4H)	6.94 (m, 3H), 7.32 (d, 2H, J = 7.5)
	Exo	3.06 (br s)	2.24 (dd)	1.67-1.90 (---)	1.29-1.38 (---)	2.94 (br s)	6.14 (m)	6.14 (m)	1.29-1.38 (---)	1.55 (br d)	1.67-1.90 (m, 4H), 3.98-4.18 (m, 4H)	6.94 (m, 3H), 7.32 (d, 2H, J = 7.5)
3.20	**Endo**	3.22 (br s)	2.98 (m)	1.91 (---)	1.41 (br d)	2.93 (br s)	6.20 (dd)	5.93 (dd)	1.30 (br d)	1.41 (br d)	1.41-1.59 (m, 4H), 1.62-1.89 (m, 4H), 3.93-4.14 (m, 4H)	6.93 (m, 3H), 7.30 (m, 2H)
	Exo	3.06 (br s)	2.23 (dd)	1.97 (---)	1.31-1.40 (---)	2.93 (br s)	6.13 (m)	6.13 (m)	1.31-1.40 (br d)	1.40-1.60 (---)	1.41-1.59 (m, 4H), 1.62-1.89 (m, 4H), 3.93-4.14 (m, 4H)	6.93 (m, 3H), 7.30 (m, 2H)

(---) Denotes a hidden peak.
Coupling constants are recorded in Hz.
Observed *endo* coupling: **3.19**: $J_{(1,6)}$=2.9, $J_{(5,6)}$=5.5, $J_{(4,5)}$=3.0 and **3.20**: $J_{(1,6)}$=2.9, $J_{(5,6)}$=5.6, $J_{(4,5)}$=3.0

Table 3.15: ^{13}C NMR Data of Monomers **3.19** and **3.20**.

δ ($CDCl_3$), ppm; (50 MHz NMR)												
M	**Endo /Exo**	**C-1**	**C-2**	**C-3**	**C-4**	**C-5**	**C-6**	**C-7**	**CH_2 Bridge**	**ArC**	**CO**	**% Yield**
3.19	**Endo**	45.63	43.25	29.10	43.09	137.71	132.26	49.54	25.43, 25.86, 63.76, 67.05	114.36, 120.55, 129.34, 159.81*	174.67	63
	Exo	46.53	43.12	30.24	42.44	137.93	135.66	46.28	25.43, 25.86, 63.89, 67.05	114.36, 120.55, 129.34, 159.81*	176.15	
3.20	**Endo**	45.65	43.27	---	43.13	137.66	132.28	49.56	25.71 (2 CH_2), 28.59, 29.12, 64.08, 67.53	114.38, 120.43, 129.33, 158.98*	174.44	61
	Exo	46.55	43.17	30.26	42.46	137.94	135.69	46.30	25.71 (2 CH_2), 28.59, 29.12, 64.33, 67.53	114.38, 120.43, 129.33, 158.98*	176.10	

--- Peak unobservable due to crowding.

* Denotes a quaternary aromatic carbon.

M = Monomer.

Table 3.16: ^{1}H NMR Spectral Information for Polymers **3.21 – 3.25**.

δ ($CDCl_3$, ppm)					
Polymer	**Aromatic H's**	**Vinyl H's**	**Methylene H's**	**Aliphatic H's**	**Others**
3.21	7.33 (br s, 5H),	5.18–5.37 (br d, 2H)	4.55 (s, 2H), 4.00–4.20 (br m, 4H), 3.64 (br s, 8H)	1.04-2.93 (br peaks, 7H)	---
3.22	6.88-6.96 (br m, 3H), 7.22-7.30 (br s, 2H)	5.19-5.36 (br d, 2H)	4.00–4.20 (br m, 4H), 3.84 (br s, 2H), 3.67 (br s, 6H)	1.12-2.95 (br peaks, 7H)	---
3.23	6.79 (br d, 2H), 7.08 (br d, 2H)	5.12-5.41 (br d, 2H)	4.01–4.20 (br m, 4H), 3.83 (br s, 2H), 3.68 (br s, 6H)	1.15-2.93 (br peaks, 7H)	2.27 (br s, 3H) (CH_3)
3.24	6.80-6.91 (br m, 3H), 7.24-7.28 (br s, 2H)	5.04-5.57 (br s, 2H)	3.77-4.28 (br d, 4H), 1.0-1.90 (br m, 4H)	0.54-2.98 (br peaks, 7H)	---
3.25	6.75-7.72 (br m, 5H)	5.18-5.53 (br s, 2H)	3.85-4.18 (br s, 4H), 1.25-1.98 (br peaks, 8H)	0.85-2.98 (br peaks, 7H)	---

Table 3.17: Mw, Mn, PDI and Yield for Aliphatic Bridged Polynorbornenes **3.21 – 3.25**.

Polymer	[a]Mw	[a]Mn	PDI	Yield (%)
3.21	66 000	33 000	2.2	38
3.22	390 000	145 000	2.7	23
3.23	288 000	104 000	2.8	37
3.24	97 000	53 000	1.8	82
3.25	110 000	82 000	1.3	78

[a] Values are reported in g/mol.

Table 3.18. Thermal Decomposition Data for Polymers **3.21 – 3.25**.

Polymer	T_{onset} (°C)	$T_{midpoint}$ (°C)	T_{endset} (°C)
3.21	393.7	427.9	454.3
3.22	403.9	431.7	451.8
3.23	395.0	430.5	455.1
3.24	391.6	424.2	454.5
3.25	394.1	423.1	449.7

4.0 Conclusion

Functionalization of the polynorbornene backbone has shown to be an effective method towards altering the thermal properties of the resulting polymeric material. It was our goal to construct polynorbornenes functionalized with pendent aromatic ether side chains in an attempt to improve the thermal stability. As aromatic ethers represent a class of materials known as engineering thermoplastics, we focused on incorporating various lengths of these chains into the polymer. Through a series of cyclopentadienyliron-mediated S_NAr reactions and DCC-mediated coupling reactions, we were able to design novel monomeric derivatives of norbornene containing one, three and five aromatic groups pendent to the norbornene structure. Complexation of the cyclopentadienyliron moiety to chloroarenes has proven to be an effective method towards preparing these novel metallated monomers. However, as we were only interested in the organic compounds at this time, we cleaved the metal moiety using photolytic demetallation.

Living polymerizations of these norbornene building blocks were accomplished in the presence of $(Cy_3P)_2Cl_2Ru{=}CHPh$ or "Grubbs catalyst". The resulting polymeric materials displayed high Mw's and Mn's with low polydispersities, as was determined by GPC. DSC and TGA thermal analyses showed that as the length of the aryl ether chain pendent to the polynorbornene backbone increased, an increase in the thermal properties of the polymeric materials was also observed. As these derivatives of polynorbornene represent greater thermal stability than the unsubstituted derivative, we were successful in attaining our goal.

The incorporation of an aliphatic spacer between the polynorbornene backbone and the rigid aromatic ring or mesogen was also explored. Synthesis of the monomers were accomplished using several steps involving an initial monoarylation step via a S_NAr with a chlorobenzene cyclopentadienyliron complex, capping with 5-norbornene-2-carboxylic acid and then photolysis. Living polymerizations yielded polymers having much higher Mw's and Mn's than the aryl ether derivatives, with similar PDI's. Thermogravimetric analysis of the polymers bridged by tri(ethylene glycol), 1,4-butanediol or 1,6-hexanediol linkages demonstrated improved thermal properties relative to the unsubstituted derivative, yet were notably lower than the aryl ether functionalized polymers.

5.0 Future Work

Current efforts in the design of SCLCPs are being directed towards materials that possess lower crystalline melting temperatures in an attempt to improve processability. Efforts toward attaining this goal have recently begun to focus on the preparation of novel copolymers with properties exhibiting reduced chain rigidity, yet maintaining high dimensional stability, strength and melting temperatures. [158] Due to the recent syntheses of both the aryl ether- and aliphatic-bridged functionalized polynorbornenes (via living polymerizations), a preliminary investigation involving the construction of a block copolymer combining each of these novel polynorbornenes was attempted.

The following scheme shows the copolymerization of two norbornene monomers with two different side chains. In a glove box, 0.006 g (0.00681 mmol) of $(Cy_3P)_2Cl_2Ru{=}CHPh$ was weighed into a 10 mL round bottom flask. To this was added 0.8 mL of dry CH_2Cl_2. The catalyst solution was then added to a stirring solution of monomer **3.26** [0.16 g (0.68 mmol)] also dissolved in 0.8 mL of CH_2Cl_2. The reaction mixture was then stirred under nitrogen until there was a thickening of the solution. Upon the appearance of this viscous solution 1 h after the ROMP reaction commenced, an aliquot of monomer **3.3** dissolved in an additional 1.0 mL of CH_2Cl_2 was added. Continued polymerization proceeded until the reappearance of a viscous solution, which was after 50 min. The ruthenium catalyst was then cleaved by the addition of ethyl vinyl ether. Purification of the copolymer proceeded upon dissolution in a minimum amount of chloroform and precipitation into cold methanol. Isolation of the tan, fibrous polymeric

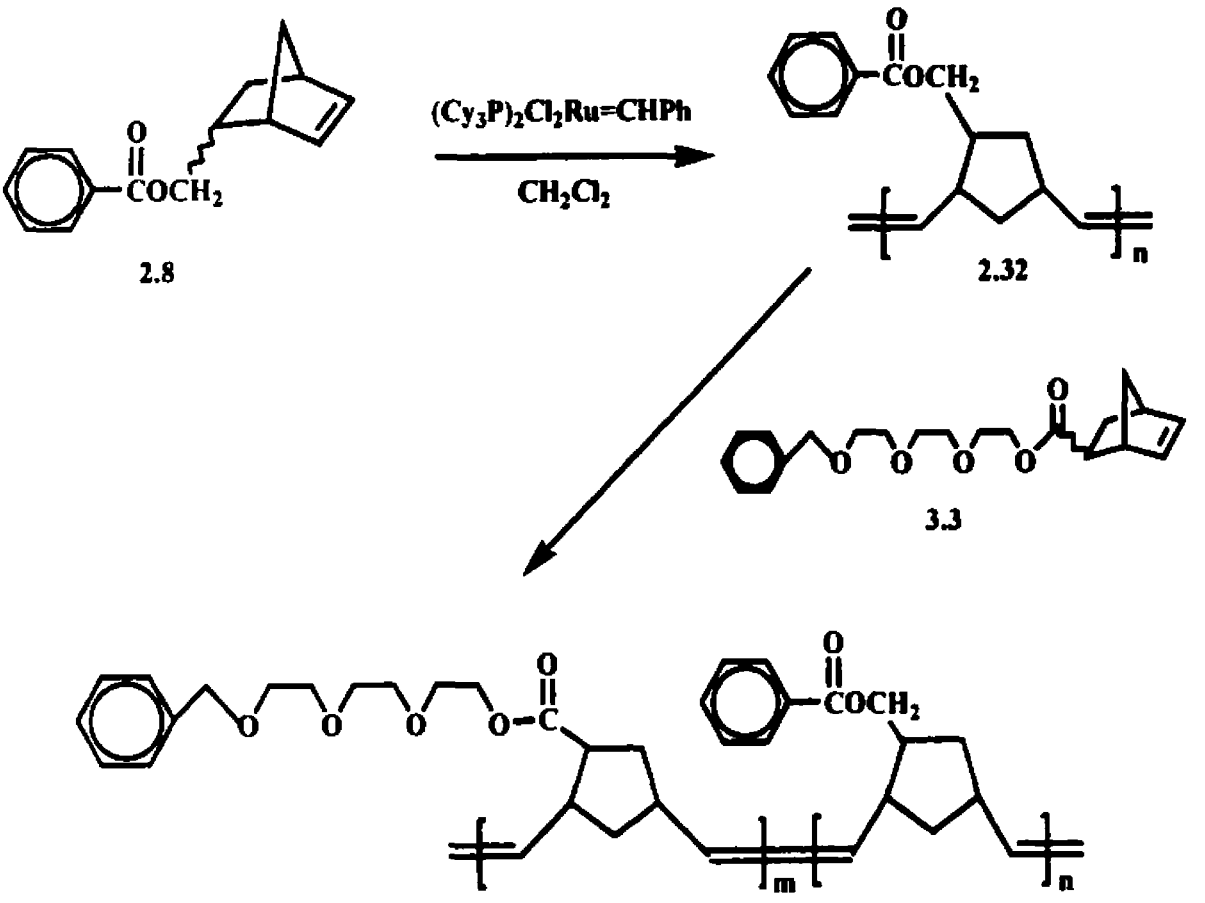

2.8 2.32 3.3 4.1

material was achieved in 31% yield. GPC analysis indicated a high Mw (89 000) and Mn (72 000) for this material with a PDI of 1.2.

In the ^{1}H NMR spectrum, two broad singlets at 4.55 ppm and at 3.64 ppm were assigned to the methylene protons in the aliphatic ether portion of the copolymer. Another broad peak ranging from 4.07 – 4.24 ppm was also representative of the remaining methylene protons in the aliphatic spacer as well as to the methylene protons arising from the ROMP of monomer **2.8**. Evidence confirming the incorporation of polymer **2.32** was found by the appearance of a strong aromatic resonance at 8.02 ppm. The presence of these aromatic signals so far downfield is characteristic of the close

proximity of the ortho protons to the highly electron-withdrawing carbonyl group. Polymer formation was also verified by the loss of olefinic resonances in the range of 5.9 – 6.2 ppm which were representative of the *endo* and *exo* H_5 and H_6 protons in each of the monomers. A broad singlet ranging from 5.22 – 5.39 ppm in the ^1H NMR spectrum represented the double bonds in the unsaturated polymer backbone. This broad singlet reflects the high trans geometry in the polymer microstructure.

As the thermal behavior of this copolymer was of interest, DSC and TGA were performed. Two distinct Tg's were observed in the DSC thermogram, the first appearing at 39.3 °C and the second at 45.3 °C. Due to the AB nature of the block copolymer, the first Tg was identified as belonging to the aliphatic-bridged component of the polymer which is what would be expected for this "soft" or more flexible segment.[41, 145, 149] The more rigid aryl ester unit referred to as the "hard" segment was assigned to the higher Tg. Determination of the thermal decomposition of **4.1** was also accomplished using TGA, which showed a single weight loss at 417 °C.

6.0 References

1. K.J. Ivin and J.C. Mol. Olefin Metathesis and Metathesis Polymerization. San Diego: Academic Press, Inc., 1997.
2. K.J. Ivin and T. Saegusa, Eds. "Cycloalkenes and Bicycloalkenes." Ring-Opening Polymerization. Vol. 1. London: Elsevier, 1984. 121-183.
3. K.J. Ivin. "Metathesis Polymerization." Encyclopedia of Polymer Science and Engineering (2nd Ed.). Ed. H.F. Mark, N.M. Bikales, C.G. Overberger and G.
4. G. Odian. Principles of Polymerization, (3rd Ed.). New York: John Wiley & Sons, Inc., 1991.
5. Z. Komiya, C. Pugh and R.R. Schrock. *Macromolecules.* **1992**, *25*, 3609.
6. C. Pugh, J. Dharia and S.V. Arehart. *Macromolecules.* **1997**, *30*, 4520.
7. C. Pugh, J. Shao, J.J. Ge and S.Z.D. Cheng. *Macromolecules.* **1998**, *31*, 1779.
8. T.J. Boyd, Y. Geerts, J-K Lee, D.E. Fogg, G.G. Lavoie, R.R. Schrock and M.F. Rubner. *Macromolecules.* **1997**, *30*, 3553.
9. W.J. Feast and L.A. Shahada. *Eur. Polym. J.* **1991**, *27*, 27.
10. W.L. Truett, D.R. Johnson, L.M. Robinson and B.A. Montague. *J. Am. Chem. Soc.*, **1960**, *82*, 2337.
11. N. Calderon, H.Y. Chen and K.W. Scott. *Tetrahedron Lett.*, **1967**, 3327.
12. N. Calderon, E.A. Ofstead and W.A. Judy. *J. Polym. Sci. A-1.*, **1967**, *5*, 2209.
13. N. Calderon, E.A. Ofstead, J.P. Ward, W.A. Judy and K.W. Scott. *J. Am. Chem. Soc.*, **1968**, *90*, 4133.
14. R.H. Grubbs, P.L. Burk and D.D. Carr. *J. Am. Chem. Soc.*, **1975**, *97*, 3265.

15. T.J. Katz and R. Rothchild. *J. Am. Chem. Soc.*, **1976**, *98*, 2519.

16. G. Dall'Asta and G. Motroni. *Europ. Polymer J.*, **1971**, *7*, 707.

17. G. Dall'Asta, G. Motroni and L. Motta. *J. Polymer Sci., A-1*, **1972**, *10*, 1601.

18. V.C. Gibson. *Adv. Mater.*, **1994**, *6*, 37.

19. D.S. Breslow. *Prog. Polym. Sci.*, **1993**, *18*, 1141.

20. R. Schrock, S. Rocklage, J. Wengrovius, G. Rupprecht and J. Fellmann. *J. Mol. Catal.*, **1980**, *8*, 73.

21. J.H. Wengrovius, R.R. Schrock, M.R. Churchill, J.R. Missert and W.J. Youngs. *J. Am. Chem. Soc.*, **1980**, *102*, 4515.

22. J. Kress, M. Wesolek and J.A. Osborn. *J. Chem. Soc., Chem. Commun.*, **1982**, 514.

23. R.P. Quirk and B. Lee. *Polym. Int.*, **1992**, *27*, 359.

24. March, J. Advanced Organic Chemistry: Reactions, Mechanisms and Structure. New York: John Wiley & Sons, 1992.

25. Fessenden, R.J. and Fessenden, J.S. Organic Chemistry, 4th Ed. California: Brooks/Cole Publishing Company, 1990.

26. D. Albagli, G.C. Bazan, R.R. Schrock and M.S. Wright. *J. Am. Chem. Soc.*, **1993**, *115*, 7328.

27. M.A. Tlenkopatchev, S. Fomine, L. Fomina, R. Gavino and T. Ogawa. *Polymer Journal*, **1997**, *29*, 622.

28. J-K Lee, R.R. Schrock, D.R. Baigent and R.H. Friend. *Macromolecules*. **1995**, *28*, 1966.

29. V. Heroguez, S. Breunig, Y. Gnanou and M. Fontanille. *Macromolecules*. **1996**, *29*, 4459.

30. M. Weck, J.J. Jackiw, R.R. Rossi, P.S. Weiss and R.H. Grubbs. *J. Am. Chem. Soc.*, **1999**, *121*, 4088.

31. D. Astruc. Electron Transfer and Radical Processes in Transition Metal Chemistry. New York: VCH Publishers, 1995.

32. Z. Komiya and R.R. Schrock. *Macromolecules*. **1993**, *26*, 1393.

33. B.R. Maughon, M. Weck, B. Mohr and R.H. Grubbs. *Macromolecules*. **1997**, *30*, 257.

34. C. Fraser and R.H. Grubbs. *Macromolecules*. **1995**, *28*, 7248.

35. B.M. Novak and R.H. Grubbs. *J. Am. Chem. Soc.*, **1988**, *110*, 960.

36. K.F. Castner and N. Calderon. *J. Mol. Cat.*, **1982**, *15*, 47.

37. S. Kanaoka and R.H. Grubbs. *Macromolecules*. **1995**, *28*, 4707.

38. G.C. Bazan, R.R. Schrock, H.N. Cho and V.C. Gibson. *Macromolecules*, **1991**, *24*, 4495.

39. M. Weck, P. Schwab and R.H. Grubbs. *Macromolecules*. **1996**, *29*, 1789.

40. R. Madan, R.C. Anand and I.K. Varma. *J. Polym. Sci: Part A: Polym. Chem.* **1997**, *35*, 2917.

41. E. Khosravi and A.A. Al-Hajaji. *Eur. Polym. J.*, **1998**, *34*, 153.

42. E. Khosravi and A.A. Al-Hajaji. *Polymer*. **1998**, *39*, 5619.

43. D.M. Lynn, S. Kanaoka and R.H. Grubbs. *J. Am. Chem. Soc.*, **1996**, *118*, 784.

44. S.C.G. Biagini, M.P. Coles, V.C. Gibson, M.R. Giles, E.L. Marshall and M. North. *Polymer*. **1998**, *39*, 1007.

45. S. Matsumoto, K. Komatsu and K. Igarashi. *Polym. Prepr.*, **1977**, *18*, 110.

46. M.P. Coles, V.C. Gibson, L. Mazzariol, M. North, W.G. Teasdale, C.M. Williams

and D. Zamuner. *J. Chem. Soc., Chem. Commun.*, **1994**, 2505.

47. R.H. Grubbs and W. Tumas. *Science*. **1989**, *243*, 907.

48. R.H. Grubbs and L.R. Gilliom. Proceedings of the 4th International Symposium on Homogeneous Catalysis. New York: Gordon and Breach. 1984, 24-28.

49. L.R. Gilliom and R.H. Grubbs. *J. Am. Chem. Soc.*, **1986**, *108*, 733.

50. B.M. Novak, W. Risse and R.H. Grubbs. *Adv. in Polym. Sc.*, **1992**, *102*, 47.

51. L.F. Cannizzo and R.H. Grubbs. *Macromolecules*. **1988**, *21*, 1961.

52. G.C. Bazan, E. Khosravi, R.R. Schrock, W.J. Feast, V.C. Gibson, M.B. O'Regan, J.K. Thomas and W.M. Davis. *J. Am. Chem. Soc.*, **1990**, *112*, 8378.

53. G.C. Bazan, J.H. Oskam, H-N. Cho, L.Y. Park and R.R. Schrock. *J. Am. Chem. Soc.*, **1991**, *113*, 6899.

54. J.H. Oskam and R.R. Schrock. *J. Am. Chem. Soc.*, **1993**, *115*, 11831.

55. R.O'Dell, D.H. McConville, G.E. Hofmeister and R.R. Schrock. *J. Am. Chem. Soc.*, **1994**, *116*, 3414.

56. W.J. Feast, V.C. Gibson, K.J. Ivin, A.M. Kenwright and E. Khosravi. *J. Chem. Soc., Chem. Commun.*, **1994**, 1399.

57. S. Matsumoto, K. Komatsu and K. Igarashi. *ACS Symp. Ser., 59 (Ring-opening Polym. Int. Symp.)*. **1977**, 303.

58. R. Madan, R.C. Anand and I.K. Varma. *Indian J. Chem. Technol.*, **1998**, *5*, 74.

59. J.L. Herisson and Y. Chauvin. *Makromol. Chem.*, **1970**, *141*, 161.

60. C.J. Schaverien, J.C. Dewan and R.R. Schrock. *J. Am. Chem. Soc.*, **1986**, *108*, 2771.

61. R.R. Schrock, J. Feldman, L.F. Cannizzo and R.H. Grubbs. *Macromolecules.*

1987, *20*, 1169.

62. R.R. Schrock. *J. Am. Chem. Soc.*, **1986**, *108*, 2771.

63. R.R. Schrock, R.T. Depue, J. Feldman, C.J. Schaverien, J.C. Dewan and A.H. Liu. *J. Am. Chem. Soc.*, **1988**, *110*, 1423.

64. R.R. Schrock. *Acc. Chem. Res.*, **1990**, *23*, 158.

65. B.M. Novak and R.H. Grubbs. *J. Am. Chem. Soc.*, **1988**, *110*, 7542.

66. M. Lautens, A.S. Abd-El-Aziz and J. Reibel. *Macromolecules*. **1989**, *22*, 4133.

67. S.T. Nguyen, L.K. Johnson, R.H. Grubbs and J.W. Ziller. *J. Am. Chem. Soc.*, **1992**, *114*, 3974.

68. S.T. Nguyen and R.H. Grubbs. *J. Am. Chem. Soc.*, **1993**, *115*, 9858.

69. E.L. Dias, S.T. Nguyen and R.H. Grubbs. *J. Am. Chem. Soc.*, **1997**, *119*, 3887.

70. P. Schwab, M.B. France, J.W. Ziller and R.H. Grubbs. *Angew. Chem. Int. Ed. Engl.*, **1995**, *34*, 2039.

71. P. Schwab, R.H. Grubbs and J.W. Ziller. *J. Am. Chem. Soc.*, **1996**, *118*, 100.

72. D.M. Lynn, B. Mohr and R.H. Grubbs. *J. Am. Chem. Soc.*, **1998**, *120*, 1627.

73. E.L. Dias and R.H. Grubbs. *Organometallics*. **1998**, *17*, 2758.

74. M.F. Semmelhack. *J. Organomet. Chem. Lib.*, **1976**, *1*, 361.

75. R.D. Pike and D.A. Sweigart. *Synlett*, **1990**, 565.

76. D. Astruc. *Topics Curr. Chem.*, **1991**, *160*, 48.

77. A.J. Pearson. Iron Compounds in Organic Synthesis. San Diego: Academic Press, Ltd., 1994.

78. S.G. Davies. Organotransition Metal Chemistry: Applications to Organic Synthesis. Oxford: Pergamon Press, 1982.

79. A.C. Knipe, S.J. McGuiness and W.E. Watts. *J. Chem. Soc. Perkin Trans. II*, **1981**, 193.

80. A.C. Knipe, S.J. McGuiness and W.E. Watts. *J. Chem. Soc. Chem. Commun.*, **1979**, 842.

81. T.H. Coffield, V. Sandel and R.D. Closson. *J. Am. Chem. Soc.*, **1957**, *79*, 5826.

82. A.N. Nesmeyanov, N.A. Vol'kenau and I.N. Bolesova. *Dokl. Akad. Nauk. SSSR*, **1963**, *149*, 615.

83. A.N. Nesmeyanov, N.A. Vol'kenau and I.N. Bolesova. *Tetrahedron Lett.*, **1963**, *24*, 1725.

84. E.I. Sirotkina, A.N. Nesmeyanov and N.A. Vol'kenau. *Dokl. Akad. Nauk. SSSR*, **1969**, *155*, 615.

85. A.N. Nesmeyanov, N.A. Vol'kenau and V.A. Petrakova. *J. Organomet. Chem.*, **1977**, *136*, 363.

86. R.G. Sutherland. *J. Organomet. Chem. Lib.*, **1977**, *3*, 311.

87. I.U. Khand, P.L Pauson and W.E. Watts. *J. Chem. Soc. C*, **1968**, 2257.

88. I.U. Khand, P.L Pauson and W.E. Watts. *J. Chem. Soc. C*, **1968**, 2261.

89. I.U. Khand, P.L Pauson and W.E. Watts. *J. Chem. Soc. C*, **1969**, 116.

90. Q. Dabirmanesh and R.M.G. Roberts. *J. Organomet. Chem.*, **1993**, *460*, C28.

91. Q. Dabirmanesh, S.I.S. Fernando and R.M.G. Roberts. *J. Chem. Soc. Perkin Trans. I.*, **1995**, 743.

92. B. Nicholls and M.C. Whiting. *J. Chem. Soc.*, **1956**, 551.

93. A.N. Nesmeyanov, N.A. Vol'kenau and I.N. Bolesova., *Dokl. Akad. Nauk SSSR*, **1967**, *175*, 606.

94. A.N. Nesmeyanov, N.A. Vol'kenau, L.S. Isaeva and I.N. Bolesova. *Dokl. Akad. Nauk SSSR.* **1968**, *183*, 834.

95. R.J. Cotter. Engineering Plastics: A Handbook of Polyarylethers. Basel: Gordon and Breach Publishers, 1995.

96. A.A. Moroz and M.S. Shvartsberg. *Russ. Chem. Rev.*, **1974**, *43*, 679.

97. J.E. Douglas and Z.Y. Wang. *Can. J. Chem.*, **1997**, *75*, 1340.

98. Z.Y. Wang and P.W. Broughton. *Can. J. Chem.*, **1997**, *75*, 1346.

99. I. Colon and D.R. Kelsey. *J. Org. Chem.*, **1986**, *51*, 2627.

100. I. Colon and G.J. Kwiatkowski. *J. Polym. Sci., Part A, Polym. Chem.*, **1990**, *23*, 367.

101. A.S. Abd-El-Aziz and D.C. Schriemer. *Inorg. Chim. Acta*, **1992**, *202*, 123.

102. A.S. Abd-El-Aziz, D.C. Schriemer and C.R. de Denus. *Organometallics*. **1994**, *13*, 374.

103. A.S. Abd-El-Aziz, C.R. de Denus and K.M. Epp. *Proc. Indian Acad. Sci. (Chem. Sci.)*. **1995**, *107*, 877.

104. A.S. Abd-El-Aziz and C.R. de Denus. *J. Chem. Soc., Chem. Commun.*, **1994**, 663.

105. A.S. Abd-El-Aziz, C.R. de Denus, M.J. Zaworotko and L.R. MacGillivray. *J. Chem. Soc. Dalton Trans.*, **1995**, 3375.

106. A.S. Abd-El-Aziz, E.K. Todd and K.M. Epp. *Polym. Prepr., Am. Chem. Soc. Div. Polym. Chem.*, **1998**, *29*, 300.

107. A.S. Abd-El-Aziz, E.K. Todd and K.M. Epp. *J. Inorg. Organomet. Polym.* **1998**, *8*, 127.

108. A.S. Abd-El-Aziz, K.M. Epp and C.R. de Denus. *Polym. Prepr., Am. Chem. Soc. Div. Polym. Chem.*, **1998**, *39*, 408.

109. A.S. Abd-El-Aziz, C.C. Lee, A. Piorko and R.G. Sutherland. *Synth. Commun.* **1988**, *18*, 291.

110. C.C. Lee, C.I. Azogu, P.C. Chang and R.G. Sutherland. *J. Organomet. Chem.*, **1981**, *220*, 181.

111. A. Darchen. *J. Chem. Soc. Chem. Commun.*, **1983**, 768.

112. A. Darchen. *J. Organomet. Chem.*, **1986**, 302, 389.

113. T.P. Gill and K.R. Mann. *Inorg. Chem.*, **1980**, *19*, 3007.

114. T.P. Gill and K.R. Mann. *J. Organomet. Chem.*, **1981**, *216*, 65.

115. A.M. McNair, J.L. Schrenk and K.R. Mann. *Inorg. Chem.*, **1984**, *23*, 2633.

116. J.L. Schrenk, M.C. Palazzotta and K.R. Mann. *Inorg. Chem.*, **1983**, *22*, 4047.

117. A.N. Nesmeyanov, N.A. Vol'kenau and L.S. Shilovtseva. *Dokl. Akad. Nauk SSSR.*, **1970**, *190*, 857.

118. A.N. Nesmeyanov, N.A. Vol'kenau and E.I. Sirotkina. *Izv. Akad. Nauk SSSR, Ser. Khim.*, **1967**, 1170.

119. A.N. Nesmeyanov, N.A. Vol'kenau, E.I. Sirotkina and V.V. Deryabin. *Dokl. Akad. Nauk SSSR.*, **1967**, *177*, 1110.

120. E.I. Sirotkina, A.N. Nesmeyanov and N.A. Vol'kenau. *Izv. Akad. Nauk SSSR, Ser. Khim.*, **1969**, 1524.

121. W. Steglich and G. Höfle. *Angew. Chem. Internat. Edit.*, **1969**, 8, 981.

122. G. Höfle and W. Steglich. *Synthesis*. **1972**, 619.

123. B. Neises and W. Steglich. *Angew. Chem. Int. Ed. Engl.*, **1978**, *17*, 522.

124. G. Höfle, W. Steglich and H. Vorbrüggen. *Angew. Chem. Int. Ed. Engl.*, **1978**, *17*, 569.

125. A. Hassner and V. Alexanian. *Tetrahedron Lett.*, **1978**, 4475.

126. E.F.V. Scriven. *Chem. Soc. Rev.*, **1983**, 129.

127. F. Kurzer and K.Douraghi-Zadeh. *Chem. Rev.*, **1967**, *67*, 107.

128. A.N. Nesmeyanov, I.F. Leshchova, Y.A. Ustynyuk, I. Sirotkina, I.N. Bolesova, L.S. Isayeva and N.A. Vol'kenau. *J. Organometal. Chem.*, **1970**, *22*, 689.

129. B.R. Steele, R.G. Sutherland and C.C. Lee. *J. Chem. Soc. Dalton.*, **1981**, 529.

130. A.E. Derome. Modern NMR Techniques for Chemistry Research. New York: Pergamon Press, 1987.

131. D.A. Skoog and J.J. Leary. Principles of Instrumental Analysis, 4th Ed., Orlando: Saunders College Publishing, 1992.

132. R.M. Silverstein, G.C. Bassler and T.C. Morrill. Spectrometric Identification of Organic Compounds. New York: John Wiley & Sons, Inc., 1963.

133. R.R. Fraser. *Can. J. Chem.*, **1962**, *40*, 78.

134. K.L. Williamson. *J. Am. Chem. Soc.*, **1963**, *85*, 516.

135. P. Laszlo and P. von Ragué Schleyer. *J. Am. Chem. Soc.*, **1963**, *85*, 2709.

136. J.I. Musher. *Mol. Phys.*, **1963**, *6*, 93.

137. H.G. Kuivila and C.R. Warner. *J. Org. Chem.*, **1964**, *29*, 2845.

138. K. Tori, Y. Hata, R. Muneyuki, Y. Takano, T. Tsuji and H. Tanida. *Can. J. Chem.*, **1964**, *42*, 926.

139. E.I. Snyder and B. Franzus. *J. Am. Chem. Soc.*, **1964**, *86*, 1166.

140. E.W.C. Wong and C.C. Lee. *Can. J. Chem.*, **1964**, *42*, 1245.

141. P. Laszlo and P. von Ragué Schleyer. *J. Am. Chem. Soc.*, **1964**, *86*, 1171.

142. J. Fisher and M.J. Gradwell. *Magn. Reson. Chem.*, **1991**, *29*, 1068.

143. W. Apichatachutapan and L.J. Mathias. *J. Appl. Polym. Sci.*, **1998**, *67*, 183.

144. F. Cataldo. *Polym. Int.*, **1994**, *34*, 49.

145. E.A. Turi. Thermal Characterization of Polymeric Materials. 2nd Ed., San Diego: Academic Press, Inc., 1997.

146. T. Hatakeyama and F.X. Quinn. Thermal Analysis – Fundamentals and Applications to Polymer Science. West Sussex: John Wiley & Sons Ltd., 1994.

147. F. Reinitzer. *Monatsh. Chem.*, **1888**, *9*, 421.

148. V. Percec and C. Pugh. Side Chain Liquid Crystal Polymers. Ed. C.B. McArdle. New York: Chapman and Hall, 1989, 30.

149. M. Weck, B. Mohr, B.R. Maughon and R.H. Grubbs. *Macromolecules*. **1997**, *30*, 6430.

150. S-H. Kim, H-J. Lee, S-H. Jin, H-N. Cho and S-K. Choi. *Macromolecules*. **1993**, *26*, 846.

151. C.Pugh and R.R. Schrock. *Macromolecules*. **1992**, *25*, 6593.

152. C. Pugh. *Macromol. Symp.*, **1994**, *77*, 325.

153. V. Percec and D. Schlueter. *Macromolecules*. **1997**, *30*, 5783.

154. H. Finkelmann, H. Ringsdorf, J.H. Wendorff. *Makromol. Chem.*, **1978**, *179*, 273.

155. H. Finkelmann, M. Happ, M. Portugall and H. Ringsdorf. *Makromol. Chem.*, **1978**, *179*, 2541.

156. C.B. Allan and L.O. Spreer. *J. Org. Chem.*, **1994**, *59*, 7695.

157. A.J. Pearson and A.M. Gelormini. *J. Org. Chem.*, **1995**, *60*, 281.

158. Z. Komiya and R.R. Schrock. *Macromolecules*. **1993**, *26*, 1387.